

**GEOMORPHOLOGY AND HYDROLOGY OF THE
COLVILLE RIVER DELTA, ALASKA, 1995**

Fourth Annual Report

Prepared for:

ARCO Alaska, Inc.
P.O. Box 100360
Anchorage, AK 99510

and

Kuukpik Unit Owners

Prepared by:

M. Torre Jorgenson
Erik R. Pullman
Yuri Shur
Michael D. Smith
Alice A. Stickney

ABR, Inc.
P.O. Box 80410
Fairbanks, AK 99708

and

James W. Aldrich
Scott R. Ray

Shannon and Wilson, Inc.
2055 Hill Road
P.O. Box 70843
Fairbanks, AK 99707-0843

and

H. Jesse Walker

Dept. of Geography and Anthropology
Howe-Russel Geosciences
Louisiana State University
Baton Rouge, LA 70803

August 1996



TABLE OF CONTENTS

LIST OF TABLES.....	iii
LIST OF FIGURES	iii
ACKNOWLEDGMENTS	vii
INTRODUCTION	1
STUDY AREA	3
PART 1. 1995 SPRING BREAKUP	5
BACKGROUND.....	5
METHODS	5
RESULTS AND DISCUSSION.....	5
CROSS SECTION E27.09.....	5
FLOW DISTRIBUTION	8
PART 2. CHANNEL GEOMETRY AND BED MATERIAL.....	10
BACKGROUND.....	10
METHODS	10
CHANNEL CROSS SECTIONS.....	10
THALWEG PROFILES	10
BED MATERIAL.....	12
RESULTS AND DISCUSSION.....	12
CHANNEL GEOMETRY	12
THALWEG PROFILES	12
BED MATERIAL.....	12
PART 3. STAGE-DISCHARGE-VELOCITY RELATIONSHIPS	25
BACKGROUND.....	25
METHODS	25
DISCHARGE MEASUREMENTS	25
STAGE-DISCHARGE CURVES.....	25
VELOCITY-DISCHARGE CURVES.....	27
RESULTS AND DISCUSSION.....	27
PART 4. FLOOD MAGNITUDE AND FREQUENCY	35
BACKGROUND.....	35
METHODS	35
FLOOD MAGNITUDE.....	35
FLOOD FREQUENCY	36
RESULTS AND DISCUSSION.....	37
FLOOD MAGNITUDE.....	37
FLOOD FREQUENCY	37
PART 5. FLOOD DISTRIBUTION.....	41
BACKGROUND.....	41
METHODS	41
RESULTS AND DISCUSSION.....	43
OVERALL FLOOD DISTRIBUTION.....	43
RELATIONSHIP BETWEEN FLOODING AND TERRAIN UNITS	44
PART 6. SUMMER- THROUGH WINTER-FLOW CONDITIONS.....	61
BACKGROUND.....	61
METHODS	61
RESULTS AND DISCUSSION.....	61

DISCHARGE	60
SALINITY.....	60
WATER TEMPERATURES	60
PART 7. BARGE ACCESS	61
BACKGROUND	61
METHODS.....	61
OFFSHORE.....	61
WITHIN CHANNELS	61
RESULTS AND DISCUSSION	62
OFFSHORE.....	62
WITHIN CHANNELS	68
PART 8. ICE-ROAD CROSSINGS.....	83
BACKGROUND	83
METHODS	83
OFFSHORE ROUTE	83
RESULTS AND DISCUSSION	83
OFFSHORE ROUTE	83
OVERLAND ROUTE.....	83
PART 9. DRAINAGE NETWORK.....	88
BACKGROUND	88
METHODS.....	88
RESULTS AND DISCUSSION	88
PART 10. SOIL STRATIGRAPHY AND PERMAFROST DEVELOPMENT	91
BACKGROUND	91
METHODS.....	92
CLASSIFICATION AND MAPPING	92
SOIL STRATIGRAPHY.....	92
RESULTS AND DISCUSSION	94
CLASSIFICATION AND MAPPING OF TERRAIN UNITS	94
SOIL STRATIGRAPHY.....	94
GRAVEL RESOURCES.....	110
CONCEPTUAL MODEL OF FLOODPLAIN EVOLUTION ON THE DELTA.....	111
PART 11. LANDSCAPE CHANGE	117
BACKGROUND	117
METHODS.....	117
RESULTS AND DISCUSSION	118
PART 12. GEODETIC CONTROL NETWORK AND SPOT BASE MAP.....	121
BACKGROUND	121
METHODS.....	121
GEODETIC CONTROL NETWORK	121
SPOT BASE MAP REGISTRATION AND PRODUCTION	121
RESULTS AND DISCUSSION	123
GEODETIC CONTROL NETWORK	123
SPOT BASE MAP	123
PART 13. HYDROLOGIC CONSIDERATIONS FOR A PIPELINE CROSSING AT E20.56.....	126
BACKGROUND	127
METHODS.....	127
DESIGN FLOOD	127
SCOUR DEPTH.....	127
RESULTS AND DISCUSSION	128

DESIGN FLOOD.....	128
SCOUR DEPTH	128
ADDITIONAL DATA REQUIREMENTS	130
LITERATURE CITED.....	132

LIST OF TABLES

Table 1–1. Summary of water-surface elevations (WSE) during breakup monitoring of the Colville River, spring 1995.....	6
Table 1–2. Summary of breakup data at the head of the Colville River Delta, 1962–1995.....	7
Table 2–1. Bed material data collected in June 1995, Colville River Delta.....	24
Table 4–1. Kuparuk and Colville rivers data used in flood frequency analysis.....	38
Table 5–1. Flood-frequency classes associated with terrain units within three flooding regions, Colville River Delta, 1995.....	52
Table 7–1. Cross section width at specific depths in the lower Nechelik Channel.....	77
Table 7–2. Cross section width at specific depths in the upper Nechelik Channel.....	79
Table 7–3. Cross section width at specific depths in the Putu Channel.....	80
Table 9–1. Descriptions of stream orders for the drainage network in the Transportation Corridor adjacent to the Colville River Delta, 1995.....	89
Table 10–1. Descriptions of terrain units mapped within the Colville River Delta.....	95
Table 12–1. Coordinates of geodetic control points in three coordinate systems for new monuments tied to USGS monument "River", Colville River Delta, 1995.....	123
Table 12–2. Summary of positional error (mean \pm SE) of the SPOT panchromatic image compared to vector layers from various sources, Colville River Delta, 1995.....	126
Table 13–1. Scour depth estimates based on Blench equations at Cross Section E20.56, Colville River Delta, 1995.....	129

LIST OF FIGURES

Figure 1–1. Water surface elevation and discharge data for the head of the Colville River Delta.....	9
Figure 2–1. Location map.....	11
Figure 2–2. West side of Cross Section E16.32.....	13
Figure 2–3. East side of Cross Section E16.32.....	14
Figure 2–4. Cross Section E20.56.....	15
Figure 2–5. Cross Section E27.09.....	16
Figure 2–6. Cross Section N7.46.....	17

Figure 2-7.	Cross Section S9.80.....	18
Figure 2-8.	Cross Section T12.62.....	19
Figure 2-9.	Upper East Channel thalweg profile.....	20
Figure 2-10.	Lower East Channel thalweg profile.....	21
Figure 2-11.	Upper Nechelik Channel thalweg profile.....	22
Figure 2-12.	Lower Nechelik Channel thalweg profile.....	23
Figure 3-1.	Stage-discharge relationship for the Colville River at Cross Section E27.09.....	28
Figure 3-2.	Mean main channel velocity-discharge relationship for the Colville River at Cross Section E27.09.....	29
Figure 3-3.	Stage-discharge relationship for the Colville River at Cross Section E20.56.....	30
Figure 3-4.	Mean main channel velocity-discharge relationship for the Colville River at Cross Section E20.56.....	32
Figure 3-5.	Stage-discharge relationship for the Colville River at Cross Section N7.46.....	33
Figure 3-6.	Main mean channel velocity-discharge relationship for the Colville River at Cross Section N7.46.....	34
Figure 4-1.	Flood-frequency relationship for the Colville River at the head of the delta.....	39
Figure 4-2.	Summary of annual peak discharge and return period at the head of the Colville River Delta (Cross Section E27.09).....	40
Figure 5-1.	Map of flooding study areas and flooding regions, Colville River Delta, 1995.....	42
Figure 5-2.	Map of flood distribution in the Alpine study area, Colville River Delta, 1995.....	45
Figure 5-3.	Map of flood distribution in the Itkillik study area, Colville River Delta, 1995.....	46
Figure 5-4.	Map of flood distribution in the Tamayayak study area, Colville River Delta, 1995.....	47
Figure 5-5.	Map of flood distribution in the Kupigrak study area, Colville River Delta, 1995.....	48
Figure 5-6.	Map of flood distribution in the Nechelik study area, Colville River Delta, 1995.....	49
Figure 5-7.	Percentage of total area covered by flood water in five study areas in the Colville River Delta, 1995.....	50
Figure 5-8.	Percentage of each terrain unit covered by flooding in five study areas in the Colville River Delta, 1995.....	51
Figure 5-9.	Relationship between percent area flooded and peak discharge for the major terrain units, Colville River Delta, 1995.....	52
Figure 5-10.	Mean elevations (\pm SD) of the surface of inactive-floodplain cover deposits relative to distance in river miles from the outer edge of the delta, Colville River Delta, 1995.....	54
Figure 5-11.	Mean relative heights (\pm SD) of terrain units relative to inactive floodplain cover deposits occurring along cross-sectional profiles, Colville River Delta, 1995.....	54
Figure 5-12.	Predicted flood frequency, Colville River Delta, 1995.....	57
Figure 5-13.	Map of flood distribution on 30 May 1943, Colville River Delta (adapted from Walker, unpubl. data).....	58

Figure 5–14.	Map of flood distribution in early June 1971, Colville River Delta (adapted from Walker 1976).....	59
Figure 7–1.	Offshore bathymetry location map.	63
Figure 7–2.	Water depth offshore of Kupigruak Channel (North).....	64
Figure 7–3.	Water depth offshore of Kupigruak Channel (South).....	65
Figure 7–4.	Contours offshore from the Nechelik Channel.	66
Figure 7–5.	Contours offshore from the Kupigruak Channel.	67
Figure 7–6.	Kupigruak Channel cross sections.	69
Figure 7–7.	East Channel cross sections.	70
Figure 7–8.	East Channel cross sections (continued).....	71
Figure 7–9.	Kupigruak Channel contour maps.....	72
Figure 7–10.	Kupigruak Channel contour maps (continued).....	73
Figure 7–11.	Kupigruak Channel contour maps (continued).....	74
Figure 7–12.	East Channel contour map.	75
Figure 7–13.	Cross section location map for evaluation of barge access in the lower Nechelik Channel.	76
Figure 7–14.	Cross section location map for evaluation of barge access in the upper Nechelik Channel.	77
Figure 7–15.	Comparison of 1962 and 1995 cross sections of the Nechelik Channel.....	78
Figure 7–16.	Comparison of 1962 and 1995 cross sections of the Nechelik Channel.....	79
Figure 8–1.	Water depth offshore of East Channel.....	84
Figure 8–2.	Potential East Channel ice road crossings.	85
Figure 8–3.	Potential Nechelik Channel ice road crossings.....	87
Figure 9–1.	Drainage network in the Transportation Corridor, 1995.	89
Figure 10–1.	Map of soil core locations in 1992 and 1995, Colville River Delta.	93
Figure 10–2.	Map of terrain units, Colville River Delta, 1995.	97
Figure 10–3.	Soil stratigraphy profiles grouped by terrain unit, Colville River Delta, 1995.	98
Figure 10–4.	Soil stratigraphy along a terrain sequence (Cross Section N7.46) near Nanuk Lake, Colville River Delta, 1995.	99
Figure 10–5.	Soil stratigraphy along a terrain sequence (Cross Section S9.80) along Sakoonang Channel, Colville River Delta, 1995.....	100
Figure 10–6.	Soil stratigraphy along a terrain sequence near Nanuk Lake (Transect 11), Colville River Delta, 1995.	101
Figure 10–7.	Soil stratigraphy along a terrain sequence along the East Channel (Cross-Section E20.56), Colville River Delta, 1995.	102

Figure 10–8.	Mean (\pm SD) percentages of sand, silt, and clay of soils associated with various terrain units on the Colville River Delta.....	104
Figure 10–9.	Mean (\pm SD) salinity (electrical conductivity) values for soils associated with various terrain units on the Colville River Delta.....	105
Figure 10–10.	Mean (\pm SD) thickness of the top layer of organic matter (left) and cumulative thickness of organic layers in top 1 ft (right) for soils associated with various terrain units on the Colville River Delta, 1995.....	106
Figure 10–11.	Photographs of common ice types: structureless and lenticular ice (upper left), reticulate and suspended ice (upper right), sheet ice (lower right), and wedge ice (lower left) on the Colville River Delta, 1995.....	108
Figure 10–12.	Volumetric ice contents near the soil surface grouped by terrain unit (upper four graphs) and summarized by depth (lower left) and terrain unit (lower right) Colville River Delta, 1995.....	109
Figure 10–13.	Mean (\pm SD) rates of accumulation of material (sediments, organics, and ice) for various terrain units on the Colville River Delta, 1995.....	110
Figure 10–14.	Relative importance of the processes of fluvial and eolian deposition, and organic matter and ice accumulation in common floodplain deposits on the Colville River Delta.....	112
Figure 11–1.	Map of landscape change within the proposed Alpine Development Area, Colville River Delta, 1955–1992.....	119
Figure 11–2.	Percentage of landscape change in four study areas (above) and within the Alpine Development Area only (below) on the Colville River Delta, 1955–1992.....	120
Figure 12–1.	Location of new geodetic control monuments and lakes surveyed by differential GPS technology on the Colville River Delta, 1995.....	122
Figure 12–2.	SPOT image of the Colville River Delta.....	124
Figure 12–3.	SPOT image of the proposed Transportation Corridor west of the Colville River Delta.....	125
Figure 13–1.	Cross Section E29.09.....	131

APPENDICES

(Separate Attachment)

- Appendix A. Summary of TBM data.
- Appendix B. Summary of discharge, and water-surface elevation and slope data.
- Appendix C. Summary of cross section data.
- Appendix D. Summary of thalweg profile data.
- Appendix E. Summary of bed material data.
- Appendix F. Water depths offshore of Kupigruak and East channels.
- Appendix G. Water depths at potential ice road crossings.
- Appendix H. Borehole logs from siple core and soil data listings.

ACKNOWLEDGMENTS

We acknowledge the many participants who contributed to this project. The project was funded by ARCO, Alaska, Inc., and the Kuukpik Unit Owners and was managed by John Eldred, Senior Project Engineer for ARCO.

Numerous individuals helped with the field work. Mark Prins, of Imanda Placer, helped with soil coring. Many villagers in Nuiqsut also contributed to this study. Jobe Woods performed ably as a boatman during long days. Lanston Chinn, Manager of Kuukpik Corporation, helped arrange field personnel and contractual arrangements.

Numerous people from ABR contributed to this study: Ed Ashmead helped with surveying. Tom DeLong and George Zusi-Cobb helped with field logistics and coordinated services provided by Kuukpik Corporation. Allison Zusi-Cobb, Stan Bearup, and Will Lentz helped with GIS analysis. Robert Day and Stephen Murphy provided editorial review, and Terrence Davis and Cecilia Barkley provided clerical work.

INTRODUCTION

The Colville River drains ~29% of the North Slope of Alaska and its delta is the largest in arctic Alaska. The river's volume and heavy sediment load produces a dynamic deltaic system with diverse geomorphic, hydrologic, and ecological systems. Recognizing these characteristics and in preparation for oil development on the Colville River Delta, ARCO Alaska, Inc., and the Kuukpik Unit Owners, contracted ABR, Inc., along with Shannon and Wilson Consultants, Inc., to conduct both this study on geomorphology and hydrology and a companion study on wildlife and their habitats. The geomorphology and hydrology studies were designed to provide information that is essential for designing bridge and pipeline crossings and for locating roads and pads to minimize problems associated with flooding and terrain stability. The studies mainly focused on the delta, but also included some work in the proposed Transportation Corridor.

This report provides results from the fourth year of investigation of the geomorphology and hydrology of the delta. In 1992, this project investigated the morphology of selected channels, mapped the distribution of terrain units, analyzed the flooding regime, and quantified the rate of landscape change (Jorgenson et al. 1993). In 1993, the project was limited to measuring peak discharge after snowmelt and mapping the distribution of floodwater within five small study areas (Jorgenson et al. 1994a). In 1994, only spring breakup was monitored (Jorgenson et al. 1994b). The data are intended to provide a long-term database upon which detailed engineering and facility planning analyses can be made.

This report is divided into 13 parts. The first parts mainly focus on the hydrology of the delta by presenting the results of the monitoring of spring breakup (Part 1), development of stage-discharge-velocity relationships (Part 3), analysis of flood magnitude and frequency (Part 4), mapping and analysis of flood distribution (Part 5), and compilation of low flow conditions (Part 6). Three parts describe channel geometry and water depths at numerous sites across the delta to provide data for the analysis of flow conditions (Part 2), barge access (Part 7), and ice-road crossings (Part 8). Part 9

presents a map of the drainage network in the Transportation Corridor for use in oil spill contingency planning. Part 10 provides information on soil stratigraphy and permafrost development for various terrain units in the delta. Part 11 analyzes landscape change between 1955 and 1992 to identify areas of erosion and deposition. Part 12 describes the production of a map developed from SPOT satellite imagery that provides a common base map for the environmental and engineering studies. Finally, Part 13 identifies hydrologic information that needs to be considered for the design of a pipeline across the main channel of the Colville River.

The remarkable environment of the delta has been the subject of numerous studies conducted over the last four decades. Most information on the geomorphology and hydrology of the delta was gathered by H. J. Walker and his associates during the 1960s and 1970s (Walker 1983a). Other important studies on the geomorphology of the delta and nearby coast have been done by Carter and Galloway (1982, 1985), Reimnitz et al. (1985), and Rawlinson (1993). In addition, several major multi-disciplinary research efforts have been conducted, including a study of nearshore aquatic and marine environments by the University of Alaska (UAF 1972), the investigation of the coast and shelf of the Beaufort Sea by numerous organizations during the early 1970s (Reed and Sater 1974), and numerous studies conducted under the Outer Continental Shelf Environmental Assessment Program of the National Oceanic and Atmospheric Administration. Pertinent information from these and other studies are included in the background portions of each section of this report.

Despite the numerous studies conducted on the delta, the record of discharge measurements is short, particularly at the head of the delta. Arnborg et al. (1966, 1967) collected stage-discharge information in 1962 and the U. S. Geological Survey (USGS) collected stage-discharge measurements in 1977 (USGS 1978). The USGS also collected selected discharge measurements in 1979, 1980, and 1981 (USGS 1980, 1981, 1982).

Attempts to characterize flooding in the delta also have been limited. Small-scale maps of the distribution of flood water across the delta in 1943 and 1971 were developed by Walker (1974).

Relative frequencies of flooding have been mapped on a small scale for the delta by using geomorphic characteristics to delineate active and inactive portions of the floodplain (Cannon and Rawlinson 1981, Cannon and Mortensen 1982). However, those maps were not of sufficient detail to be useful to this project.

All elevations referenced in this report were based on a set of vertical control points established using GIS technology in 1995. In 1996, ground surveys of this control network resulted in minor changes in elevations that are not incorporated in this report (see Part 10).

STUDY AREA

This study focuses on the Colville River Delta and the proposed Transportation Corridor (hereafter referred to as the Transportation Corridor) adjacent to the delta (Figure S-1). Current plans for oil development on the delta include a road and two drill sites within the proposed Development Area (hereafter referred to as the Development Area) and a pipeline to the Kuparuk Oilfield. A road has been included with the current plans as an alternative that may or may not be developed. The village of Nuiqsut, established in 1971, is near the head of the delta.

The Colville River is the largest river on Alaska's North Slope and is one of eight major rivers with significant freshwater input to the Arctic Ocean (Walker 1983a). The Colville enters the Beaufort Sea just west of the Kuparuk Oilfield and midway between Barrow and Kaktovik. The Colville River drains about 20,700 mi² (29%) of the North Slope. Most of the watershed is situated in the foothills (64%), with smaller amounts situated in the Brooks Range (26%) and coastal plain (10%; Walker 1976). The head of the delta is located about 2 mi upstream from the mouth of the Itkillik River (Arnborg et al. 1966). Below the Itkillik River, the area encompassed by the floodplain of the delta and water within the fringe of the delta covers 257 mi².

The delta is bounded on both sides by old alluvial terraces that are traceable from the coast to above the Itkillik River (Carter and Galloway 1982). Fossil wood collected at the base of exposures yielded ages of 48,000–50,600 ybp, suggesting that the terraces and underlying deposits of gravelly sand were formed during the last interglacial period (Carter and Galloway 1982). These deposits are part of the Gubik Formation (Black 1964, Carter et al. 1977), a series of unconsolidated deposits that record a complex marine and alluvial history spanning ~3.5 million years (Carter et al. 1986). The terraces are capped by eolian silt and derived from the delta. The surficial geology of the central Arctic Coastal Plain has been mapped (1:63,360 scale) by Rawlinson (1993).

The delta has two main distributaries, the Nechelik (western) Channel and the Colville East Channel (Figure S-1). These two channels carry about 90% of the water through the delta during

flooding and 99% during low water (Walker 1983a). Smaller channels branching from the East Channel, include the Sakoonang, Tamayayak, and Elaktoveach channels. The delta also is characterized by numerous lakes and ponds, sandbars, mud flats, sand dunes, and low- and high-centered polygons (Walker 1976). Most water bodies are shallow (<6 ft deep) ponds that freeze to the bottom in winter and thaw by June. Larger lakes typically are deeper (up to 33 ft) and freeze only in the upper 6 ft.

The delta study area has a typical arctic maritime climate. Winters last about eight months and are generally cold and windy. Summers are cool, with temperatures ranging from 12°F in mid-May to 60°F in July and August (Simpson et al. 1982); summers also are characterized by low precipitation, overcast skies, fog, and persistent winds from the northeast. Occasional northwesterly winds usually bring storms, with high, wind-driven tides and rain (Walker and Morgan 1964).

Integrated terrain unit maps (based on 1:18,000-scale photography) that classified and delineated terrain units, surface-forms, and vegetation components of the landscape were produced for the delta by Jorgenson et al. (1993) and revised in 1995 (Jorgenson et al. 1996). In addition, land-cover maps (1:30,000 scale) of the delta have been generated by the U. S. Fish and Wildlife Service (USFWS) (Rothe et al. 1983). Wetlands (1:63,360 scale) classified under the National Wetlands Inventory system also have been mapped by the USFWS. The North Slope Borough has mapped the delta for vegetation, surface form, and landforms (1:250,000 scale). Vegetation-soil-landform associations have been described for the Prudhoe Bay region (Walker et al. 1980).

The delta has long been recognized as one of the most productive deltas for fish and wildlife on the Arctic Coast of Alaska (Gilliam and Lent 1982, Divoky 1983). The area is important for Tundra Swans, Brant, Yellow-billed Loons, and Greater White-fronted Geese (Rothe et al. 1983). Arctic and least cisco overwinter in the delta (NOAA/OCSEAP 1983) and support the only commercial fishery on the North Slope. Caribou from both the Central Arctic Herd and the Teshekpuk Herd use the delta (Gilliam and Lent 1982). Finally, the area's resources are important to the subsistence economy of the Nuiqsut villagers.

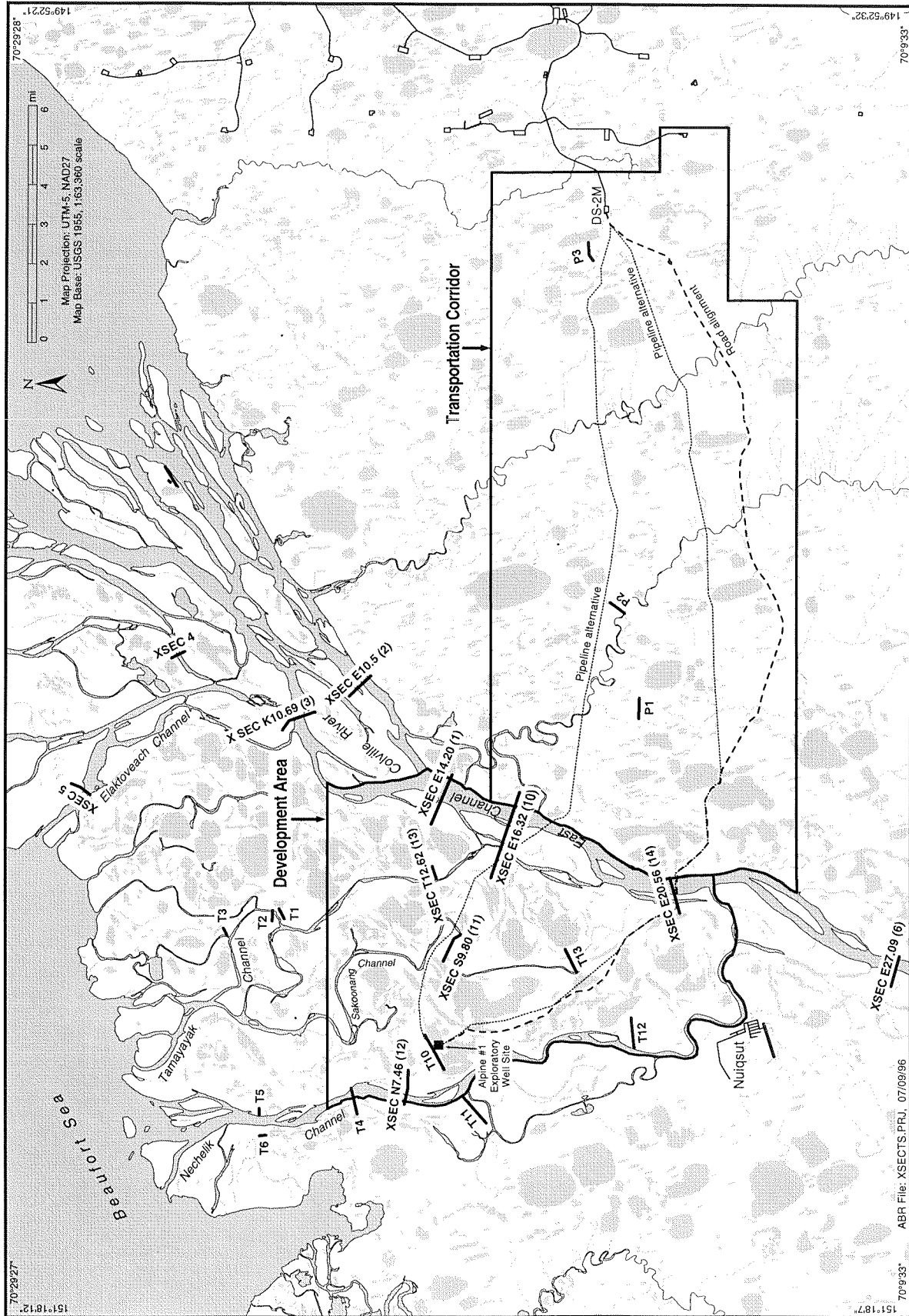


Figure S-1. Map of study area showing the Alpine Development Area, Transportation Corridors and sampling cross-sections, Colville River Delta, 1995.

PART 1. 1995 SPRING BREAKUP

by Scott R. Ray and James W. Aldrich

BACKGROUND

On North Slope rivers, the highest flood peak each year (annual flood-peak discharge) usually occurs during spring breakup. Measurements of the annual flood-peak discharge are used to estimate the magnitudes of less-frequent floods, such as the 50 to 200-yr flood peak discharges, which typically are used in the design of oil pipelines and facilities. The size and abundance of ice floes, the velocity of the water, the sediment transport rate, and the depth of scouring of the riverbed also are important aspects of breakup and of pipeline and facilities design. Additionally, the hydrologic and hydraulic information collected during breakup are important in assessing and mitigating environmental concerns related to development.

This section describes the conditions observed during the 1995 spring breakup on the Colville River Delta and compares those conditions observed in 1995 to those observed in the past. The data collected during the 1995 breakup also are discussed in sections on flood frequency and magnitude, stage-discharge-velocity relationships, and pipeline crossing considerations.

METHODS

Water-surface elevations at each cross section were measured periodically between 11 and 19 May 1995. The elevation of high-water marks along the river banks also were recorded. Temporary bench marks (TBMs) were established at each cross section as control points for measuring water-surface elevations and water-surface slopes. The locations of these TBMs and other TBMs used in this project are presented in Appendix A. The water-surface elevation and water-surface slope measurements are summarized in Appendix B.

The peak discharge at each cross section was estimated based on the peak water surface elevation, after adjusting it for the effects of ice in the channel, using the stage-discharge curve developed at each cross section (see Parts 3 and 4). The parameters required to compute the stage-discharge curves are

the water-surface elevation, water-surface slope, channel geometry, and hydraulic roughness.

RESULTS AND DISCUSSION

CROSS SECTION E27.09

Field observations began on 11 May 1995. The water-surface elevation at Cross Section E27.09 (Cross Section 6) was 8.05 ft (above mean sea level [msl], based on U. S. Coast and Geodetic Survey [USCGS] monument "River") at 15:00 on 11 May 1995 (Table 1-1). At this time, the sandbar on the west side of the river was exposed, and the east side of the channel was ice covered, with ice extending approximately 1400 ft from the east bank. There were no ice floes observed in the river at this time.

The water level in the river began to rise rapidly after 11 May. Over the next 27 hours the water surface rose nearly 5 ft at E27.09, and had reached an elevation of 12.93 ft at 18:30 on 12 May (Table 1-1). At that time, the large ice sheet on the east bank remained intact. A few ice floes were observed in the open river.

Because of inclement weather, we were unable to fly to the Colville River on 13 May. Consequently, no river stage observations were made on that date. Measured water-surface elevations at E27.09 included 14.11 ft at 14:00 on 14 May, 15.27 ft at 13:00 on 15 May, and 15.35 ft at 18:10 on 15 May (Table 1-1). Some ice floes were observed in the river on both days, with some minor ice-choked areas occurring near the mouth of the Tamayyak Channel. However, the large ice sheet on the east side of E27.09 remained intact.

The weather began to change on 16 May, bringing cooler temperatures and snow. Inclement weather again prevented access to the river on 16-17 May. By 18 May, significantly cooler temperatures had settled in over the North Slope. Reflecting this decrease in temperature, the water-surface elevation in the river had begun to fall, and ice was reforming along the edges of the channel. The water-surface elevation at E27.09 was 12.37 ft at 10:20 on 18 May. Based on high-water marks, the peak water-surface elevation at E27.09 between 15 and 18 May was estimated to be 15.87 ft. The peak probably occurred on 16 May.

Table 1-1. Summary of water-surface elevations (WSE) during breakup monitoring of the Colville River, spring 1995.

Date	Parameter	Cross Section ^d					
		E27.09	E16.32	E14.20	N7.46	S9.80	T12.62
11 May	WSE ^b (ft)	8.05					
	Time	15:30					
12 May	WSE (ft)	12.93	7.63 ^c				
	Time	18:35	14:50				
12 May	WSE (ft)		8.07 ^d				
	Time		15:20				
14 May	WSE (ft)	14.11	9.70 ^c	8.47	6.57	4.26	8.73
	Time	14:00	18:15	18:50	15:00	16:00	16:45
14 May	WSE (ft)		9.57 ^d				
	Time		18:35				
15 May	WSE (ft)	15.27	10.74 ^c	9.31	7.26	5.45	8.87
	Time	13:00	14:40	18:00	16:00	17:00	17:30
15 May	WSE (ft)	15.35	10.78 ^d				
	Time	18:20	15:30				
High Water	WSE (ft)	15.87	11.43	9.51	7.26	7.15	9.99
	Time						
18 May	WSE (ft)	12.37	8.64 ^d	7.86	6.21	6.82	6.90
	Time	10:00	11:00	15:00	12:10	13:00	14:30
19 May	WSE (ft)	9.96					
	Time	12:30					

^aIn previous reports, Cross Section E27.09 was referred to as Cross Section 6, Cross Section E16.32 was referred to as Cross Section 10, Cross Section E14.20 was referred to as Cross Section 1, Cross Section N7.46 was referred to as Cross Section 12, Cross Section S9.80 was referred to as Cross Section 11, and Cross Section T12.62 was referred to as Cross Section 13.

^bWater-surface elevations (WSE) are based on USCGS monument "River" (elevation = 41.99 ft).

^cThe water-surface elevation was measured on the east side of the mid-channel island.

^dThe water-surface elevation was measured on the west side of the channel.

Due to the continuing cold weather, the water surface continued to fall and was down to 9.96 ft at E27.09 at 12:00 on 19 May. We decided to return to Fairbanks and wait for breakup to resume. Crest gages were installed at each cross section prior to returning to Fairbanks. The weather remained cold until 23 May, when temperatures above 10°C were reported in both Anaktuvik Pass and Umiat. Observations reported from Nuiqsut indicated that the river continued to drop until 27 May, when it again began to rise. An observer in the village reported that the ice in the Nechelik Channel

at Nuiqsut went out sometime during the night of 29–30 May (J. Woods 1995, pers. comm.).

Observers returned to Cross Section E27.09 on 3 June. The water-surface elevation was 9.18 ft at 18:00. Between 19 May and 3 June, the water surface at E27.09 did not reach the bottom of the crest gage (elevation 14.5 ft). Therefore, the peak water-surface elevation that occurred on or about May 16 (15.87 ft) was the peak for the 1995 breakup. The 1995 peak discharge at E27.09 was estimated to be 233,000 cfs (Table 1–2).

Table 1-2. Summary of breakup data at the head of the Colville River Delta, 1962–1995.

Year	Approximate Date Water Began To Flow	Peak Water-Surface Elevation ^a (ft)	Peak Breakup Discharge (cfs)	Date of Peak Water-Surface Elevation	Date of First Clear Channel/Open Water ^b
1995	8 May	15.9	233,000	16 May	30 May
1994 ^c	16 May	13.2	159,000	25 May	9 June
1993 ^d	—	20.2	379,000	31 May	1 June
1992 ^e	—	14.9	188,000	2 June	4 June
1977 ^f	—	20.1	407,000	7 June	9 June
1973 ^g	25 May	—	—	8 June	8 June
1971 ^g	23 May	—	—	2 June	2 June
1964 ^g	28 May	—	—	3 June	5 June
1962 ^h	19 May	13.4	215,000	14 June	10 June

^a Water-surface elevations are based on USCGS monument "River" (elevation= 41.99 ft).

^b Approximate date the main channel was generally clear of ice.

^c Data from Jorgenson et al. (1994b).

^d Data from Jorgenson et al. (1994a).

^e Data from Jorgenson et al. (1993).

^f Data from U. S. Geological Survey (1978).

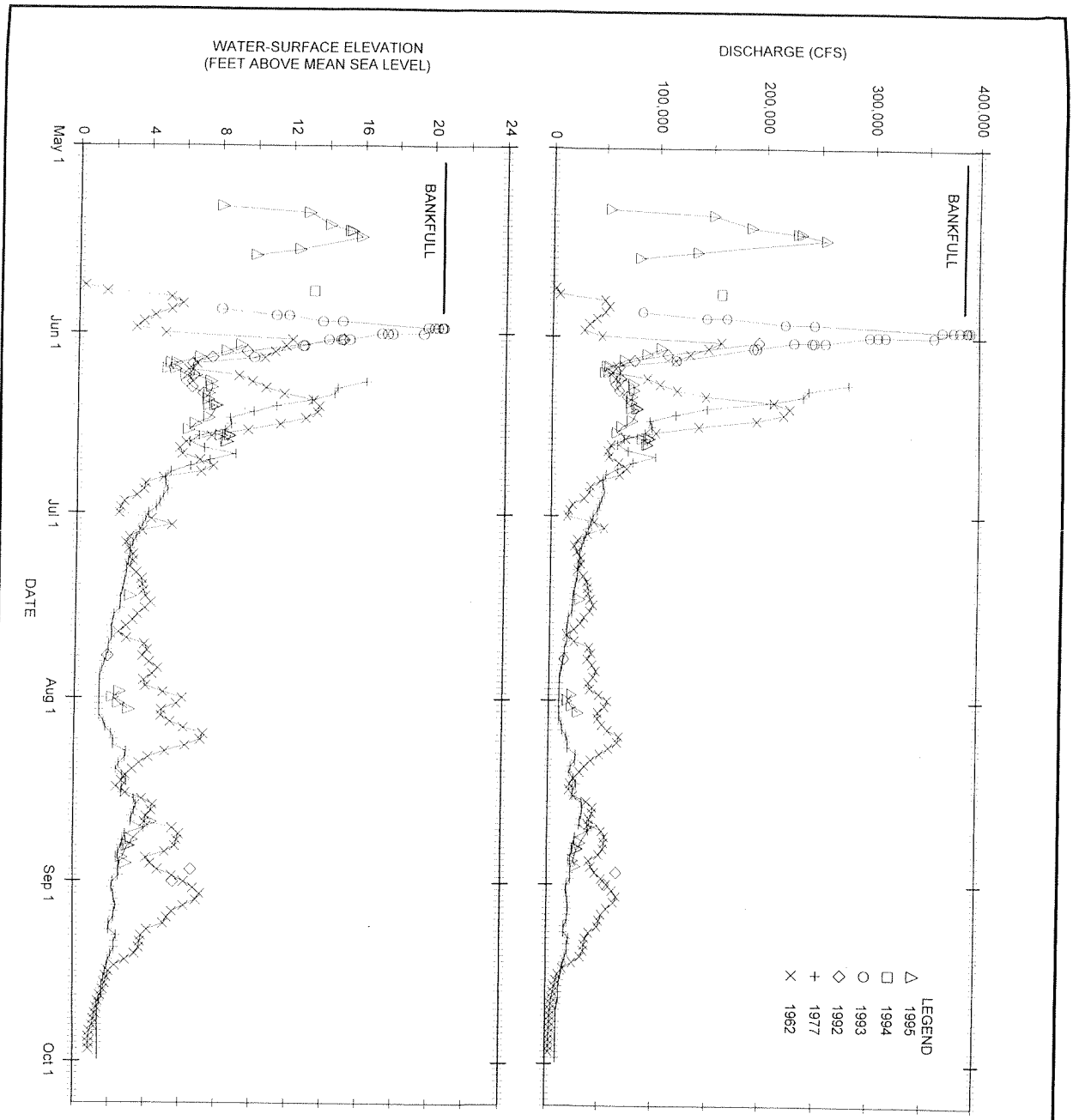
^g Based on data collected near Nuiqsut (Walker 1974).

^h Data from Arnborg et al. (1966).

FLOW DISTRIBUTION

The 1995 peak discharge at Cross Section E20.56 (Cross Section 14) was estimated to be 144,000 cfs (Table 1-2), or approximately 62% of the peak flow (233,000 cfs) at the head of the delta. Assuming the downstream attenuation of the peak discharge was small between E27.09 and E20.56, the peak discharge at the upstream end of the Nechelik Channel was approximately 38% of the peak discharge at the head of the delta (i.e. 89,000 cfs). The peak discharge at Cross Section N7.46 (Cross Section 12; 18.5 mi downstream from E27.09) was approximately 37,000 cfs, suggesting that the peak was attenuated in the Nechelik Channel. Arnborg et al. (1966) estimated the flow at high stages to be distributed as approximately 80% of the total discharge in the East Channel and its distributaries, and 20% in the Nechelik Channel. The proportion of the total flow in the East and Nechelik channels may vary annually and with stage. It may depend in part on the location of open water, the percentage of ice cover, and the presence and location of ice jams.

The peak spring-breakup discharge for the Colville River typically occurs sometime between mid-May and mid-June (Table 1-2). Generally, the main channel is free of ice within a few days before or after the peak discharge. In both 1994 and 1995, however, the ice did not clear the main channel for approximately 2 weeks after the peak discharge. Sub-freezing temperatures, which reduced the amount of meltwater available for runoff, occurred near the date of peak discharge in both of these years. Hydrographs of the available discharge and water-surface elevation data for the head of the delta are presented in Figure 1-1. The discharge data presented in Figure 1-1 were collected in the vicinity of E27.09 and are summarized in Appendix B.



- NOTES:
1. DATA WERE OBTAINED AT A LOCATION ONE MILE DOWNSTREAM FROM THE ITKLIK RIVER.
 2. ELEVATIONS ARE BASED ON USCGS MONUMENT "RIVER" AT AN ELEVATION OF 41.99 FEET.
 3. 1992-1995 DISCHARGES ARE BASED ON WATER SURFACE ELEVATION MEASUREMENTS AND THE RATING CURVE IN FIGURE 3-1 OF THIS REPORT.
 4. 1977 DISCHARGES ARE MEAN DAILY DISCHARGES OBTAINED FROM USGS WATER RESOURCE DATA (USGS, 1978). 1977 WATER SURFACE ELEVATIONS ARE BASED ON THE USGS MEAN DAILY DISCHARGES AND THE RATING CURVE IN FIGURE 3-1 OF THIS REPORT.
 5. 1962 DATA WERE BASED ON THE HYDROGRAPH AND RATING CURVE IN ARNBORG ET AL. (1966).

ARCO Alaska, Inc.
 COLVILLE GEOMORPHOLOGY
 AND HYDROLOGY

Figure 1-1: Water Surface Elevation And
 Discharge Data For The Head
 Of The Colville River Delta

SHANNON & WILSON, INC.
 TECHNICAL AND ENVIRONMENTAL CONSULTANTS

Date: 13 Feb 1996 File: FIG1-1.DRW

PART 2. CHANNEL GEOMETRY AND BED MATERIAL

by Scott R. Ray and James W. Aldrich

BACKGROUND

This section provides data on channel geometry (cross sections and thalweg profiles) and bed material (size and gradation). The channel cross sections are used in the hydraulic analyses to estimate water-surface elevations and velocities at discharges of a specified magnitude. The cross-section and thalweg data also are used in assessing the potential for barges to haul equipment to the Alpine Development (see Part 7). Data on bed material size and gradation are used in estimating the depth of riverbed scour (see Part 13). This section summarizes the available data.

METHODS

CHANNEL CROSS SECTIONS

Numerous cross sections were measured for this study. There were three levels of effort used in measuring the cross sections, which resulted in three levels of relative measurement accuracy. The methods used in measuring the cross sections are described below.

The highest level of measurement accuracy was used at cross sections where discharge measurements were made. The portion of each cross section located below the water surface was measured by recording the elevation of the water surface and measuring the depth with a sounding reel and a 75-lb weight. During the measurement, the boat operator kept the boat on the cross section by lining it up with two rows of flags on each shore. The location of the boat along the cross section was determined by measuring the angle between the boat and a TBM on the river bank, from the river bank. The angle was measured with a theodolite from a location at a known distance from the cross section. The portion of each cross section above the water surface was measured with an automatic level and was tied to TBMs that were established at each end of the cross section. The TBMs were tied to the USCGS monument "River" with an highly accurate

Differential Global Positioning System (DGPS; see Part 12).

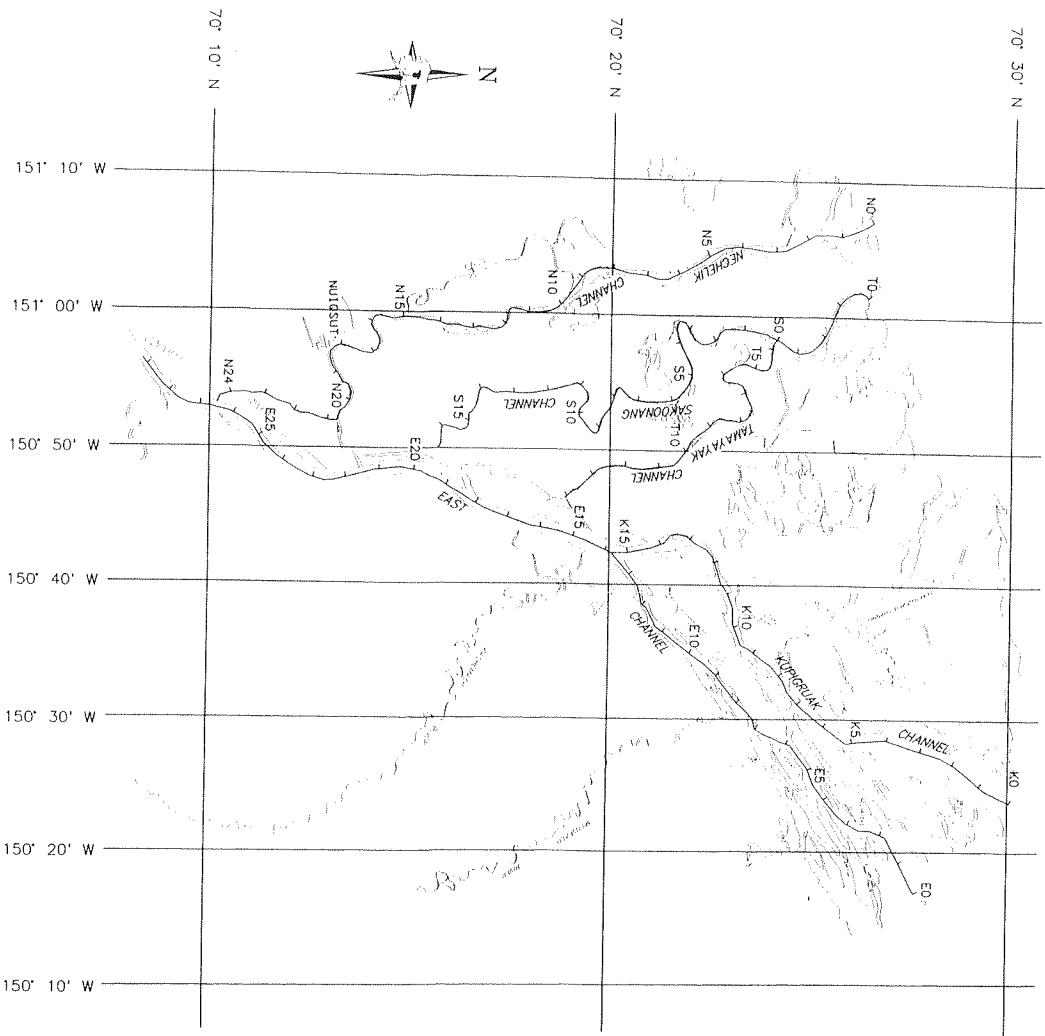
A moderate level of accuracy was obtained with the use of a DGPS and a fathometer. The portion of each cross section located above the water surface was measured with an automatic level and was tied to TBMs that were established at each end of the cross section. These TBMs were not tied to a common datum but were left so that they might be tied to a common datum at a later date. The portion of each cross section located below the water surface was measured by recording the elevation of the water surface and determining the depth with a Lowrance Model X25 fathometer (accurate within approximately 5%). The position of the boat was determined with a Trimble Pro XL DGPS (typical horizontal error less than 16 ft).

The lowest level of accuracy was obtained with the use of a GPS and a fathometer. The cross section above the water surface was not surveyed, and TBMs were not set. The cross section below the water surface was estimated by measuring the depth with the Lowrance Model X25 fathometer. The position of the boat was estimated with a Garmin 45 GPS (typical horizontal error less than 328 ft).

Each cross section is identified by a letter-number designation. The letter prefix represents the channel in which the cross section is located. The East Channel is represented by "E," the Kupigruak Channel is represented by "K," the Nechelik Channel is represented by "N," the Sakoonang Channel is represented by "S," and the Tamayayak Channel is represented by "T." The number suffix represents the distance in river miles upstream from the mouth of the channel (Figure 2-1). For example, Cross Section E16.32 is a cross section on the East Channel located 16.32 river miles upstream from the mouth.

THALWEG PROFILES

Channel thalweg profiles were measured in both June and August 1995. The water-surface elevation at Cross Section E27.09 (Cross Section 6) was recorded at the start of the thalweg measurements. In June, the profiles were measured with a Garmin 45 GPS and a Lowrance Model X25 fathometer. The profile was measured starting at the upstream end of the channel to be measured. We traversed



NOTES FOR FIGURES 2-2 TO 2-12:

1. ELEVATIONS ARE BASED ON THE NATIONAL GEODETIC VERTICAL DATUM OF 1929 (NGVD 29). HORIZONTAL COORDINATES ARE BASED ON THE 1927 NORTH AMERICAN DATUM (NAD 27).
2. THE CROSS SECTIONS ARE NAMED BASED ON RIVER MILES FROM THE MOUTH OF THE CHANNEL. FOR EXAMPLE, THE DESIGNATION E7.00 REFERS TO A CROSS SECTION ON THE EAST CHANNEL LOCATED 7.00 MILES FROM THE MOUTH OF THE EAST CHANNEL. THE MILEAGE ALONG EACH CHANNEL IS SHOWN ON THE LOCATION MAP ON THIS SHEET.
3. IN PREVIOUS REPORTS, CROSS SECTION E16.32 WAS REFERRED TO AS CROSS SECTION 10; CROSS SECTION E20.56 WAS REFERRED TO AS CROSS SECTION 14; CROSS SECTION E27.09 WAS REFERRED TO AS CROSS SECTION 6; CROSS SECTION N7.46 WAS REFERRED TO AS CROSS SECTION 12; CROSS SECTION S9.60 WAS REFERRED TO AS CROSS SECTION 11; AND CROSS SECTION T12.62 WAS REFERRED TO AS CROSS SECTION 13.
4. THE THALWEG IS THE LINE FOLLOWING THE DEEPEST PART OF A RIVER CHANNEL.
5. THE EAST CHANNEL THALWEG WAS MEASURED ON 17 JUNE AND 25 AUGUST 1996. DISCHARGE AT THE HEAD OF THE DELTA (E27.09) AT THE START OF THE MEASUREMENTS WERE APPROXIMATELY 62,000 AND 32,000 CFS, RESPECTIVELY. THE NECHELEK CHANNEL THALWEG WAS MEASURED ON 18 JUNE 1995. THE DISCHARGE AT THE HEAD OF THE DELTA (E27.09) WAS APPROXIMATELY 87,000 CFS.
6. HORIZONTAL LOCATIONS ALONG THE THALWEG WERE ESTIMATED WITH A GARMIN MODEL 45 GPS (POSITION ACCURACY WITHIN 328 FEET). DURING THE JUNE 1995 MEASUREMENTS, HORIZONTAL LOCATIONS ALONG THE THALWEG WERE ESTIMATED WITH A TRIMBLE PRO XL DGPS (POSITION ACCURACY WITHIN 16 FEET) DURING THE AUGUST 1995 MEASUREMENTS.
7. VERTICAL MEASUREMENTS ALONG THE THALWEG WERE MADE WITH A LOWRANCE MODEL X25 FATHOMETER (EXPERIENCE INDICATES THAT MEASURED DEPTH IS WITHIN FIVE PERCENT OF ACTUAL DEPTH).
8. ON FIG. 2-9 AND 2-10, THE CROSS SECTION LOCATIONS SHOWN ON THE PROFILES REFER TO THE 25 AUGUST 1995 THALWEG PROFILE.
9. ON FIG. 2-9 AND 2-10, SOME OF THE DIFFERENCES BETWEEN THE TWO THALWEG PROFILES ARE DUE TO THE SLIGHT DIFFERENCES IN THE PATH TRAVELED AND THE NUMBER OF POINTS RECORDED. THE TWO THALWEG PLOTS WERE MATCHED AT DISTANCE OF 90,000 FEET FROM THE BEGINNING OF THE PROFILES. POINTS AT THE SAME LOCATION BEGIN TO DEVIATE FROM EACH OTHER, ON THE PROFILE, AT SIGNIFICANT DISTANCES UPSTREAM AND DOWNSTREAM FROM THE MATCH POINT (I.E. 90,000 FEET).

KEY

- E10.0 RIVER MILES FROM MOUTH OF CHANNEL
- E = EAST CHANNEL
- K = KUYUGRAK CHANNEL
- N = NECHELEK CHANNEL
- S = SAKOOVANG CHANNEL
- T = TAMAYAYAK CHANNEL

ARCO Alaska, Inc.
COLVILLE GEOMORPHOLOGY AND HYDROLOGY

Figure 2-1: Location Map

SHANNON & WILSON, INC.
GEOTECHNICAL AND ENVIRONMENTAL CONSULTING

Date: 01 Jul 1996 File: 2LOCATIO.DWG

the channel, recording the location of the deepest portion of the channel with the GPS. We then traveled downstream along the shore 500–800 ft, turned and crossed the channel, and again recorded the location of the deepest portion of the channel with the GPS. This process continued to the mouth of the channel. The distance along the thalweg is based on the straight-line distance between two adjacent points. The same method was used in August, with the exception that a Trimble Pro XL DGPS was used to mark the location of the deepest portion of the channel.

BED MATERIAL

Samples of bed material were taken at selected cross sections using a pipe dredge and a boat. Grain-size analyses were conducted with the washed-sieve method (ASTM D-422-72).

RESULTS AND DISCUSSION

CHANNEL GEOMETRY

Cross sections that were measured in 1995 at the highest level of accuracy and have elevations based on the USCGS monument "River" are presented in Figures 2–2 through 2–8. Additional cross sections measured on the Nechelik and East channels are presented in Parts 7 and 8 of this report. The station and elevation data for these cross sections are presented in Appendix C. Also presented in Appendix C are cross sections that were measured in 1962 by Walker (1983b) and in 1992 by Jorgenson et al. (1993).

THALWEG PROFILES

Plan and profile views of the East and Nechelik channel thalwegs are presented in Figures 2–9 through 2–12. The East Channel thalweg was measured on 17 June and 25 August. The Nechelik Channel thalweg was measured on 18 June. Water-surface elevations at Cross Section E27.09, at the time the thalweg measurements were started on 17 June, 18 June, and 25 August, were 6.3, 8.1 and 3.3 ft, respectively. The data used to create the figures are presented in Appendix D.

Most of the differences between the two profiles of the East Channel (Figures 2–9 and 2–10)

probably can be attributed to two uncontrolled variables. Some of the differences are due to slight differences in the path traveled by the boat and the number of points measured. The two thalweg profiles were matched at a point 90,000 ft from the start of the August profile and begin to deviate from each other at significant distances up- or downstream from the match point. Because the thalweg profile depths were measured from the water surface, the difference in the water-surface elevation at the time of the measurements also accounts for some of the differences in the profiles. Differences in the thalweg depth that are due to differences in the water-surface elevation are greater at the head of the delta than at the ocean.

During normal summer flows, the width of the water surface in the East Channel is on the order of 2000 ft (Figures 2–2 to 2–5). Thalweg depths generally are between 15 and 25 ft (Figures 2–9 and 2–10), but maximal depths of greater than 40 ft were measured at a few locations.

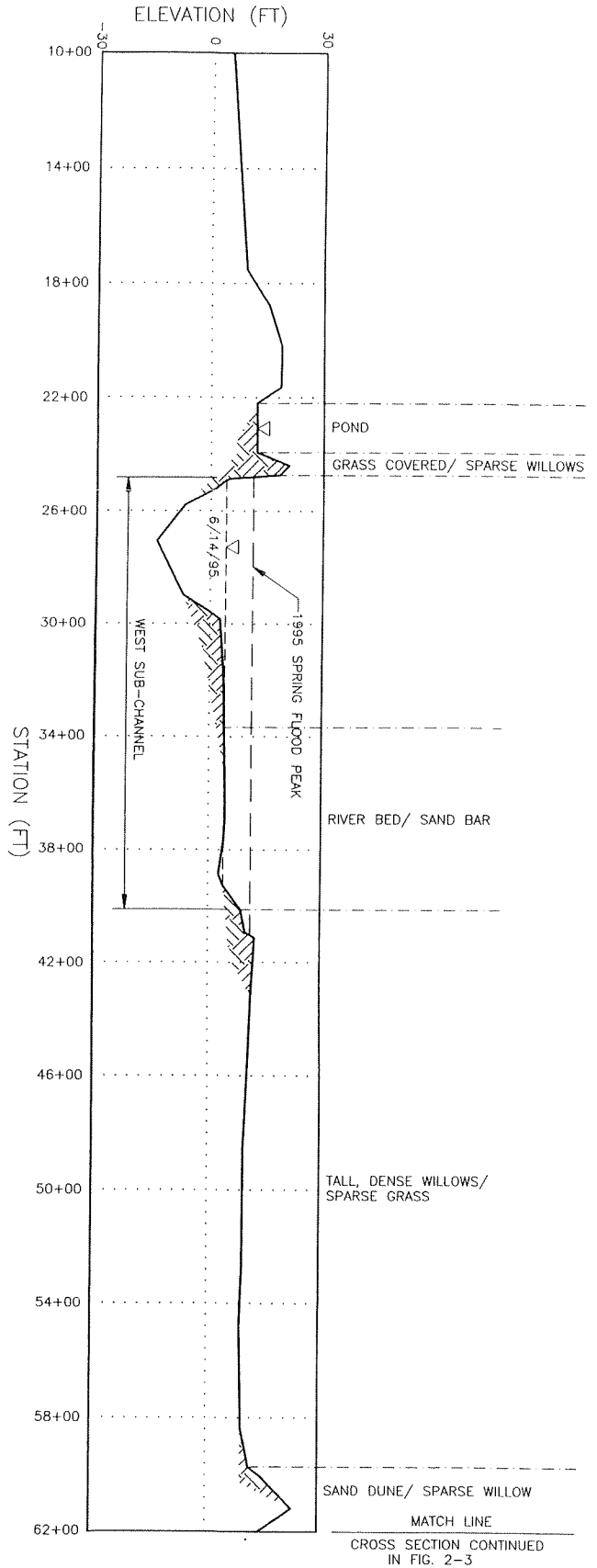
The width of the water surface in the Nechelik Channel during normal summer flows is on the order of 600 ft (Figure 2–6). Thalweg depths generally are between 10 and 30 ft (Figures 2–11 and 2–12), but maximal depths are on the order of 40 ft.

The width of the water surface in the Sagoonang and Tamayayak channels generally are on the order of 100 and 300 ft, respectively (Figures 2–7 and 2–8). The maximal depths of these two channels are on the order of 30 ft.

BED MATERIAL

Based on the median grain size (D_{50}) of all the samples collected in the East Channel, the bed material generally can be classified as fine sand (Table 2–1). The median bed material size of the samples collected near the thalweg of the East Channel, however, are classified as fine gravel (Table 2–1). The D_{50} of the bed material samples collected in both the Tamayayak and Sagoonang channels are fine sands (Table 2–1). A sandbar in the Nechelik Channel at N7.46 (Cross Section 12) also is fine sand. The material from the deep part of the Nechelik Channel at N7.46, however, is silt (Table 2–1). Additional data on bed material from Walker (1983b), Jorgenson et al. (1993), and the 1995 gradation curves are presented in Appendix E.

CROSS SECTION E16.32 (EAST CHANNEL)

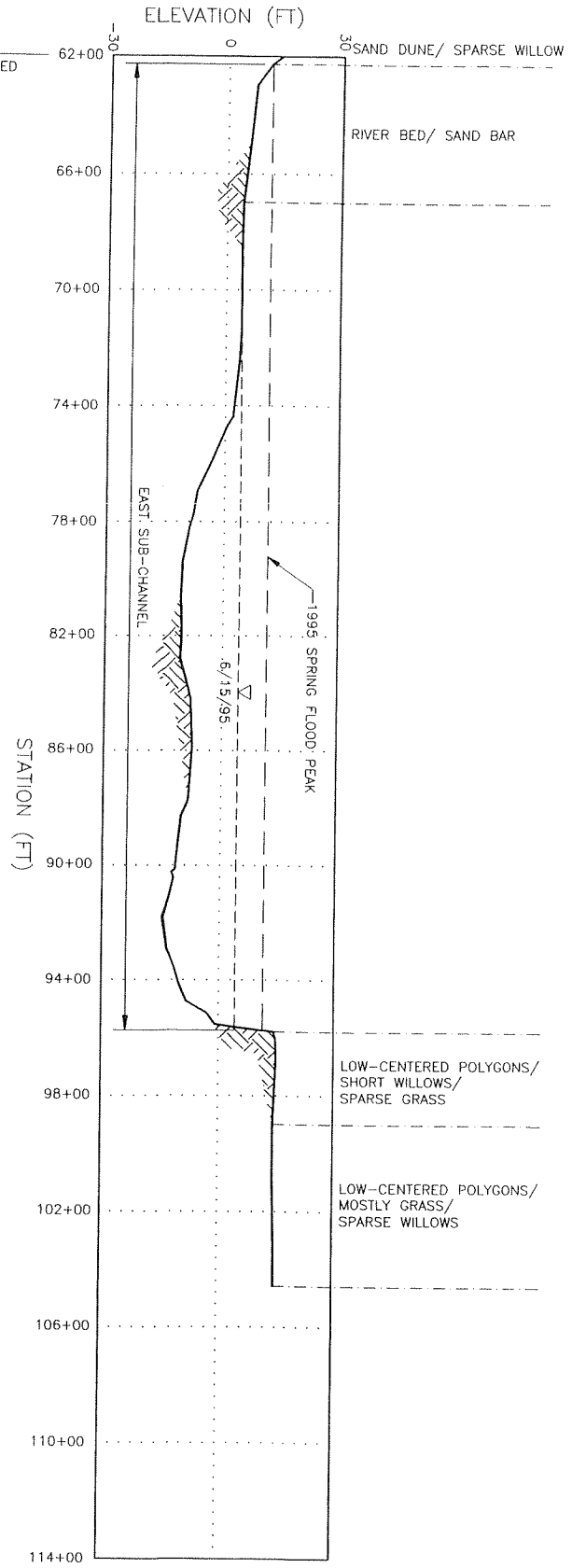


- NOTES:
1. THE 1995 SPRING FLOOD PEAK PROBABLY OCCURRED ON 16 MAY 1995 AND HAD AN ELEVATION OF 11.43 FEET BETWEEN STATION 24+78 AND STATION 41+05, AND HAD AN ELEVATION OF 11.35 FEET BETWEEN STATION 62+27 AND STATION 95+75.
 2. ELEVATIONS ARE BASED ON USCGS MONUMENT RIVER, ELEVATION= 41.99 FEET.
 3. IN PREVIOUS REPORTS, CROSS SECTION E16.32 HAS BEEN REFERRED TO AS CROSS SECTION 10. DUE TO THE INCREASED NUMBER OF CROSS SECTIONS BEING USED ON THE PROJECT, THE CROSS SECTION DESIGNATION WAS CHANGED SUCH THAT IT IS NOW BASED ON RIVER MILES, MEASURED FROM THE MOUTH, THEODOLITE, AND SOUNDING WEIGHT.
 4. THE GROUND PROFILE WAS OBTAINED USING LEVEL, THEODOLITE, AND SOUNDING WEIGHT.
 5. CROSS SECTION IS LOOKING DOWNSTREAM.


ARCO Alaska, Inc.	
COVILLE GEOMORPHOLOGY AND HYDROLOGY	
Figure 2-2: West Side Of Cross Section E16.32	
SHANNON & WILSON, INC. TECHNICAL AND ENVIRONMENTAL CONSULTANTS	
Date: 13 Feb 1996	File: 2XSEC2.2.DWG

CROSS SECTION CONTINUED IN FIG. 2-3

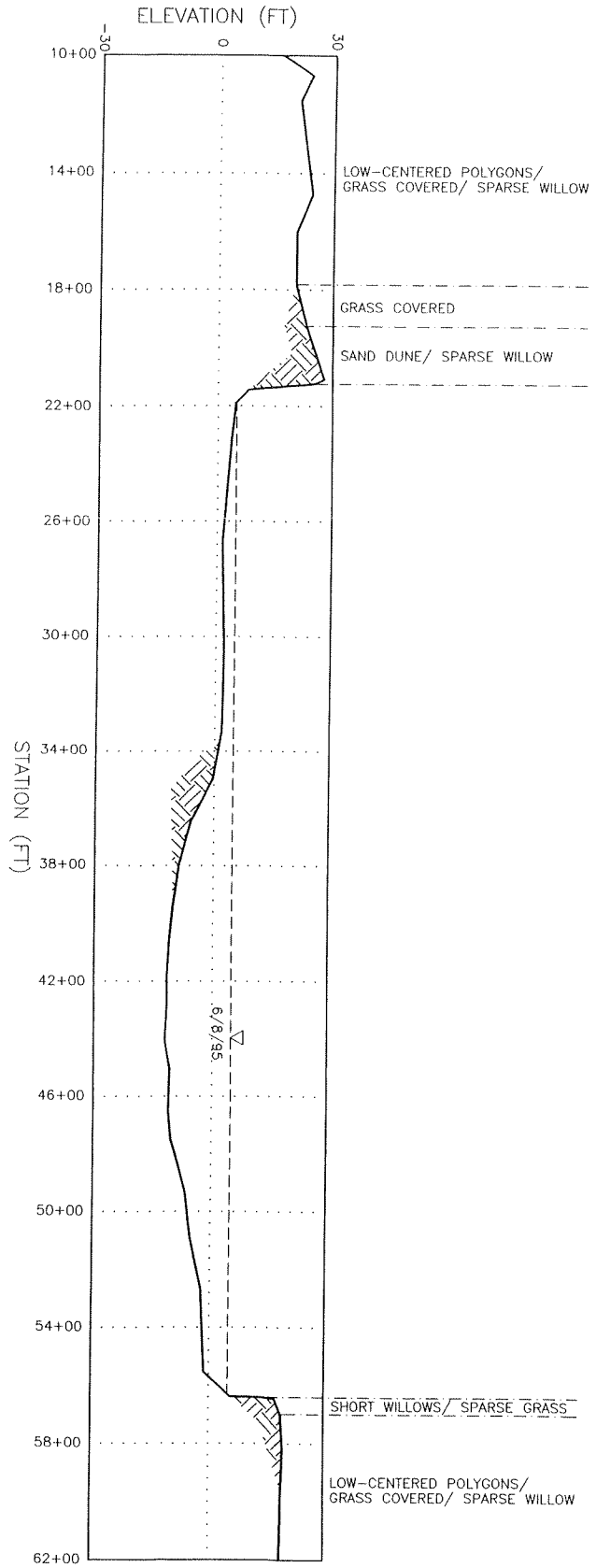
CROSS SECTION E16.32 (EAST CHANNEL)



NOTE:
1. SEE FIG. 2-2 FOR NOTES.

ARCO Alaska, Inc.	
COLVILLE GEOMORPHOLOGY AND HYDROLOGY	
Figure 2-3: East Side Of Cross Section E16.32	
 SHANNON & WILSON, INC. <small>GEOTECHNICAL AND ENVIRONMENTAL CONSULTANTS</small>	
Date: 13 Feb 1996	File: 2XSEC2_3.DWG

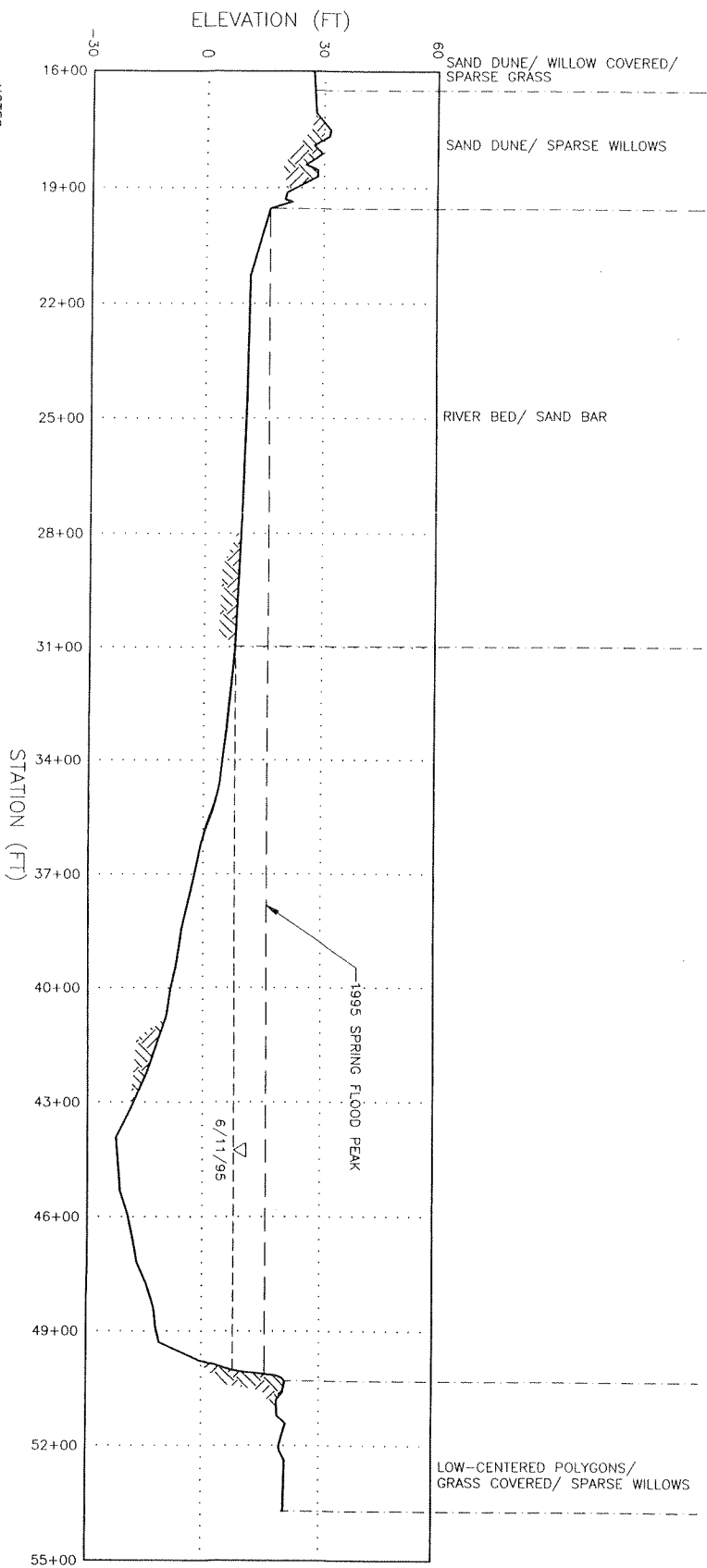
CROSS SECTION E20.56 (EAST CHANNEL)



- NOTES:
1. THE 1995 SPRING FLOOD PEAK ELEVATION WAS NOT MEASURED AT THIS CROSS SECTION.
 2. ELEVATIONS ARE BASED ON USCGS MONUMENT "RIVER", ELEVATION = 41.99 FEET.
 3. IN PREVIOUS REPORTS, CROSS SECTION E20.56 HAS BEEN REFERRED TO AS CROSS SECTION 14. DUE TO THE INCREASED NUMBER OF CROSS SECTIONS BEING USED ON THE PROJECT, THE CROSS SECTION DESIGNATION WAS CHANGED SUCH THAT IT IS NOW BASED ON RIVER MILES, MEASURED FROM THE MOUTH.
 4. THE GROUND PROFILE WAS OBTAINED WITH LEVEL, THEODOLITE, AND SOUNDING WEIGHT.
 5. CROSS SECTION IS LOOKING DOWNSTREAM.

ARCO Alaska, Inc.	
COLVILLE GEOMORPHOLOGY AND HYDROLOGY	
Figure 2-4: Cross Section E20.56	
SHANNON & WILSON, INC. <small>ENGINEERING AND ENVIRONMENTAL CONSULTANTS</small>	
Date: 13 Feb 1996	File: 2XSE02_4DWG

CROSS SECTION E27.09 (MAIN CHANNEL)

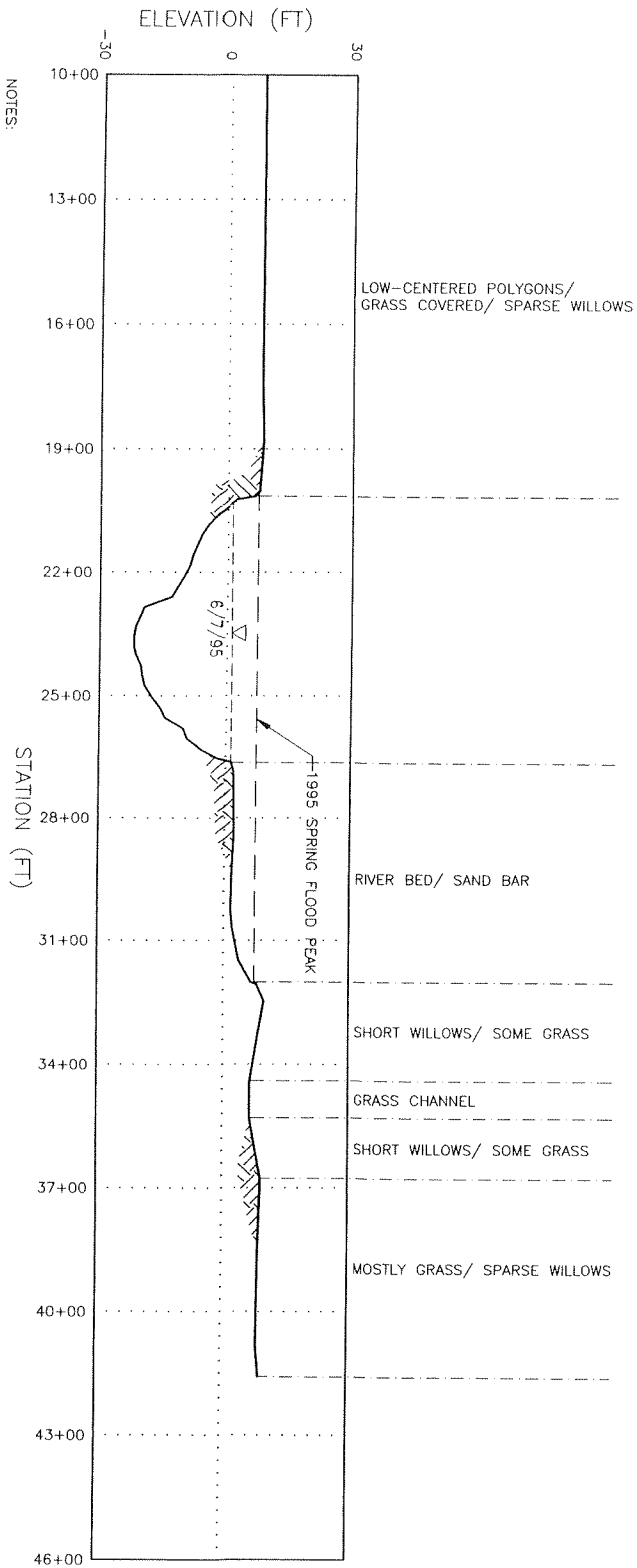


NOTES:

1. THE 1995 SPRING FLOOD PEAK PROBABLY OCCURRED ON 16 MAY 1995 AND HAD AN ELEVATION OF 15.87 FEET.
2. ELEVATIONS ARE BASED ON USGS MONUMENT "RIVER", ELEVATION= 41.99 FEET.
3. IN PREVIOUS REPORTS, CROSS SECTION E27.09 HAS BEEN REFERRED TO AS CROSS SECTION 6. DUE TO THE INCREASED NUMBER OF CROSS SECTIONS BEING USED ON THE PROJECT, THE CROSS SECTION DESIGNATION WAS CHANGED SUCH THAT IT IS NOW BASED ON RIVER MILES, MEASURED FROM THE MOUTH.
4. THE GROUND PROFILE WAS OBTAINED WITH LEVEL, THEODOLITE, AND SOUNDING WEIGHT.
5. CROSS SECTION IS LOOKING DOWNSTREAM.

ARCO Alaska, Inc.	
COLVILLE GEOMORPHOLOGY AND HYDROLOGY	
Figure 2-5: Cross Section E27.09	
<small>DESIGN AND DRAWING BY: J. W. SHANNON</small>	
Date: 13 Feb 1996	File: 2XSEC2_5.DWG

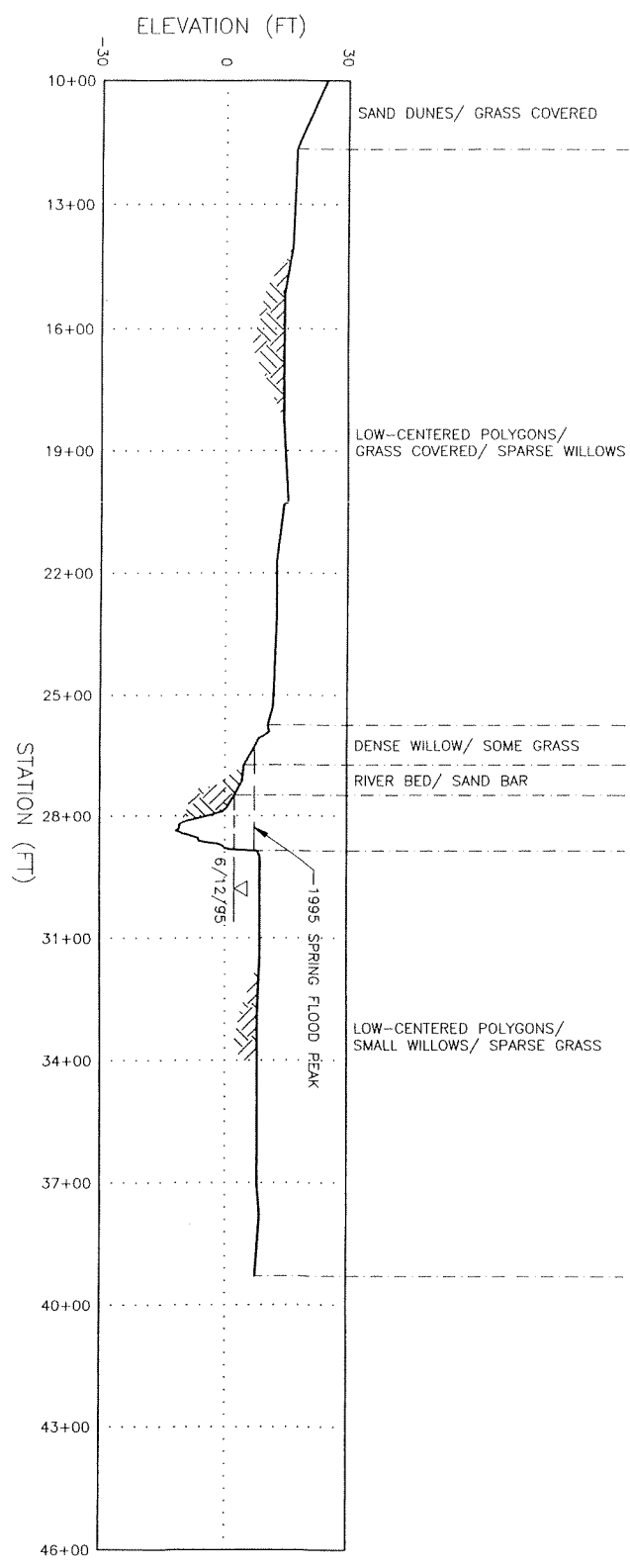
CROSS SECTION N7.46 (NECHELIK CHANNEL)



- NOTES:
1. THE 1995 SPRING FLOOD PEAK PROBABLY OCCURRED ON 16 MAY 1995 AND HAD AN ELEVATION OF 7.3 FEET.
 2. ELEVATIONS ARE BASED ON USGS MONUMENT "RIVER", ELEVATION= 41.99 FEET.
 3. IN PREVIOUS REPORTS, CROSS SECTION N7.46 HAS BEEN REFERRED TO AS CROSS SECTION 12. DUE TO THE INCREASED NUMBER OF CROSS SECTIONS BEING USED ON THE PROJECT, THE CROSS SECTION DESIGNATION WAS CHANGED SUCH THAT IT IS NOW BASED ON RIVER MILES, MEASURED FROM THE MOUTH.
 4. THE GROUND PROFILE WAS OBTAINED WITH LEVEL, THEODOLITE, AND SOUNDING WEIGHT.
 5. CROSS SECTION IS LOOKING DOWNSTREAM.

<p>ARCO Alaska, Inc.</p> <p>COLVILLE GEOMORPHOLOGY AND HYDROLOGY</p>	
<p>Figure 2-6: Cross Section N7.46</p>	
<p>SHANNON & WILSON, INC. <small>GEOTECHNICAL AND ENVIRONMENTAL CONSULTANTS</small></p>	
Date: 13 Feb 1996	File: 2XSEC2_6.DWG

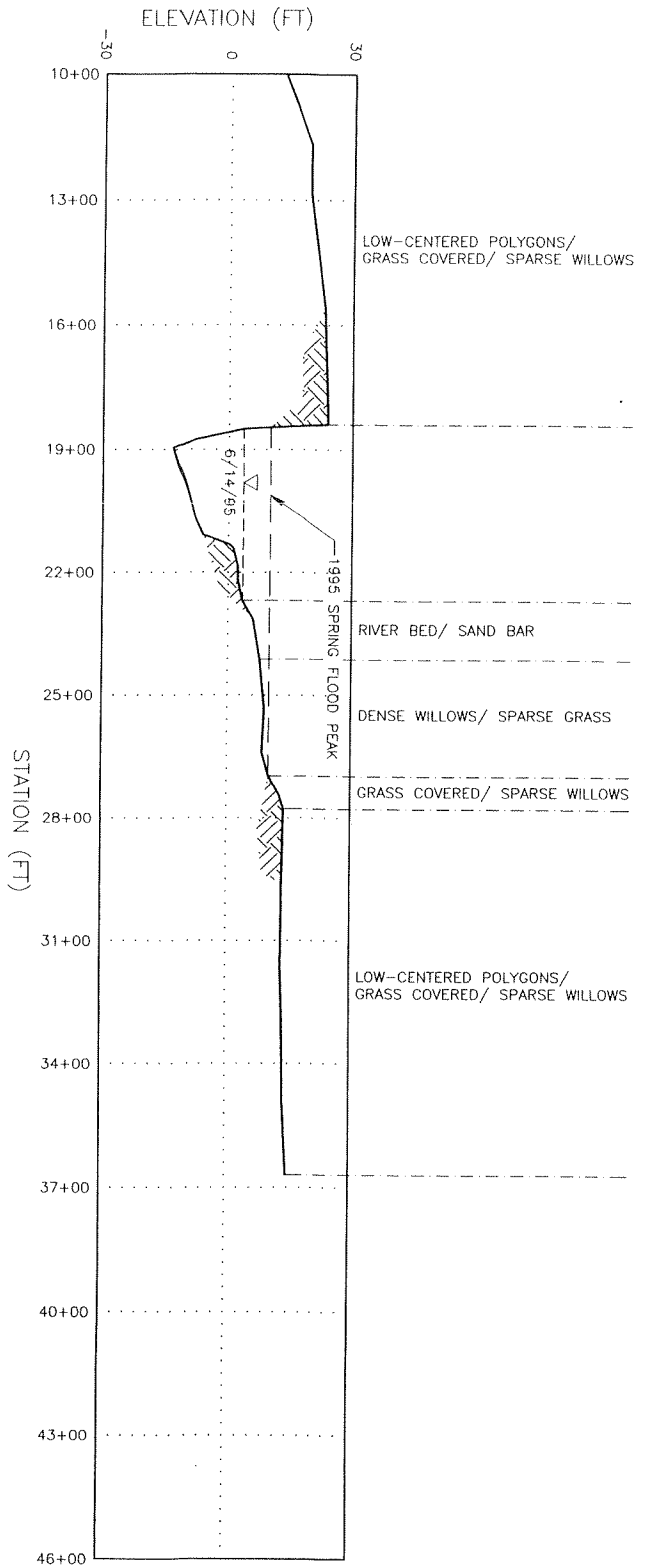
CROSS SECTION S9.80 (SAKOOKANG CHANNEL)



- NOTES:
1. THE 1995 SPRING FLOOD PEAK PROBABLY OCCURRED ON 16 MAY 1995 AND HAD AN ELEVATION OF 7.15 FEET.
 2. ELEVATIONS ARE BASED ON USGS MONUMENT "RIVER", ELEVATION= 41.99 FEET.
 3. IN PREVIOUS REPORTS, CROSS SECTION S9.80 HAS BEEN REFERRED TO AS CROSS SECTION 11. DUE TO THE INCREASED NUMBER OF CROSS SECTIONS BEING USED ON THE PROJECT, THE CROSS SECTION DESIGNATION WAS CHANGED SUCH THAT IT IS NOW BASED ON RIVER MILES, MEASURED FROM THE MOUTH.
 4. GROUND PROFILE WAS OBTAINED WITH LEVEL, TAGLINE, AND SOUNDING WEIGHT.
 5. CROSS SECTION IS LOOKING DOWNSTREAM.

<p>ARCO Alaska, Inc.</p> <p>COLVILLE GEOMORPHOLOGY AND HYDROLOGY</p>	
<p>Figure 2-7: Cross Section S9.80</p>	
<p>SHANNON & WILSON, INC. <small>GEOTECHNICAL AND ENVIRONMENTAL CONSULTANTS</small></p>	
<p>Date: 13 Feb 1996</p>	<p>File: 2XSEC2-7.DWG</p>

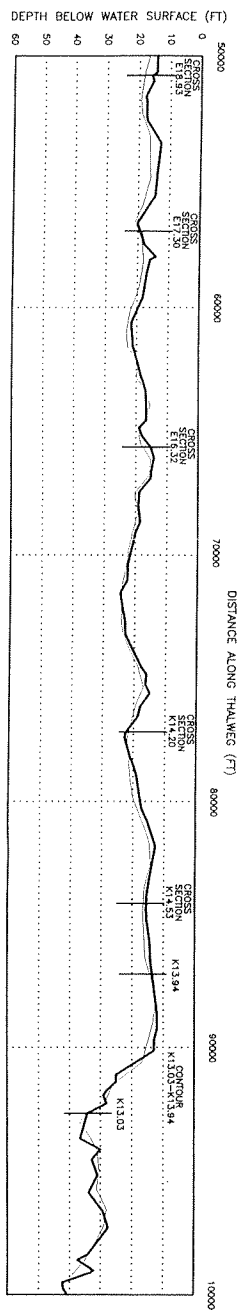
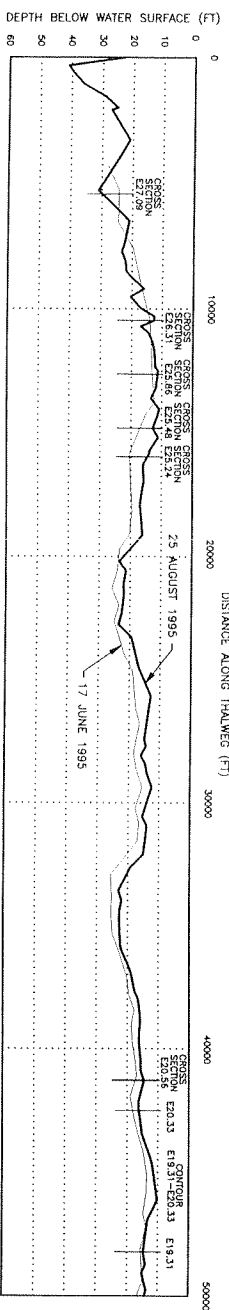
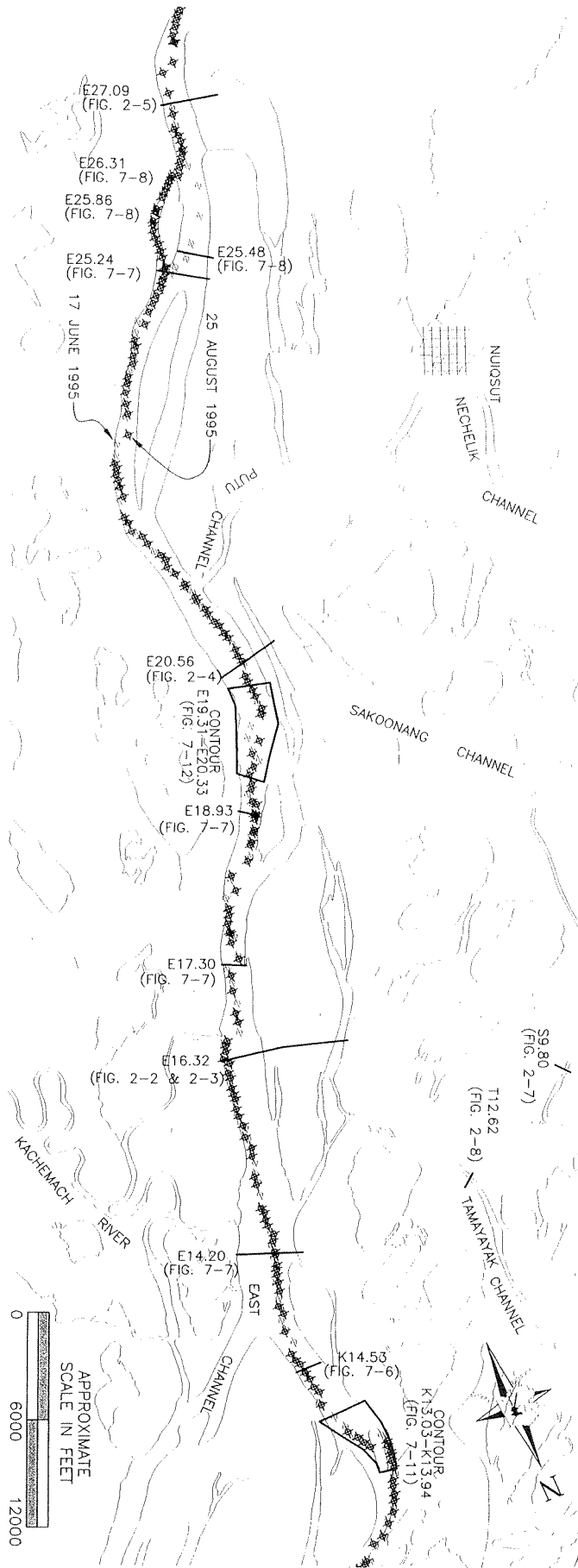
CROSS SECTION T12.62 (TAMAYAYAK CHANNEL)



NOTES:

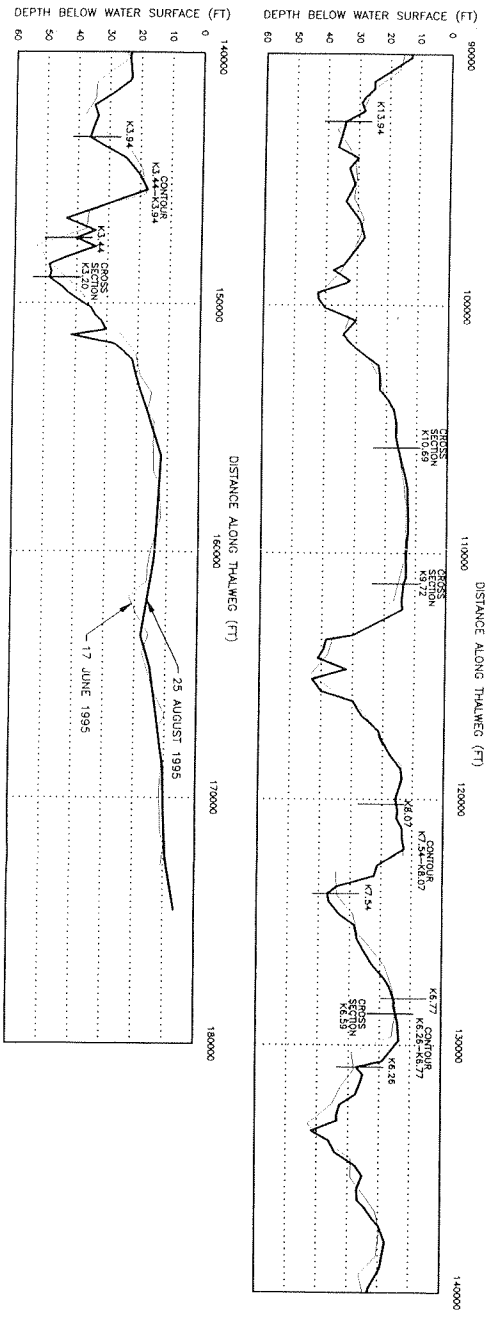
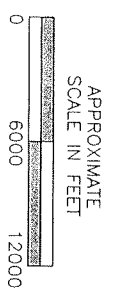
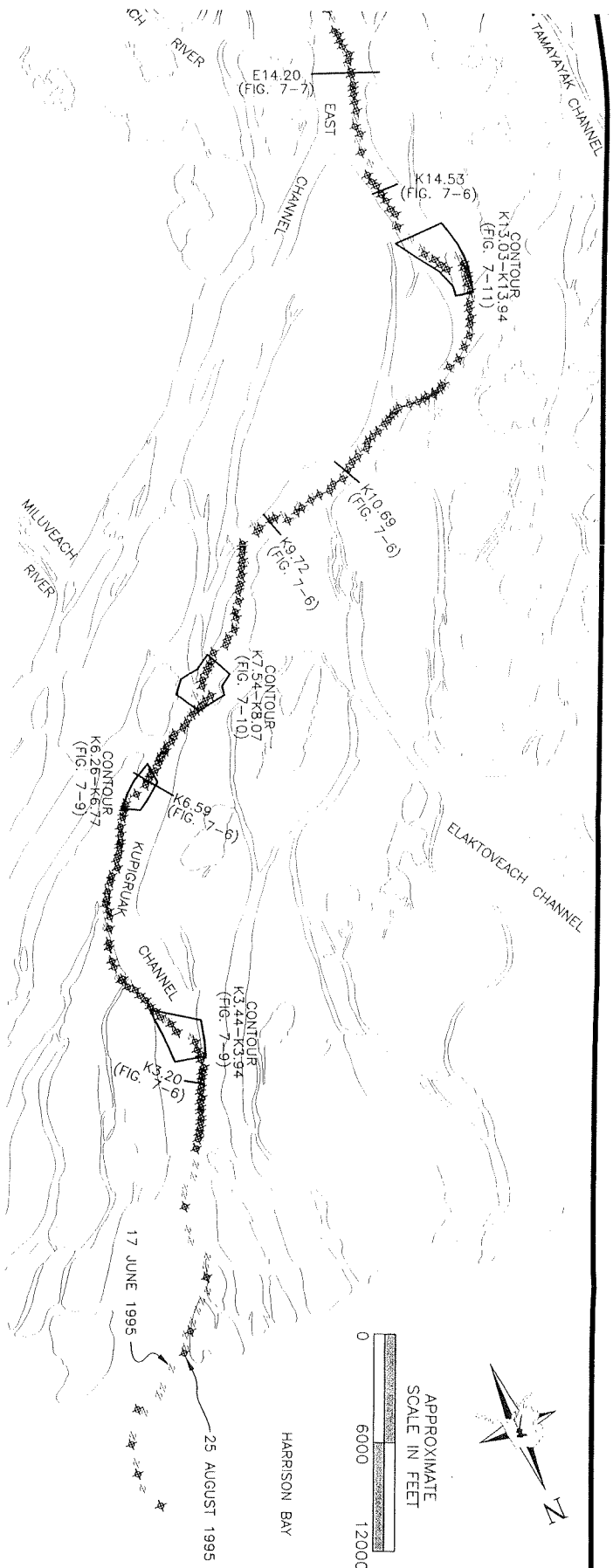
1. THE 1995 SPRING FLOOD PEAK PROBABLY OCCURRED ON 16 MAY 1995 AND HAD AN ELEVATION OF 9.99 FEET.
2. ELEVATIONS ARE BASED ON USCGS MONUMENT "RIVER", ELEVATION= 41.99 FEET.
3. IN PREVIOUS REPORTS, CROSS SECTION T12.62 HAS BEEN REFERRED TO AS CROSS SECTION 13. DUE TO THE INCREASED NUMBER OF CROSS SECTIONS BEING USED ON THIS PROJECT, THE CROSS SECTION DESIGNATION WAS CHANGED SUCH THAT IT IS NOW BASED ON RIVER MILES, MEASURED FROM THE MOUTH.
4. HORIZONTAL POSITION MEASURED WITH LEVEL AND STADIA ROD.
5. SHALLOW DEPTHS WERE MEASURED WITH LEVEL AND ROD. THE DEEPER DEPTHS WERE MEASURED WITH FAHOMETER.
6. CROSS SECTION IS LOOKING DOWNSTREAM.

ARCO Alaska, Inc.	
COLVILLE GEOMORPHOLOGY AND HYDROLOGY	
Figure 2-8: Cross Section T12.62	
SHANNON & WILSON, INC.	
<small>CONSULTING ENGINEERS AND ENVIRONMENTAL SCIENTISTS</small>	
Date: 13 Feb 1996	File: 2XSEC2_8.DWG



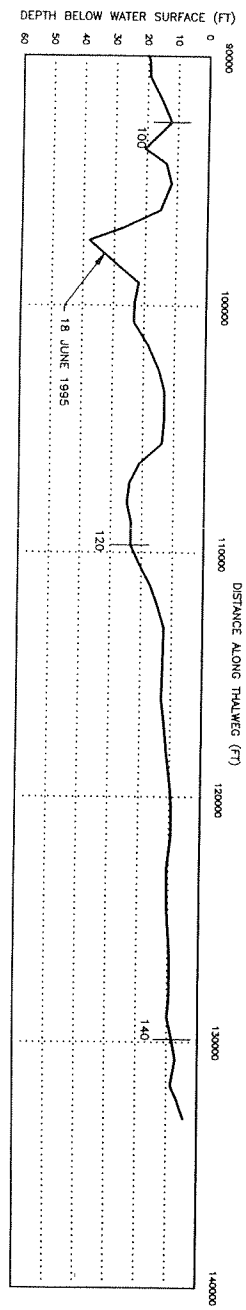
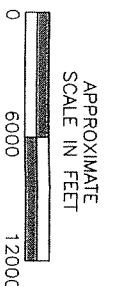
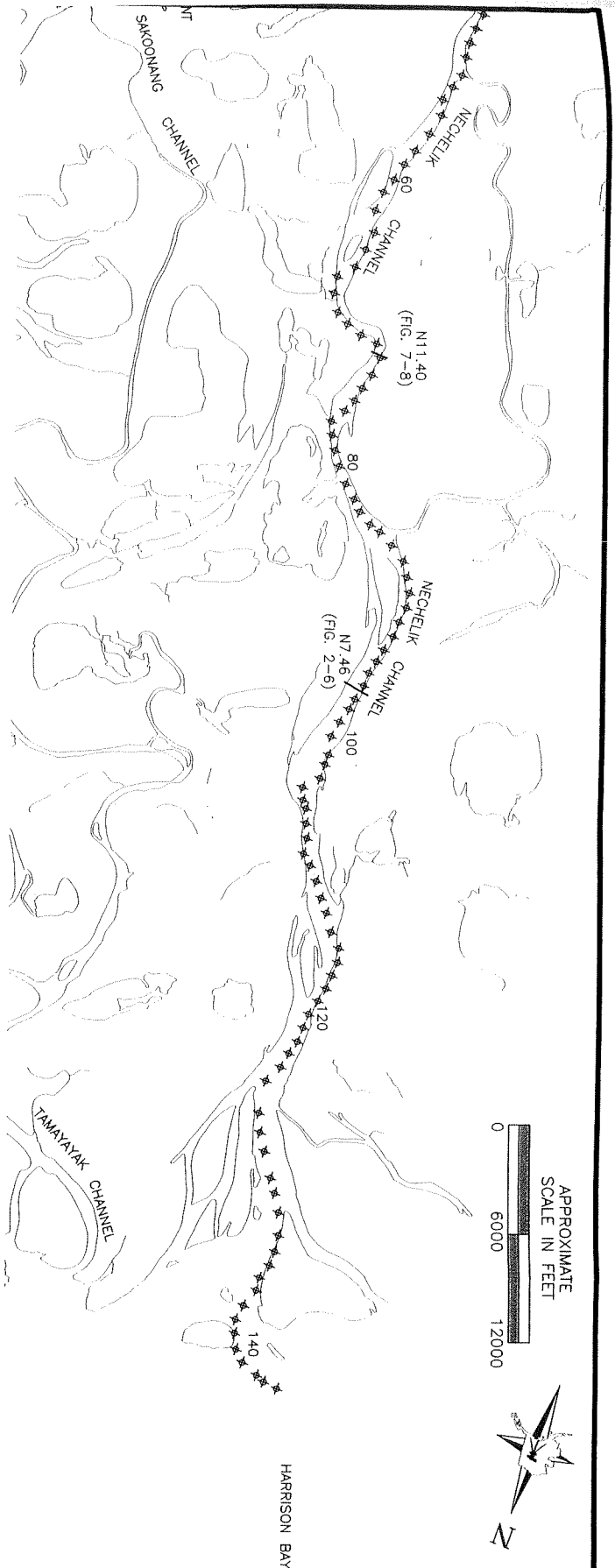
SEE FIG. 2-1 FOR APPLICABLE NOTES

ARCO Alaska, Inc.	
COVILLE GEOMORPHOLOGY AND HYDROLOGY	
Figure 2-9: Upper East Channel Thidweg Profile	
SHANNON & WILSON, INC.	
GEOTECHNICAL AND ENVIRONMENTAL CONSULTANTS	
Date: 13 Feb 1996	File: 2PLANZ_9.DWG



SEE FIG. 2-1 FOR APPLICABLE NOTES

ARCO Alaska, Inc.	
COLVILLE GEOMORPHOLOGY AND HYDROLOGY	
Figure 2-10: Lower East Channel Thlweg Profile	
SHANNON & WILSON, INC. GEOTECHNICAL AND DEVELOPMENTAL CONSULTANTS	
Date: 13 Feb 1996	File: 2PLAN210.DWG



SEE FIG. 2-1 FOR APPLICABLE NOTES

ARCO Alaska, Inc.	
COLVILLE GEOMORPHOLOGY AND HYDROLOGY	
Figure 2-12: Lower Nechelik Channel Thalweg Profile	
SHANNON & WILSON, INC. ENGINEERING AND ENVIRONMENTAL CONSULTANTS	
Date: 13 Feb 1996	File: ZPLAN212.DWG



Table 2-1. Bed-material data collected in June 1995, Colville River Delta.

Cross Section ^a	Distance From Bank ^b (ft)	D ₂₅ ^c (mm)	D ₅₀ ^d (mm)	D ₇₅ ^e (mm)	Percentage >0.062 mm ^f (by weight)
E20.56	R 940	0.36	5.36	7.14	100
E20.56	R 1540	0.22	0.30	0.37	99
E20.56	R 2140	0.12	0.17	0.21	96
E16.32	L 367	0.18	0.22	0.28	99
E16.32	R 608	0.43	5.01	6.91	99
E16.32	R 1458	0.22	0.29	0.36	99
N7.46	L 335	<0.075	<0.075	<0.075	7
N7.46	L 821	0.16	0.22	0.30	91
S9.80	R 56	0.17	0.21	0.28	98
T12.62	L 136	0.15	0.19	0.23	96

^a Location designation is based on river miles measured upstream from the mouth. The letter prefix indicates the channel as follows: E=East; K=Kupigruak; N=Nechelik; S=Sakoonang; T=Tamayayak.

^b Distance from the bank is approximate. L indicates distance from the left bank (looking downstream), and R indicates distance from the right bank.

^c D₂₅ refers to the particle size at which 25% of the material (by weight) is finer.

^d D₅₀ refers to the particle size at which 50% of the material (by weight) is finer.

^e D₇₅ refers to the particle size at which 75% of the material (by weight) is finer.

^f A particle size of 0.062 mm represents the division between silt and sand-sized particles according to the Massachusetts Institute of Technology soil classification system.

PART 3. STAGE-DISCHARGE-VELOCITY RELATIONSHIPS

by Scott R. Ray and James W. Aldrich

BACKGROUND

This section provides information on stage- and velocity-discharge relationships at three locations: Cross Section E27.09 (Cross Section 6), Cross Section E20.56 (Cross Section 14), and Cross Section N7.46 (Cross Section 12). These relationships are useful in estimating the magnitude of discharge and velocity at elevations below bankfull. This information is useful in preparing preliminary estimates of scour associated with conceptual pipeline river-crossing designs and for oil-spill contingency planning. This information also provides a portion of the information that will be required to estimate water-surface elevations during a design flood. The cross sections, however, do not extend far enough inland from the river banks to estimate the water-surface elevation associated with flows significantly above bankfull.

METHODS

DISCHARGE MEASUREMENTS

One discharge measurement was made at Cross Sections E27.09, E20.56, and N7.46 to assist in estimating the stage-discharge and velocity-discharge relationships. The discharge measurements were made from a boat with a Price AA current meter suspended with a 75-lb weight. The horizontal position of the boat was estimated by measuring the angle between a TBM on the river bank and the boat with a theodolite. The water-surface elevation was recorded periodically during these discharge measurements, and a weighted-average water-surface elevation was used as the water-surface elevation corresponding to the discharge measurement. The water-surface slope was measured immediately after the discharge measurement.

The hydraulic roughness at the time of the discharge measurement was calculated based on normal depth, from the measured discharge and the associated water-surface elevation and slope

(Henderson 1966). For computational purposes, the main channel within each cross section was divided into subsections based on the criteria presented by Davidian (1984).

STAGE-DISCHARGE CURVES

Cross Section E27.09

Stage- and velocity-discharge relationships were developed for the Colville River at the head of the delta (E27.09) after the 1992 field season. The stage-discharge relationship was developed using data from 1962, 1977, and 1992 (Jorgenson et al. 1993), and a datum based on USCGS monument "Kinik." The upper end of the relationship was revised in 1993 (Jorgenson et al. 1994a), with data collected in 1993. No flow measurements were made in 1994. Significant revisions of the curve were made after the 1995 field season. These changes are discussed below.

The first change in the relationship involves the change in datum. In 1995, all the major cross sections were tied to a common datum with a precise DGPS (see Part 12). This new datum is based on USCGS monument "River." Elevations at E27.09 are 1.46 ft higher when referenced to the new datum. Thus, the entire stage-discharge curve was shifted up by 1.46 ft. For example, a discharge that had a water-surface elevation of 18.80 ft on the 1993 stage-discharge curve now has a water-surface elevation of 20.26 ft.

The second change involved the reevaluation of the 1962 data. During a site visit with H. J. Walker in August 1995, it was discovered that the 1962 measurements were made at essentially the same location where our measurements were made in 1992–1995. It also was determined that the elevations associated with the 1962 measurements were tied to USCGS monument "Kinik," the same datum used for the cross section survey in 1992. Use of the same measurement location and the same USCGS datum allowed the 1962 data to be plotted directly on the new curve, after adjusting the elevations to the new datum (USCGS monument "River"). Using the 1962 data in this way suggested that the lower end of the 1993 stage-discharge curve might be in error, in that the elevation associated with a discharge of 10,000 cfs might be several feet

higher than was suggested by the 1993 stage-discharge curve alone.

A reevaluation of the 1977 data produced the final change of the stage-discharge curve. The U. S. Geological Survey (USGS) did not tie its water-surface elevation measurements to a known datum. Instead, they were tied to an assumed datum. Although the water-surface elevation was measured whenever a discharge measurement was made, there was no way (in 1992) to tie the USGS measurements to a known datum. Therefore, the water-surface elevations associated with the 1977 discharge measurements were computed from the cross-sectional area of flow and the 1992 cross section survey. This computation assumed that all of the USGS discharge measurements were made at a location with the same cross-sectional geometry as that in Cross Section E27.09.

The reevaluation of the 1962 measurements, when combined with our measurements in 1993 and 1995, gave us considerable confidence in the middle part of the stage-discharge curve. Plotting of the two highest 1977 USGS discharge measurements (232,000 and 212,000 cfs), which were similar to measured discharges in 1962 and 1993, allowed us to develop an adjustment factor between the USGS assumed datum and the USCGS monument "River" datum. Water-surface elevations for the five other USGS discharge measurements were converted to the USCGS monument "River" datum and plotted. These USGS discharge measurements were similar to those of the other data; thus, a best-fit curve was plotted through all of the data (1962, 1977, 1992, 1993, and 1995). This new curve is referred to as the January 1996 stage-discharge curve.

Cross Section E20.56

The stage-discharge curve for Cross Section E20.56 is based on normal depth computations, water-surface slope measurements, and one discharge measurement. To assign hydraulic roughness values to this cross section, the main channel was divided into two subsections, following the guidelines presented by Davidian (1984).

A relationship describing hydraulic roughness in sandbed rivers, based on bedform, bed material size, and stream power (Simons, Lion & Associates 1982) was used to estimate hydraulic roughness within each subsection of the main channel. An

iterative process was used to determine the bedform likely to exist under the estimated hydraulic conditions at each water-surface elevation. Once the most likely bedform had been estimated, the discharge was estimated based on the likely range in roughness associated with the selected bedform. Thus, at each water-surface elevation, two discharges were estimated, based on minimal and maximal likely hydraulic roughness.

The discharge and water-surface slope measurements taken on 8 June 1995 were used to verify the hydraulic roughness estimates for the east and west sides of the channel. Roughness values estimated from discharge measurements were 0.034 and 0.031 for the east and west sides, respectively. Based on the bedform analysis, the bedform on the east side of the channel probably was dunes, which have a hydraulic roughness value of 0.030–0.035. The bedform on the west side of the channel probably was ripples, which have a roughness value of 0.022–0.030. Thus, both the method used to estimate the bedform and the hydraulic roughness associated with the bedform fit the actual discharge measurement data very closely.

When estimating discharge, the water-surface slope was varied with the water surface elevation. A relationship between water-surface elevation and water-surface slope was derived at Cross Section E20.56, from the water-surface slopes observed during spring breakup (measured between E27.09 and E16.32) and summer (measured between E27.09 and E20.56). Only one measured water-surface slope per day was used in the analysis (Appendix B).

Cross Section N7.46

The stage-discharge curve for Cross Section N7.46 is based on normal depth computations, water-surface slope measurements, and one discharge measurement. As at E20.56, this cross section was divided into two subsections (Davidian 1984).

Hydraulic roughness was estimated with the same method as that used at E20.56. Once the most likely bedform had been estimated, the discharge was estimated from the likely range in roughness associated with the selected bedform. Thus, two discharges were estimated at each water-surface

elevation, based on minimal and maximal likely hydraulic roughness.

As at E20.56, the water-surface slope varied with water-surface elevation when estimating discharge. Water-surface slopes at this cross section, however, can be nearly flat. An example is the water-surface slope (0.00001 ft/ft) at the time of the discharge measurement. The TBMs used to measure these slopes are 4872 ft apart. Based on the slope, the difference in the water-surface elevation between the two TBMs was only 0.05 ft. Because waves often are present here, the error in estimating the water-surface elevation at each TBM is on the order of the difference in the water surface elevation between the two TBMs. Thus, the confidence in any one slope measurement was low, particularly at the lower water-surface elevations.

For this reason, it was decided to base the relationship between water-surface elevation and water-surface slope on two points. The first point was derived by taking the average of the water-surface elevations and the water-surface slopes for the two breakup measurements made in May 1995. The average water-surface elevation was 6.92 ft and the average water-surface slope was 0.000095 ft/ft. The second point was derived from the data collected during the discharge measurement. Based on the discharge and the water-surface slope measured, the hydraulic roughness was estimated to be 0.041. However, the relationship developed by Simons, Li & Associates (1982) suggests that the bedform was ripples, which have an average hydraulic roughness of 0.026. Because the water-surface slope has the potential for significant error, it was decided to calculate the slope for the water-surface elevation at the time of the discharge measurement (1.20 ft) and based on a hydraulic roughness of 0.026. The resulting slope was 0.000044 ft/ft. The two water-surface elevations and their corresponding water-surface slopes were plotted, and a line was drawn between the points (Appendix B). The water-surface slope for each water-surface elevation used in the stage-discharge analysis was then estimated using the plot. The stage-discharge curve was not extrapolated below the elevation of the water surface at the time of the discharge measurement, because of the uncertainty of the water-surface slope measurements below this elevation.

VELOCITY-DISCHARGE CURVES

Velocity-discharge curves were estimated for Cross Sections E27.09, E20.46, and N7.46. These curves were derived from the stage-discharge curves and channel cross sections. The average main channel velocity at a given discharge was calculated by dividing the main channel discharge by the cross-sectional area of the main channel flow. The velocities associated with several discharges were estimated and plotted for each cross section.

RESULTS AND DISCUSSION

CROSS SECTION E27.09

The January 1996 stage-discharge curve for Cross Section E27.09 is presented in Figure 3-1. The curve remains unchanged from the 1993 curve (Jorgenson et al. 1994a) in the high-flow region, with most of the change occurring at flows less than 100,000 cfs. The bankfull discharge remains the same as that estimated in 1993 (385,000 cfs; the bankfull elevation is approximately 20.5 ft).

The velocity-discharge curve is presented in Figure 3-2. This curve represents the mean main-channel velocity. In 1993, the ratio between the "maximal average velocity in any vertical" and the mean main-channel velocity was calculated (Jorgenson et al. 1994a). The "average velocity in any vertical" is based on a method of measuring the discharge in which the velocity is estimated at two depths at the same location and averaged to obtain the average velocity at that "vertical." The maximum of all the "average velocity in a vertical" measurements is referred to as the "maximal velocity in any vertical." Based on the 1993 calculation, average main-channel velocities in the velocity-discharge curve can be multiplied by 1.40 (the multiplier ranged between 1.24 and 1.60) to estimate the maximal average velocity at any "vertical" (Jorgenson et al. 1994a). The multiplier for the 1993 discharge measurement was 1.35 (Jorgenson et al. 1994a) and the multiplier for the 1995 measurement was 1.27. Thus, a range of 1.24 to 1.60 still seems reasonable.

CROSS SECTION E20.56

The stage-discharge curve for Cross Section E20.56 is presented in Figure 3-3. The single discharge measurement made in 1995 at this

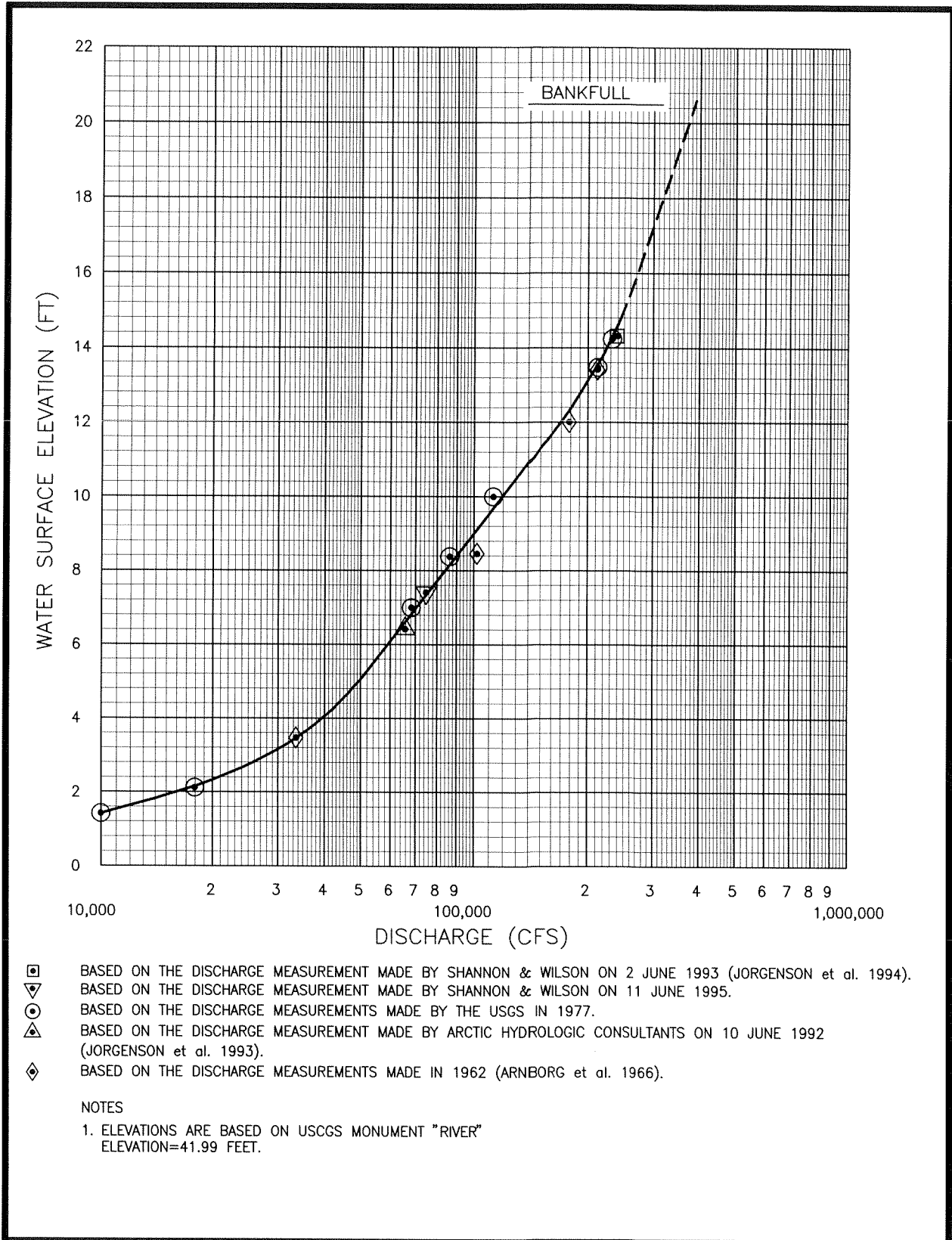


Figure 3-1. Stage-discharge relationship for the Colville River at Cross Section E27.09.

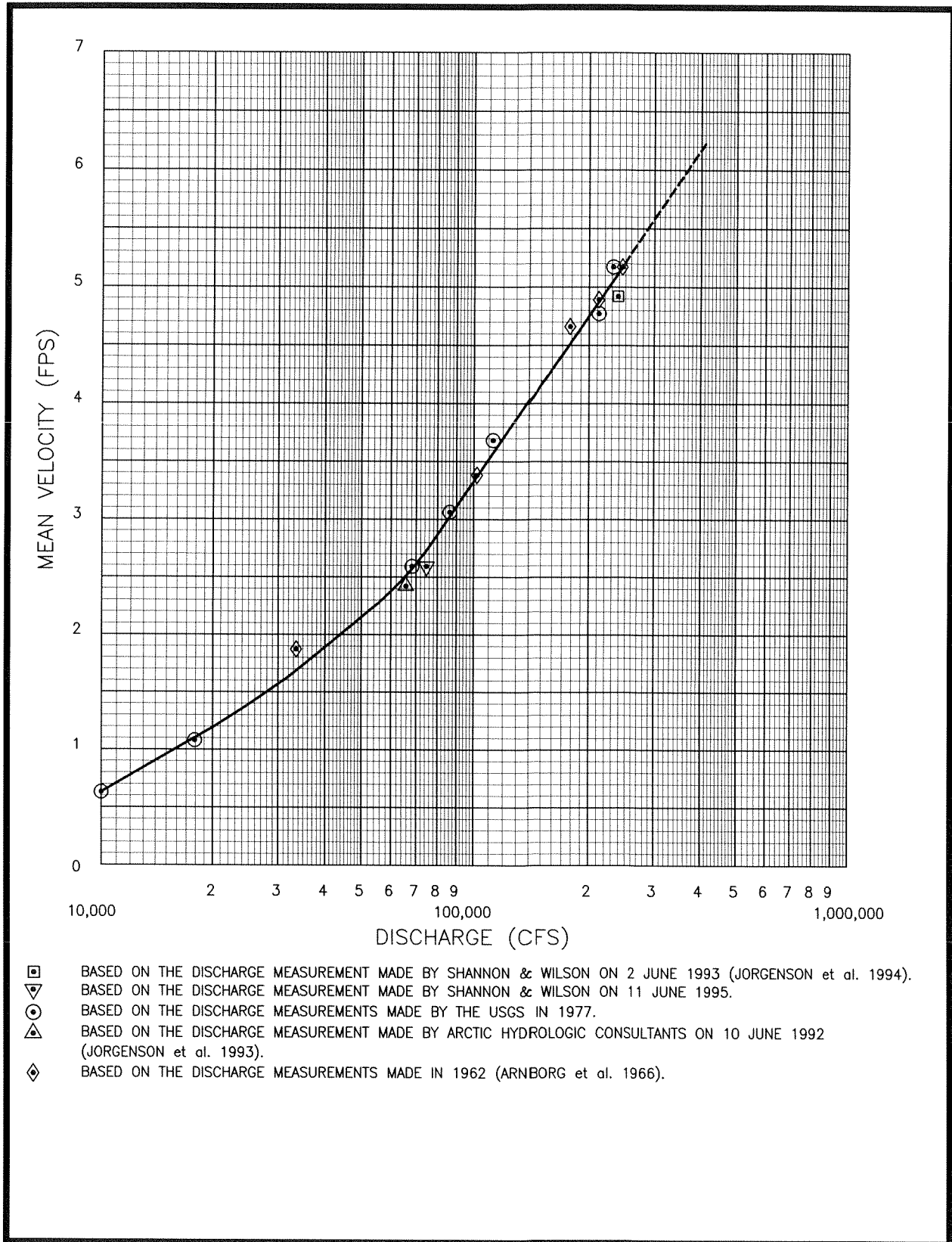


Figure 3-2. Mean main channel velocity-discharge relationship for the Colville River at Cross Section E27.09.

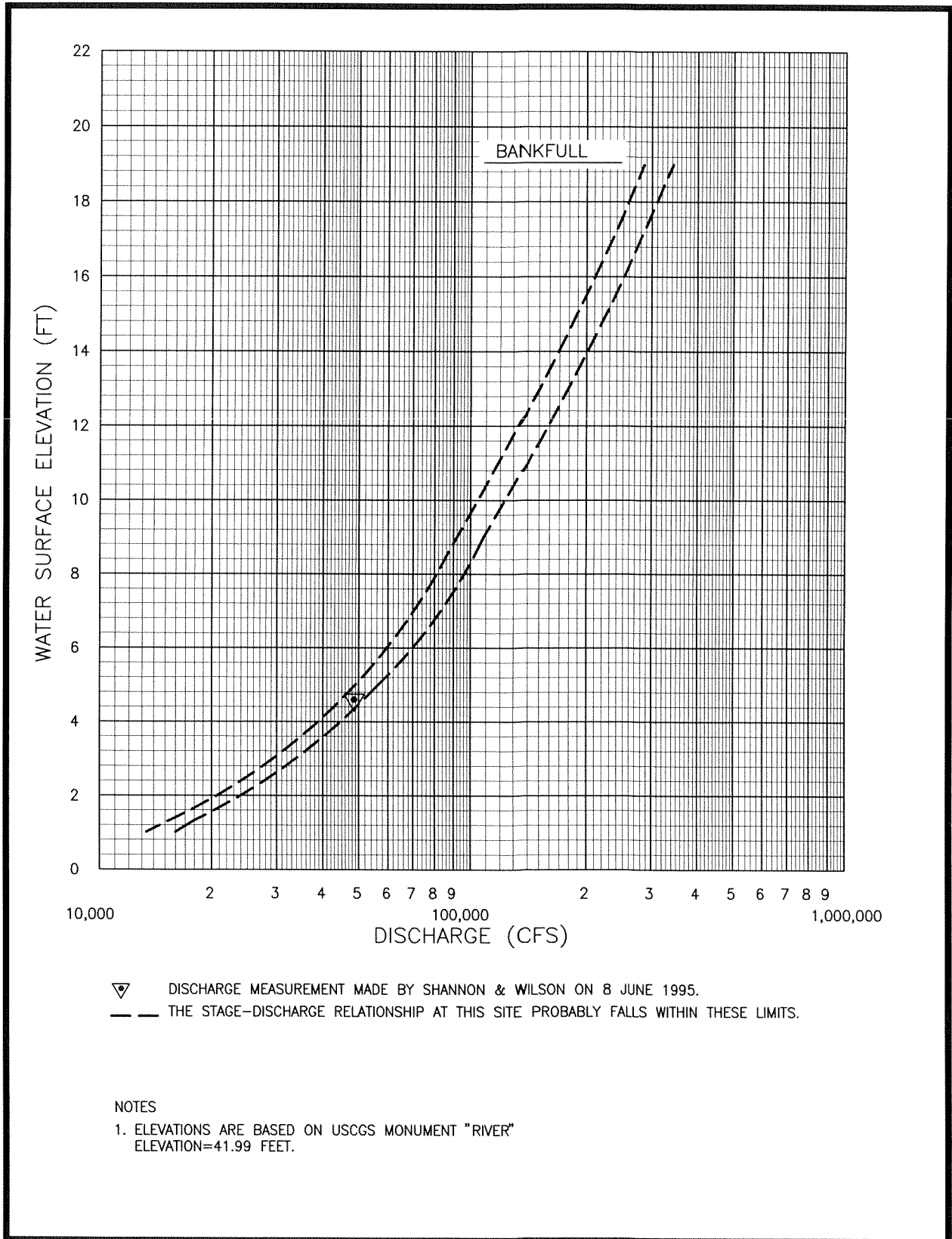


Figure 3-3. Stage-discharge relationship for the Colville River at Cross Section E20.56.

location also is plotted on the curve. The bankfull discharge at a water-surface elevation of about 19 ft is approximately 307,000 cfs. Because there was insufficient information available to estimate the flow conditions at lower flows, the stage-discharge curve is not plotted below a water-surface elevation of 1 ft.

The velocity-discharge curve for Cross Section E.20.56 is presented in Figure 3-4. This curve represents the mean main-channel velocity. During the discharge measurement (48,400 cfs) the maximal average velocity measured at any location within the cross section was 2.10 fps, which is 1.24 times the average main channel velocity of 1.69 fps.

CROSS SECTION N7.46

The stage-discharge curve for Cross Section N7.46 is presented in Figure 3-5. The single discharge measurement made in 1995 also is plotted on the curve. The bankfull discharge at a water-surface elevation of about 8.4 ft is approximately 63,000 cfs. As at Cross Section E20.56, there was insufficient information available to estimate the flow at low water-surface elevations.

The velocity-discharge curve for Cross Section N7.46 is presented in Figure 3-6. This curve represents the mean main-channel velocity. During the discharge measurement (6040 cfs), the maximal average velocity measured at any location within the cross section was 0.87 fps, which is 1.26 times the average main-channel velocity of 0.69 fps.

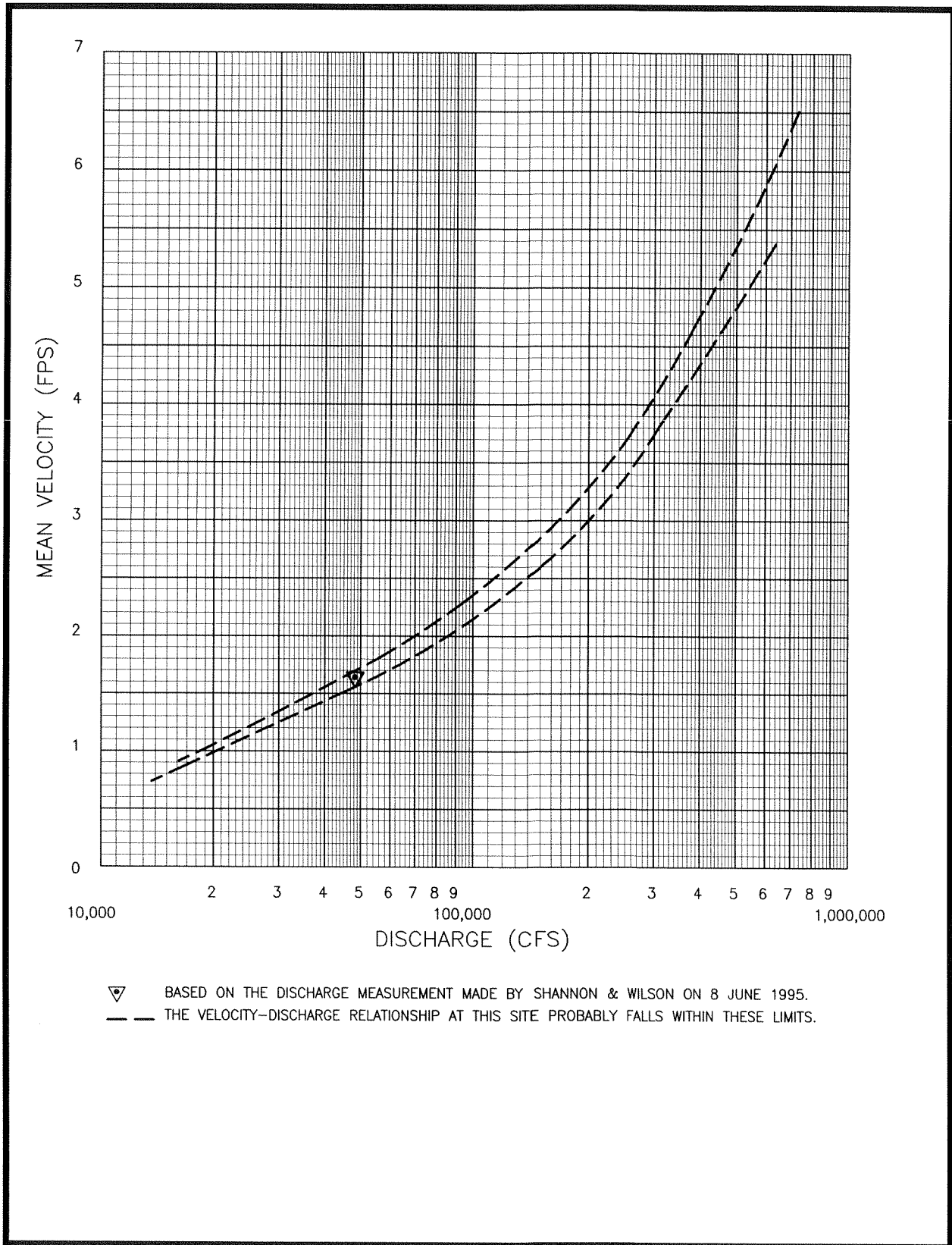


Figure 3-4. Mean main channel velocity-discharge relationship for the Colville River at Cross Section E20.56.

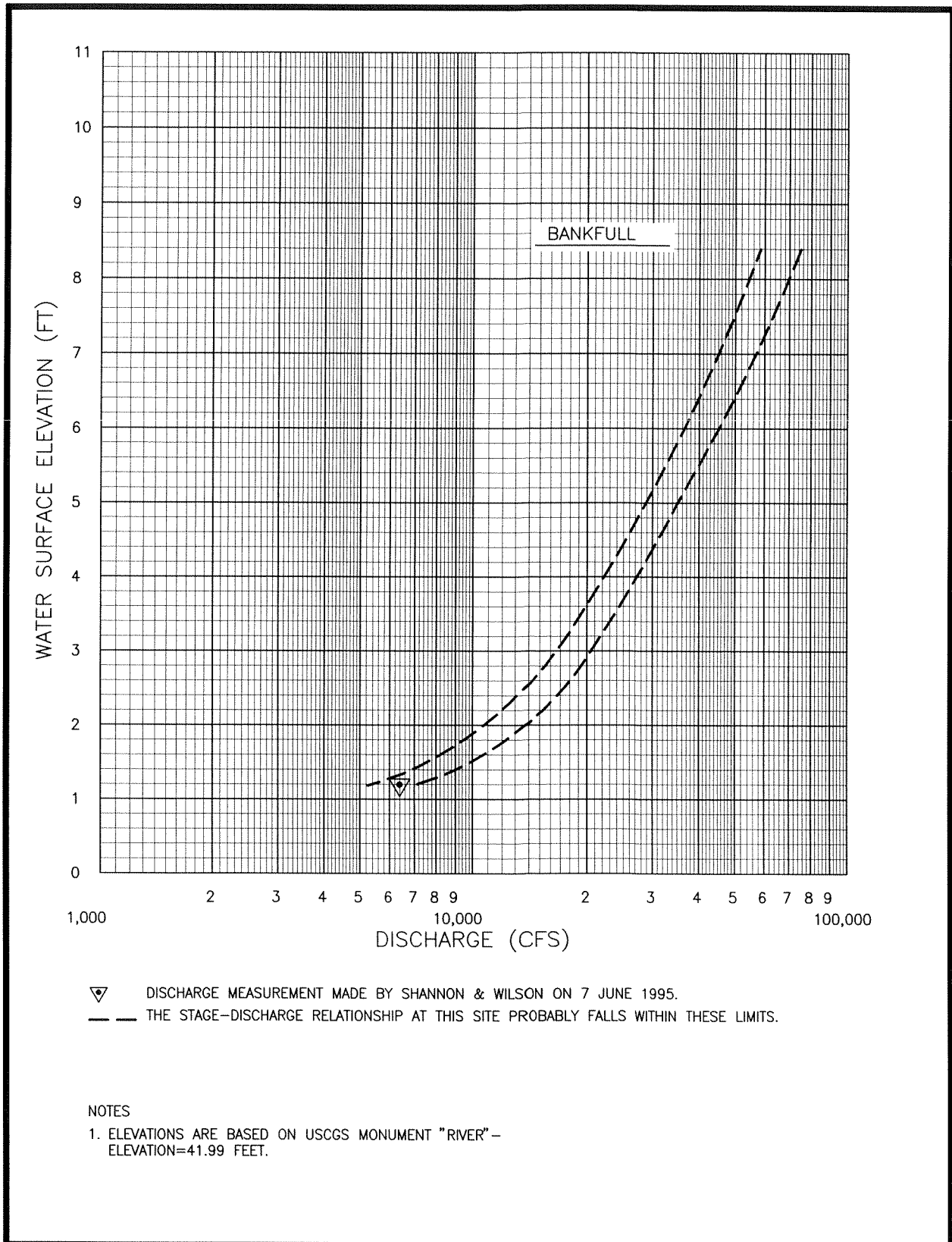


Figure 3-5. Stage-discharge relationship for the Colville River at Cross Section N7.46.

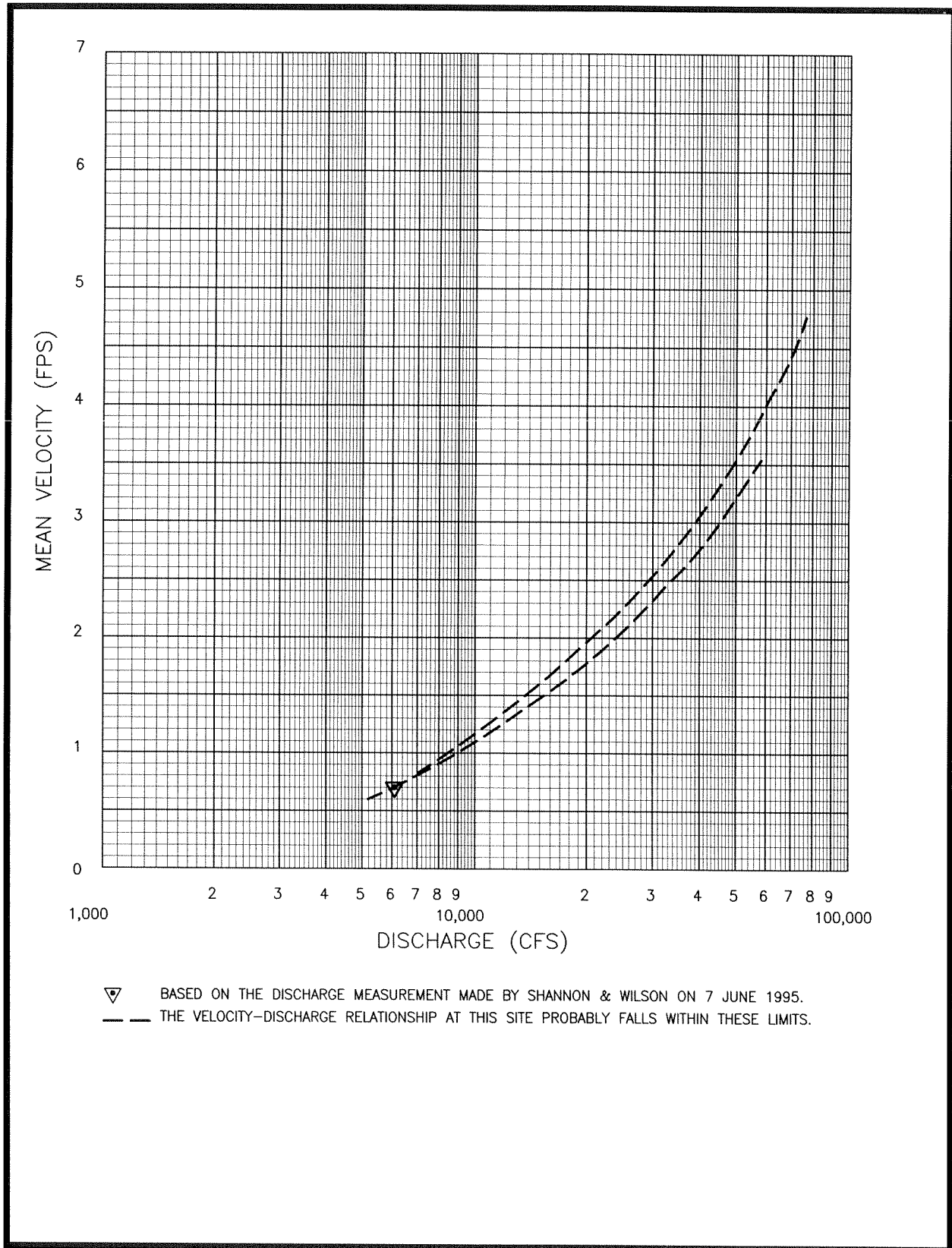


Figure 3-6. Main mean channel velocity-discharge relationship for the Colville River at Cross Section N7.46.

PART 4. FLOOD MAGNITUDE AND FREQUENCY

by Scott R. Ray and James W. Aldrich

BACKGROUND

Understanding the flooding regime of the Colville River Delta is critical to the design and placement of potential oilfield facilities. Despite the numerous studies conducted on the delta, there is no long-term record of discharge measurements or flood stages. This study uses 6 years of peak discharge data collected at the head of the delta, and data from a nearby river, to help estimate the flood magnitude and frequency on the Colville River.

METHODS

FLOOD MAGNITUDE

The methods used to estimate the peak discharge for each of 6 years of data are detailed below. The peak discharges were estimated for the years 1962, 1977, 1992, 1993, 1994, and 1995.

1962

The 1962 peak discharge was estimated by Arnborg et al. (1966).

1977

The estimate of the 1977 peak discharge was based on information collected by the USGS. Although the USGS (1978) reported a peak stage, it was ice-affected, so they did not report a peak discharge. Thus, for this project, the average of two estimates was used to produce the most likely estimate of the 1977 peak discharge. The first estimate uses the January 1996 rating curve and the average increase in stage due to ice, based on our experiences in 1994 and 1995. The peak stage occurred on 7 June, but the USGS did not measure the discharge until 10 June, when the flow was 232,000 cfs at a stage of 53.04 ft. If the assumption is made that the discharge rating curve has not changed significantly then, according to the January 1996 stage-discharge curve, the water-surface elevation associated with a discharge of 232,000 cfs

is 14.31 ft (based on USCGS monument "River"). The peak water-surface elevation that occurred on 7 June was 8.25 ft higher than the water-surface elevation during the discharge measurement on 10 June. Therefore, the peak water-surface elevation was 22.56 ft. However, the peak stage was affected by ice. Based on estimates of the affect of the ice on water-surface elevations in 1994 and 1995, the ice probably increased the peak water-surface elevation by an average of 1.57 ft. If the affect of the ice is subtracted from the peak water-surface elevation, the resulting stage is 20.99 ft. Thus, a discharge estimate for the first method was prepared using a stage of 20.99 ft and the January 1996 stage-discharge curve.

The second estimate uses the average daily flow on the second day after the peak and a ratio to estimate the 1977 peak discharge. The ratio relates the instantaneous peak discharge and the average daily discharge two days after the peak. The average ratio, for the years in which data are available (1962, 1993, and 1995), is 1.48. The average daily flow on 9 June 1977 was 277,000 cfs. The discharge estimate for the second method was prepared by multiplying the flow two days after the peak by the average ratio. The average of the two methods was adopted as the most likely estimate of the 1977 peak discharge.

1992

The peak water-surface elevation for 1992 was obtained from high-water marks and not by direct observations (Jorgenson et al. 1993). Because the slope of the high water marks is considerably less than the water-surface slope at the peak discharge in 1993 and 1995, it seems likely that the peak discharge was affected by ice. Essentially the same methods that were used to estimate the 1977 peak discharge were used to estimate the 1992 peak discharge.

1993

The peak discharge in 1993 was observed and believed to be unaffected by ice (Jorgenson et al. 1994a). The average water-surface elevation based on measurements from both sides of the river was 20.15 ft. The final discharge estimate was prepared using a stage of 20.15 ft and the January 1996 stage-discharge curve.

1994

The peak water-surface elevation during the 1994 spring breakup was affected by ice so, prior to computing the discharge, it was necessary to adjust the elevation for the effect of the ice. In addition, because the geometry of Cross Section E27.09 (Cross Section 6) changed slightly between 1992 and 1995, two estimates of the 1994 peak discharge were averaged to obtain the final discharge estimate.

The first estimate used the 1992 cross section at E27.09 to compute the peak discharge. The cross-sectional area of the ice (4782 ft²) was subtracted from the total cross-sectional area (45,271 ft²), estimated from the elevation of the high-water marks and the 1992 cross section. Using the January 1996 stage-discharge curve, a discharge estimate was calculated from the water-surface elevation (11.63 ft) associated with the adjusted cross sectional area (40,489 ft²).

The second estimate used the 1995 cross section at E27.09 to compute the peak discharge. Again, the cross-sectional area of the ice (4782 ft²) was subtracted from the total cross-sectional area (43,666 ft²), estimated from the elevation of the high-water marks and the 1995 cross section. Using the January 1996 stage-discharge curve, a discharge estimate was prepared based on the water-surface elevation (11.59 ft) associated with the adjusted cross-sectional area (38,884 ft²).

1995

The peak water-surface elevation during the 1995 spring breakup also was affected by ice, so we adjusted the peak water-surface elevation for the effect of the ice, as described above. Thus, the peak discharge was estimated by subtracting the cross-sectional area of ice (4600 ft²) from the total cross-sectional area (51,640 ft²), estimated from the elevation of the high-water marks and the 1995 cross section. Using the January 1996 stage-discharge curve, a discharge estimate was calculated from the water-surface elevation (14.35 ft) associated with the adjusted cross-sectional area (47,040 ft²).

FLOOD FREQUENCY

Although 6 years of data on peak discharge are available for the Colville River, the length of record

is considered marginal for a single-station flood-frequency analysis. Consequently, peak discharge data from a nearby North Slope river were used to extend the Colville River peak discharge record. A flood-frequency relationship was developed from the extended peak-discharge record.

Of the North Slope rivers with a significant peak discharge record, the Kuparuk River, with 25 years of records, probably is the most similar to the Colville River. Additionally, as we suspect is the case with the Colville River, the annual peak discharge on the Kuparuk River nearly always is the result of snowmelt.

The six annual peak discharges on the Colville River, which all resulted from snowmelt, were related to the spring peak discharge on the Kuparuk River. The annual peak discharge on the Kuparuk River in 1977, 1993, 1994, and 1995 resulted from snowmelt, but the 1992 annual peak resulted from rainfall. To estimate the peak snowmelt discharge in 1992, a ratio between the instantaneous peak snowmelt discharge and the average daily discharge occurring on the same day as the instantaneous peak was calculated from the Kuparuk River data. The instantaneous peak snowmelt discharge for the Kuparuk River in 1992 was estimated using this ratio.

A regression equation then was developed that used the peak snowmelt discharge data from the Colville River (1977, 1992, 1993, 1994, and 1995) and the peak snowmelt discharge data from the Kuparuk River for the same years. This regression equation was used to estimate peak discharges for the Colville River for the entire period during which data had been collected on the Kuparuk River. A flood frequency-discharge relationship was developed from the extended data set (following Interagency Advisory Committee On Water Data 1982). Both the generalized skew (0.13) and the standard error of the generalized skew (1.15), used to produce a weighted skew for the flood-frequency analysis, were taken from the data presented for Region 3 by Jones and Fahl (1994). Because structures ultimately may be constructed based on these discharge estimates, the flood-frequency-discharge relationship that was developed was based on the expected probability associated with an event of a given magnitude, rather than the true probability associated with an event of an average magnitude.

RESULTS AND DISCUSSION

FLOOD MAGNITUDE

The results of the flood-magnitude analyses are presented in Table 1–2, along with the peak water-surface elevations and date of the peak discharge. Of the 6 years of flood peak data collected at the head of the Colville River Delta, only two of the years (1962 and 1977) had complete discharge records from breakup to freezeup. The peak discharges at breakup for 1962 and 1977 also are the annual peak discharges for these years. We assumed that the peak breakup discharges for 1992–1995 also were the annual peak discharges for these years. This assumption is supported by isolated stage readings and observations made by researchers and area residents.

FLOOD FREQUENCY

The annual flood-peak estimates used in the flood-frequency analysis are presented in Table 4–1. A flood-frequency relationship was developed for the Colville River at E27.09 from these data. Based on the flood-frequency curve (Figure 4–1), the 1995 peak discharge has an estimated recurrence interval of approximately 1.5 yr. The recurrence interval for each of the 6 years of data, based on the flood-frequency curve, are summarized in Table 4–2. Peak discharges associated with the 50-, 100-, and 200-yr floods are estimated to be on the order of 805,000, 947,000, and 1,110,000 cfs, respectively.

As was mentioned previously, all six of the flood peaks at the head of the delta were produced by snowmelt runoff during breakup. Additionally, 24 of the 25 years of data for the Kuparuk River were produced by snowmelt runoff (EarthInfo 1993; USGS 1994, 1995). In general, floods on North Slope rivers are influenced by the type of physiographic region drained. Snowmelt flooding occurs annually in all rivers on the North Slope. On rivers having drainage basins entirely within the Arctic Coastal Plain, snowmelt flooding nearly always produces the annual peak discharge. Large rainfall floods are rare because the rainfall intensity generally is low, and the thaw lakes and tundra have a large capacity to absorb rainfall and retard runoff.

The flooding regime of the Colville River is more complicated because the basin drains the

Brooks Range and foothills in addition to the coastal plain. Basins that drain the Brooks Range and foothills, such as the upper Sagavanirktok River, experience significant summer floods caused by large rainstorms. Large rainfall floods are not as frequent as snowmelt floods, but they may be large. The two largest floods on the Sagavanirktok River, during the 27 years in which data have been collected, were caused by rainfall. Long-term discharge records do not exist for the Colville River. However, rainfall floods have not produced overbank flow in 40 years of observations (J. Helmericks 1996, pers. comm.). Thus, if significant rainfall floods occur on the Colville River Delta, they are rare.

Ice jams also may lead to significant flooding, even during periods of only moderate discharge. In 1966, an ice jam in the vicinity of the Putu Channel caused water to flow overbank at distances up to 4 mi east of the East Channel, and caused ice floes to be deposited up to 1 mi east of the East Channel (J. Helmericks 1996, pers. comm.).

As discussed in Part 1, the distribution of the flow (based on minimal data) between the East and Nechelik channels is on the order of 60–80% and 20–40%, respectively. Flood peaks on the channels near the head of the delta were estimated using this distribution of flow. Thus, a 50-yr flood on the East Channel is on the order of 483,000–644,000 cfs, a 100-yr flood is on the order of 568,000–758,000, and a 200-yr flood is on the order of 660,000–880,000 cfs. A 50-yr flood on the Nechelik channel is on the order of 161,000–322,000 cfs, a 100-yr flood is on the order of 189,000–379,000, and a 200-yr flood is on the order of 220,000–440,000 cfs. The distribution of flow between these channels probably varies annually, however, and may vary with the location of open water, ice cover, and ice jams. The distribution of flow probably also depends on the water-surface elevation. In this regard, we emphasize that there is no information on the distribution of flow occurring during a discharge anywhere near the magnitude of a design event. We also emphasize that, as flood peaks move downstream from the head of the delta, they may be attenuated by in-channel storage. At this time, no information on the possible magnitude of the attenuation is available.

Table 4-1. Kuparuk and Colville rivers data used in flood frequency analysis.

Year	Kuparuk River Peak Discharge (cfs)	Colville River Peak Discharge		
		Based On Regression Equation ^a (cfs)	Based On Colville River Data (cfs)	Discharge Used In Frequency Analysis (cfs)
1962			215,000	215,000
1971	77,000	466,000		466,000
1972	45,800	297,000		297,000
1973	82,000	493,000		493,000
1974	24,000	179,000		179,000
1975	22,600	171,000		171,000
1976	55,000	347,000		347,000
1977	66,800		407,000	407,000
1978	118,000	688,000		688,000
1979	24,300	181,000		181,000
1980	40,500	268,000		268,000
1981	27,500	198,000		198,000
1982	104,000	612,000		612,000
1983	68,400	419,000		419,000
1984	56,800	356,000		356,000
1985	34,500	236,000		236,000
1986	38,000	255,000		255,000
1987	15,500	133,000		133,000
1988	38,700	258,000		258,000
1989	75,400	457,000		457,000
1990	70,000	428,000		428,000
1991	37,100	250,000		250,000
1992	28,000 ^b		188,000	188,000
1993	52,300		379,000	379,000
1994	36,500		159,000	159,000
1995	23,500		233,000	233,000

^a Estimate of Colville River discharge based on regression equation developed from Kuparuk and Colville river data.

^b Based on peak average-discharge (2 June 1992) and the ratio developed between instantaneous peak discharge and average daily discharge.

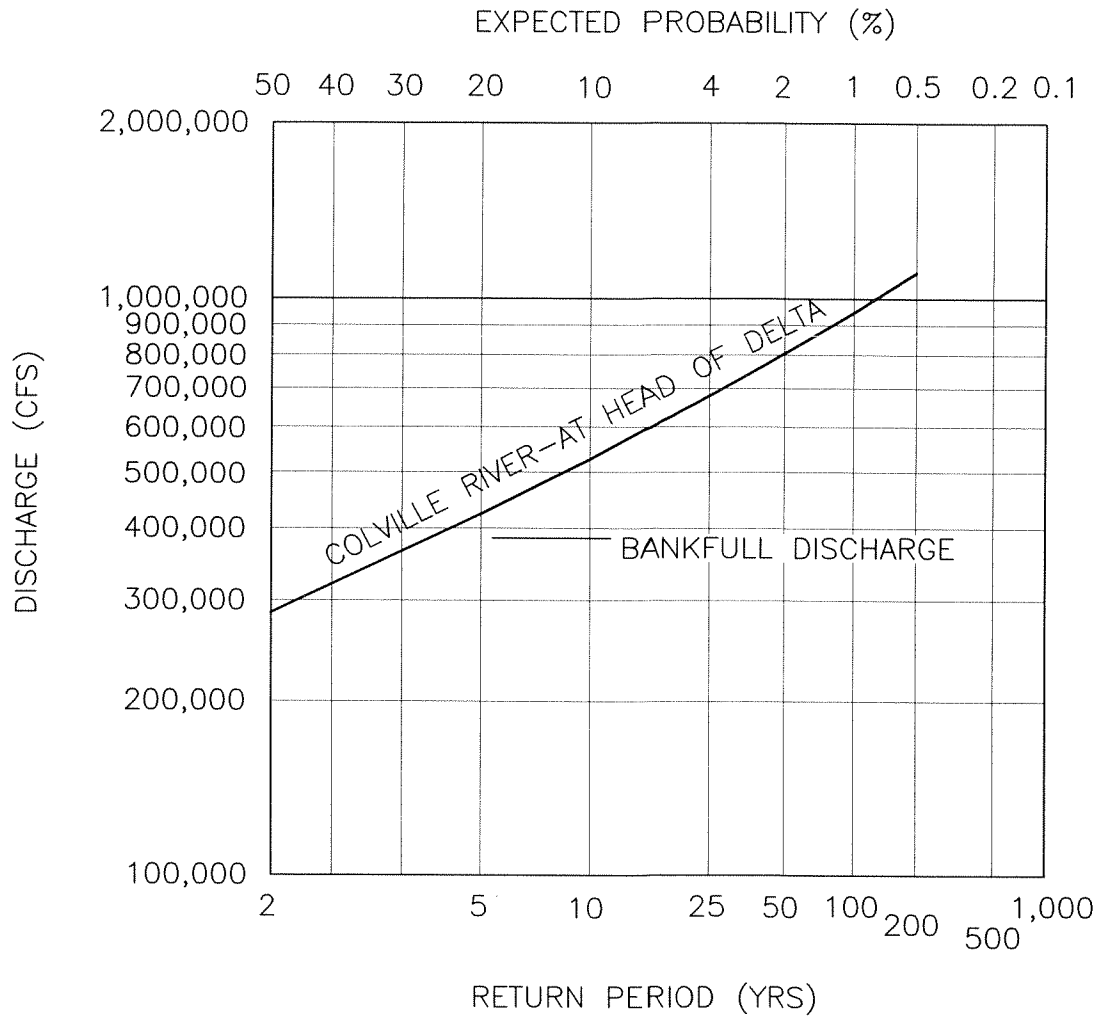


Figure 4-1. Flood-frequency relationship for the Colville River at the head of the delta.

Table 4–2. Summary of annual peak discharge and return period at the head of the Colville River Delta (Cross Section E27.09).

Year	Annual Peak Discharge (cfs)	Approximate Return Period (Years)
1995	233,000	1.5
1994	159,000	1.1
1993	379,000	3.7
1992	188,000	1.2
1977	407,000	4.4
1962	215,000	1.4

PART 5. FLOOD DISTRIBUTION

By M. Torre Jorgenson, Erik Pullman, and H. Jesse Walker

BACKGROUND

The distribution of flood water during spring breakup has been monitored within small, representative study areas in the Colville River Delta from 1992 to 1995; this information has been used to delineate the extent of annual flooding, analyze the patterns of flooding across the delta, and develop a spatially explicit model for predicting flooding frequency across the delta. Such information will aid the selection of sites for oilfield facilities on the delta that will minimize flooding and avoid the obstruction of flood water.

To provide a record of flood distribution, flood waters near peak stage during breakup have been photographed from small aircraft during the years 1992–1995. Due to the large area of the delta, the photography and subsequent mapping were limited to small study areas that represent different flooding regimes. These study areas, however, have changed over the years because there have been different areas of interest for oil exploration. Initially, oil exploration focused on the outer delta, whereas more recent oil exploration and development planning has focused on the central delta.

Because the delta is flat with only small changes in topography, these analyses of flood distribution have focused on determining relationships between flooding and terrain units (rather than actual elevations). High-resolution (e.g., 2-ft interval) contour mapping has not been done here and, even if it was done, it might not be adequate for delineating small differences in floodplain steps that are important in affecting the distribution of flood water at high-flood stages. Instead, we have analyzed flood distribution relative to terrain units because they reflect environments that differ in sediment deposition and in relative heights above the surface of the river.

Analyses of flood distribution and the relative heights of terrain units were used to develop a predictive model of flood distribution across the delta. This model relies on the use of empirical data of flood frequency for the more-frequently flooded terrain units. To help assign approximate flooding

frequencies for areas with low-frequency flooding but for which we have no direct observations, we relied on indirect evidence from a large flooding event in 1989 and inferences from data collected for the soil surveys (see Part 10).

METHODS

Mapping of flood distribution within five small study areas on the delta was conducted annually between 1992–1995 (Figure 5–1). Mapping of the study areas changed over the years in response to redirection of oil exploration activities during that period. Aerial photography and mapping methods were similar for all years, although minor modifications were necessary, depending on the weather. Specific details for each year are provided below.

In 1992, the extent of flood-water coverage within three study areas (Nechelik, Tamayayak, and Kupigruak) was mapped by using aerial photography acquired on 4 and 8 June. Oblique photographs were taken on 4 June, 2 days after peak stage occurred at the head of the delta, with a 35-mm camera at 500 ft above ground level (agl) and just below the lowest cloud layer. On 8 June, when weather improved, vertical color photographs (1:17,000 scale) were taken at 11,000 ft agl with a large-format camera (6x7-cm Hasselblad). Complete photographic coverage of all study areas was obtained on this 8 June flight.

In 1993, oblique aerial photographs were obtained for four study areas (Tamayayak, Kupigruak, Kachemach, and Itkillik) on 1 June and for the fifth study area (Nechelik) on 2 June. Thus, most of the photography was acquired one day after peak stage occurred at the head of the delta. Photographs were taken with a 35-mm camera at 500–700 ft agl, just below the lowest cloud layer. Because of poor weather, vertical photographs could not be obtained with the large-format camera. In 1993, the photography obtained was incomplete (approximately 20–30% of each study area), because of lack of overlapping coverage between flight lines.

In 1994, oblique aerial photography was obtained only for the Itkillik study area because monitoring effort was reduced that year. Photographs were taken on 25 May, which was the

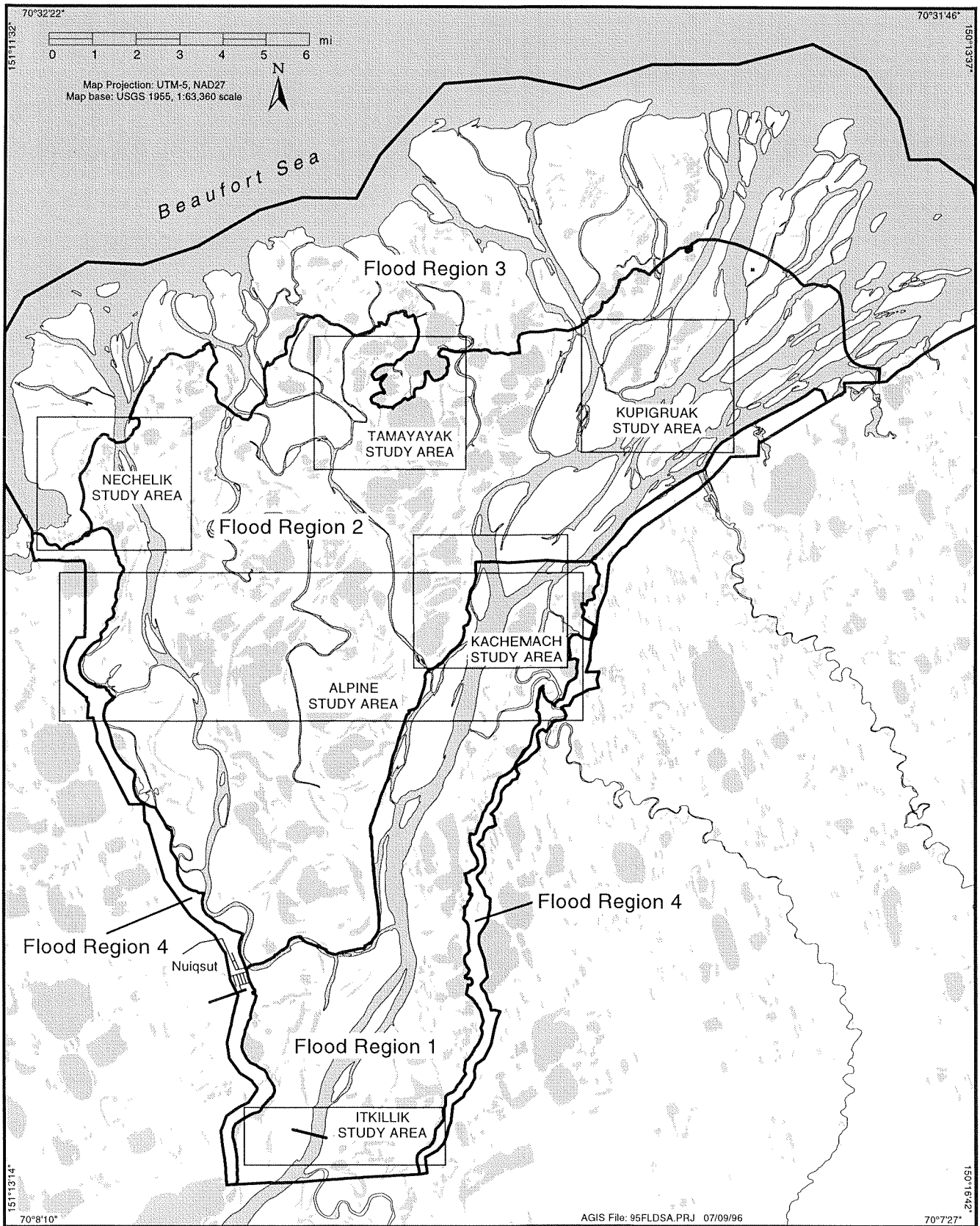


Figure 5-1. Map of flooding study areas and flooding regions, Colville River Delta, 1995.

day of peak stage, with a 35-mm camera at 500–700 ft agl, just below the lowest cloud layer.

In 1995, oblique aerial photography was obtained for the Itkillik, Alpine, and Tamayayak study areas on 16 May, which was the day of peak stage. Photographs were taken with a 35-mm camera at 500–700 ft agl, just below the lowest cloud layer.

For each of these years, the extent of flooding within these study areas was determined from the oblique photography and was delineated on the color infrared photography (1:18,000 scale) that was used to map integrated terrain units, ITUs. Flood water was identified by its light brown color, which was caused by the presence of large amounts of suspended sediments, whereas standing water from snowmelt in depressions and ponds typically appeared clear or black. Lakes and channels having flood water around the ice margins were mapped as entirely flooded. In 1992, 1994, and 1995, flood water in the study areas was mapped entirely from the oblique aerial photography. In 1993, flood distribution was mapped in two phases because of the incomplete photographic coverage. First, the extent of flood water was delineated within those areas covered by the aerial photography. Then, the distribution of flood waters in the intervening gaps was interpolated along ITU boundaries. The lines were digitized with a geographic information system (AtlasGIS, San Jose, CA) and rectified to the ITU map initially produced in 1992 and later revised in 1995.

For analysis of flood distribution relative to terrain units, the flooding layer was overlaid on the ITU map, and the percentage of each terrain unit covered by flood water was determined. The analysis was done only for terrain units, instead of the full ITUs (terrain unit, surface form, and vegetation), to reduce the complexity of the analysis and because terrain units accounted for most of the variation. In 1993, however, only those areas mapped directly with the aerial photography in the first phase of mapping were used for this analysis. For all years, the data were summarized within each study area and for all areas combined.

The development of a model for predicting flood distribution and flooding frequency across the delta involved five steps: (1) ranking the relative heights of terrain units, (2) ranking the percentage of areas flooded at various flood stages, as described

above, (3) analyzing sediment deposition and driftwood occurrence (see Part 10), (4) comparing the stage-discharge and flood-frequency relationships at the head of the delta (see Part 2) with relative heights of terrain units, and (5) minor adjustment of flood-frequency classes within three flooding regions. A flood-frequency class then was assigned to each terrain unit within each flooding region, and these were used to create a map of flood distribution.

Relative heights of the terrain units were calculated from the elevational data obtained from the surveying of cross sections (includes measurements of the underwater riverbed) and transects (includes only measurements on the riverbanks). Relative heights were calculated by dividing the mean elevation of a terrain-unit segment along the cross section or transect by the mean elevation of a segment of inactive-floodplain cover deposits. Inactive-floodplain cover deposits were used as the standard terrain unit for the top of the bank, because their interbedded organic and mineral horizons indicated occasional flooding and that these deposits are in equilibrium with the current flooding regime. If there was more than one segment of inactive-floodplain cover deposit along a cross section, the mean elevation of one of the segments was arbitrarily assigned as the value by which the mean elevations of all other terrain units were divided. We used mean elevations of each terrain-unit segment along the cross sections for our subsequent analyses, instead of individual readings within each segment, to avoid pseudoreplication. Thus, the mean elevation for each terrain-unit segment represented one sample, and the total number of segments along all cross sections and transects combined represented the sample population.

RESULTS AND DISCUSSION

OVERALL FLOOD DISTRIBUTION

Overall, the average percentage of flooding for all study areas varied from 33% in 1995, when peak discharge was estimated to be 233,000 cfs, to 55% in 1993, when peak discharge was estimated to be 379,000 cfs. Flooding in 1992 was intermediate, covering 42%. In 1994, flooding covered 13%, but

this value was skewed because only the Itkillik study area was monitored.

The amount of flooding varied considerably among areas for any given year (Figures 5-2 to 5-7). In 1993, when flooding was the greatest, the amount of flooding ranged from 39% in the Tamayayak area in the central delta to 69% on the Kachemach area (later incorporated into the Alpine area), which encompassed the East Channel.

The amount of flooding also varied considerably among years for any given area. In the Itkillik area at the head of the delta, where the floodplain is narrower and constrained by high banks on either side, there was large variation in the percentage of area flooded: from 13% in 1994 to 52% in 1993 (Figures 5-3 and 5-7). In contrast, in the Tamayayak area of the central delta, flooding varied only from 36% in 1992 to 40% in 1995 (Figure 5-4). This area is in one of the oldest portions of the delta and surrounds only one small distributary (Tamayayak). Hence, the area appears to be affected more by the backup of flood water on the sea ice than from bank overflow from the Tamayayak.

The amount of annual variation in the other study areas was intermediate between the above two study areas. In the Alpine study area, flooding ranged from 32% in 1995 to 69% in 1993 (Figures 5-2 and 5-7). The value for 1993, however, was relatively large because only a small portion of the area (Kachemach area) that centered on the East Channel was mapped that year, thus amplifying the flood coverage. Of particular interest in the Alpine study area is the extensive flooding around the Alpine #1 Exploratory Well Site in 1995. We attribute this extensive flooding to the tapping of Nanuk Lake at an outside bend of the Nechelik Channel. Consequently, flood water was directed into this lake, where it backed up and overflowed the bank, even at a relatively low flood stage.

In the Nechelik study area, which encompassed an extensive area of tidal flats on the outer delta, flooding coverage ranged from 41% in 1992 to 65% in 1993 (Figures 5-6 and 5-7). Similarly, in the Kupiguak study area, which was mainly centered on a portion of the East Channel in the outer delta, flooding coverage ranged from 49% in 1992 to 62% in 1993 (Figure 5-5).

In summary, those areas having the most extensive flooding in 1993, the year of highest peak

discharge, were floodplains along the East Channel. In particular, there was extensive overbank flooding at the head of the delta (Itkillik study area) and near the mouth of the Kachemach River (Kachemach study area), where most of the flow is constrained by high banks on the eastern side of the floodplain and by high sand dunes on the western side of the East Channel. Frequent overbank flooding also occurred near Nanuk Lake at the Alpine #1 Exploratory Well Site. We attributed this flooding, which occurred at fairly low flood stages, to the tapping of Nanuk Lake, the occurrence of a low-lying, ice-rich thaw basin around the exploratory well site, and the occurrence of low-lying, ice-poor thaw basins east of this well site. In contrast, most of the central portion of the delta west of the sand dunes bordering the East Channel did not flood during our monitoring. This area is the oldest portion of the delta, and there are numerous abandoned-floodplain cover deposits in this area (see Part 10).

RELATIONSHIP BETWEEN FLOODING AND TERRAIN UNITS

Patterns in flood distribution were strongly related to terrain units and differed among years, with 1994 having the least flooding and 1993 having the most flooding overall (Figure 5-8). Delta riverbed/sandbar deposits were nearly entirely flooded (82-95%) every year, as would be expected. Active-floodplain cover deposits had up to 47% flooding coverage at the highest flood stage. In contrast, flooding coverage on abandoned-floodplain and inactive-floodplain cover deposits were relatively low, up 11% and 16%, respectively. Terrain units that were not considered to be affected by the current flooding regime, such as sand dunes and alluvial terraces, also had minor amounts of flooding along their margins (up to 5% and 6% of the area, respectively).

The amount of flooding in each terrain unit also was strongly related to discharge (Figure 5-9). Riverbed/sandbar deposits became nearly entirely flooded at intermediate levels of discharge. In contrast, the inactive- and abandoned-floodplain cover deposits showed only small, but consistent, increases in flood coverage at the discharge rates (up to 379,000 cfs) observed in this study.

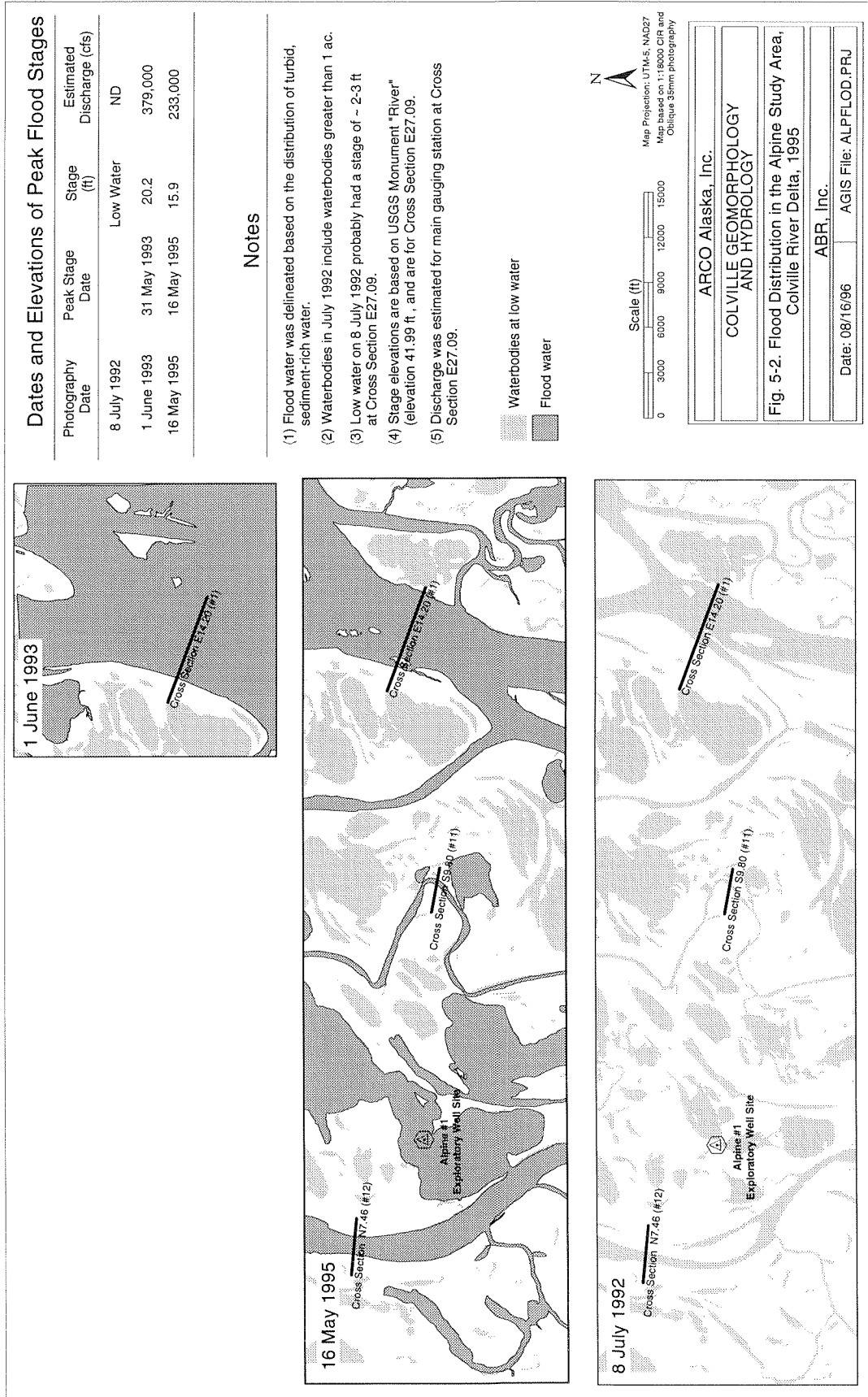


Figure 5-2. Map of flood distribution in the Alpine study area, Colville River Delta, 1995.

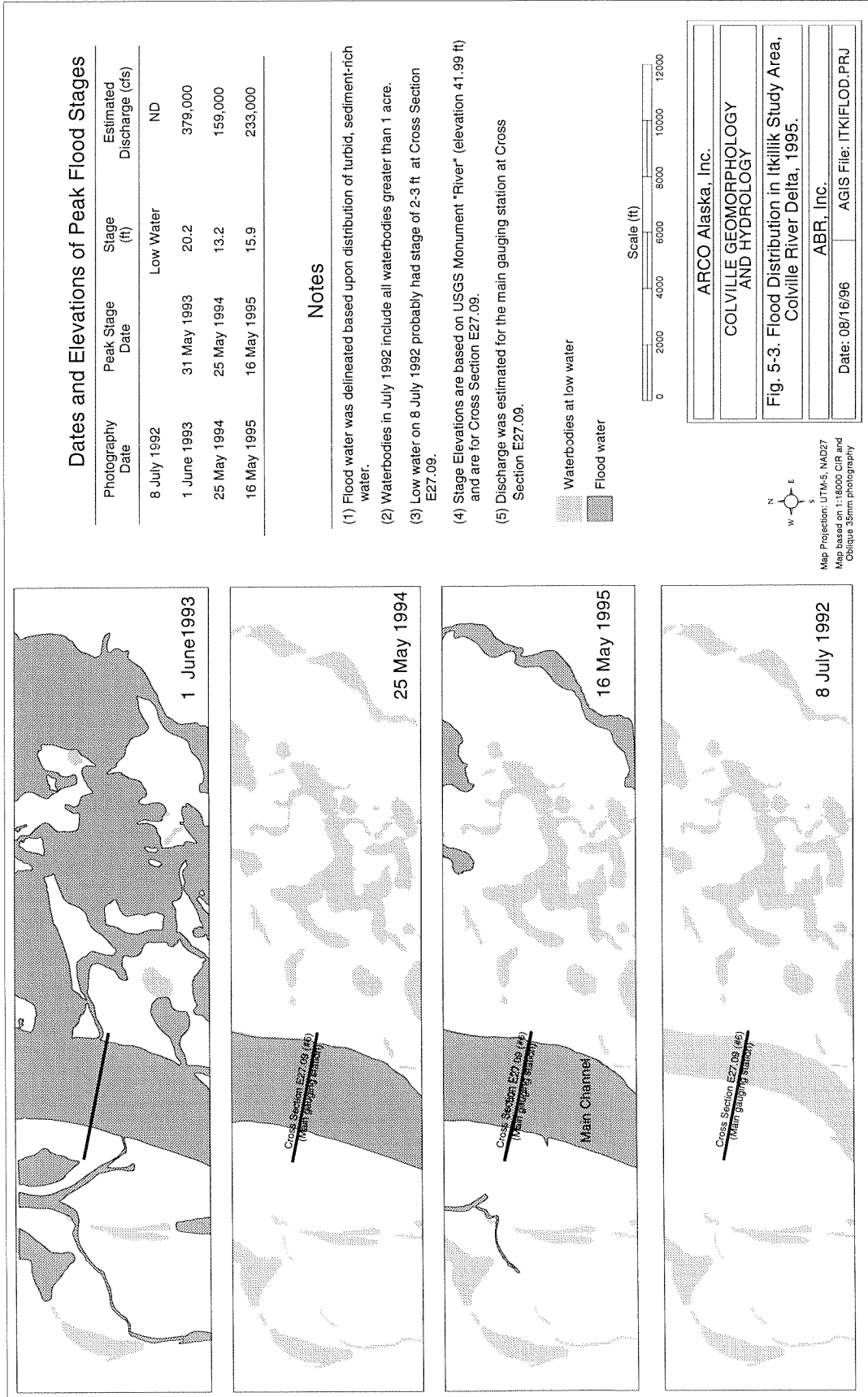


Figure 5-3. Map of flood distribution in the Itkillik study area, Colville River Delta, 1995.

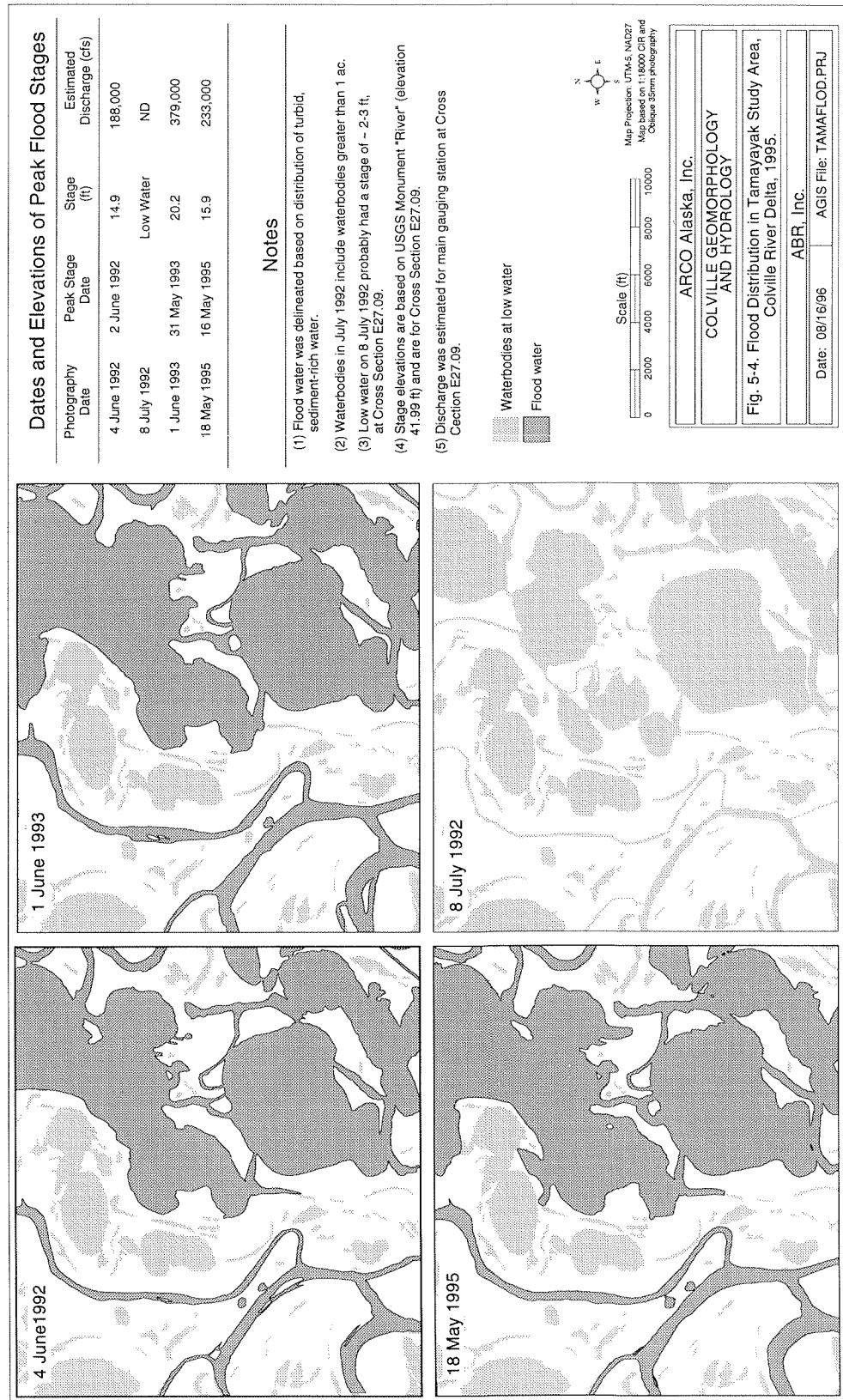


Figure 5-4. Map of flood distribution in the Tamayyak study area, Colville River Delta, 1995.

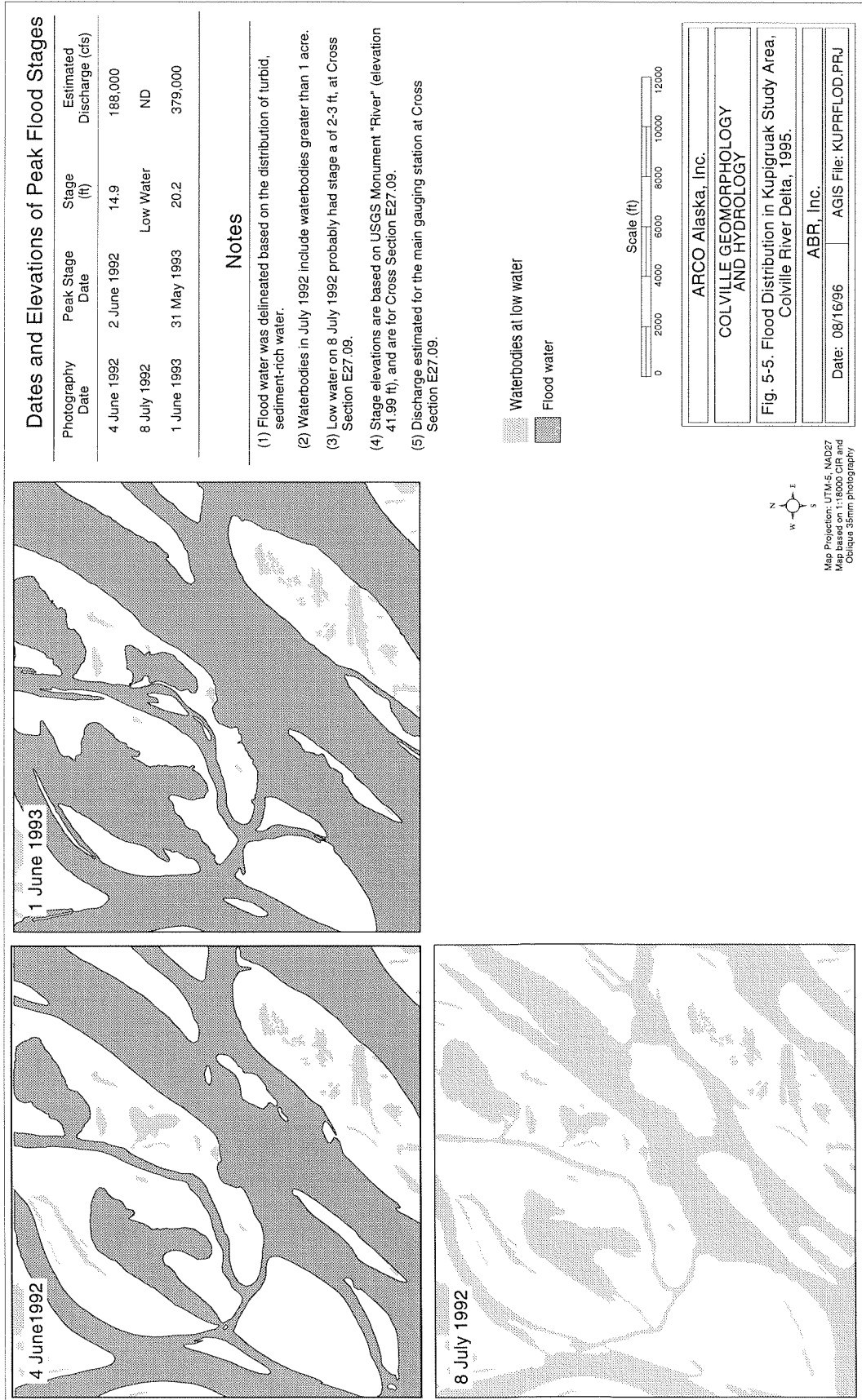


Figure 5-5. Map of flood distribution in the Kupiguak study area, Colville River Delta, 1995.

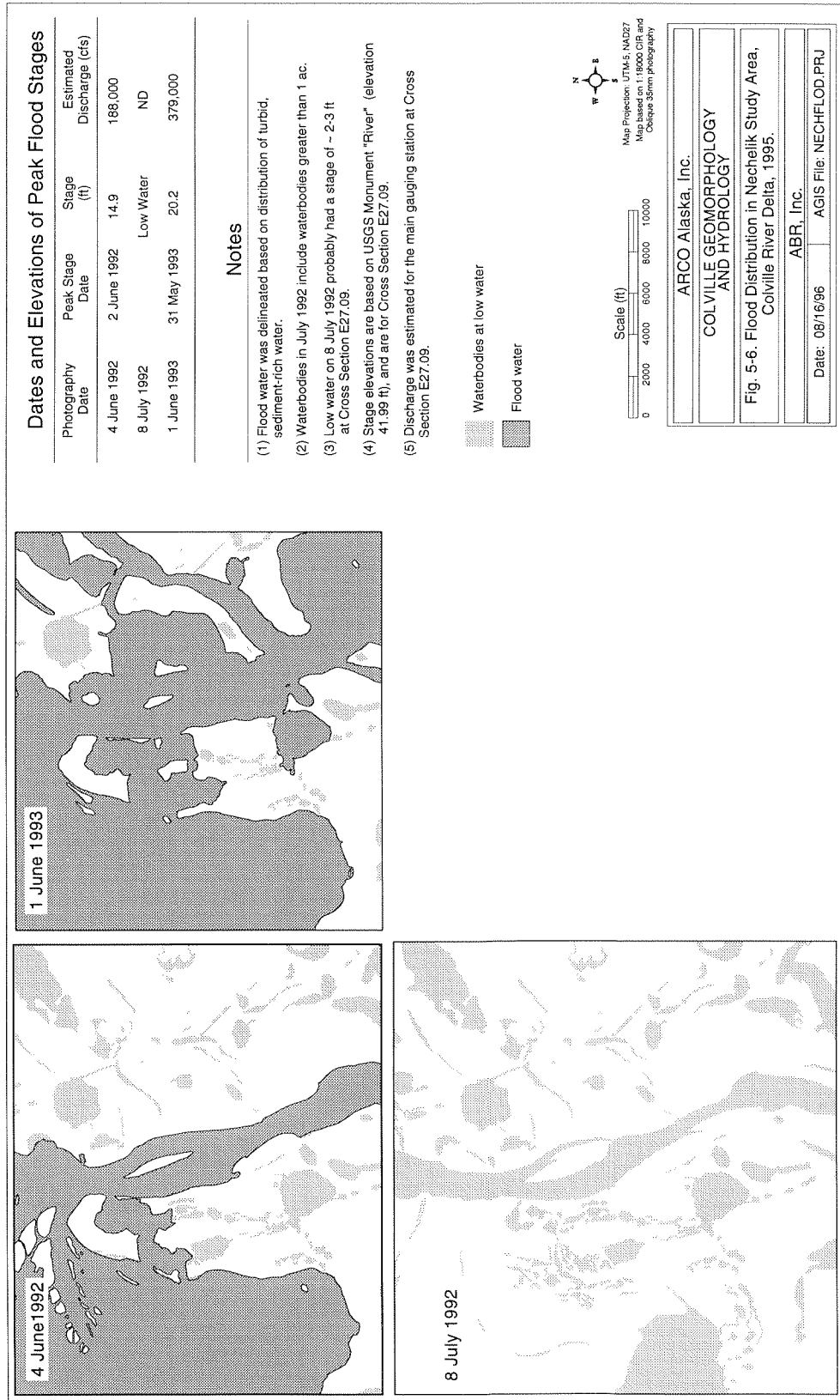
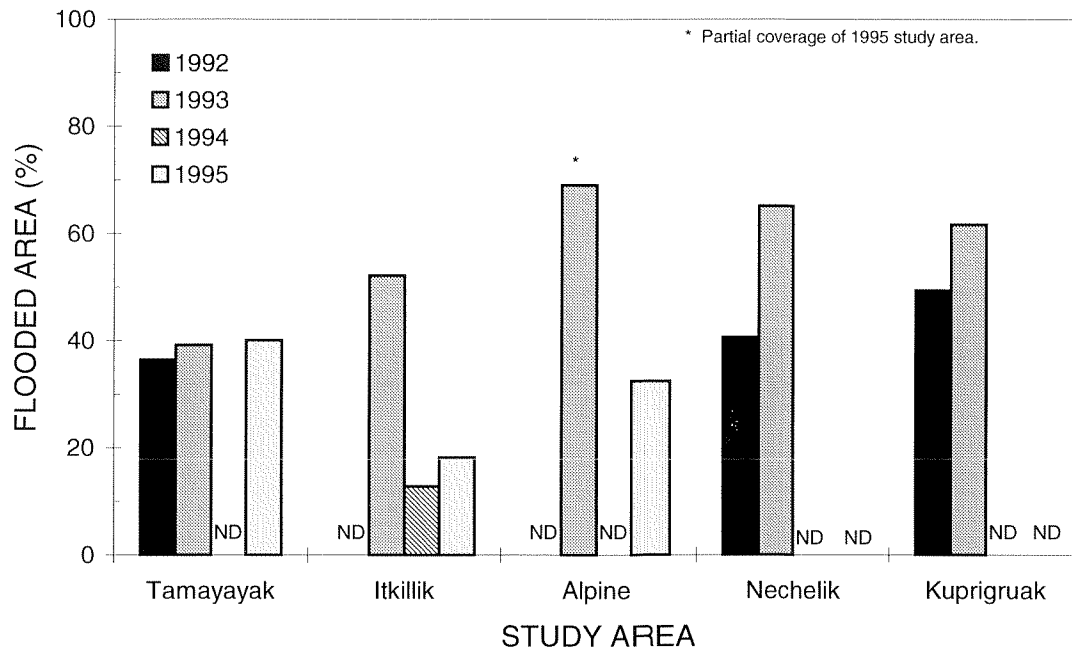


Figure 5-6. Map of flood distribution in the Nechelek study area, Colville River Delta, 1995.

Figure 5-7. Percentage of total area covered by flood water in five study areas in the Colville River Delta, 1995.



Small inconsistencies among years in the percentage of area of some terrain units that were flooded can be attributed to several factors. First (and most importantly), different study areas were mapped during different years. These different study areas occur in different flooding regions and they have different percentages of terrain units. Second, there is a time lag between peak discharge at the head of the delta and flooding in the central and outer delta. Finally, some channel features, such as the tapping of Nanuk Lake and ice jamming at river bends, can strongly affect overbank flooding. Despite these problems, strong differences among terrain units in extent of flooding have emerged and can form the basis for modeling flood distribution of flooding frequency (see Part 4). Because of the lack of data for flood distribution at higher flood stages, the estimation of flooding frequency for the least-frequently flooded terrain units relied on the analysis of differences in sediment deposition among terrain units (see Part 10). The flood frequency classes for the various terrain units were modified slightly based on their occurrence in three flooding regions.

There is a gradual and consistent decrease in mean elevation of the inactive-floodplain cover deposits from the head of the delta, decreasing from 20.5 ft and 19.7 feet at two segments at the head of

the delta (Cross Section E27.09) to 3.2 and 6.3 ft at two segments on the outer delta (Cross Section 5; Figure 5-10). Inactive-floodplain cover deposits along the Nechelik Channel and in the central delta had similar mean elevations relative to river mile as those along the East Channel but tended to be slightly higher.

Because of the gradual change in elevation from the head to the outer delta, the mean elevations of the various terrain units along our cross sections and transects were calculated as relative heights (relative to the top of the banks) to allow comparison of terrain units across the entire delta. Inactive-floodplain cover deposits were used as the standard terrain unit for the top of the bank (as opposed to abandoned-floodplain cover deposits and eolian sand deposits), because the interbedded organic and mineral horizons indicated that the deposits occasionally are flooded and are in equilibrium with the current flooding regime. A comparison of mean relative heights among terrain units reveals large differences among most terrain units (Figure 5-11). The difference in mean relative height between abandoned-floodplain (1.12) and inactive-cover deposits (0.97) was small, however, indicating that small changes in flood stage can result in large changes in the distribution of floodwaters. The

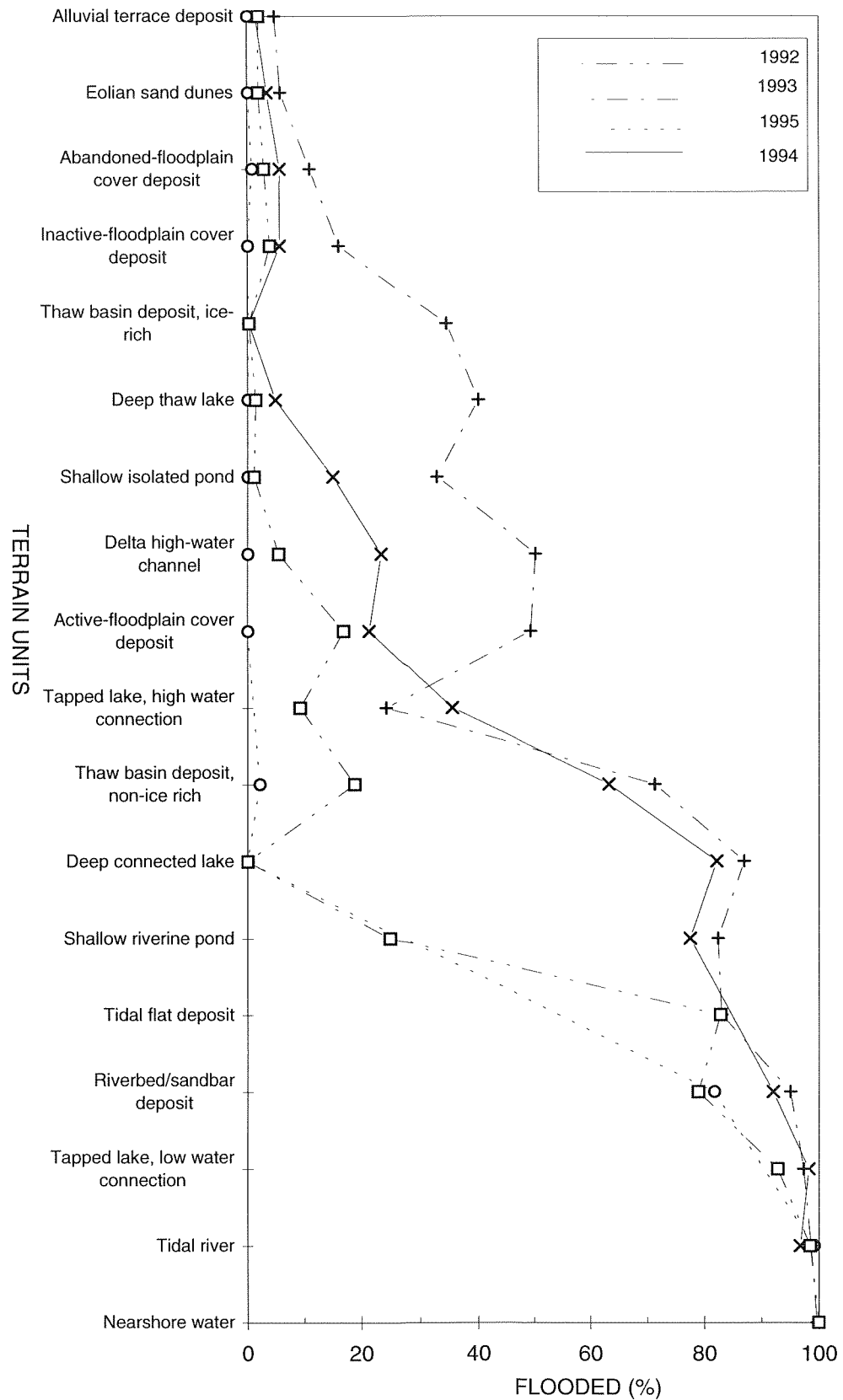
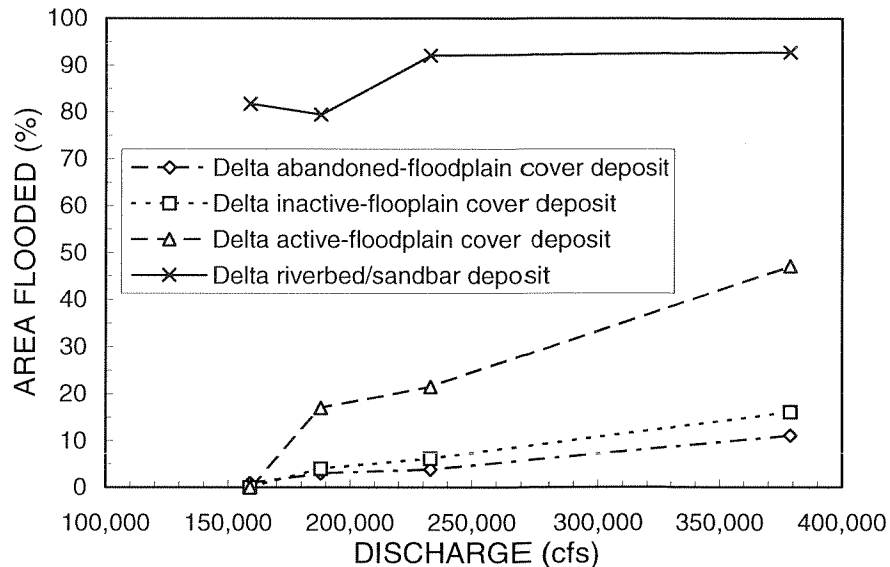


Figure 5-8. Percentage of each terrain unit covered by flooding in five study areas in the Colville River Delta, 1995.

Figure 5-9. Relationship between percent area flooded and peak discharge for the major terrain units, Colville River Delta, 1995.



small standard deviations associated with the means indicate that the relationships between relative heights and terrain units are consistent throughout the delta.

The differences in relative heights and amount of flooding among terrain units that we observed from 1992 to 1995 were used to classify terrain units into classes having different flood frequencies. The flood-frequency classes assigned to terrain units, however, were modified with respect to their occurrence within four flooding regions that we have tentatively identified on the delta (Figure 5-1, Table 5-1). These four regions were interpreted from features of the terrain that could constrain flood distribution by comparing the amount of flooding within the small study areas and by comparing the amount of sediment deposition on abandoned-floodplain cover deposits among the regions. In the following discussion, the flooding regions are described first, followed by descriptions of the flood-frequency classes.

Flooding Region 1 includes the area at head of the delta above the Nechelik Channel and the upper portion of the East Channel (Figure 5-1). In this region, the floodplain is narrow and is constrained by alluvial terraces at the head of the delta and by large sand dunes along the western borders of the riverbed/sandbars on the upper

portion of the East Channel. Maps of flood distribution in 1993 revealed more extensive overbank flooding in this region than in other regions. More frequent flooding of the abandoned-floodplain cover deposits in this region also was indicated by more extensive cover of riverine shrubs, prevalence of driftwood, and occurrence of fluvial sediment near the surface. Therefore, the abandoned-floodplain cover deposits in Region 1 were assigned to Flood-frequency Class 3 (every 5–25 yr) instead of Class 4 (every 26–150 yr), as was done for Region 2.

Flooding Region 2 includes the central delta but excludes the upper portion of the East Channel. This region contains older portions of the delta, and the abandoned-floodplain and inactive-floodplain cover deposits generally are slightly higher than those found along the East Channel (Figure 5-10). On many of the abandoned-floodplain cover deposits in this region, we did not observe driftwood or sedimentation in the surface organic layer, the presence of either of which would indicate occasional flooding. This region differs from the other two regions in that we have assigned a Flood-frequency Class 4 (every 26–150 yr) to the abandoned-floodplain cover deposits (Table 5-1).

Flooding Region 3 includes the outer delta, which is dominated by tidal flats and salt-killed tundra. The presence of the salt-killed tundra

Table 5-1. Flood-frequency classes associated with terrain units within three flooding regions, Colville River Delta, 1995.

Terrain Unit	Flooding Region			
	1 (Delta head, Upper East Channel)	2 (Central Delta)	3 (Outer Delta)	4 (Alluvial Terraces on Both Sides of Delta)
Eolian sand deposit	5	5	5	5
Alluvial terrace deposit	5	5	5	5
Gravel fill	5	5	5	5
Delta abandoned-floodplain cover deposit	3	4	3	4
Delta inactive-floodplain cover deposit	3	3	2	3
Shallow thaw pond	3	3	2	5
Deep thaw lake	3	3	2	5
Thaw basin deposit, ice-rich	3	3	2	5
Delta active-floodplain cover deposit	2	2	2	3
Tapped lake, high-water connection	2	2	2	2
Deep thaw lake, connected	2	2	2	2
Delta thaw basin deposit, ice-rich	2	2	2	2
Thaw basin deposit, ice-poor	2	2	2	5
Delta thaw basin deposit, ice-poor	1	1	1	1
Shallow riverine pond	1	1	1	1
Tapped lake, low-water connection	1	1	1	1
Delta riverbed/sandbar deposit	1	1	1	1
Tidal flat deposit	1	1	1	1
Tidal river	1	1	1	1
Nearshore water	1	1	1	1

Flood frequency classes: 1 (every 1–2 yr), 2 (every 3–4 yr), 3 (every 5–25 yr), 4 (every 26–150 yr), 5 (non-flooded).

indicates that this region is no longer in equilibrium with the current flooding regime, presumably as a result of sea level rise, and its distribution was used as the basis for defining the inner edge of this region. The few data we have from the Tamayyak study area indicate that the inactive-floodplain cover deposits in this region are flooded more frequently here than in other regions. Thus, the inactive-cover deposits, along with their associated deep and shallow thaw ponds, were assigned to Flood-frequency Class 2 (every 3–4 yr), and abandoned-floodplain cover deposits were assigned to Class 3 (Table 5–1).

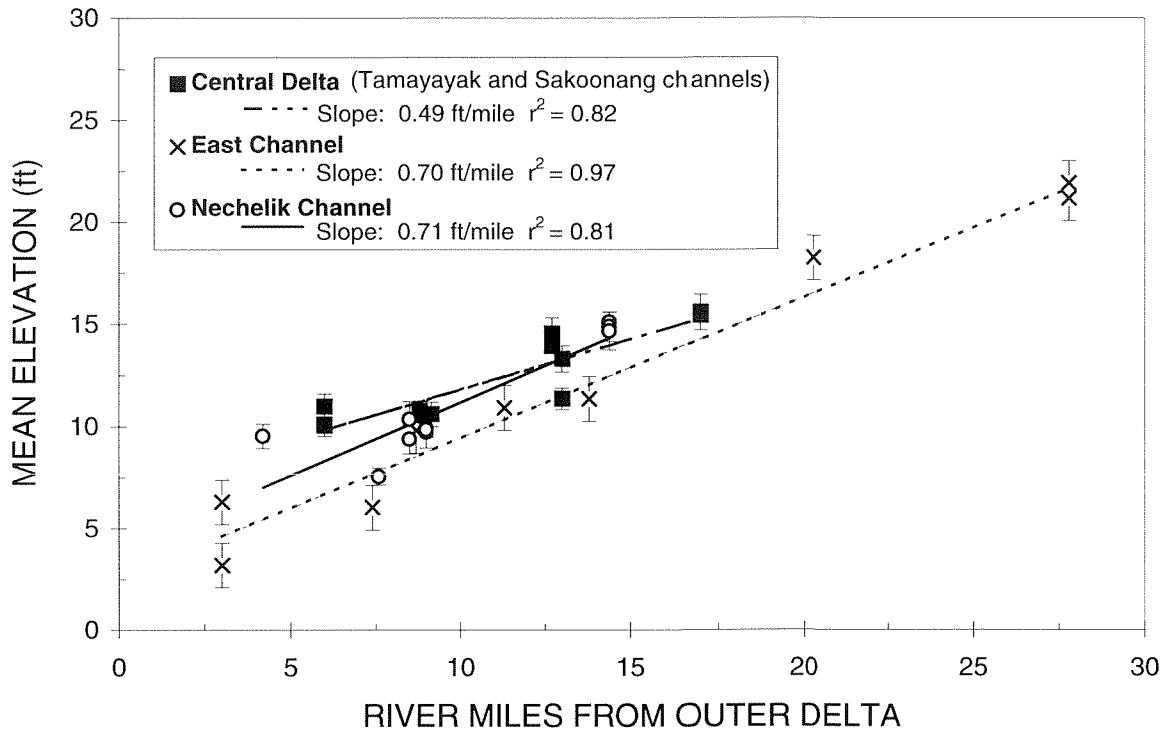
Flooding Region 4 includes the alluvial terraces and thaw basins on both sides of the delta.

Thaw basins that occur in the region were assigned to Class 5 because they are isolated from the floodplain.

Within these four broad regions, the terrain units were assigned a flood-frequency class. The rationale for assigning terrain units to the various flood-frequency classes, the range in relative heights of terrain units grouped into the classes, and how these relative heights correspond to flood stages at the head of the delta are described below.

Flood-frequency Class 1 includes delta riverbed/sandbars, tidal flats, shallow riverine ponds, and tidal rivers (Table 5–1). On delta riverbed/sandbar deposits, flooding is sufficiently frequent that vegetation cannot develop (except

Figure 5-10. Mean elevations (\pm SD) of the surface of inactive-floodplain cover deposits relative to distance in river miles from the outer edge of the delta, Colville River Delta, 1995.



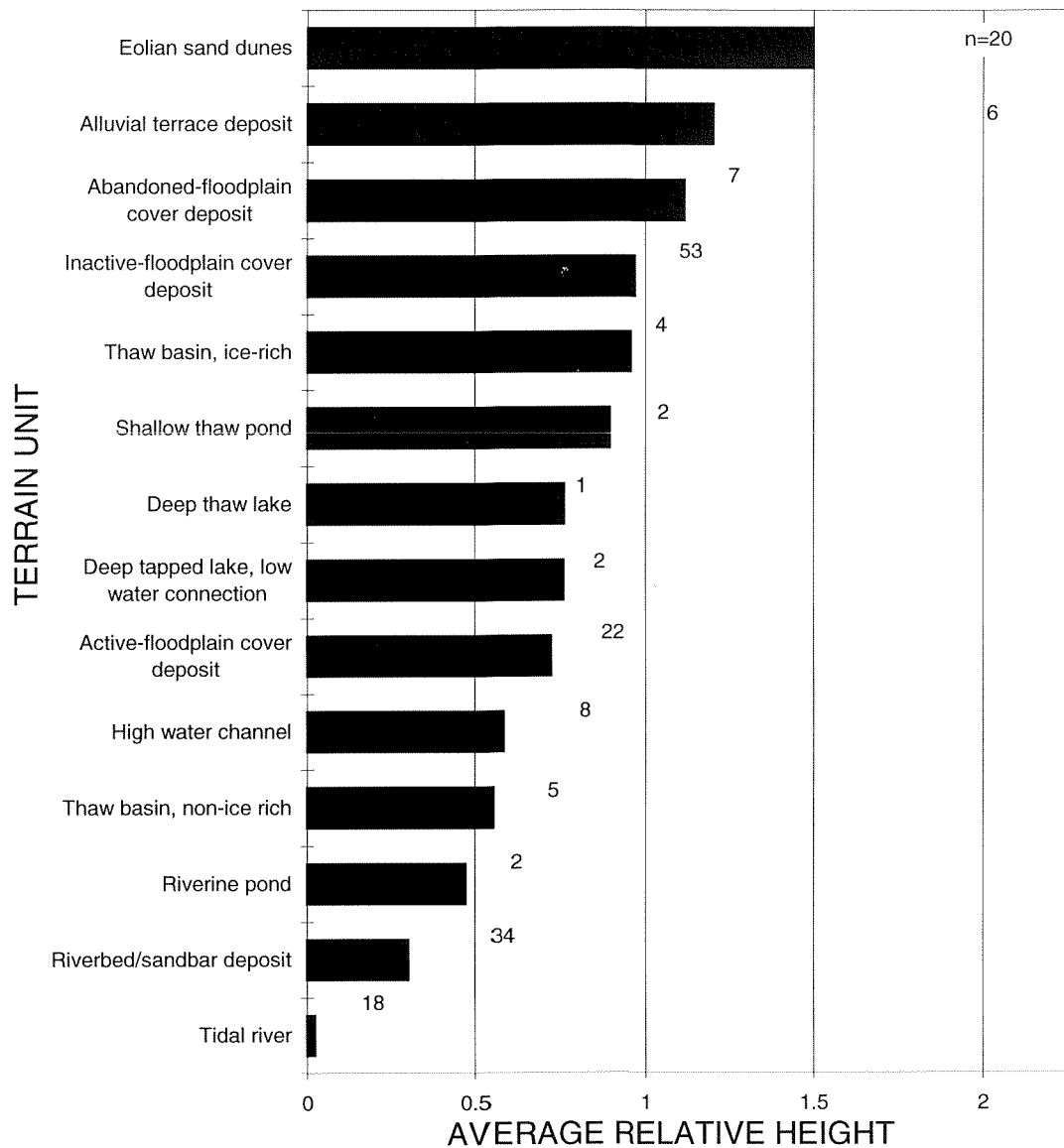
pioneer vegetation along margins) and organic matter cannot accumulate. This class was assigned a flood frequency of every 1–2 yr, because most of the terrain units in this class have been flooded every year from 1992 to 1995. The mean relative heights, plus one standard deviation (1 SD was added so that values represent 82% of the deposits instead of 50%), of these terrain units range from 0.10 to 0.56. At the head of the delta (Cross Section E27.09), a relative height of 0.56 corresponds to a flood stage of 11.5 ft.

Flood-frequency Class 2 includes delta active-floodplain cover deposits, ice-poor thaw basins, high-water channels, and tapped lakes with high-water connections (Table 5-1). On active-floodplain cover deposits, the extensive development of riverine shrub communities that depend on the input of nutrients associated with sediment deposition, the lack of organic matter accumulation, and the abundance of driftwood indicate that flooding is still frequent. This class was assigned a flood frequency of every 3–4 yr because none of its terrain units were entirely flooded during our monitoring, but they were

partially flooded (26.8 to 58.9%) during the highest flood water in 1993. The mean relative heights, plus one standard deviation, range from 0.67 to 0.84. At the head of the delta (Cross Section E27.09), a relative height of 0.84 corresponds to a flood stage of 17.2 ft.

Flood-frequency Class 3 includes inactive-floodplain cover deposits and the deep and shallow thaw ponds that usually are associated with these ice-rich deposits. On inactive-floodplain cover deposits, the development of a well-established vegetation community and accumulation of peat indicate that flood frequency has decreased substantially. The surface soils show distinct interceding of peat and mineral horizons, however, indicating periodic flooding. This class was assigned a flood frequency of every 5–25 yr because most of these terrain units were not flooded during 1992–1995. The upper limit of 25 yr was assigned because the presence of driftlines and sediment deposition (see Part 10) indicates that nearly all inactive-floodplain cover deposits were flooded in 1989 (the largest flood that Jim Helmericks has observed in his ~30 yr on

Figure 5–11. Mean relative heights (\pm SD) of terrain units relative to inactive cover deposits occurring along cross-sectional profiles, Colville River Delta, 1995.



the delta). Obviously, there is substantial uncertainty about the upper flood-frequency estimate, because we have no observations at high-flood stages. Mean relative heights, plus one standard deviation, of these terrain units range from 0.75 to 1.07. At the head of the delta (Cross Section E27.09), a relative height of 1.07 corresponds to a flood stage of 21.9 ft.

Flood-frequency Class 4 includes abandoned-floodplain cover deposits in the central delta. Our

inability to detect fluvial sediment and the lack of driftwood on most deposits in the central delta indicate that flooding is rare. This class was assigned a flood frequency of every 26–150 yr because most of these units were not flooded during 1992–1995, but the presence of driftlines and sediment deposition indicates that at least some of these deposits were flooded in 1989. As with Class 3, there is great uncertainty about the flood frequency of this class. Mean relative height, plus

one standard deviation, of this terrain unit is 1.23. At the head of the delta (Cross Section E27.09), a relative height of 1.23 corresponds to a flood stage of 25.2 ft.

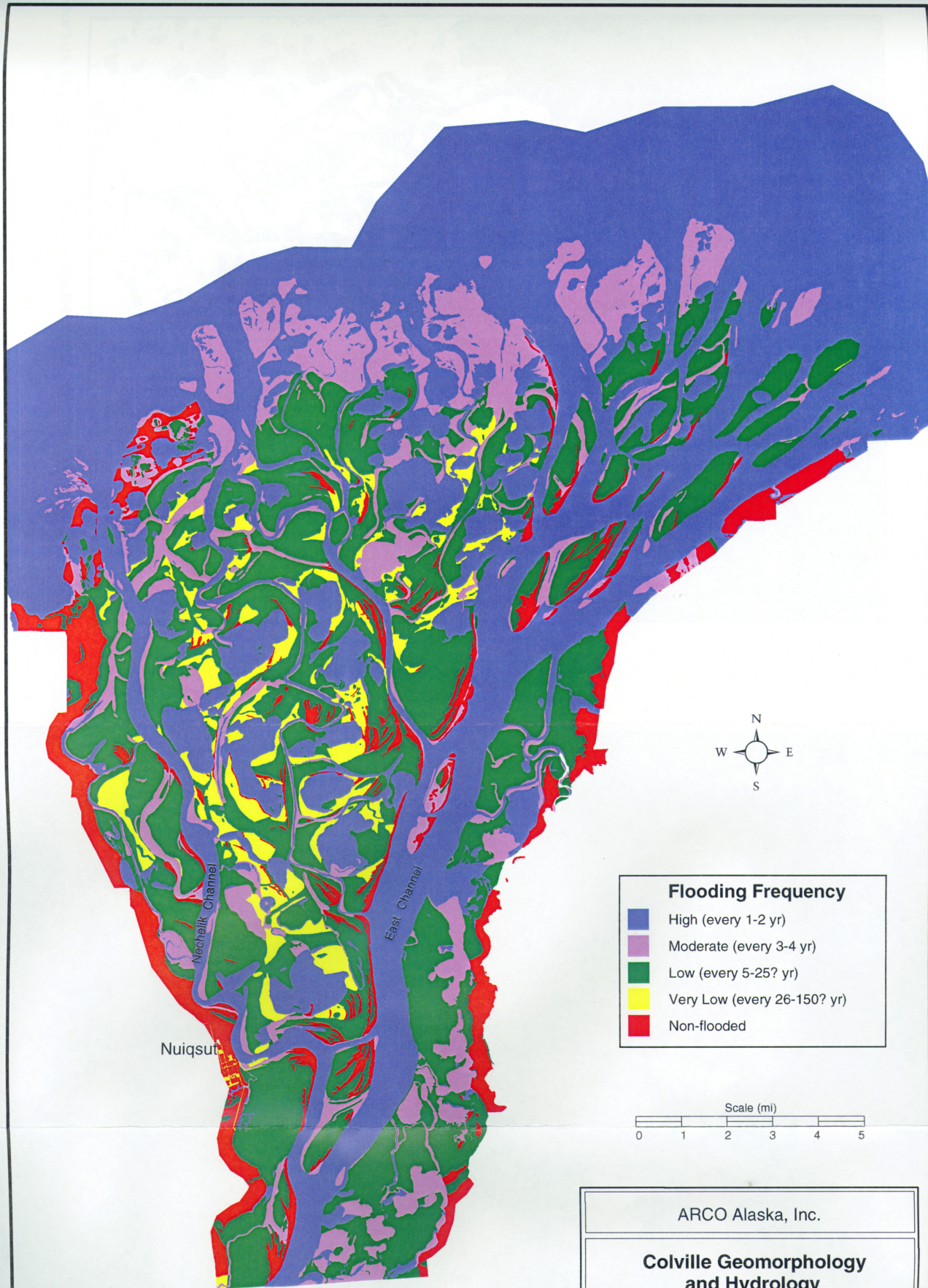
Estimating flood frequency for the abandoned-floodplain cover deposits is problematic because of the lack of data, but an analysis of material accumulation rates also suggest that flooding of the abandoned-floodplain cover deposits in the central delta is rare. Using values for peat depths (1.80 ft and 2.07 ft) at the surface and ages at the bottom of the peat (1950 and 3550 yr, respectively) for two sites (X11.9, X12.9) in the central delta, estimates of flood frequency were calculated using two sets of assumptions. Based on values that assume (1) that 20% of each profile is mineral material deposited by flooding (although very little mineral material was observed) and (2) a silt deposition rate of 0.003 ft/flood (although depths of 0.05–0.06 ft were observed from the 1989 flood), flooding intervals of 17–28 yr were calculated for these profiles. Based on a more realistic value that assumed that 5% of the profile is mineral material deposited by flooding and a low silt deposition rate of 0.007 ft/flood, flood intervals of 142–225 yr were calculated. Given the uncertainty involved, we believe that an appropriate estimate of the flood frequency is 25–150 yr.

Flood-frequency Class 5 includes eolian sand and alluvial terraces. We do not consider these units to be affected by flooding under the current flooding regime. The small amount of flooding observed on these terrain units during 1992–1995 occurred almost entirely along the margins of the units. There are some small, low patches of eolian sand, however, that occur in the middle the barren riverbed/sandbar deposits that are subject to flooding. Mean relative heights, plus one standard deviation, of this unit range from 1.79 to 1.88.

Results of the model of flood distribution are presented in Figure 5–12. Comparison of the predicted flood distribution, developed from data collected in 1992–1995, with actual flood distributions from flooding maps (Figures 5–13 and 5–14) developed by Walker (1976 and unpubl. data), reveals a fairly high correspondence at the higher flood-frequency classes (Classes 1 and 2). Thus, the delineation of areas with different flooding frequencies through this simplified modeling approach should be useful in locating oilfield facilities in areas that are least prone to

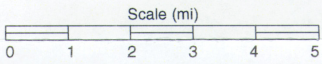
flooding and that will minimize the obstruction of flood water.

Although there is uncertainty over the flood-frequency estimates for the less-frequently flooded classes (3 and 4), improving the reliability of these estimates for both inactive-floodplain and abandoned-floodplain cover deposits will be difficult; it will take decades of observations to provide sufficient data for adequate analysis. In addition, the topographic differences between the two deposits are small, so developing high-resolution topographic maps to differentiate this small amount of relief is impractical. The results of the soil stratigraphy surveys (Part 10), however, indicate that the differences in flood frequency between these two deposits are substantial. Additional data, particularly from Flooding Region 1 along the eastern side of the East Channel (where data are sparse), would help confirm differences in flood frequencies among terrain units and flooding regions.



Flooding Frequency

- High (every 1-2 yr)
- Moderate (every 3-4 yr)
- Low (every 5-25? yr)
- Very Low (every 26-150? yr)
- Non-flooded



ARCO Alaska, Inc.	
Colville Geomorphology and Hydrology	
Figure 5-12. Predicted flood frequency, Colville River Delta, 1995	
08/15/1996	File: FLODFREQ.PRJ

Flood-frequency model based on relative heights of terrain units and analysis of flood distribution, 1992-1995
 Map registered to SPOT image base map.
 Projection: UTM Zone 5, Datum NAD 27

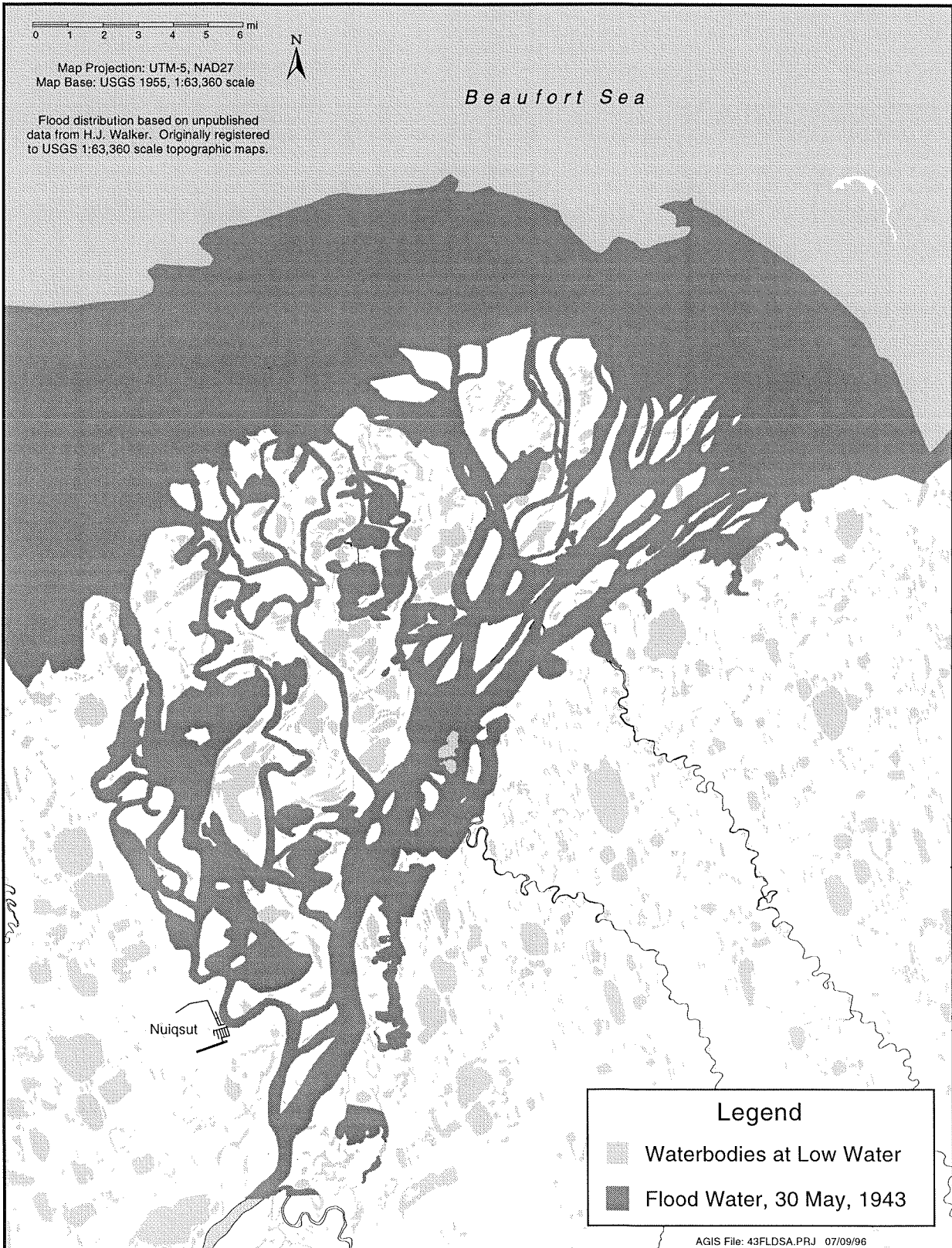


Figure 5–13. Map of flood distribution on 30 May 1943, Colville River Delta (adapted from Walker, unpubl. data).

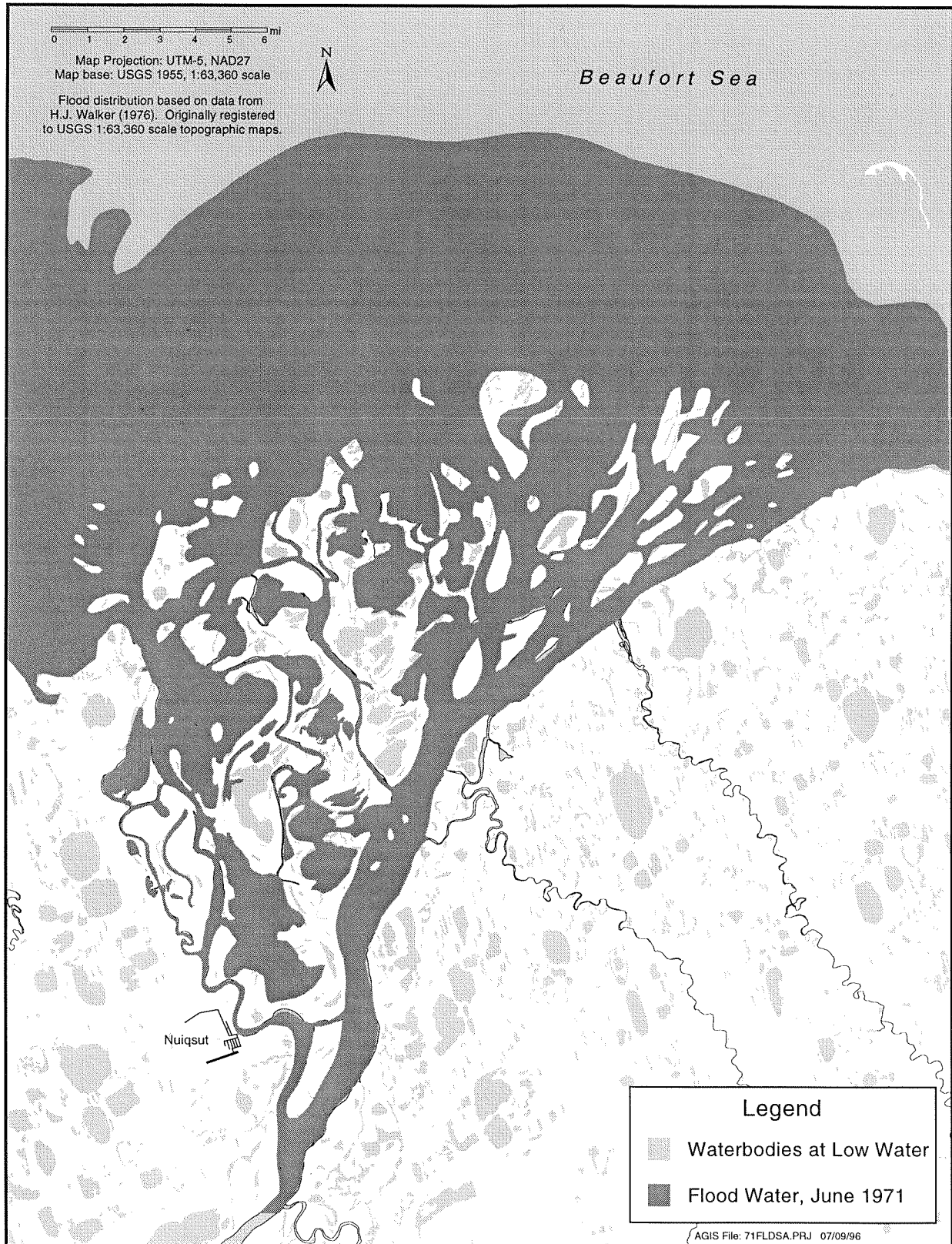


Figure 5-14. Map of flood distribution in early June 1971, Colville River Delta (adapted from Walker 1976).

PART 6. SUMMER- THROUGH WINTER-FLOW CONDITIONS

by Scott R. Ray and James W. Aldrich

BACKGROUND

The flows in the Colville River during the summer, fall, and winter are typically much less than those experienced during spring breakup. Because these flow conditions occur during most of the year, this information is useful for oil-spill contingency planning. Additionally, the low flow during the winter months allows seawater to intrude up the river, possibly creating corrosive conditions for a period of time and influencing the behavior of fish.

METHODS

The data presented in this section were collected primarily by others. The information is presented here to provide a more complete picture of the hydrology of the Colville River Delta.

RESULTS AND DISCUSSION

DISCHARGE

Walker and McCloy (1969) described the summer flow in the Colville River as a period of low flow during dry periods and higher flows during rainy periods. Data collected thus far support this description. Continuous flow data (Figure 1-1) were collected at the head of the delta in both 1962 and 1977 (Arnborg et al. 1966, USGS 1978). In general, flows after breakup are lower and range between 10,000 and 75,000 cfs. The average flows between 1 July and 30 September were 38,000 cfs and 20,000 cfs during 1962 and 1977, respectively. Scattered measurements made in 1992 and 1995 generally were between the 1962 and 1977 measurements (Figure 1-1).

The rate of flow in the Colville River continues to decrease in the fall until, according to Walker (1983a), it ceases to flow sometime during the winter. Several attempts to measure the discharge during the winter have yielded velocity readings of zero (Walker 1973b). However, the possible flow

area of channels under the ice may be as high as 10,000 ft². Because the minimal detectable velocity for many current meters is 0.1 fps, flows as high as 1000 cfs could go undetected. In discussions following Walker (1973b), researchers reported flow upstream of the delta in March and April. In particular, a discharge measurement note from the USGS reported that on 1 May 1969 water movement was seen 1 mi southeast of Umiat but was insufficient to turn the vanes on the current meter. The USGS estimated that the observed flow could have been as high as 300 cfs. Thus, based on the information at this time, late-winter flows probably range between 0 and something less than 1000 cfs.

SALINITY

As river discharge decreases, the freshwater within the lower channels is replaced by seawater (Arnborg et al. 1966). Moulten (1995) reported salinity measurements as high as 17 ppt near Nuiqsut and 23 ppt near Nanuk Lake in the Nechelik Channel during late November. By late winter, when maximal freshwater/seawater exchange has occurred, the influence of seawater can reach as far as 37 mi upstream (Walker 1973a). Salinities within the delta during this time can be as high as 44 ppt (Walker 1973a), with isolated pockets as high as 50 to 60 ppt (Schell and Hall 1972).

WATER TEMPERATURES

Water temperatures in the Colville River probably are near or slightly above 0°C early in breakup, while there is still ice in the channel. However, the water warms quickly once the ice is gone. In 1977, the discharge at the head of the delta peaked on 7 June, and the channel was free of ice by 9 June (USGS 1978). The water temperature only 1 day later (10 June) was 6°C, and temperatures for most of the summer of 1977 varied between 10°C and 18°C (USGS 1978). The water temperature began to drop in late August and was approximately 6°C in early September. Water temperatures measured in late August 1995 generally were between 6°C and 11°C. Water temperatures in November and December ranged between -1°C and 2°C (Moulten 1986).

PART 7. BARGE ACCESS

by Scott R. Ray and James W. Aldrich

BACKGROUND

Barges have been used on the Colville River in the past to supply Nuiqsut with cargo ranging from fuel to construction materials. Supplies for oil-well drilling were barged in the early 1960s. However, sediment deposits offshore may limit the size of the barges that can enter the channels on the delta. In addition, travel upriver by the large barges may be limited by shallow reaches within the river. The purpose of this task was to evaluate the potential for barge access on the East, Kupigruak, and Nechelik channels

METHODS

OFFSHORE

Kupigruak Channel

Barge access offshore from the Kupigruak Channel was evaluated by developing a bathymetric map of the entrance to the channel. The map was developed with data on water depths that were collected in late August 1995 with a Lowrance Model X25 fathometer and a Trimble Pro XL DGPS. A staff gage in the Colville River at the Helmerick's residence was read and the water level recorded periodically during the day (Appendix B).

Nechelik Channel

Bathymetric data were not collected offshore from the Nechelik Channel. Instead, a preliminary estimate of the length of channel that might require dredging, to provide access to the lower Nechelik Channel from Harrison Bay, was based primarily on mapping previously prepared by Aeromap Inc. (hereafter referred to as "the Aeromap drawing"). The Aeromap drawing was prepared from USGS 1:63,360-scale quadrangle maps. Bathymetric data were collected at the mouth of the Nechelik Channel in mid June 1995 with a Lowrance Model X25 fathometer and a Garmin 45 GPS.

The distance between the 6-ft-depth offshore contour on the Aeromap drawing and the end of the 6-ft-deep channel in the lower Nechelik Channel

was estimated. This distance approximates the length of dredging that might be required to bring in a barge with a draft on the order of 5 ft. To evaluate how well the Aeromap drawing represents present conditions, the Aeromap drawing offshore from the Kupigruak Channel was compared with the 1995 bathymetric data collected offshore from the Kupigruak Channel. For lack of a better method, we assumed that the accuracy of the Aeromap drawing in the vicinity of the Kupigruak Channel is representative of the accuracy of the drawing in the vicinity of the Nechelik Channel.

WITHIN CHANNELS

Kupigruak And East Channels

Cross sections were measured at locations that might limit the movement of barges upriver; i.e., shallow locations identified by the thalweg profile measurements (see Part 2). The data for the cross sections were collected in late August 1995 with a Lowrance Model X25 fathometer and a Trimble Pro XL DGPS. In areas where the thalweg shifted from one side of the river to the other, multiple cross sections were obtained and a bathymetric map of the channel bottom was developed.

Nechelik Channel

The width of the Nechelik Channel at depths of 5, 8, and 11 ft was estimated from the cross section data collected by H. J. Walker in late July 1962 (Walker 1983b) and from the cross section data collected for this project in mid June 1995. The analysis of channel bathymetry included 79 cross sections from 1962 and 6 cross sections from 1995.

A cursory comparison of the six cross sections from 1995 and the closest cross sections from 1962 indicates that channel bathymetry may have changed significantly. These differences in channel widths may be due to a variety of factors, including inaccuracies in the 1962 and 1995 measurements and changes in channel geometry. Because the 1995 measurements used more sophisticated technology, the measurements are believed to be considerably more precise than the 1962 measurements. The 1962 depth measurements were made with a fathometer. Horizontal distances were estimated from the estimated speed of the boat and the time to cross the channel. The 1995 depth measurements

were made using a sounding weight or a Lowrance Model X25 fathometer (experience indicates that measured depth is within 5% of actual depth). Horizontal distances in 1995 were measured using a Garmin Model 45 GPS (position accuracy within 328 ft), a Trimble Pro XL DGPS (position accuracy within 16 ft), or a theodolite. As a result, a range of likely channel widths were estimated for the Nechelik Channel at each of the above-referenced depths.

For each of the six cross sections measured in 1995, ratios were developed between the 1962 and the 1995 cross section widths. The maximal 1962/1995 width ratio for depths of 5, 8, and 11 ft were 1.67, 1.28, and 1.31, respectively. Dividing the width of the other 1962 cross sections by these ratios results in an estimate of the smallest probable width. The maximal likely width was taken as the unadjusted widths of the 1962 cross sections.

In developing the width ratios, no adjustment was made for possible differences in water-surface elevations at the time of the measurements. Although no data on water-surface elevation are available for the 1962 cross sections, stage observations and stage-discharge relationships at the head of the delta on the days of the measurements indicate that the elevations at the time of the two measurements probably were within 1 ft of each other along the lower and middle Nechelik Channel.

Putu Channel

An analysis of cross section widths similar to that for the Nechelik Channel also was conducted for the Putu Channel. However, no adjustment factors were applied to the widths of the 1962 cross sections, because there were no 1995 data to use in calculating adjustment factors.

RESULTS AND DISCUSSION

OFFSHORE

Kupigruak Channel

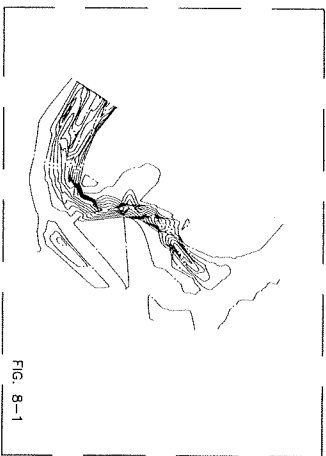
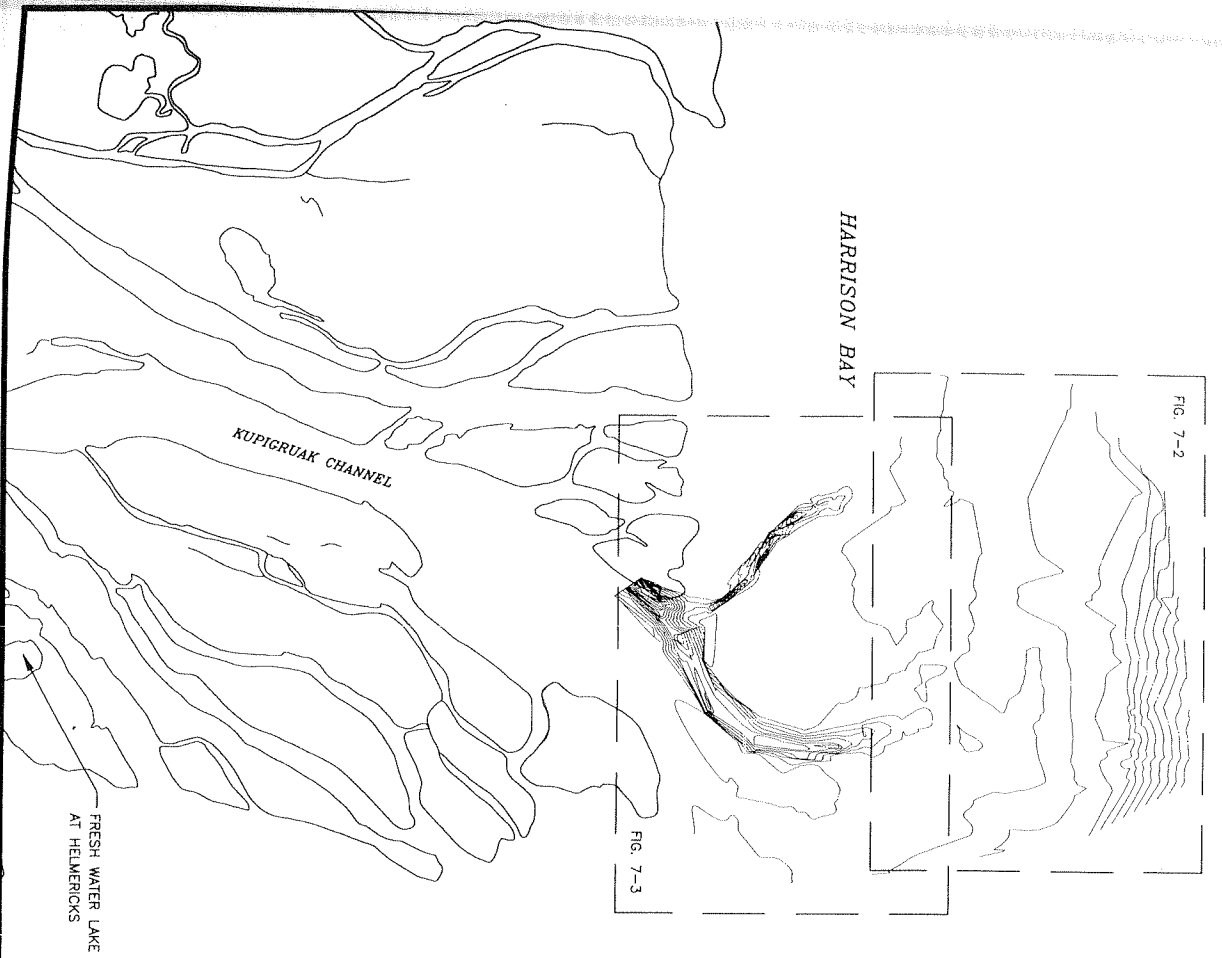
The bathymetric map created offshore from the Kupigruak Channel is presented in Figures 7-1 through 7-3. D-size drawings of Figures 7-1 through 7-3 and the data collected offshore and used to create the bathymetric maps are presented in Appendix F. Near its mouth the channel forks into a

small, poorly defined channel that flows towards the north west, and a well-defined channel that continues towards the north. Thalweg depths in the well-defined channel are approximately 15 ft at the channel fork and gradually decline to 6 ft approximately 1.9 mi downstream from the fork, at a location where the channel loses its definition. The depth of water beyond the channel generally averages 3-4 ft. Farther offshore from this point, the depth of water increases rapidly. The distance between the downstream end of the 6-ft-depth contour in the Kupigruak Channel and the 6-ft-depth contour in Harrison Bay is approximately 1.6 mi. It probably is another 0.2 mi to the 8-ft-depth contour in Harrison Bay.

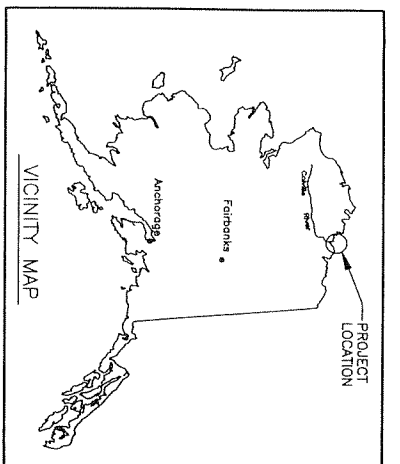
Nechelik Channel

Based on the 1995 field measurements at the mouth of the Nechelik Channel and the Aeromap drawing, the distance from the 6-ft-depth contour in the Nechelik Channel to the 6-ft-depth contour in Harrison Bay is approximately 4 mi (Figure 7-4). The depth of water between the two 6-ft-depth contours probably averages about 3-4 ft. However, this depth estimate is based only on two spot depths that appear on the Aeromap 1:63,360-scale drawing. From limited experience, we know that the area immediately offshore from the Nechelik Channel is shallow. The additional distance to the 8-ft-depth contour in Harrison Bay probably is 0.7 mi.

The 1995 field measurements were used to locate the 6-ft-depth contour at the mouth of the Kupigruak Channel, and the Aeromap drawing was used to locate the 6-ft-depth contour in Harrison Bay. Based on this technique, the estimated distances between the 6-ft-depth contour in the Kupigruak Channel and the 6-ft-depth contour in Harrison Bay is approximately 2 mi (Figure 7-5). The 8-ft-depth contour in Harrison Bay is an additional 0.2 mi. If only the 1995 field data are used, however, these estimated distances are approximately 1.6 mi and an additional 0.2 mi, respectively. Based on the difference between these estimates, the actual distance between the two 6-ft-depth contours at the mouth of the Nechelik Channel may be on the order of ± 0.5 mi of the estimated distance presented above (i.e., 4 mi ± 0.5 mi).



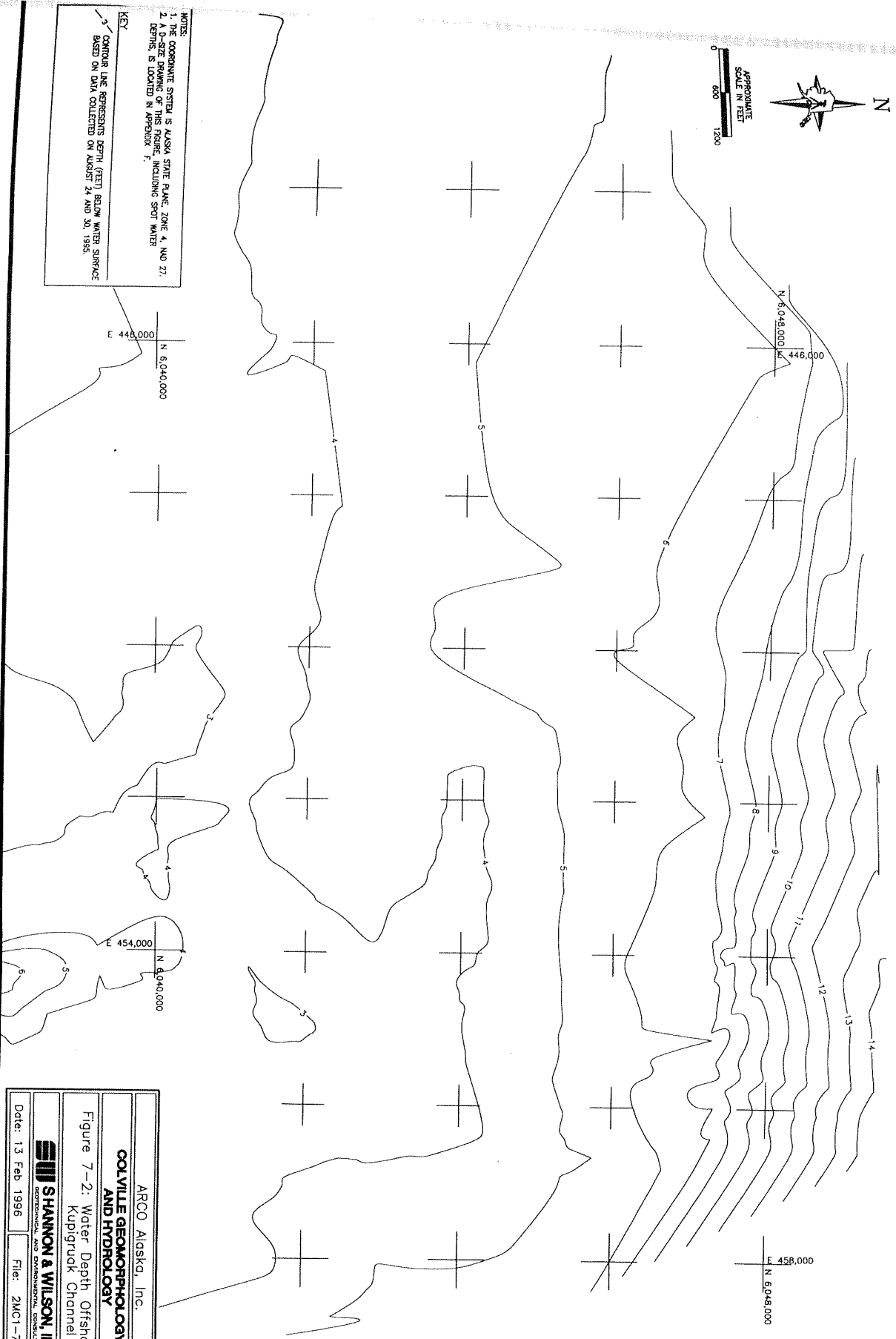
APPROXIMATE
SCALE IN FEET
0 2500 5000



ARCO Alaska, Inc.	
COVILLE GEOMORPHOLOGY AND HYDROLOGY	
Figure 7-1: Offshore Bathymetry Location Map	
SHANNON & WILSON, INC. <small>GEOTECHNICAL AND ENVIRONMENTAL CONSULTANTS</small>	
Date: 13 Feb 1996	File: 21007-1.DWG



APPROPRIATE
SCALE IN FEET
0 500 1000



NOTES:
1. THE COORDINATE SYSTEM IS ALASKA STATE PLANE, ZONE 4, NAD 27.
2. A D-SIZE DRAWING OF THIS CHART, INCLUDING SPOT WATER DEPTHS, IS LOCATED IN APPENDIX 7.
KEY:
3. CONTOUR LINE REPRESENTS DEPTH (FEET) BELOW WATER SURFACE BASED ON DATA COLLECTED ON AUGUST 24 AND 26, 1995.

ARCO Alaska, Inc.
**COLVILLE GEOMORPHOLOGY
AND HYDROLOGY**
Figure 7-2: Water Depth Offshore of
Kupigruok Channel (North)
SHANNON & WILSON, INC.
GEOTECHNICAL AND ENVIRONMENTAL CONSULTANTS
Date: 13 Feb 1996 File: 2MC1-7.2.DWG




NOTES:

1. THE COORDINATE SYSTEM IS ALASKA STATE PLANE, ZONE 4, NAD 27.
2. A D-SIDE DRAWING OF THIS FIGURE, INCLUDING SPOT WATER DEPTHS, IS LOCATED IN APPENDIX F.

KEY:

— CONTOUR LINE REPRESENTS DEPTH (FEET) BELOW WATER SURFACE
 BASED ON DATA COLLECTED ON AUGUST 24 AND 30, 1995.

ARCO Alaska, Inc. COLVILLE GEOMORPHOLOGY AND HYDROLOGY	
Figure 7-3: Water Depth Offshore of Kupigruak Channel (South)	
 SHANNON & WILSON, INC. <small>GEOTECHNICAL AND ENVIRONMENTAL CONSULTANTS</small>	
Date: 13 Feb 1996	File: 2MCI-7-3.DWG

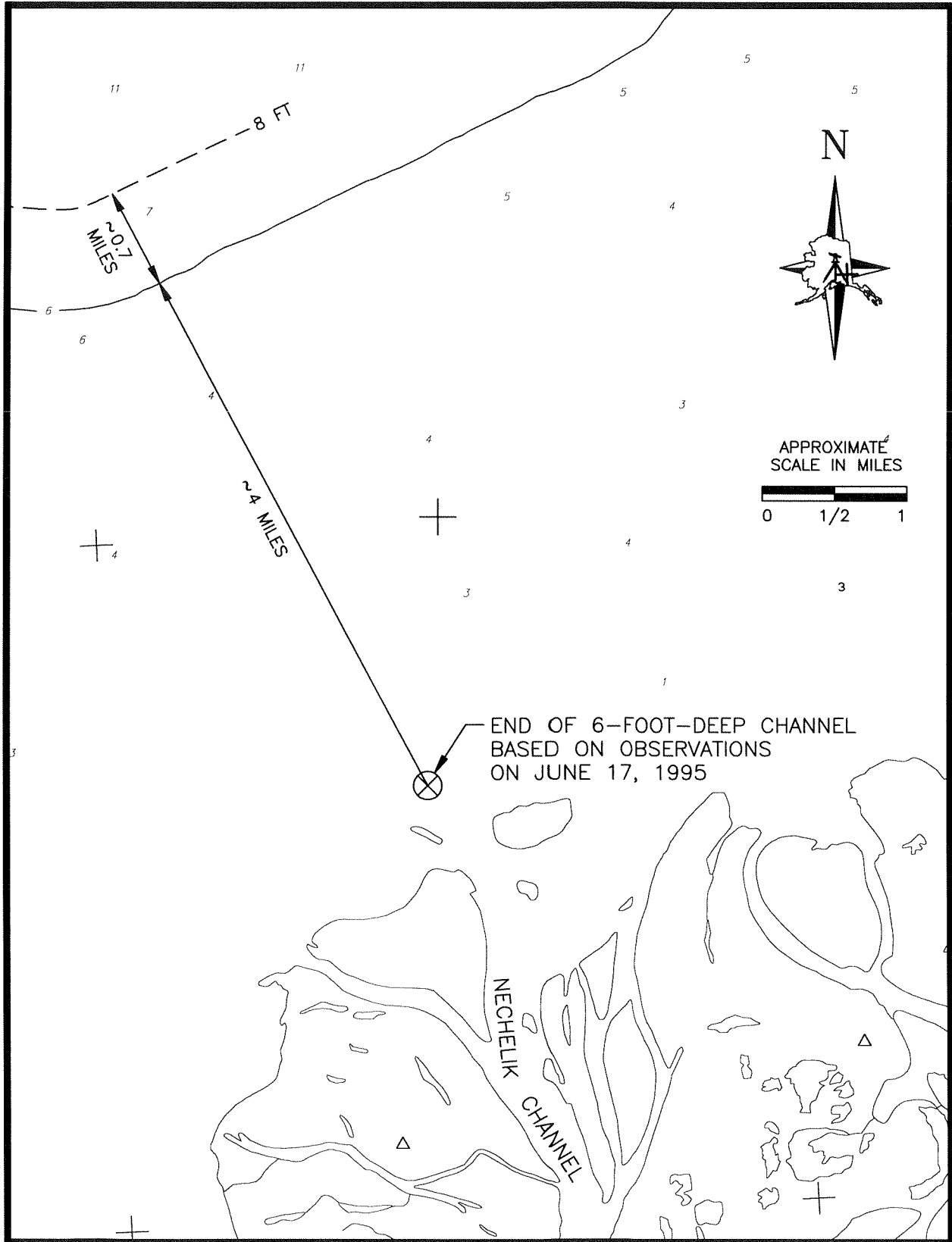


Figure 7-4. Contours offshore from the Nechelik Channel.

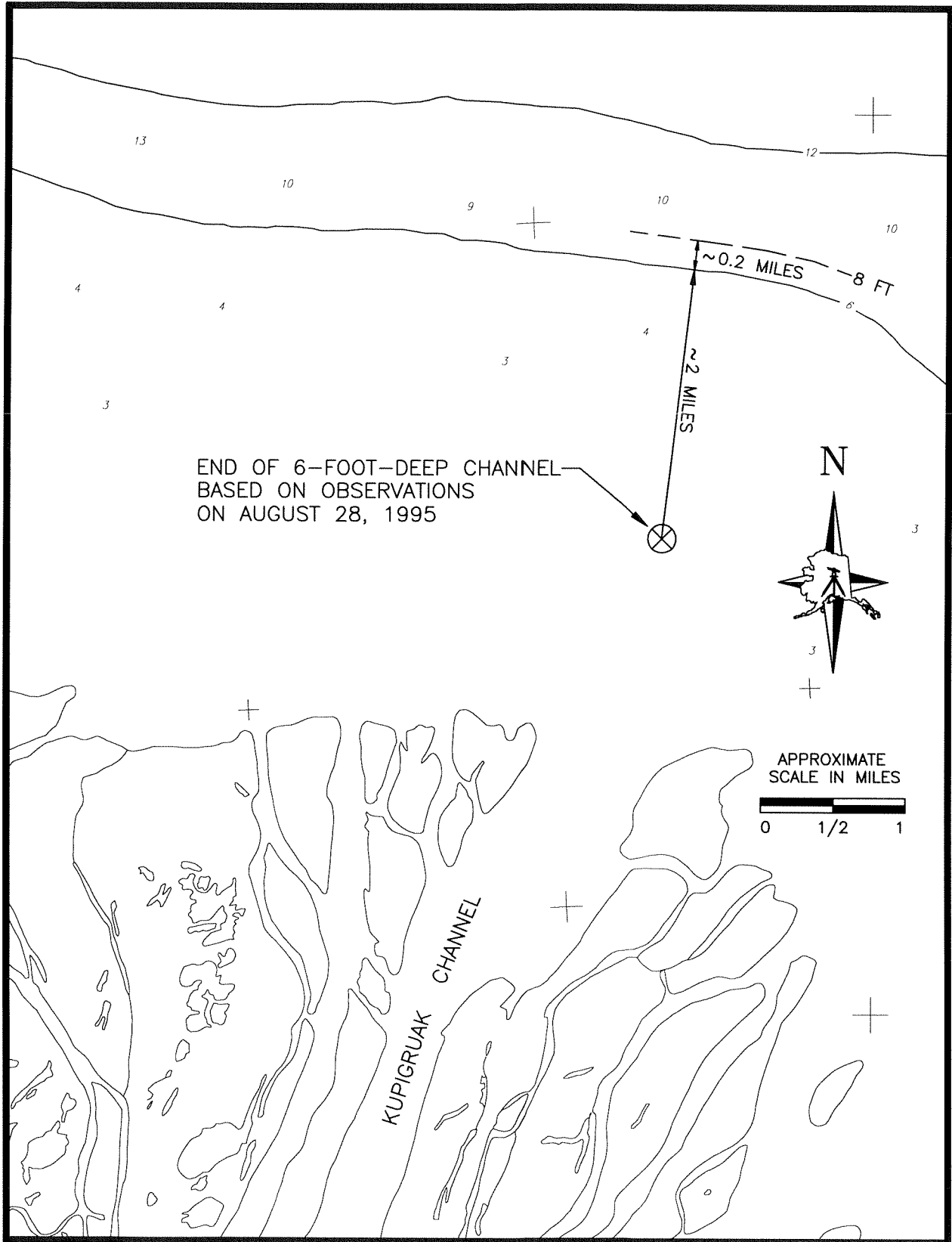


Figure 7-5. Contours offshore from the Kupiguak Channel

WITHIN CHANNELS

Kupigruak and East Channel

Because the water depth at a location varies with the water-surface elevation, it should be noted that the water-depth data were collected in late August 1995 on the Kupigruak and East channels, and in mid June 1995 on the Nechelik Channel. In general, the summer water-surface elevation at the head of the delta varies between 1 ft and 7 ft (msl). The water-surface elevations at E27.09 in late August 1995 ranged between 2.8 ft and 3.0 ft (msl). The water-surface elevations at N7.46 were 1.6 ft and 0.7 ft (msl) in mid June and late August 1995, respectively. The variation of the water-surface elevation is greater at the head of the delta than it is at the outer delta. Thus, it is important when comparing cross section depths, to note when the data were collected and the relative location of the cross section within the delta.

In general, thalweg depths in the Kupigruak and East channels are greater than 10 ft (Figures 2–9 and 2–10). Cross sections were measured at selected locations within the channel where the thalweg depth approached 10 ft (Figures 7–6 through 7–8). Channel widths at a depth of 10 ft generally are greater than a few hundred feet. The only exceptions occur near the head of the delta, in a location downstream from where the Nechelik Channel leaves the East Channel (Cross Sections E25.24 and E25.48). The width at a depth of 10 ft at Cross Section E25.24 is on the order of 100–150 ft. The maximal depth at Cross Section E25.48 is approximately 9 ft, and the width at a depth of 8 ft is on the order of 450 ft.

Bathymetric contour maps were developed in areas where the thalweg shifts from one side of the river to the other, or in areas where the channel seemed particularly shallow (Figures 7–9 through 7–12). These maps show that a depth of at least 10 ft is maintained as the thalweg moves from one side of the river to the other. The exception occurs at E19.31–E20.33 (Figure 7–12). At this location, there is an area that is less than 10 ft deep, but is approximately 400-ft wide at a depth of 8 ft.

Nechelik Channel

It appears that the lower Nechelik Channel between Cross Sections W42 and W80

(Figures 7–13 through 7–16) will probably have widths of at least 261 ft at depths of 5 and 8 ft (Table 7–1). We believe these widths are representative of those widths occurring during August.

At most of the cross sections between W10 and W41 (Figure 7–14), the width of the Nechelik Channel is at least 126 ft at a depth of 5 ft (Table 7–2). In 1962, however, the maximal depth of the channel at Cross Section W35 was only 3 ft. In June 1995, the maximal depth of the channel near this cross section was approximately 9 ft. Thus, the channel has deepened at this section. Between W29 and W35, the channel widths at a depth of 8 ft are considerably less than widths at other cross sections between W10 and W41. In one case, the width is 0 ft, and in another case, it is as little as 16 ft (Table 7–2).

The Nechelik Channel between Nuiqsut (Cross Section W10) and the Putu Channel has been dredged, and it is doubtful that meaningful data could be extrapolated from the 1962 cross sections. Based on the thalweg survey conducted in June 1995 and observations made in August, shallow areas (on the order of 3 ft) downstream from the Putu Channel hinder boat travel within this reach during periods of low flow.

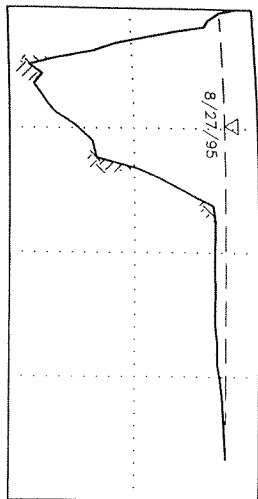
The width of the Nechelik Channel between the Putu Channel and the East Channel was not analyzed in this study. It is our experience that there are shallow areas within this reach (2–3 ft) that hinder boat travel during periods of low flow.

Putu Channel

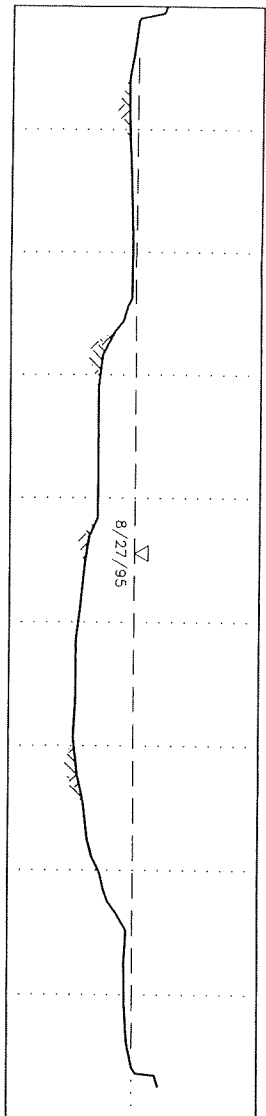
The results of the analysis suggests that the available width is significant (Table 7–3), however, it is likely that this is misleading. The Putu Channel has changed since the cross sections were measured in 1962, particularly at the confluence with the East Channel. The following is from Walker (1994b):

During the 1960's it [the Putu Channel] was traversable easily even during low stage. During the 1970's, some difficulty was encountered and, by the early 1990's, it became impossible to use it at low stage as a route between Nuiqsut and the main channel.

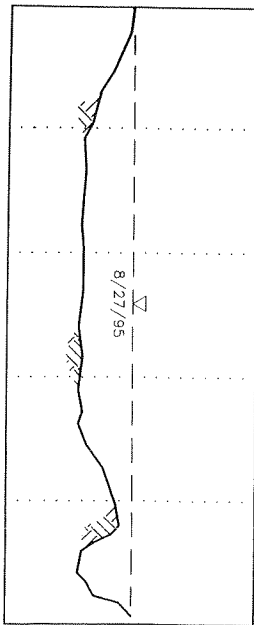
CROSS SECTION K3.20



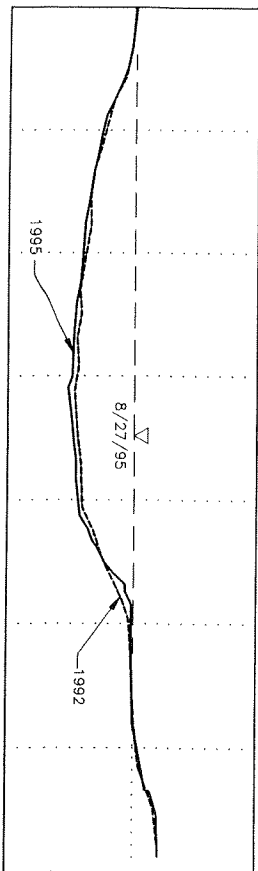
CROSS SECTION K6.59



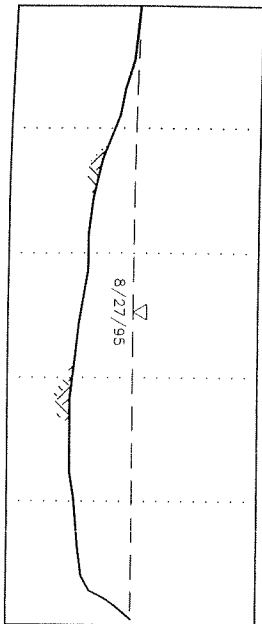
CROSS SECTION K9.72



CROSS SECTION K10.69



CROSS SECTION K14.53



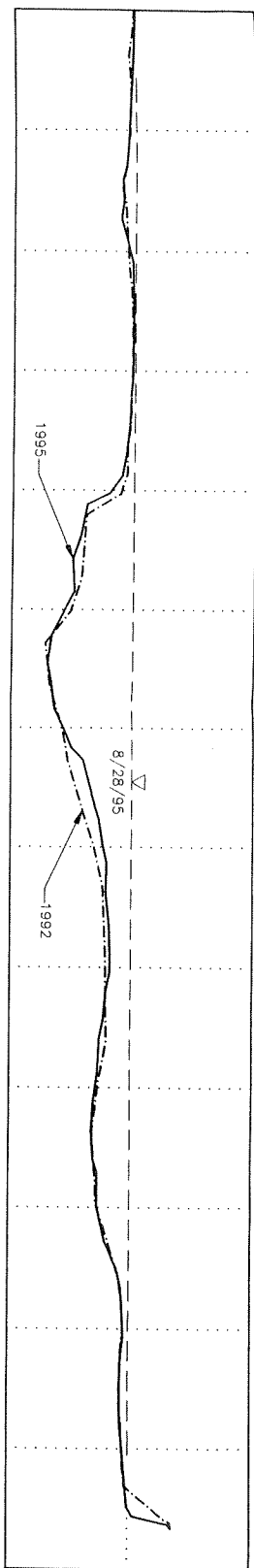
NOTES:

1. THESE CROSS SECTIONS WERE NOT TIED TO A KNOWN ELEVATION. TEMPORARY BENCH MARKS (TBM) WERE ESTABLISHED AT A FEW OF THE CROSS SECTIONS. THE DISTANCE ABOVE THE WATER SURFACE FOR EACH OF THE TBMS PLACED AT CROSS SECTIONS ON THIS SHEET ARE PRESENTED IN APPENDIX A.
2. HORIZONTAL LOCATIONS ALONG THE CROSS SECTION WERE ESTIMATED WITH A TRIMBLE PRO XL DGPS (POSITION ACCURACY WITHIN 16 FEET).
3. DEPTH MEASUREMENTS ALONG THE CROSS SECTION WERE MADE WITH A LOWRANCE MODEL X25 FATHOMETER. EXPERIENCE INDICATES THAT THE MEASURED DEPTH IS WITHIN FIVE PERCENT OF THE ACTUAL DEPTH.
4. THE APPROXIMATE LOCATION OF THE CROSS SECTIONS ARE SHOWN ON FIGURES 2-1 AND 2-10.
5. CROSS SECTION K10.69 HAS BEEN REFERRED TO AS CROSS SECTION 3 IN PREVIOUS REPORTS.

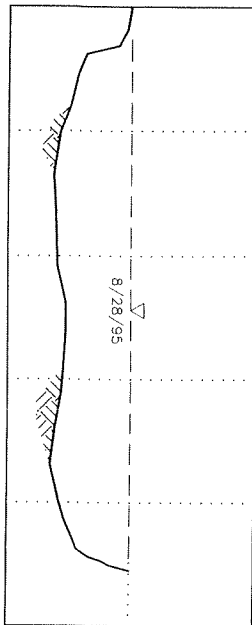
SCALE
 H: 1" = 300'
 V: 1" = 30'

ARCO Alaska, Inc.	
COLVILLE GEOMORPHOLOGY AND HYDROLOGY	
Figure 7-6:	Kupignuk Channel
Cross Sections	
SHANNON & WILSON, INC.	
GEOTECHNICAL AND ENVIRONMENTAL CONSULTANTS	
Date: 13 Feb 1996	File: 2XSECT-6.DWG

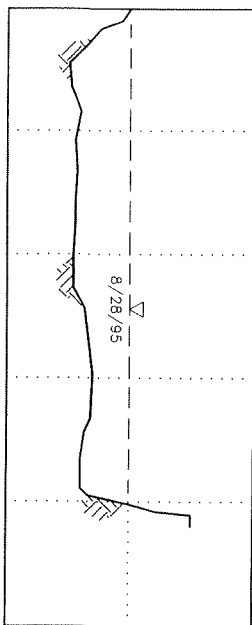
CROSS SECTION E14.20



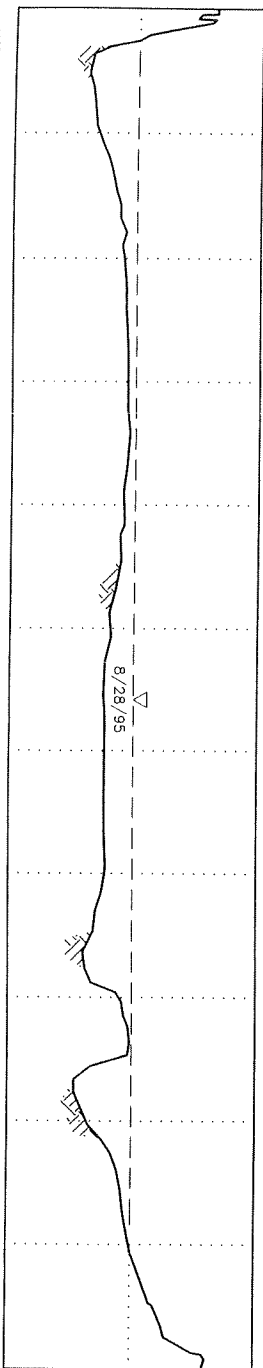
CROSS SECTION E17.30



CROSS SECTION E18.93



CROSS SECTION E25.24



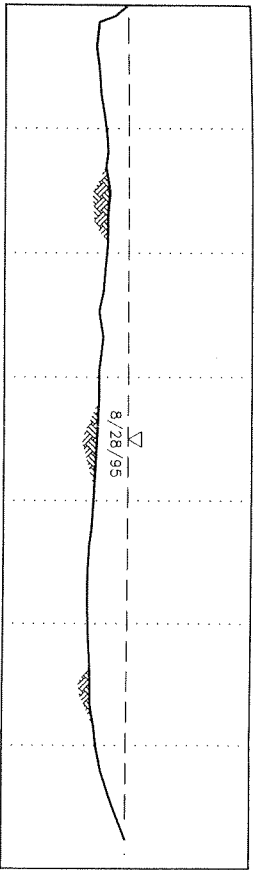
SCALE
 H: 1" = 300'
 V: 1" = 30'

NOTES:

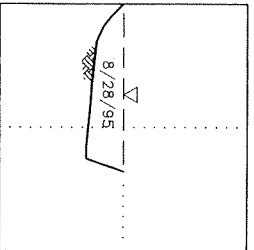
1. THESE CROSS SECTIONS WERE NOT TIED TO A KNOWN ELEVATION. TEMPORARY BENCH MARKS (TBM) WERE ESTABLISHED AT A FEW OF THE CROSS SECTIONS. THE DISTANCE ABOVE THE WATER SURFACE FOR EACH OF THE TBMS PLACED AT CROSS SECTIONS ON THIS SHEET ARE PRESENTED IN APPENDIX A.
2. HORIZONTAL LOCATIONS ALONG THE CROSS SECTION WERE ESTIMATED WITH A TRIMBLE PRO XL DGPS (POSITION ACCURACY WITHIN 16 FEET).
3. DEPTH MEASUREMENTS ALONG THE CROSS SECTION WERE MADE WITH A LOWRANCE MODEL X25 FATHOMETER. EXPERIENCE INDICATES THAT THE MEASURED DEPTH IS WITHIN FIVE PERCENT OF THE ACTUAL DEPTH.
4. THE APPROXIMATE LOCATIONS OF THE CROSS SECTIONS ARE SHOWN ON FIGURES 2-1 AND 2-9.
5. CROSS SECTION E14.20 HAS BEEN REFERRED TO AS CROSS SECTION 1 IN PREVIOUS REPORTS.

ARCO Alaska, Inc.	
COVILLE GEOMORPHOLOGY AND HYDROLOGY	
Figure 7-7:	East Channel Cross Sections
SHANNON & WILSON, INC. <small>GEOTECHNICAL AND ENVIRONMENTAL CONSULTANTS</small>	
Date: 13 Feb 1996	File: 2XSECT-7.DWG

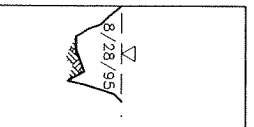
CROSS SECTION E25.48



CROSS SECTION E25.86



CROSS SECTION E26.31

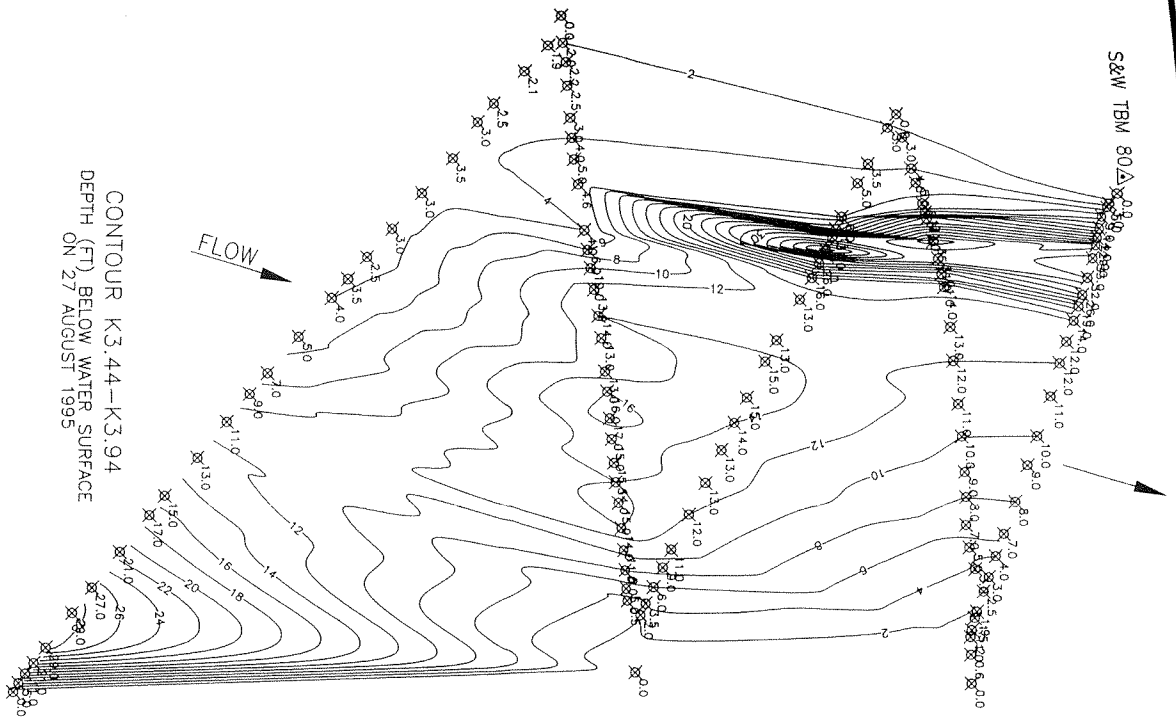


SCALE
 H: 1" = 300'
 V: 1" = 30'

NOTES:

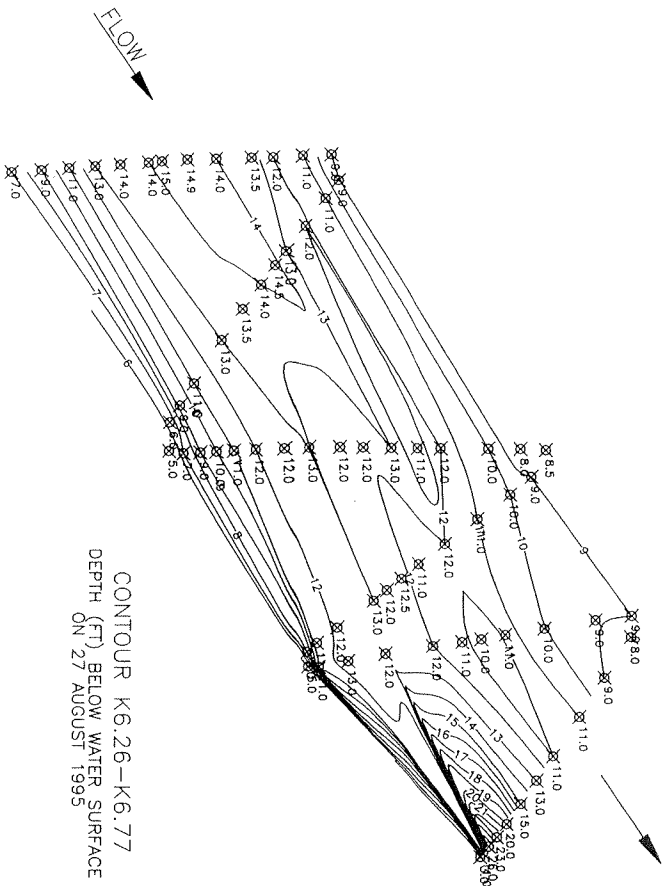
1. THESE CROSS SECTIONS WERE NOT TIED TO A KNOWN ELEVATION. TEMPORARY BENCH MARKS (TBM) WERE ESTABLISHED AT A FEW OF THE CROSS SECTIONS. THE DISTANCE ABOVE THE WATER SURFACE FOR EACH OF THE TBMS PLACED AT CROSS SECTIONS ON THIS SHEET ARE PRESENTED IN APPENDIX A.
2. HORIZONTAL LOCATIONS ALONG THE CROSS SECTION WERE ESTIMATED WITH A TRIMBLE PRO XL DGPS (POSITION ACCURACY WITHIN 16 FEET).
3. DEPTH MEASUREMENTS ALONG THE CROSS SECTION WERE MADE WITH A LOWRANCE MODEL X25 FATHOMETER. EXPERIENCE INDICATES THAT THE MEASURED DEPTH IS WITHIN FIVE PERCENT OF THE ACTUAL DEPTH.
4. THE APPROXIMATE LOCATIONS OF THE CROSS SECTIONS ARE SHOWN ON FIGURES 2-1 AND 2-9.

ARCO Alaska, Inc.	
COLVILLE GEOMORPHOLOGY AND HYDROLOGY	
Figure 7-8: East Channel Cross Sections (continued)	
SHANNON & WILSON, INC. GEOTECHNICAL AND DIMENSIONAL CONSULTANTS	
Date: 13 Feb 1996	File: 2XSECT-8.DWG

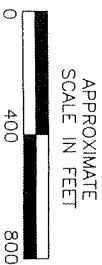


CONTOUR K3.44-K3.94
DEPTH (FT) BELOW WATER SURFACE
ON 27 AUGUST 1995

- NOTES:
1. HORIZONTAL LOCATIONS ALONG THE CROSS SECTION WERE ESTIMATED WITH A TRIMBLE PRO XL DGPS (POSITION ACCURACY WITHIN 16 FEET).
 2. DEPTH MEASUREMENTS ALONG THE CROSS SECTION WERE MADE WITH A LOWRANCE MODEL X25 FATHOMETER. EXPERIENCE INDICATES THAT THE MEASURED DEPTH IS WITHIN FIVE PERCENT OF THE ACTUAL DEPTH.
 3. A TEMPORARY BENCH MARK (TBM 80) WAS ESTABLISHED NEAR CONTOUR K3.44-K3.94 (AT LATITUDE 70.455648N AND LONGITUDE 150.481277W). PRESENTLY, THE TBM HAS NOT BEEN TIED TO A KNOWN ELEVATION. THE DISTANCE ABOVE THE WATER SURFACE FOR TBM 80 WAS 4.37 FEET ON 27 AUGUST 1995 AT 1045.
 4. THE APPROXIMATE LOCATIONS OF THE CONTOUR MAPS ARE SHOWN ON FIGURES 2-1 AND 2-10.

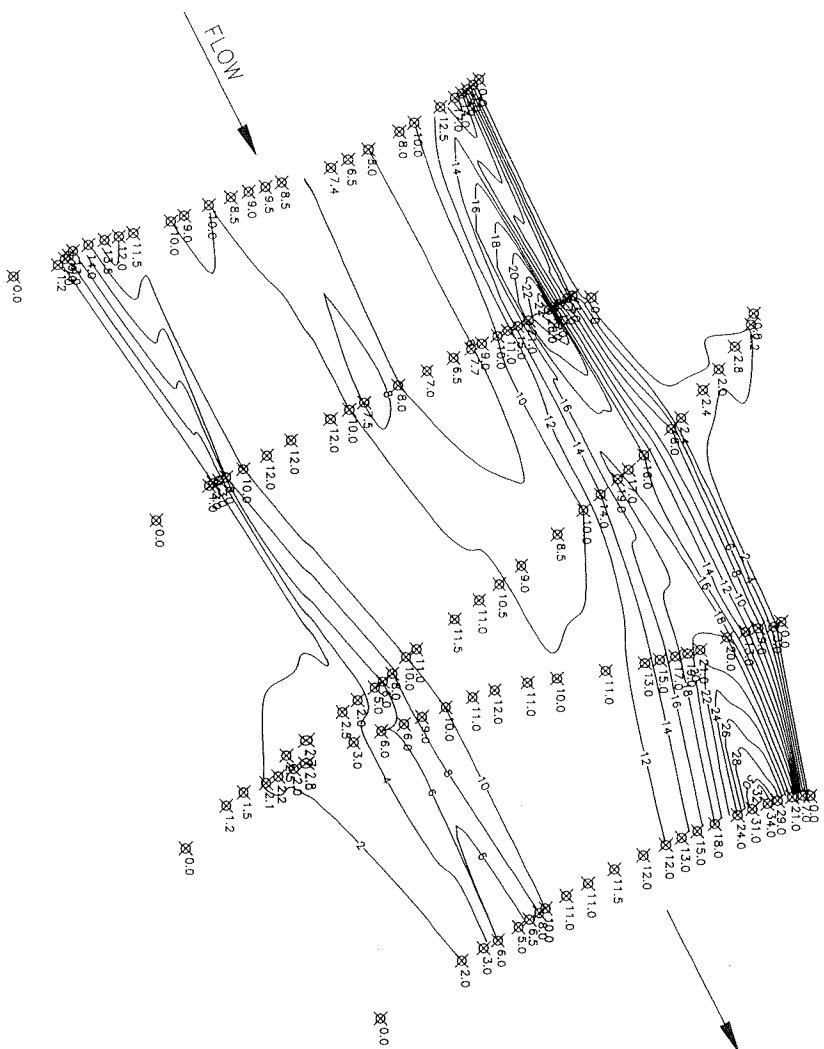


CONTOUR K6.26-K6.77
DEPTH (FT) BELOW WATER SURFACE
ON 27 AUGUST 1995

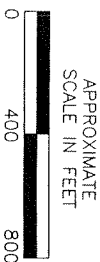


ARCO Alaska, Inc.	
COLVILLE GEOMORPHOLOGY AND HYDROLOGY	
Figure 7-9: Kupitruak Channel Contour Maps	
SHANNON & WILSON, INC. <small>GEOTECHNICAL AND ENVIRONMENTAL CONSULTANTS</small>	
Date: 13 Feb 1996	File: 2XSECT 9.DWG

CONTOUR K7.54-K8.07
 DEPTH (FT) BELOW WATER SURFACE
 ON 27 AUGUST 1995

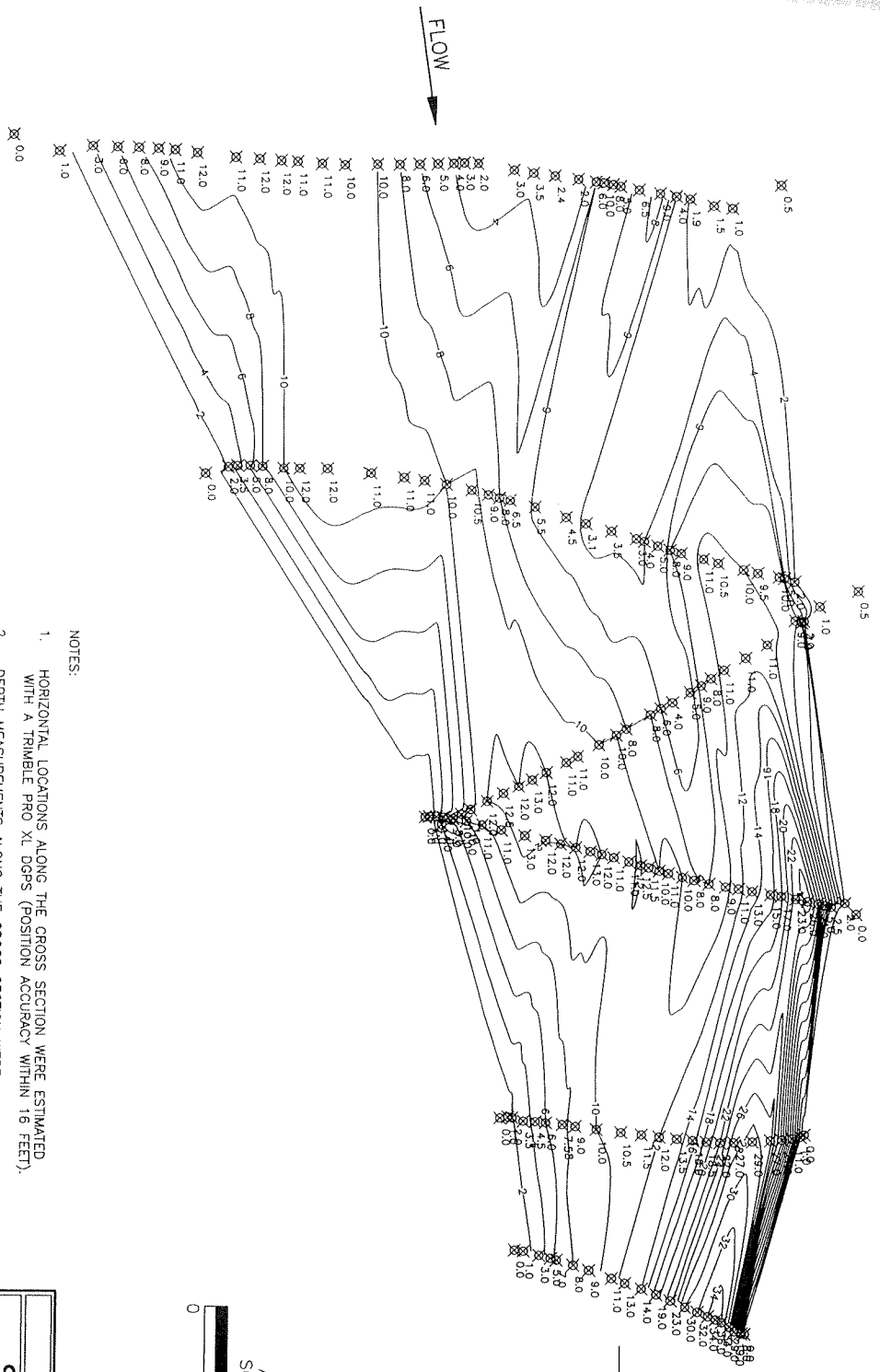


- NOTES:
1. HORIZONTAL LOCATIONS ALONG THE CROSS SECTION WERE ESTIMATED WITH A TRIMBLE PRO XL DOPS (POSITION ACCURACY WITHIN 16 FEET).
 2. DEPTH MEASUREMENTS ALONG THE CROSS SECTION WERE MADE WITH A LOWRANGE MODEL X25 FATHOMETER. EXPERIENCE INDICATES THAT THE MEASURED DEPTH IS WITHIN FIVE PERCENT OF THE ACTUAL DEPTH.
 3. THE APPROXIMATE LOCATION OF THE CONTOUR MAP IS SHOWN ON FIGURES 2-1 AND 2-10.

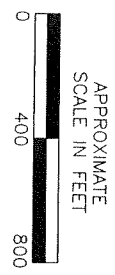


ARCO Alaska, Inc.	
COLVILLE GEOMORPHOLOGY AND HYDROLOGY	
Fig. 7-10: Kupigruak Channel Contour Maps (continued)	
S HANNON & WILSON, INC. <small>GEOTECHNICAL AND ENVIRONMENTAL CONSULTANTS</small>	
Date: 13 Feb 1996	File: 2XSEC710.DWG

CONTOUR K13.03-K13.94
 DEPTH (FT) BELOW WATER SURFACE
 ON 27 AUGUST 1995

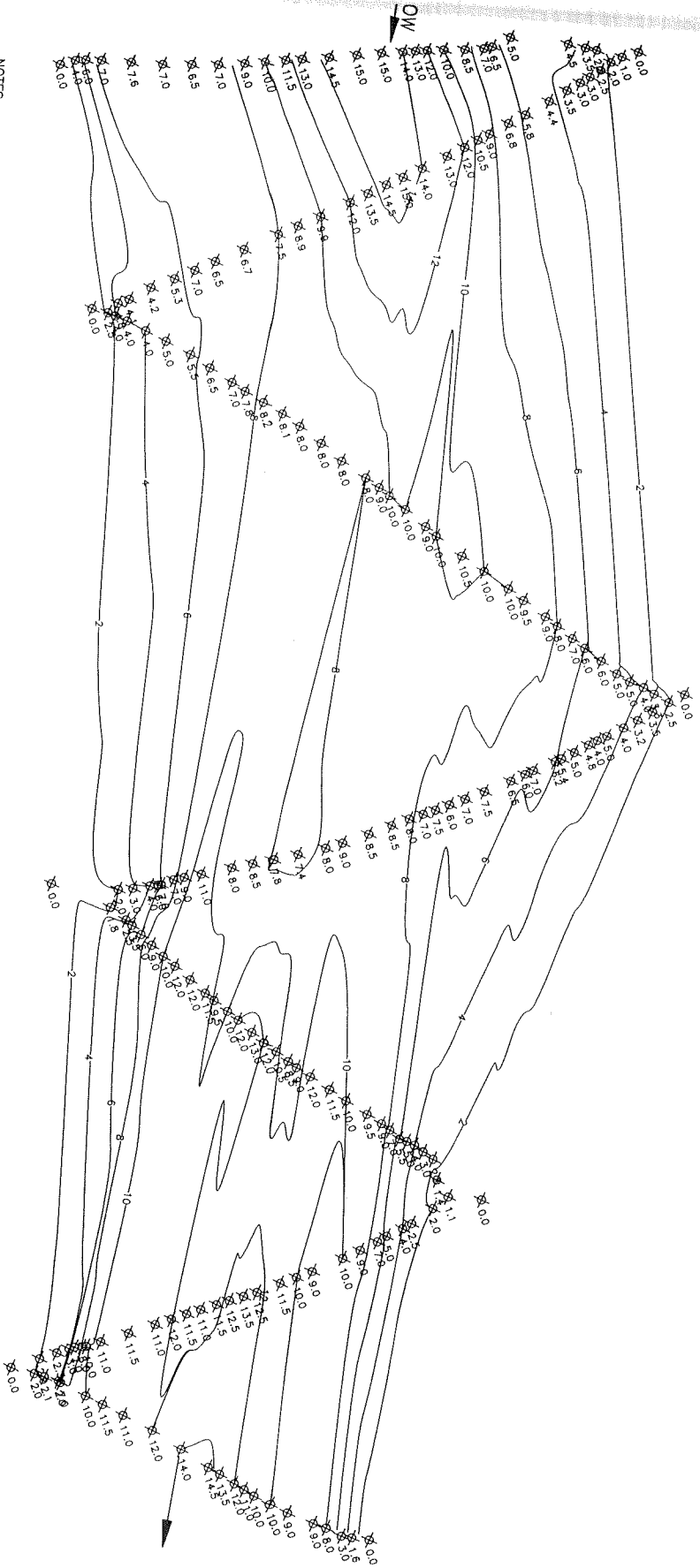


- NOTES:
1. HORIZONTAL LOCATIONS ALONG THE CROSS SECTION WERE ESTIMATED WITH A TRIMBLE PRO XL DGPS (POSITION ACCURACY WITHIN 16 FEET).
 2. DEPTH MEASUREMENTS ALONG THE CROSS SECTION WERE MADE WITH A LOWRANCE MODEL X25 FATHOMETER. EXPERIENCE INDICATES THAT THE MEASURED DEPTH IS WITHIN FIVE PERCENT OF THE ACTUAL DEPTH.
 3. THE APPROXIMATE LOCATIONS OF THE CONTOUR MAP IS SHOWN ON FIGURES 2-1 AND 2-10.

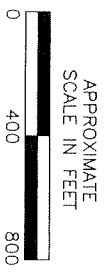


ARCO Alaska, Inc.	
COLVILLE GEOMORPHOLOGY AND HYDROLOGY	
Figure 7-11: Kupigruck Channel Contour Maps (continued)	
SHANNON & WILSON, INC. <small>CONSULTANTS AND ENVIRONMENTAL SCIENTISTS</small>	
Date: 13 Feb 1996	File: 2XSEC711.DWG

CONTOUR E19.31-E20.33
 DEPTH (FT), BELOW WATER SURFACE
 ON 28 AUGUST 1995



- NOTES:
1. HORIZONTAL LOCATIONS ALONG THE CROSS SECTION WERE ESTIMATED WITH A TRIMBLE PRO XL DGPS (POSITION ACCURACY WITHIN 16 FEET).
 2. DEPTH MEASUREMENTS ALONG THE CROSS SECTION WERE MADE WITH A LOWRANCE MODEL X25 FATHOMETER. EXPERIENCE INDICATES THAT THE MEASURED DEPTH IS WITHIN FIVE PERCENT OF THE ACTUAL DEPTH.
 3. THE APPROXIMATE LOCATION OF THE CONTOUR MAP IS SHOWN ON FIGURES 2-1 AND 2-9.



ARCO Alaska, Inc.	
COLVILLE GEOMORPHOLOGY AND HYDROLOGY	
Figure 7-12:	East Channel Contour Map
SHANNON & WILSON, INC. <small>CONSULTING ENGINEERS AND SCIENTISTS</small>	
Date: 13 Feb 1996	File: 2XSEC712.DWG

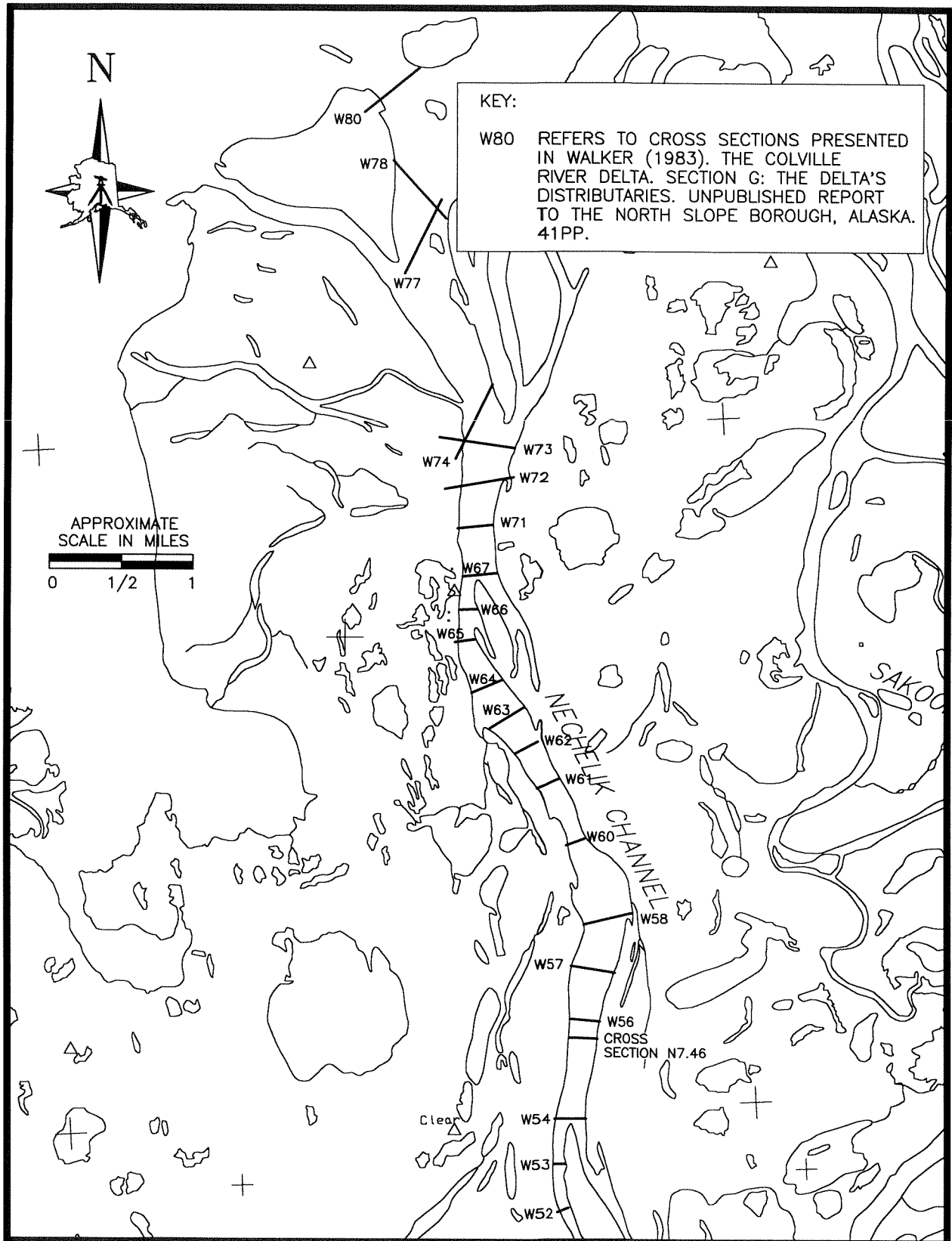


Figure 7-13. Cross section location map for evaluation of barge access in the lower Nechelik Channel.

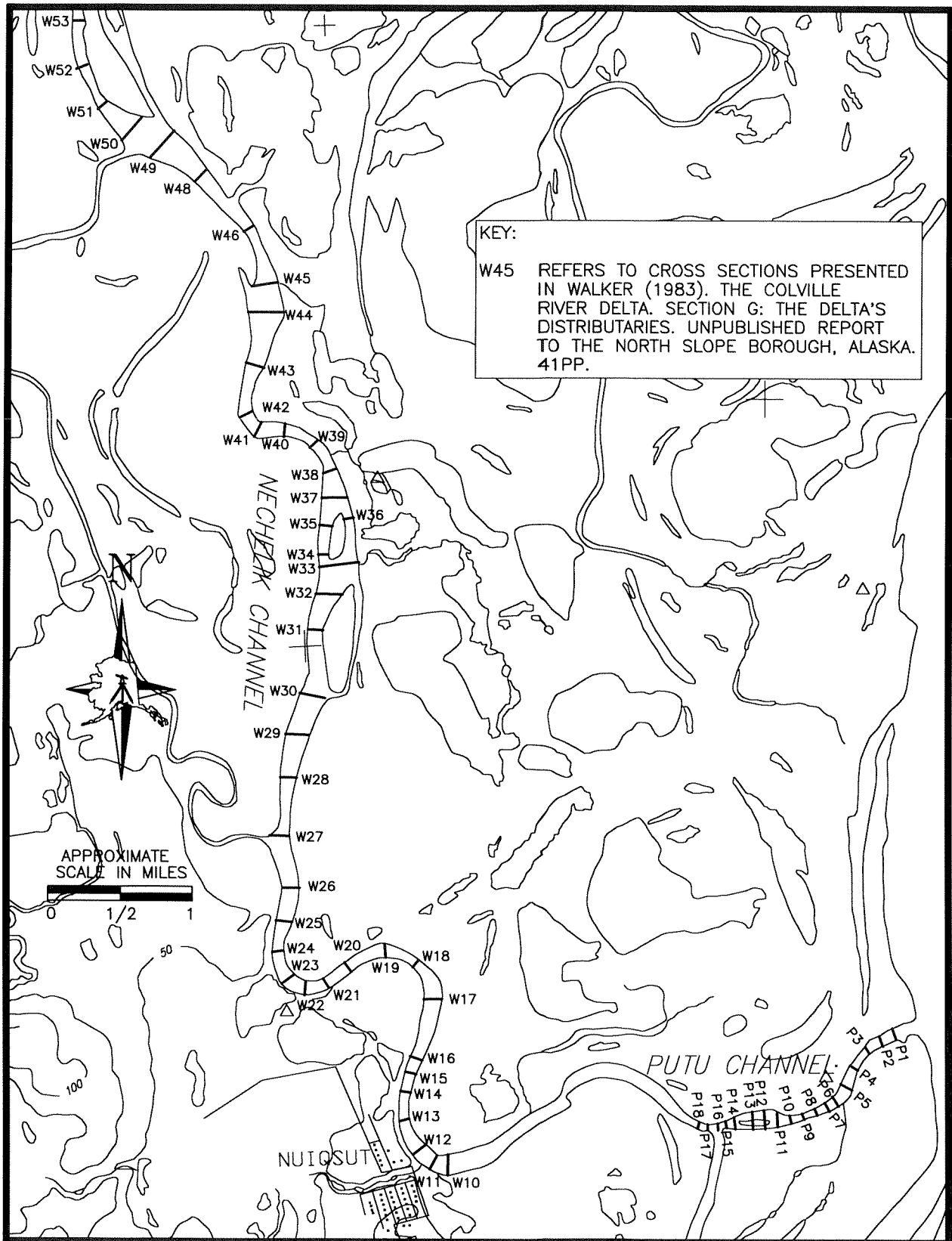


Figure 7-14. Cross section location map for evaluation of barge access in the upper Nechelik Channel.

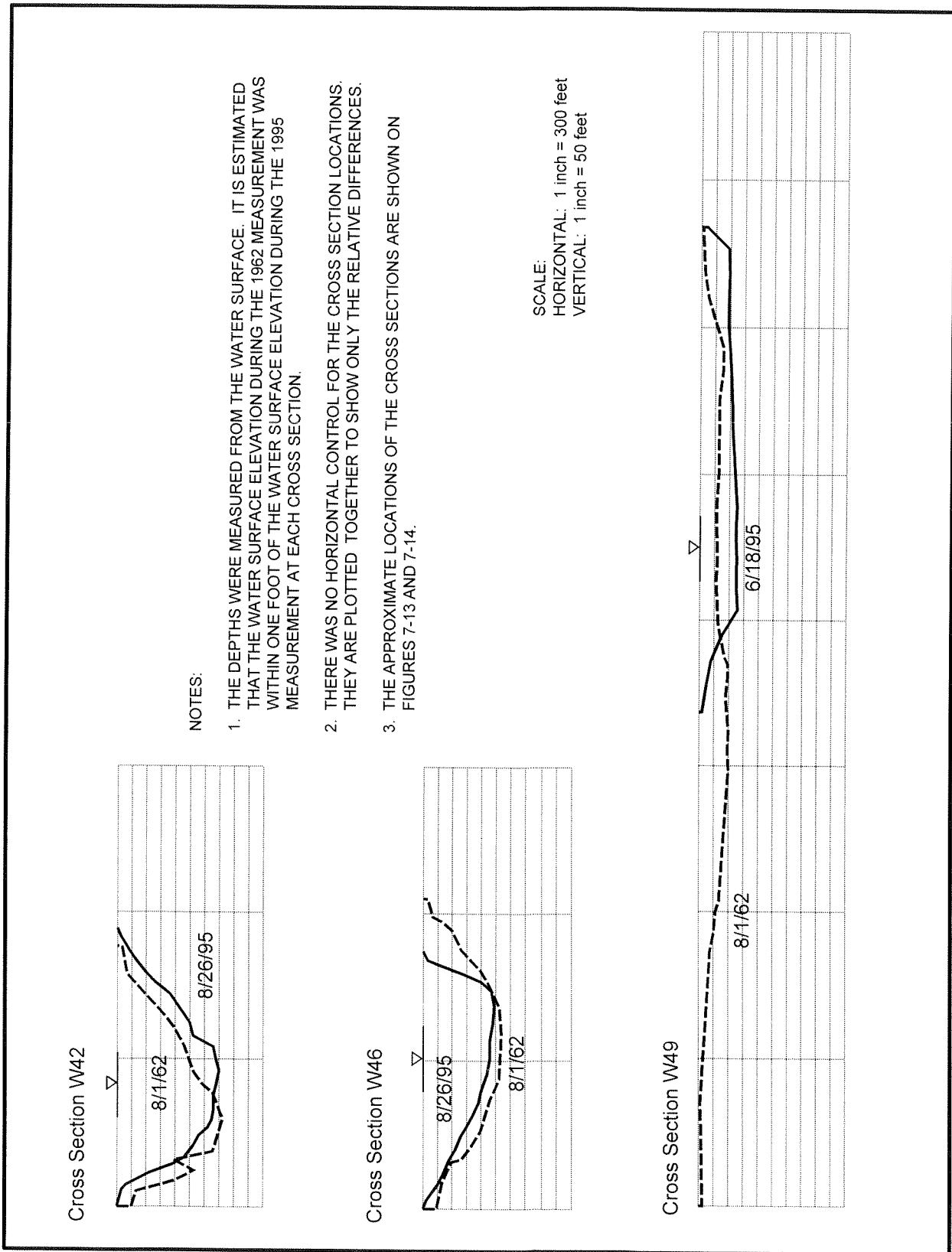


Figure 7-15. Comparison of 1962 and 1995 cross sections of the Nechelik Channel.

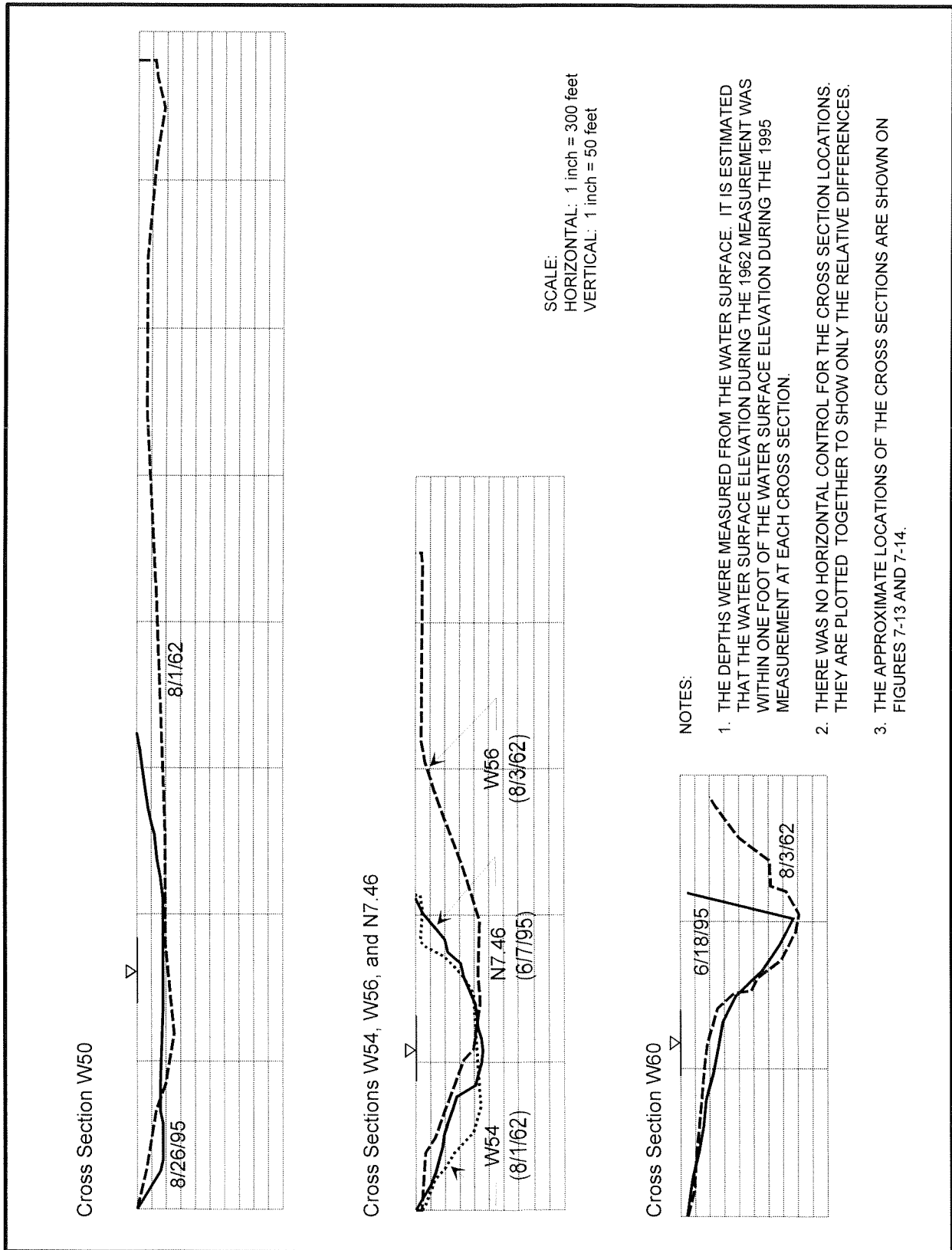


Figure 7-16. Comparison of 1962 and 1995 cross sections of the Nechelik Channel.

Table 7-1. Cross section width at specific depths in the lower Nechelik Channel.

Cross Section	Width ^a (ft)		
	At 5-ft Depth	At 8-ft Depth	At 11-ft Depth
W42	277 - 462	316 - 404	289 - 378
W43	359 - 599	410 - 525	313 - 410
W44	541 - 903	468 - 599	176 - 231
W45	371 - 620	410 - 525	340 - 446
W46	340 - 567	394 - 504	345 - 452
W48	440 - 735	525 - 672	469 - 614
W49	754 - 1260	288 - 368	[110] ^b
W50	736 - 1229	595 - 761	112 - 147
W51	261 - 436	316 - 404	273 - 357
W52	289 - 483	357 - 457	317 - 415
W53	377 - 630	452 - 578	417 - 546
W54	289 - 483	345 - 441	317 - 415
W56	447 - 746	517 - 662	389 - 509
W57	666 - 1113	718 - 919	313 - 410
W58	723 - 1208	791 - 1013	292 - 383
W59	692 - 1155	763 - 977	553 - 725
W60	440 - 735	427 - 546	356 - 467
W61	456 - 761	558 - 714	469 - 614
W62	522 - 872	587 - 751	529 - 693
W63	481 - 803	476 - 609	244 - 320
W64	862 - 1439	747 - 956	108 - 142
W65	497 - 830	541 - 693	297 - 389
W66	598 - 998	574 - 735	481 - 630
W67	289 - 483	353 - 452	324 - 425
W71	475 - 793	529 - 677	397 - 520
W72	968 - 1617	993 - 1271	144 - 189
W73	471 - 786	380 - 486	79 - 103
W74	830 - 1386	478 - 612	[110] ^b
W77	278 - 464	261 - 334	[111] ^b
W78	495 - 827	420 - 537	[111] ^b
W80	428 - 714	410 - 525	32 - 42

^a The range in widths is based on adjustment factors developed using the original 1962 cross sections and the 1995 cross sections. The maximal value shown is the width measured in 1962. The minimal widths were obtained by dividing the 1962 widths at depths of 5, 8, and 11 ft by 1.67, 1.28, and 1.31, respectively. These adjustment factors were developed from data between Cross Sections W42 and W60.

^b Thalweg depths, which are ≤ 11 ft at these cross sections, are shown in brackets [].

Table 7-2. Cross section width at specific depths in the upper Nechelik Channel.

Cross Section	Width ^a (ft)		
	At 5-ft Depth	At 8-ft Depth	At 11-ft Depth
W10	340 - 567	353 - 452	281 - 368
W11	239 - 399	254 - 326	184 - 242
W12	258 - 431	287 - 368	184 - 242
W13	264 - 441	304 - 389	232 - 305
W14	314 - 525	320 - 410	232 - 305
W15	289 - 483	246 - 315	200 - 263
W16	264 - 441	279 - 357	176 - 231
W17	321 - 536	295 - 378	192 - 252
W18	251 - 420	304 - 389	273 - 357
W19	321 - 536	328 - 420	265 - 347
W20	308 - 515	369 - 473	256 - 336
W21	289 - 483	353 - 452	329 - 431
W22	333 - 557	328 - 420	240 - 315
W23	264 - 441	263 - 336	216 - 284
W24	327 - 546	328 - 420	265 - 347
W25	377 - 630	336 - 431	120 - 158
W26	365 - 609	369 - 473	24 - 32
W27	377 - 630	287 - 368	[9] ^b
W28	283 - 473	328 - 420	289 - 378
W29	459 - 767	16 - 21	[8] ^b
W30	296 - 494	254 - 326	[10] ^b
W31	258 - 431	[8] ^b	[8] ^b
W32	415 - 693	74 - 95	[10] ^b
W33	189 - 315	74 - 95	[10] ^b
W34	126 - 210	131 - 168	112 - 147
W35	[3] ^b	[3] ^b	[3] ^b
W36	245 - 410	246 - 315	160 - 210
W37	201 - 336	246 - 315	208 - 273
W38	245 - 410	295 - 378	273 - 357
W39	358 - 599	427 - 546	313 - 410
W40	346 - 578	394 - 504	297 - 389
W41	390 - 651	410 - 525	361 - 473

^a The range in widths is based on adjustment factors developed using the original 1962 cross sections and the 1995 cross sections. The maximal value shown is the width measured in 1962. The minimal widths were obtained by dividing the 1962 widths at depths of 5, 8, and 11 ft by 1.67, 1.28, and 1.31, respectively. These adjustment factors were developed from data between Cross Sections W42 and W60.

^b Thalweg depths, which are less than the specified depth at these cross sections, are shown in brackets [].

Table 7-3. Cross section width at specific depths in the Putu Channel.^a

Cross Section	Width ^b (ft)		
	At 5-ft Depth	At 8-ft Depth	At 11-ft Depth
P1	305	32	[8] ^c
P2	336	221	[10] ^c
P3	441	[7] ^c	[7] ^c
P4	315	[7] ^c	[7] ^c
P5	263	[8] ^c	[8] ^c
P6	420	105	[10] ^c
P8	168	63	[10] ^c
P9	578	389	[11] ^c
P10	242	105	[9] ^c
P11	210	[6] ^c	[6] ^c
P12	389	378	368
P14	294	221	[10] ^c
P15	221	210	[11] ^c
P16	336	200	95
P17	441	420	305
P18	294	231	179

^aThe widths and depths presented herein are much greater than those that exist at the present time.

^bThe widths are based on the 1962 cross section data obtained by H. J. Walker (1983b).

^cThalweg depths, which are less than or equal to the specified depth at these cross sections, are shown in brackets [].

Putu Channel is one of those channels in which the water reverses direction with stage, a situation that enhances deposition and hastens its filling....

It is not surprising given this type of stage reversal that Putu Channel has become so shallow. Indeed, in July, 1994 it was completely blocked at its main channel location.

In addition, the area of the Nechelik Channel just downstream from Putu Channel is also undergoing increased sedimentation. In 1994, the channel opposite the band of dunes north west of the western end of Putu Channel was sufficiently shallow in early July that some boats could not pass through it.

Presently, boat travel in the Putu Channel is limited to periods of high flow. Without additional information, it should probably be assumed that the entire Putu Channel would require at least some dredging to pass barges at typical summer flows.

PART 8. ICE-ROAD CROSSINGS

by Scott R. Ray and James W. Aldrich

BACKGROUND

Ice roads are important for most oil exploration work on the North Slope. They provide access to remote areas in an environmentally acceptable way. Ice roads built to the Colville River Delta in the past few years usually have taken one of two basic routes. An offshore route begins near Kalubik Creek and proceeds toward the Colville River Delta. The problem with this route is the difficulty in crossing the offshore portions of the East and Kupigruak channels, which can be deep.

In the past, holes have been drilled through the sea ice ahead of the ice road construction, searching for a shallow route. A route that maintains a water depth of 3 ft or less around all of these channels has not been found. Our task was to sound the area offshore from the East and Kupigruak channels to determine if a shallow route exists around the deep channels. The task was performed during the open-water season so that a large area could be easily explored.

The overland ice road route crosses the East Channel at the southernmost mouth of the Kachemach River. Because it has been a few years since bathymetric data were collected at this crossing of the East Channel, bathymetric data were collected in 1995 to determine if the channel had changed significantly. Bathymetric data also were collected in the Nechelik Channel at a potential ice-road crossing near Nanuk Lake.

METHODS

OFFSHORE ROUTE

Possible routes around the offshore channels of the Kupigruak and East channels were evaluated by developing bathymetric maps of Harrison Bay at the mouths of these channels. The bathymetric maps were developed from data on water depths collected with a Lowrance Model X25 fathometer and a Trimble Pro XL DGPS. A staff gage in the Colville River at the Helmerick's residence was read and the

water level recorded periodically during the day (Appendix B).

OVERLAND ROUTE

A bathymetric map of the East Channel ice-road crossing was developed from data on water depths collected with a Lowrance Model X25 fathometer and a Trimble Pro XL DGPS. Prior to making these measurements, the water-surface elevation at TBM 20 (Appendix A) was measured and recorded. This measurement will allow the depth contours to be converted to elevation contours in the future, if desired.

Several cross sections were surveyed in the Nechelik Channel at the mouth of Nanuk Lake and approximately 0.7 mi downstream with a Lowrance Model X25 fathometer and a Trimble Pro XL DGPS. TBMs were established in the vicinity of the measured cross sections. The water-surface elevations were tied to the TBMs at the time the cross sections were surveyed. At the present time, these TBMs are not tied to a common datum. If the TBMs were tied to a common datum, the depth contours could be converted to elevation contours. A bathymetric map was created of the area 0.7 mi downstream from Nanuk Lake.

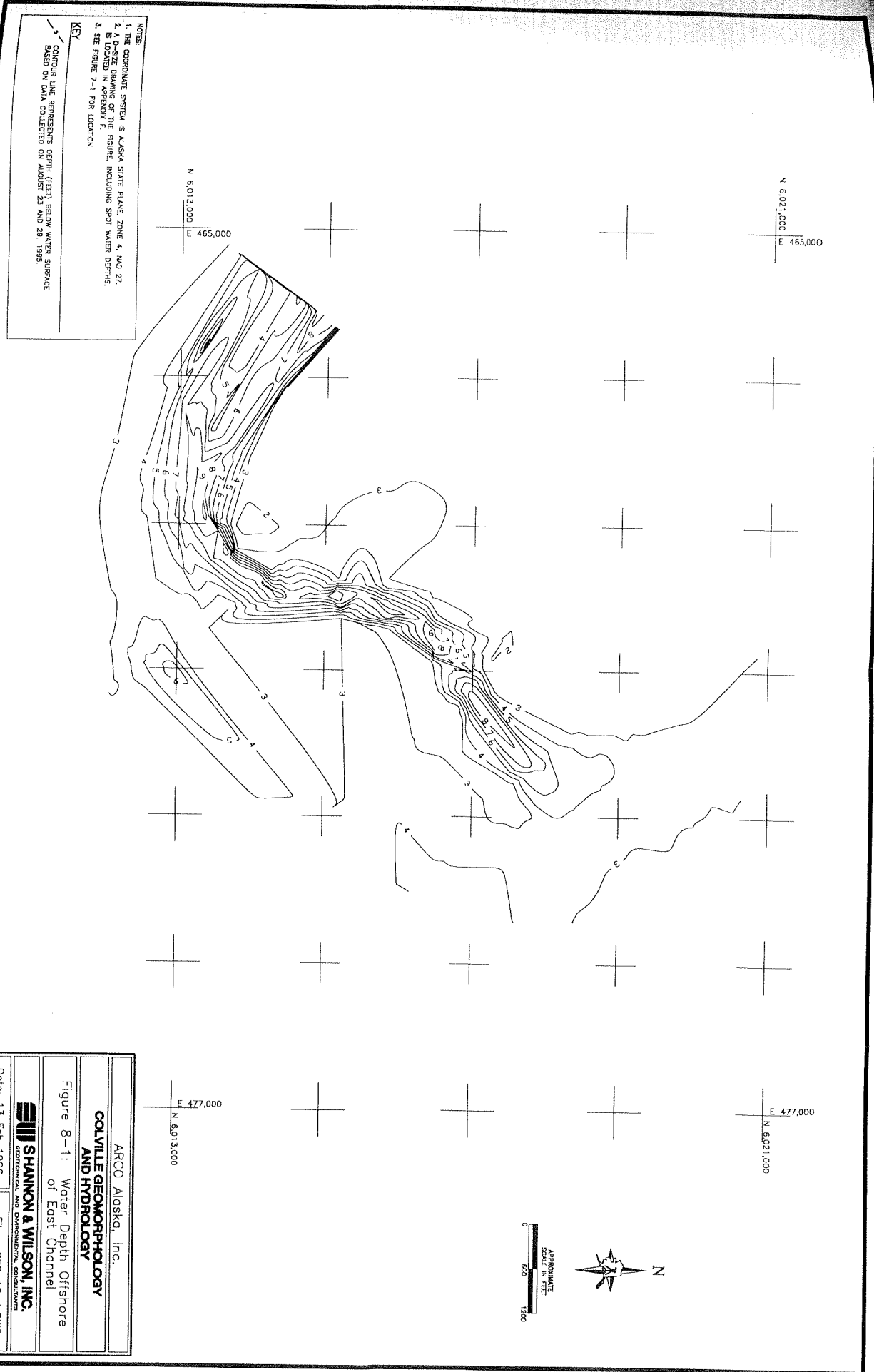
RESULTS AND DISCUSSION

OFFSHORE ROUTE

There is no obvious shallow crossing (3 ft or less) of the East Channel (Figures 7-1 and 8-1). The depth west of the deep channel appears to be at or less than 3 ft, but the depth east of the channel exceeds 3 ft in many locations. A D-size drawing of Figure 8-1 and the data used to make the bathymetric maps are presented in Appendix F. Based on the bathymetric maps offshore from the Kupigruak Channel (Figures 7-1 through 7-3), there is no obvious place to cross these channels where the water depth will always be at or less than 3 ft.

OVERLAND ROUTE

Cross Section A-A' and Cross Section B-B' on Figure 8-2 compare the depths measured in 1993 and 1995, based on the map contours. As shown, there are only slight differences in the shapes of the



- NOTES
1. THE COORDINATE SYSTEM IS ALASKA STATE PLANE, ZONE 4, NAD 27.
 2. A SCALE DRAWING OF THE FIGURE, INCLUDING SPOT WATER DEPTHS, IS LOCATED ON SHEET 7-1.
 3. SEE FIGURE 7-1 FOR LOCATION.

KEY
 CONTOUR LINE REPRESENTS DEPTH (FEET) BELOW WATER SURFACE
 BASED ON DATA COLLECTED ON AUGUST 23 AND 28, 1995.

ARCO Alaska, Inc.
COLVILLE GEOMORPHOLOGY AND HYDROLOGY
Figure 8-1: Water Depth Offshore of East Channel
SHANNON & WILSON, INC. GEOTECHNICAL AND ENVIRONMENTAL CONSULTANTS
Date: 13 Feb 1998
File: 2EC_18_1.DWG

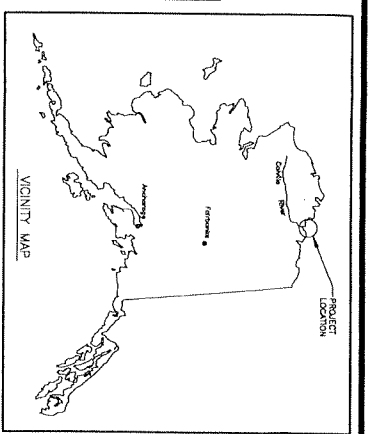
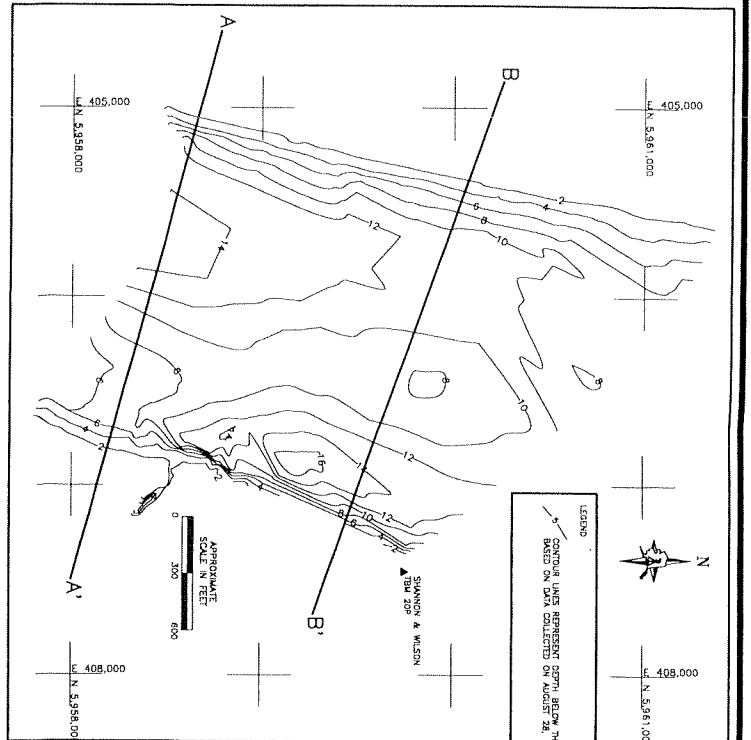
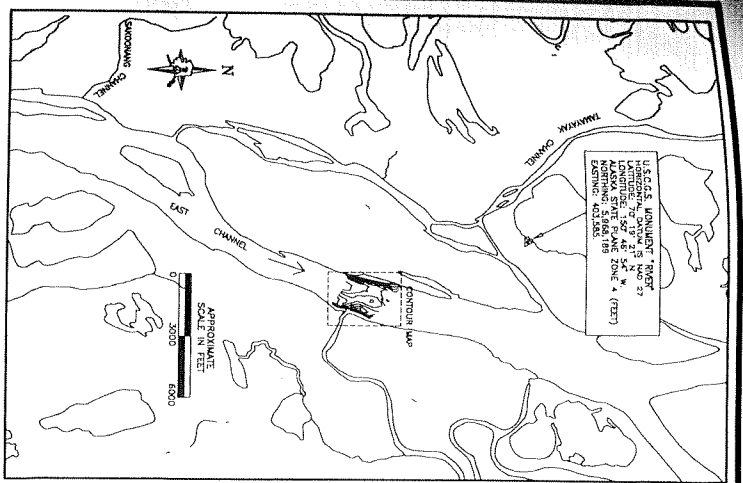
ing (3 ft
 1 and 8-
 sars to be
 the chan-
 drawing
 make a
 ppendix 1
 e from 8
 7-3), the
 nels with
 than 3 ft

in B-8
 d in 198
 As shown
 tpe of #

during the

hannel
 n water
 2.5 fath
 o making
 ation at
 e corded
 contours
 the funn

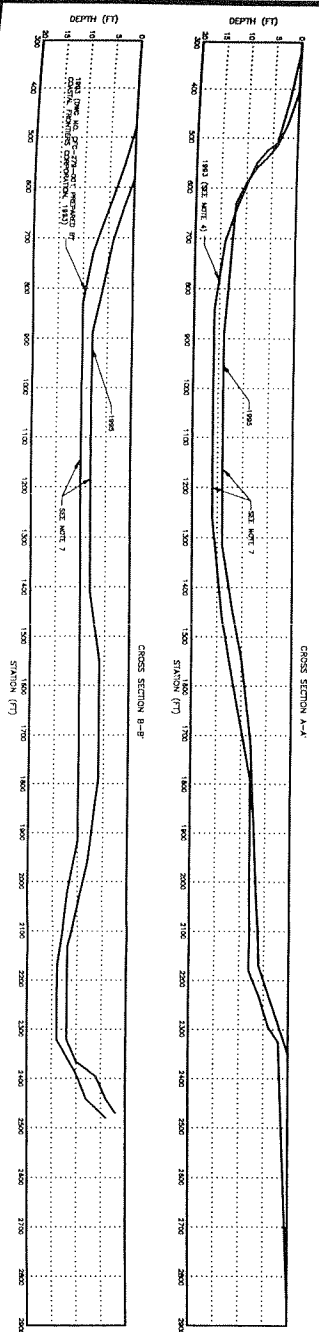
veyed in
 h a Low
 ble Pro
 vicinity
 water-s
 the time
 present
 atum. If
 n, the
 on cont
 area 0.7



LOCATION MAP

CONTOUR MAP

- NOTES:
1. THE COORDINATE SYSTEM IS ALASKA STATE PLANE, ZONE 4, NAD 27 (FEET).
 2. WATER DEPTHS WERE MEASURED ON AUGUST 28, 1985.
 3. THE WATER SURFACE ELEVATION NEAR TBM 208 AT THE TIME THE DEPTHS WERE MEASURED WAS 0.78 FEET (BASED ON U.S.G.S. MOUNTAIN RIVER, ELEVATION = 41.99 FEET).
 4. CROSS SECTION A-A' CORRESPONDS TO CROSS SECTION 90E-208 ON DRAWING NUMBER GCS-279-002, SECTION VIEW OF PROPOSED COLVILLE RIVER BRIDGE, PREPARED BY SHANNON & WILSON, INC. DRAWING NUMBER GCS-279-002, SECTION VIEW OF PROPOSED COLVILLE RIVER BRIDGE, PREPARED BY SHANNON & WILSON, INC. DRAWING NUMBER GCS-279-002, SECTION VIEW OF PROPOSED COLVILLE RIVER BRIDGE, PREPARED BY SHANNON & WILSON, INC.
 5. HORIZONTAL LOCATIONS WERE ESTIMATED WITH A TRIMBLE PRO XL DGPS (POSITION ACCURACY WITHIN 16 FEET).
 6. VERTICAL MEASUREMENTS WERE MADE WITH A LORANGE MODEL X25 FATHOMETER. EXPERIENCE INDICATES THAT MEASURED DEPTH IS WITHIN 5 PERCENT OF ACTUAL DEPTH.
 7. NO WATER SURFACE ELEVATION DATA WERE AVAILABLE FOR THE 1983 SURVEY. DUE TO THE MORE OR LESS UNIFORM DIFFERENCE IN THE CROSS SECTIONS, IT IS ANTICIPATED THAT THE DIFFERENCE IS PRIMARILY DUE TO A DIFFERENCE IN WATER SURFACE ELEVATION AT THE TIME OF THE SURVEYS.
 8. A D-SIZE DRAWING OF THIS FIGURE IS PRESENTED IN APPENDIX G.



ARCO Alaska, Inc.

COLVILLE GEOMORPHOLOGY AND HYDROLOGY

Figure 8-2: Potential East Channel Ice Road Crossings

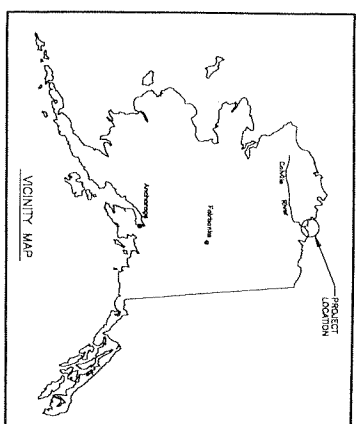
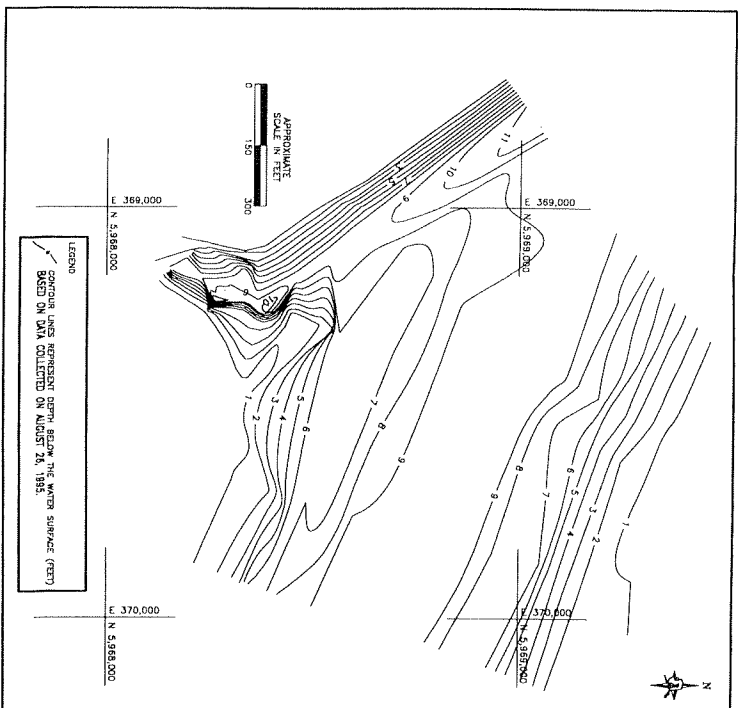
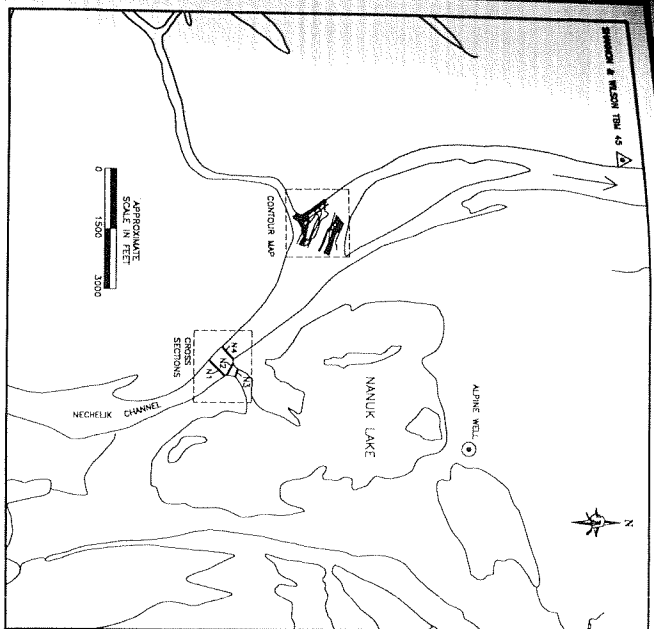
SHANNON & WILSON, INC.
ENGINEERING, ARCHITECTURAL, AND ENVIRONMENTAL CONSULTANTS

Date: 13 Feb 1996 File: 2101R8_2.DWG

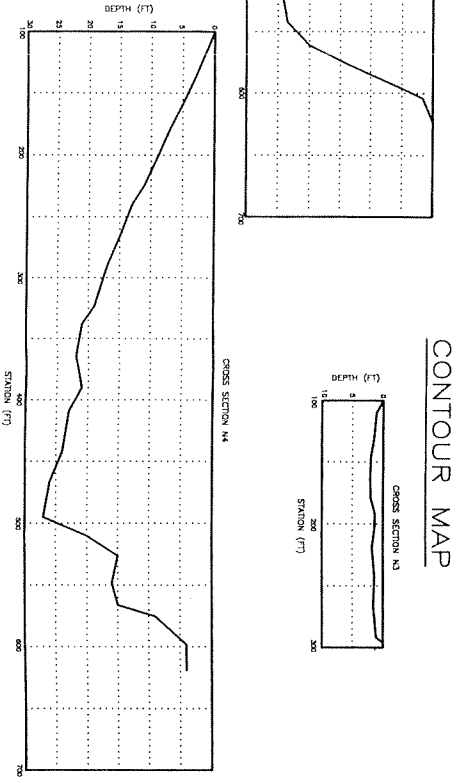
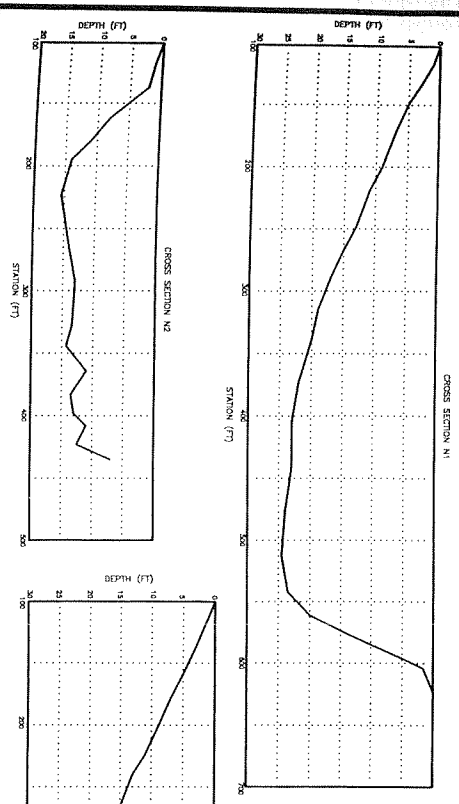
lines. The main difference between the lines is in the depths. Because the 1993 data were not based on elevation, the difference between the two lines is assumed to be the difference in the water-surface elevation at the time of the measurements. Because the lines are about the same shape, the channel probably has changed very little at this location.

The Nechelik Channel at Nanuk Lake is deep, with the cross section immediately downstream from Nanuk Lake having a thalweg depth of 27 ft (Figure 8-3). The channel leading into Nanuk Lake becomes shallow rapidly, having a thalweg depth of 2 ft approximately 100 ft from the Nechelik Channel.

A bathymetric map of the channel 0.7 mi downstream from Nanuk Lake (Figure 8-3) was developed. This area was considered a potential ice road crossing, particularly if the maximal thalweg depth was shallow. Based on the contour lines, the best crossing location would have a thalweg depth of approximately 9 ft. D-size drawings of Figures 8-2 and 8-3, and the data used to make the bathymetric maps are presented in Appendix G.



- NOTES:
1. THE COORDINATE SYSTEM IS ALASKA STATE PLANE, ZONE 4, NAD 27 (FEET).
 2. WATER DEPTHS WERE MEASURED ON AUGUST 26, 1995.
 3. THE WATER SURFACE ELEVATION NEAR TBM 45 AT THE TIME THE DEPTHS WERE MEASURED WAS 0.81 FEET (BASED ON U.S.C.G.S MONUMENT "RIVER", ELEVATION = 41.99 FEET).
 4. HORIZONTAL LOCATIONS WERE ESTIMATED WITH A TRIMBLE PRO XL DGPS (POSITION ACCURACY WITHIN 1.6 FEET).
 5. VERTICAL MEASUREMENTS WERE MADE WITH A LOWRANCE MODEL X2S FATHOMETER (EXPERIENCE INDICATES THAT MEASURED DEPTH IS WITHIN 5 PERCENT OF ACTUAL DEPTH).
- A D-SIZE DRAWING OF THIS FIGURE IS PRESENTED IN APPENDIX C.



ARCO Alaska, Inc.
COLVILLE GEOMORPHOLOGY AND HYDROLOGY
 Figure 8-3: Potential Necheлик Channel Ice Road Crossings
SHANNON & WILSON, INC.
 GEOTECHNICAL AND ENVIRONMENTAL CONSULTANTS
 Date: 13 Feb 1996 File: 2NCRB_3.DWG

PART 9. DRAINAGE NETWORK

By Torre Jorgenson and Alice Stickney

BACKGROUND

Drainages in the Transportation Corridor were mapped to aid in oil spill contingency planning and spill response. During mapping, an emphasis was placed on identifying "micro-drainages" on slopes, such as "water-tracks" and nutrient-enhanced flow zones, that would help us identify flow directions in areas where topographic changes are minimal. In addition to the drainage network, thaw basins that provide topographic catchments were delineated to identify areas where spilled oil may be expected to pool.

METHODS

The delineation of the drainage network was done in conjunction with the ecological land classification effort that mapped terrain units, waterbodies, surface-forms, and vegetation (Jorgenson et al. 1996). Waterbodies and thaw basins that were mapped during the ecological land classification were incorporated into the drainage network map. Waterbodies were classified by type (river, lake, ocean), salinity (fresh, brackish, marine), depth (<6 ft, ≥6 ft), presence of inflow/outflow streams (isolated, connected, tapped), and presence of islands; then, they were delineated on acetate overlays of 1:18,000-scale color-infrared and true-color aerial photography. Minimal polygon size for delineation of waterbodies was about 1 acre (0.5 ha). In addition, ice-poor and ice-rich thaw basins, which were terrain units delineated by the ecological land classification, also were transferred onto the drainage network map.

Drainages in the Transportation Corridor were classified with a system of stream ordering developed by Strahler (1952). In this system, (1) "fingertip" tributaries (first-order channels) combine to become a second-order channel below their confluence, (2) the confluence of two second-order channels creates a third-order channel, (3) two third-order channels join to create a fourth-order channel, and so on. A junction with a lower-order channel (e.g., a first-order with a second-order one) does not alter the designation of the higher-order stream.

Classification of first- and second-order channels on the poorly integrated drainage network typical of tundra on the Arctic Coastal Plain was problematic. We originally attempted to assign all beginnings of drainage lines on the USGS maps as second-order streams according to common practice for the Strahler system. The mapping on these USGS maps, however, was inconsistent, with some large channels missed and some indistinct channels included. Therefore, we instead classified the first- and second-order channels based on characteristics of the tundra and channel morphology. First-order channels were indistinct drainages identifiable by surface topography, surface forms (periglacial features), or vegetation that indicated ephemeral movement of water on the surface or within the seasonally active layer on top of the permafrost. We refer to these first-order channels as micro-drainages. In many instances these micro-drainages ended at the edges of thaw basins, because drainage patterns within the basins frequently were not clear.

During stream classification, many micro-drainages could join together before the channel became a second-order channel. This departure from normal stream-ordering procedures was made so that the numerous micro-drainages on the tundra could be delineated without regard to implications concerning the ordering of higher-order channels. In contrast to the micro-drainages, all second-order channels had a distinct channel or flow zone. Because second-order channels were distinct and could be identified consistently, second-order channels formed the basis for subsequent ordering of higher-order channels.

RESULTS AND DISCUSSION

The map of the drainage network within the Transportation Corridor reveals a poorly integrated drainage system that is interrupted by numerous thaw basins (Figure 9-1). Further, many of these thaw basins did not have a distinct outlet that could be mapped, and in some instances the basins had multiple outlets. The two largest channels, the Miluveach and Kachemach rivers, were designated fifth-order channels. Because it would have required mapping its entire watershed and because its stream order is not essential to this effort, the stream order for the Colville River was not determined. Descriptions of the various channel orders are presented in Table 9-1.

Table 9-1. Descriptions of stream orders for the drainage network in the Transportation Corridor adjacent to the Colville River Delta, 1995.

Stream Order	Description
First (micro-drainages)	Drainages are referred to as "micro-drainages" to indicate their indistinct and ephemeral nature. The micro-drainages denote areas on slopes and swales where water might flow across the tundra's surface during snowmelt or through the active layer during mid-summer. The distinguishing features were identified by topographic breaks across the slopes, as interconnected networks of ice-wedge polygons, or by enhanced growth of vegetation that indicates areas of subsurface water movement (e.g. "water-tracks").
Second	Seasonally active drainages that have a distinct, albeit small, channel incised in the tundra. These drainages primarily carry water during breakup and usually do not have flowing water during mid-summer. Second-order channels were classified more by their distinct channels with intermittent flow than by noting the confluences of first-order channels.
Third	Drainages that had a distinct, incised channel and that usually have water present in the channel during mid-summer. These streams probably have intermittent flow during the summer and have periods when the water may be still.
Fourth	Only one fourth-order stream was noted within the proposed Transportation Corridor. It is a small, beaded stream that probably has continuous low flow during the summer.
Fifth	Broad, gravelly riverbeds indicative of high flow during spring breakup and low flow during mid-summer. The meandering channels are bordered by high floodplain steps that receive occasional overbank flow, the floodplains are constrained by the adjacent alluvial/marine terraces, and the channels frequently alternate between pools and riffles. The Miluveach and Kachemach rivers were classified as fifth-order channels.

The map of the drainage network will help in contingency planning for oil spills by identifying where oil will flow at any point on the tundra and where the oil could be intercepted and contained. For small spills on the tundra, movement of oil would be expected to be minimal. For large spills, however, the thaw basins identified on this map would be useful for helping to contain and control large volumes of oil, thus preventing it from reaching larger streams.

ARCO Alaska, Inc.

Colville Geomorphology and Hydrology

Figure 9-1. Drainage network in the Transportation Corridor, 1995.

08/15/1996

File: TCDRAIN.PRJ

Basins and Waterbodies

- Thaw basin, ice-poor
- Thaw basin, ice-rich
- Delta thaw basin, ice-poor
- Delta thaw basin, ice-rich
- Riverbed/sandbar
- Waterbodies



Stream Order

- First
- Second
- Third
- Fourth
- Fifth

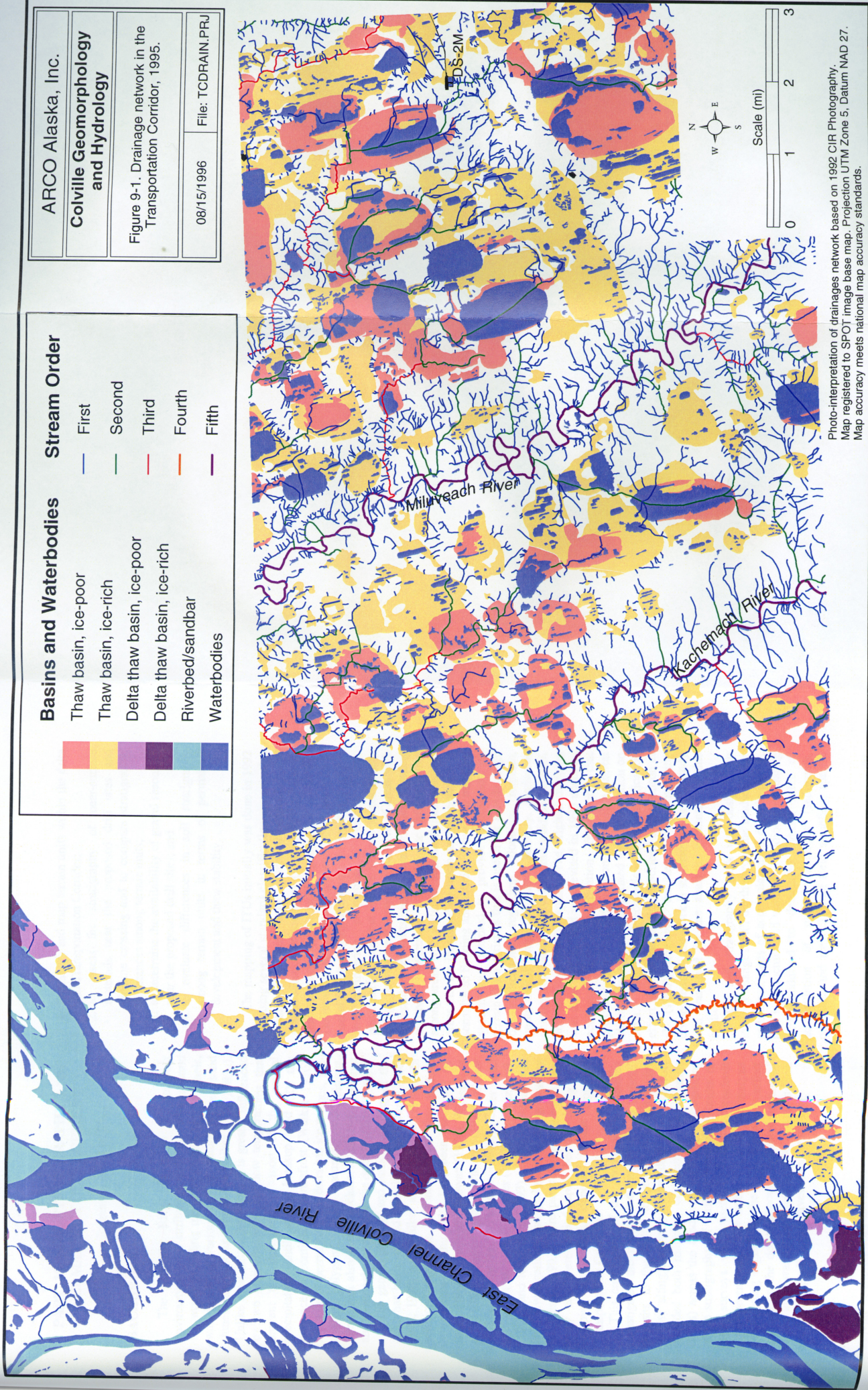


Photo-interpretation of drainages network based on 1992 CIR Photography.
Map registered to SPOT image base map. Projection UTM Zone 5, Datum NAD 27.
Map accuracy meets national map accuracy standards.

PART 10. SOIL STRATIGRAPHY AND PERMAFROST DEVELOPMENT

By Torre Jorgenson and Yuri Shur

BACKGROUND

The Colville River Delta is a complex environment with attributes similar to deltas around the world, including migrating distributary channels, waterbodies of various origins, natural levees, sand dunes, sandbars, and mudflats (Walker 1976, 1983a). Unlike most deltas, however, it is greatly influenced by two other factors: (1) low temperatures that prevent the movement of most of the annual precipitation until spring breakup, and (2) the presence of continuous permafrost (Walker 1976). Because of permafrost, the delta has ice wedges, ice-wedge polygons, frost mounds, and pingos. Permafrost also alters the character of river discharge and erosional processes on the delta (Walker 1976).

The geomorphology and surficial geology of the delta has been studied intensively by Walker (1966, 1976, 1978) and Walker and Matsukara (1979). In addition, numerous regional studies that include information on the delta have been conducted by Black (1964), Naidu and Mowatt (1975), Williams et al. (1978), Cannon and Rawlinson (1979), Carter (1981), Craig and Thrasher (1982), Carter and Galloway (1982, 1985), Foster (1988), Reimnitz et al. (1988), and Rawlinson (1993). Of these studies, the field investigations and geological mapping done by Rawlinson (1993) were particularly relevant to this study and were relied upon heavily during the mapping of surficial deposits in the proposed Transportation Corridor.

This component of the geomorphology studies investigated the nature and distribution of surficial deposits in the delta, to provide information for facility siting and engineering design. This effort included both mapping of integrated terrain units (ITUs) across the landscape and field investigations of the stratigraphy of surficial materials. Results of these surveys were used to evaluate permafrost development and thaw stability and to help analyze the flooding regime in the delta. The field effort focused on the delta, although a limited amount of work also was conducted in the Transportation Corridor. Specific objectives of this study were.

1. to classify and map terrain units within the delta and Transportation Corridor;
2. to assess the stratigraphy of near-surface materials near the proposed drill sites and pipeline crossing and to compare stratigraphic differences among terrain units;
3. to determine the availability of gravel resources near the proposed drill sites; and
4. to evaluate differences in soil stratigraphy among terrain units in terms of permafrost development and thaw stability.

The mapping of ITUs initially was done in 1992 by using several standard classification systems that classified terrain units (surficial deposits and waterbodies), surface-form (ice- and frost-related) features, and vegetation (Jorgenson et al. 1993). Delineating the landscape in terms of terrain units is useful for identifying areas with different soil genesis and engineering properties. Surface forms, particularly those that reflect various stages of ice-wedge development, may be indicative of areas with different ice contents, ages, elevations, and flooding regimes. Vegetation is useful for differentiating among areas with different sedimentation rates and areas that are inundated by storm surges because it is sensitive to flooding and salinity. Thus, the mapping system was designed to provide information on terrain characteristics that is useful for a wide range of applications regarding flooding regimes, geotechnical properties, thaw stability, landscape change, soil productivity, fish and wildlife habitats, and sensitivity to oil spills. The original mapping was done in 1992 and was revised in 1995 under an ecological land classification framework that provided additional information on wildlife habitat characteristics and incorporated new information on soils. The overall ecological land classification effort is more thoroughly described by Jorgenson et al. (1996); however, the terrain unit mapping component of that work is summarized in this study and was used for the analyses presented in this section.

The soil stratigraphy work was designed to identify changes with depth across the landscape for sediments, rates of accumulation of organic matter, and ice structure and volumes. Radiocarbon dating was conducted to determine overall rates of accumulation of surface materials (sediments, organics, and ice). During field sampling, special

attention was paid to identifying mineral and organic horizons near the surface that provided a record of sedimentation related to flooding events. Differences in surficial characteristics among terrain units were evaluated in terms of permafrost development and thaw stability and were used to develop a conceptual model of floodplain evolution.

The field investigation also included a reconnaissance-level effort to assess the availability of gravel resources near the proposed drill sites. Accordingly, the effort was limited to drilling a few shallow (10–18 ft) boreholes with a portable drill. In addition, potential gravel sources farther away from the proposed drill sites were identified.

METHODS

CLASSIFICATION AND MAPPING

We used a compound classification system based on standard classification systems developed for Alaska that integrated information about terrain units, surface forms, and vegetation. The terrain unit classification and mapping is presented here, but a more complete description of the entire system is presented in Jorgenson et al. (1996). The terrain unit classification system was developed by Kreig and Reger (1982) and has been adopted by the Alaska Division of Geological and Geophysical Surveys for their engineering-geology mapping scheme. This classification system was modified slightly to incorporate surficial geology units in the Transportation Corridor that have been identified by Rawlinson (1993) and to differentiate better deltaic sediments that are related to flooding regimes.

The ITUs represent ecological land classes and were classified and delineated with color-infrared (CIR) photography (1:18,000 scale) acquired by AeroMap, Inc., (Anchorage, AK) on 8 July 1992. The mapping was done on acetate overlays of the photos with a mirror stereoscope. Minimal mapping size for features was 1 acre (0.4 ha), although waterbodies as small as 0.5 acre occasionally were mapped to provide additional geodetic reference points. Lines and codes then were digitized and encoded with Atlas GIS software (Strategic Mapping, Inc., Santa Clara, CA). During digitizing, the photos were registered to UTM coordinates obtained from prominent features along waterbody shorelines identified on a base map developed from SPOT

imagery (see Part 12). After digitizing, the digital features on each photo were geometrically rectified by performing a three-point transformation (rubber-sheeting) to match waterbodies on the SPOT base map and, thus, to compensate for distortion caused by tilt. After rectification, features on adjacent photos were joined to create a seamless map of the entire area.

SOIL STRATIGRAPHY

A field survey conducted from 28 July to 8 August 1995 characterized soil stratigraphy along toposequences related to the hydrologic cross sections (includes ground surface below channels) and along additional transects (includes terrain adjacent to rivers) subjectively chosen to cross a variety of terrain units (Figure 10–1). The cross sections were initially numbered consecutively in the field, but the numbering system was changed after the field work to denote river miles. The transects were numbered consecutively. Sampling location identifications used the field cross-section or transect number and a consecutive number for its position along the profiles (e.g., X11.9 or T12.3).

The stratigraphy of the near-surface soil (i.e., the active layer) was described from soil cores or soil pits to determine the occurrence of flood deposition. For sampling frozen soils below the active layer, a 3"-diameter SIPRE corer with a portable power head was used to obtain cores down to 8 ft. Several profiles also were described from cutbanks after unfrozen material was removed with a shovel to expose undisturbed frozen sediments. Descriptions for each profile included the texture of each horizon, the depth of organic matter, depth of thaw, and ice volume and structure. In the field, soil texture was classified according to the Soil Conservation Service system (SSDS 1993). Cryogenic structure (forms, distribution, and volumes of ice) was classified in the field according to Russian (Katsonov 1969) and North American systems (Philainen and Johnston 1963), but were reclassified following Murton and French (1994) after review of field descriptions and examination of close-up photography. Similar data were collected in 1992 (Jorgenson et al. 1993), although they did not include ice descriptions.

During field sampling, the occurrence of thin fluvial and organic layers was noted and two measures of organic accumulation were analyzed to

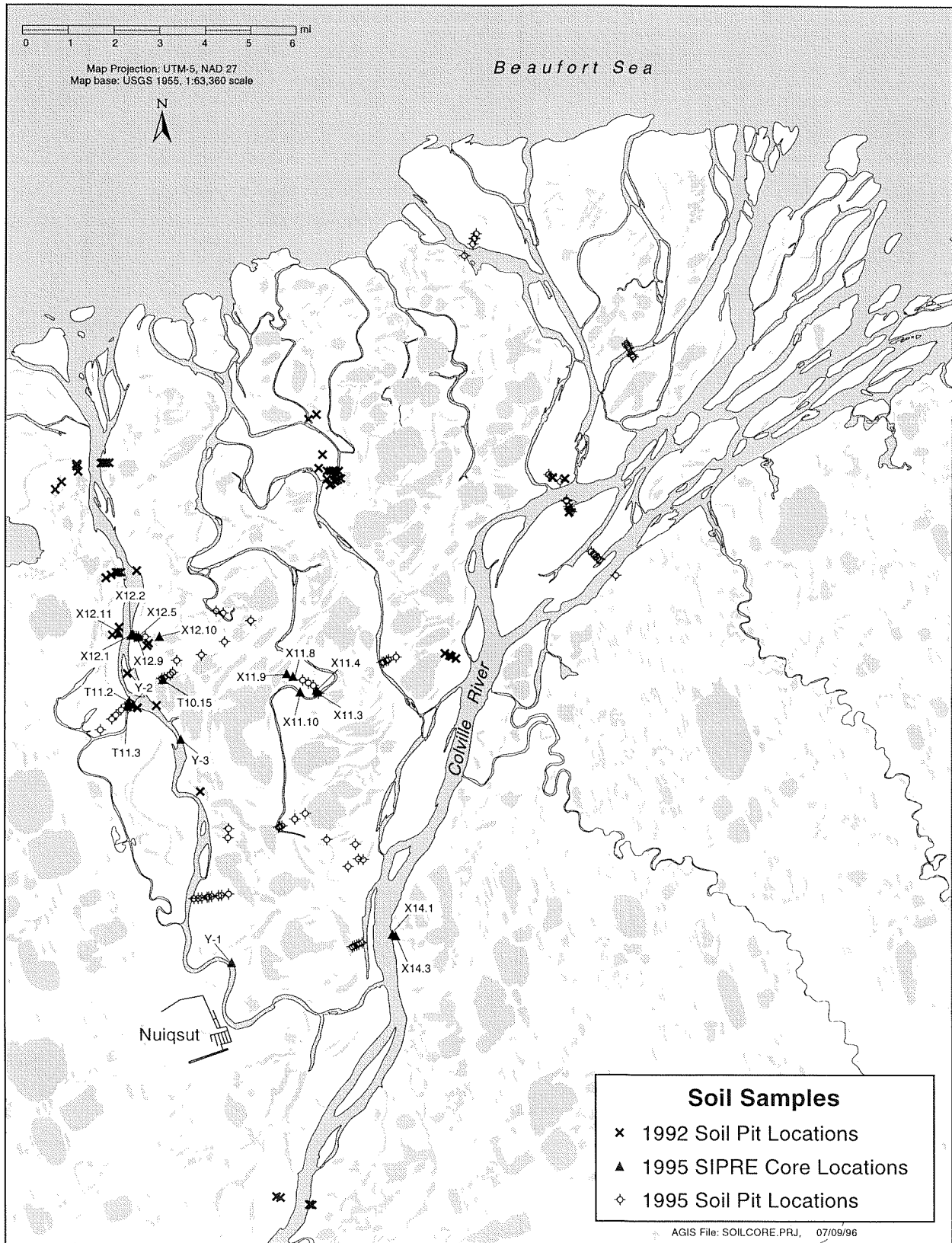


Figure 10–1. Map of soil core locations in 1992 and 1995, Colville River Delta.

assess differences among terrain units and to evaluate differences in the frequency of flooding. First, the thickness of organic material above the uppermost distinct mineral horizon of fluvial origin was measured to evaluate how much material had accumulated since the previous major flood. Then, the cumulative amount of organic material that had accumulated in the top 1 ft of soil was calculated by summing the thicknesses of all the individual organic layers; these data were used to assess rates of sediment accumulation. The first approach provides a short-term measure of flood frequency by identifying those areas affected by the 1989 flood, whereas the second approach is a long-term indicator of flood frequency.

Numerous samples were taken from the frozen core for analysis of gravimetric water content, particle size, and electrical conductivity. In 1995, measurements of water content and conductivity were taken by ABR, Inc., and determination of particle-size distributions was done by Shannon and Wilson, Inc. Data were collected in a similar manner in 1992 but also included collection of samples for laboratory analyses of particle-size distributions, pH, and electrical conductivity. Those laboratory analyses were conducted by the Soil Testing Laboratory of Colorado State University (Fort Collins, CO), following standard methods (Klute 1986).

To establish minimal ages for the older terrain units, samples to be used for radiocarbon dating were collected from organic material in some of the deeper profiles. In a few instances, fragments of wood stems were collected for dating. Laboratory analyses were performed by Beta Analytic, Inc. (Coral Gables, FL). The dates were reported as radiocarbon years before 1950 AD and include the error (± 1 SD) associated with each analysis.

RESULTS AND DISCUSSION

CLASSIFICATION AND MAPPING OF TERRAIN UNITS

Eighteen terrain units were identified within the delta and the Transportation Corridor, and there were large differences in distribution of terrain units between the two areas (Table 10-1, Figure 10-2). Deposits on the delta included: delta riverbed/sandbar deposits, high-water channels, active-floodplain cover deposits, inactive-floodplain

cover deposits, abandoned-floodplain cover deposits, tidal flat deposits, eolian sand deposits, and ice-rich and ice-poor thaw basin deposits. In contrast, deposits within the Transportation Corridor off the delta included: meander floodplain riverbed deposits, active-floodplain cover deposits, inactive-floodplain cover deposits, alluvial and alluvial-marine terraces, alluvial plain, and gravel and peat fill deposits.

The classification of floodplain deposits within the delta emphasized differences in sediments that are related to flooding regimes. Delta riverbed/sandbar deposits have interbedded silt and sand layers and are differentiated easily by numerous thin interbedded layers of shredded peat formed from thin drifted layers. High-water channels are similar to riverbed/sandbar deposits but the channels do not have water during periods of low flow. Active-floodplain cover deposits occur along low riverbanks and are mostly composed of silt; thin shredded, drifted peat layers are absent. A lack of accumulation of peat at the surface indicates frequent flooding. Inactive-floodplain cover deposits are characterized by distinct interbedded layers of silt and peat, indicating frequent flooding. Abandoned-floodplain cover deposits have thick accumulations of peat at the surface, but distinct interbedded layers of silt are absent. Although these latter deposits may be flooded rarely, the deposits at the surface no longer reflect fluvial origin.

SOIL STRATIGRAPHY

The following section analyses those factors that have contributed to changes in terrain characteristics across the delta landscape. These analyses include comparisons of sediment characteristics, organic matter accumulation, ice structures and volumes, and overall accumulation rates of these materials.

When stratigraphic profiles for the most common terrain units are grouped together, large differences in soil texture and ice structure are evident among them (Figure 10-3). The delta/riverbed sandbar deposit has a sandy texture, and the ice is mostly structureless and of low volume. Active-floodplain cover deposits generally had a silty (or interbedded silts and sands) cover deposit over the sandier riverbed deposit, and lenticular cryostructures were more common.

Table 10-1. Descriptions of terrain units mapped within the Colville River Delta.

Unit	Description
Eolian Sand Deposit	Unconsolidated, wind-deposited accumulations of primarily very fine and fine sand. Surficial patterns associated with ice-aggradation generally are absent. These active sand dunes are being built by deposition of sand from adjacent sandbars and are prone to wind erosion, giving them distinctive, highly dissected patterns. Active dunes occur at the inner edge of extensive mudflats, the outer delta, and along the western and southwestern sides of river channel bars. Only distinct dunes were mapped, whereas smooth sand sheets overlying other deposits were not.
Delta Floodplain Riverbed/Sandbar Deposit	Silty and sandy riverbed or lateral accretion deposits laid down from the bed load of a river in areas of channeled flow. Riverbed alluvium includes point bars, lateral bars, mid-channel bars, unvegetated high-water channels, and broad riverbed/sandbars exposed during low water. In general, texture of the sediments decreases in a seaward direction along the distributaries and in a bankward direction from the thalweg. Organic matter, including driftwood (mostly small willows), peat shreds, and other plant remains, usually is interbedded with the sediments. Only those riverbed deposits that are exposed at low water are mapped, but they also occur under rivers and cover deposits. Frequent flooding (every 1–2 yr) prevents the establishment of permanent vegetation.
Delta Floodplain High-water Channel	Riverbed deposits that occur in channels flooded only during periods of high flow. Because of river meandering, these channels no longer are active during low-flow conditions. Deposits in this unit are similar to those described for riverbed alluvium. These old channels show little surface polygonization indicative of ice-wedge development, although there infrequently are high-water channels that are older and have developed disjunct polygon rims. Very old channels that have distinct low-centered polygons are not included in this unit.
Delta Active-Floodplain Cover Deposit	Thin (0.5–1 ft) fine-grained cover deposits (primarily silt) that are laid down over sandier riverbed deposits during flood stages. Deposition occurs sufficiently frequently (every 3–4 yr) to prevent the development of a surface organic horizon. Supra-permafrost groundwater generally is absent or occurs only at the bottom of the active layer during mid-summer. This unit usually occurs on the upper portions of point and lateral bars and supports riverine willow vegetation.
Delta Inactive-Floodplain Cover Deposit	Fine-grained cover or vertical accretion deposits of a braided floodplain that are laid down over coarser riverbed deposits by streams at bank overflow (flood) stages. The surface contains a sequence (0.5–2 ft thick) of interbedded organic and silt layers near the surface, indicating occasional flood deposition. Under the organic horizons is a thick layer (1–5 ft thick) of silty cover deposits overlying riverbed deposits. Surface forms range from nonpatterned to disjunct and low-density, low-centered polygons. Lenticular and reticulate forms of segregated ice and massive ice in the form of ice wedges are common.
Delta Abandoned Floodplain Cover Deposit	Peat, silt, or fine sand (or mixtures or interbeds of all three), deposited in a deltaic overbank environment by fluvial, eolian, and organic processes. These deposits generally consist of an accumulation of peat 2–6 ft thick that overlies cover and riverbed alluvium. Because these are older surfaces, eolian silt and sand may be common as distinct layers or as intermixed sediments. The surface layer, however, lacks interbedded silt layers associated with occasional flood deposition. Lenticular and reticulate forms of segregated ice and massive ice in the form of ice wedges are common in these deposits. The surface is characterized by high density, low-relief polygons and represents the oldest surface on the floodplain.
Meander Floodplain Riverbed Deposit	Sandy gravel, and occasionally sand, deposited as lateral accretion deposits in channels of active floodplains by fluvial processes. Subrounded to rounded pebbles and cobbles are common in the sandy gravel. Frequent deposition and scouring from flooding prevents the establishment of vegetation. The channel has a meandering configuration.
Meander Active-Floodplain Cover Deposit	Thin (0.5–1 ft), fine-grained cover deposits (primarily silt) that are laid down over sandy or gravelly riverbed deposits during flood stages. Deposition occurs sufficiently frequently (probably every 3–4 years) to prevent the development of a surface organic horizon. This unit usually occurs on the upper portions of point and lateral bars and supports riverine willow vegetation.
Meander Inactive-Floodplain Cover Deposit	Interbedded layers of peat and silty very fine sand material (0.5–2 ft thick), indicating a low frequency of flood deposition. Cover deposits below this layer generally consist of silt but may include pebbly silt and sand and usually are in sharp contact with underlying gravelly riverbed deposits. This unit has substantial segregated and massive ice, as indicated by the occurrence ice-wedge polygons.

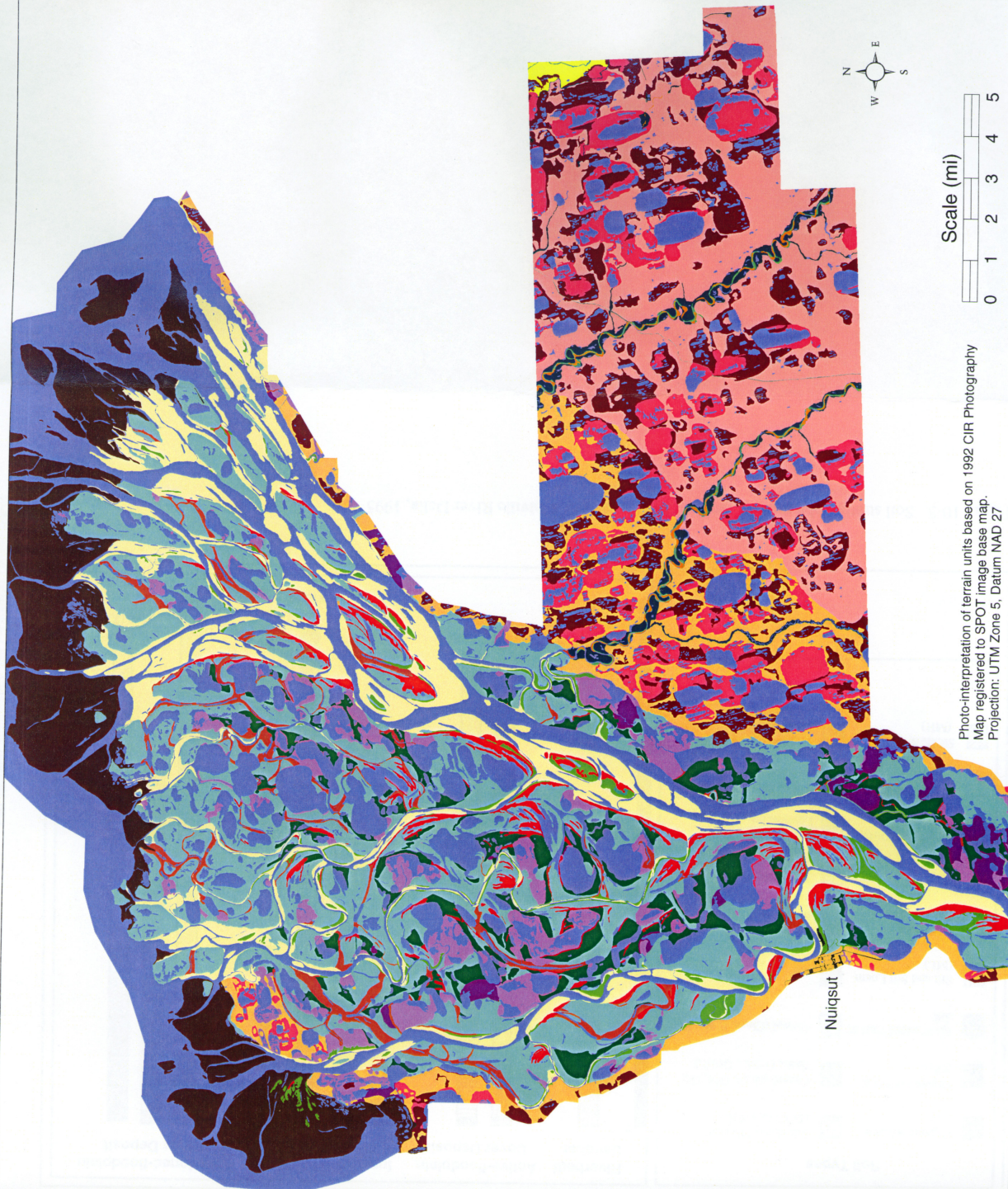
Table 10–1. continued

Thaw Basin Deposit, Ice Poor	Thaw basin deposits, which are caused by the thawing of ground ice; they typically are fine-grained and organic-rich, and the stratigraphy of the original sediments has been deformed by the subsidence. On the terraces and coastal plain west of the delta, pebbly silt or fine sand is more common. The presence of nonpatterned ground or disjunct polygonal rims indicates that ground ice is low and that lake drainage has occurred recently. Ponds in these basin typically have irregular shorelines and are highly interconnected.
Thaw Basin Deposit, Ice Rich	Sediments similar to non-ice rich thaw lake deposits but having much more ground ice, as indicated by the development of low-centered or high-centered polygons. Waterbodies within these basins tend to be rectangular, to have smooth, regular shorelines, and to be poorly interconnected.
Delta Thaw Basin Deposit, Ice Poor	Deposits occurring in thaw lakes having a connection to a river or nearshore water (tapped lake); they occur only in deltaic environments. Most connections occur when a meandering distributary cuts through a lake's bank; once connected, the lake is influenced by changes in river level. During breakup, large quantities of sediment-laden water flow into the lake, forming a lake delta at the point of breakthrough. Sediments typically consist of fine sands, silts, and clays and typically are slightly saline.
Delta Thaw Basin, Ice-rich	Similar to the above unit, except that sediments are ice-rich, as indicated by the development of ice-wedge polygons. Typically, the sediments contain a sequence of a thick (1–2 ft) layer of interbedded silt and peat, fine-grained cover deposits, and silty clay lacustrine deposits. They still are subject to flooding
Alluvial Terrace	Fluvial gravelly sand, sand, silty sand, and peat. The old terraces were deposited at an earlier age and are not subject to flooding under the current regime. Deposits usually are overlain by eolian silt and sand and organic-rich thaw basin deposits. This unit has a high content of segregated and massive ice, as indicated by the presence of ice-wedge polygons and the abundance of thaw ponds.
Alluvial-Marine Terrace	A sequence of alluvial and marine terraces (A, B, and C of Rawlinson 1993) that have variable composition but generally consist of undifferentiated gravelly sand overlain by fluvial gravelly sand, silty sand, and organic silt. Stratified layers of marine gravelly sand, silty sand, silt and minor clay occur in some locations beneath the fluvial deposits. The deposits generally are overlaid by pebbly eolian sand and silt and organic-rich lacustrine deposits. This unit is not subject to flooding.
Alluvial Plain Deposit	Peat, eolian loess and sand, lacustrine sediments, and sandy gravel deposited by braided river processes on an alluvial plain. A typical sequence consists of 0.5–2 ft of peat or mixed sand and peat typical of lacustrine material, 4–7 ft of sand and pebbly fine sand (Beechey Sand), and thick beds (below 5–10 ft) of sandy gravel and gravel (Ugnuravik Gravel). The surface is ice-rich, as indicated by polygonal development and the prevalence of thaw lakes. Water depths in thaw lakes generally are 3–7 ft, indicating that ice contents are high and sediments are not thaw stable.
Tidal Flat Deposit	Areas of nearly flat, barren mud or sand that are periodically inundated by tidal waters. Tidal flats occur on seaward margins of deltaic estuaries, leeward portions of bays and inlets, and at mouths of rivers. Tidal flats frequently are associated with lagoons and estuaries and may vary widely in actual salinity, depending on how exposed the flat is to salt-water incursion and the rate of influx of fresh water.
Fill, Gravel and Peat	Gravel and sandy gravel that has been placed as fill for roads and pads in the village of Nuiqsit and the Kuparuk Oilfield. Peat fill ("peat road") includes a mixture of organic and fine-grained sediments that has been obtained by taking peat material from the active layer and piling it into a roadbed

Inactive-floodplain cover deposits had a layer of interbedded silt and peat at the surface and silty cover deposits below that. Cryostructures revealed a complex assemblage of lenticular, reticulate, suspended, and sheet ice. Finally, abandoned-floodplain cover deposits typically had a thick organic layer at the surface with occasional eolian material mixed in.

Terrain sequences noting changes in elevation, soils, surface-forms, and vegetation at selected locations within the development area are illustrated

in Figures 10–4 through 10–7. Cross Section N7.46 (12), located approximately 1 mi south of the Alpine 1 Exploratory Well Site along the Nechelik Channel, also includes a complete floodplain sequence but is missing sand dunes that typically form on the western side of channels (Figure 10–4). Cross Section S9.80 (11), near one of the proposed well sites adjacent to the Sakoong Channel, represents a nearly complete sequence of landscape evolution that goes from a barren riverbed/sandbar deposit to an abandoned-floodplain cover deposit to a thaw



Nuiqsut

Key

- Eolian sand dunes
- Delta, riverbed/sandbar deposit
- Delta high-water channel
- Delta active-floodplain cover deposit
- Delta inactive-floodplain cover deposit
- Delta abandoned-floodplain cover deposit
- Meander floodplain riverbed deposit
- Meander active-floodplain cover deposit
- Meander inactive-floodplain cover deposit
- Alluvial terrace deposit
- Alluvial-marine terrace deposit
- Alluvial plain deposit
- Thaw basin deposit, ice-poor
- Thaw basin deposit, ice-rich
- Delta thaw basin deposit, ice-poor
- Delta thaw basin deposit, ice-rich
- Tidal flat deposit
- Gravel fill
- Peat fill
- Waterbodies

ARCO Alaska, Inc.

Colville Geomorphology
and Hydrology

Figure 10-2. Map of terrain units,
Colville River Delta, 1995.

08/15/1996

File: TERRAIN.PRJ

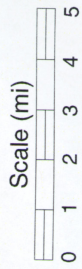


Photo-interpretation of terrain units based on 1992 CIR Photography
Map registered to SPOT image base map.
Projection: UTM Zone 5, Datum NAD 27

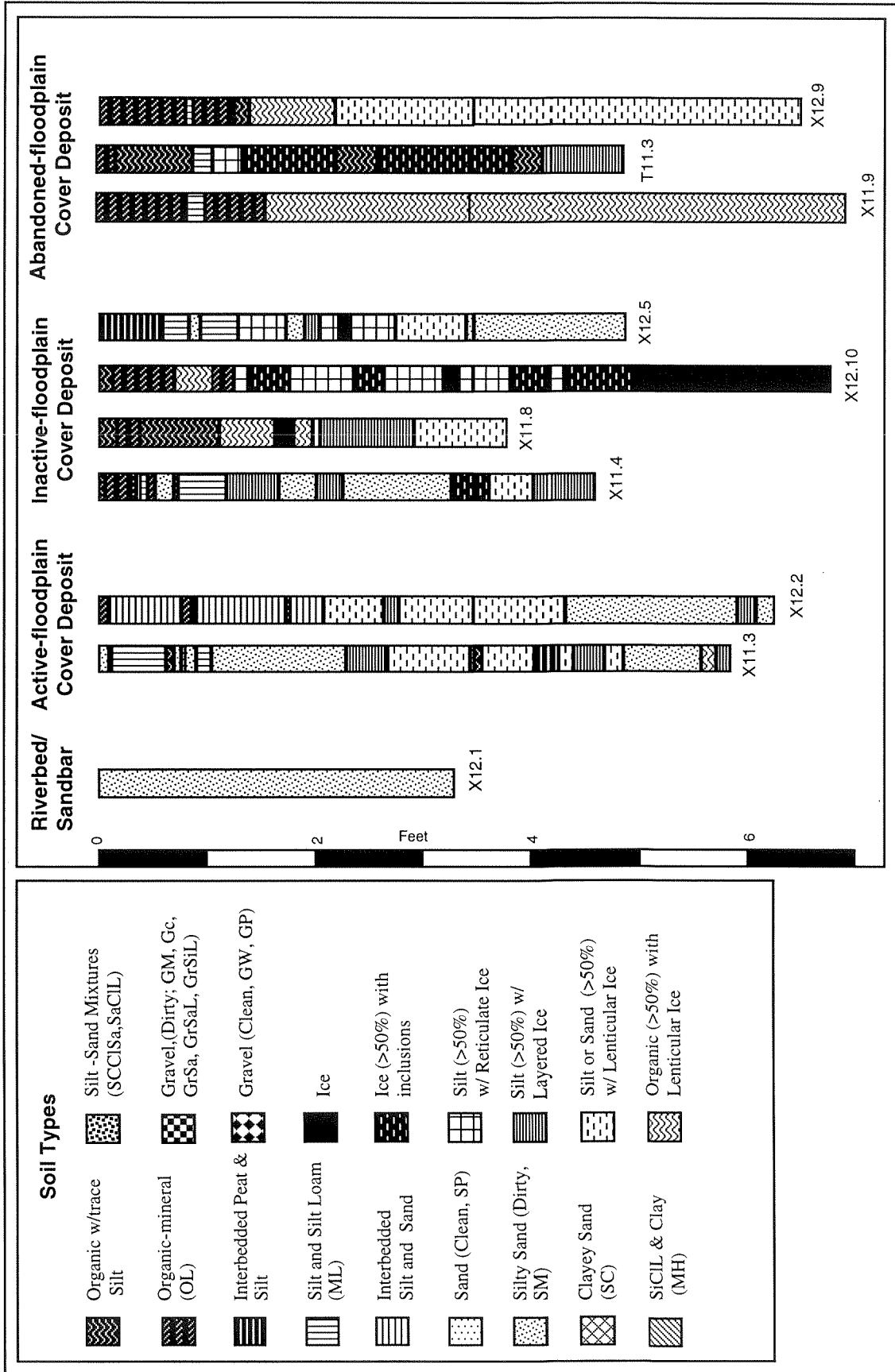


Figure 10-3. Soil stratigraphy profiles grouped by terrain unit, Colville River Delta, 1995

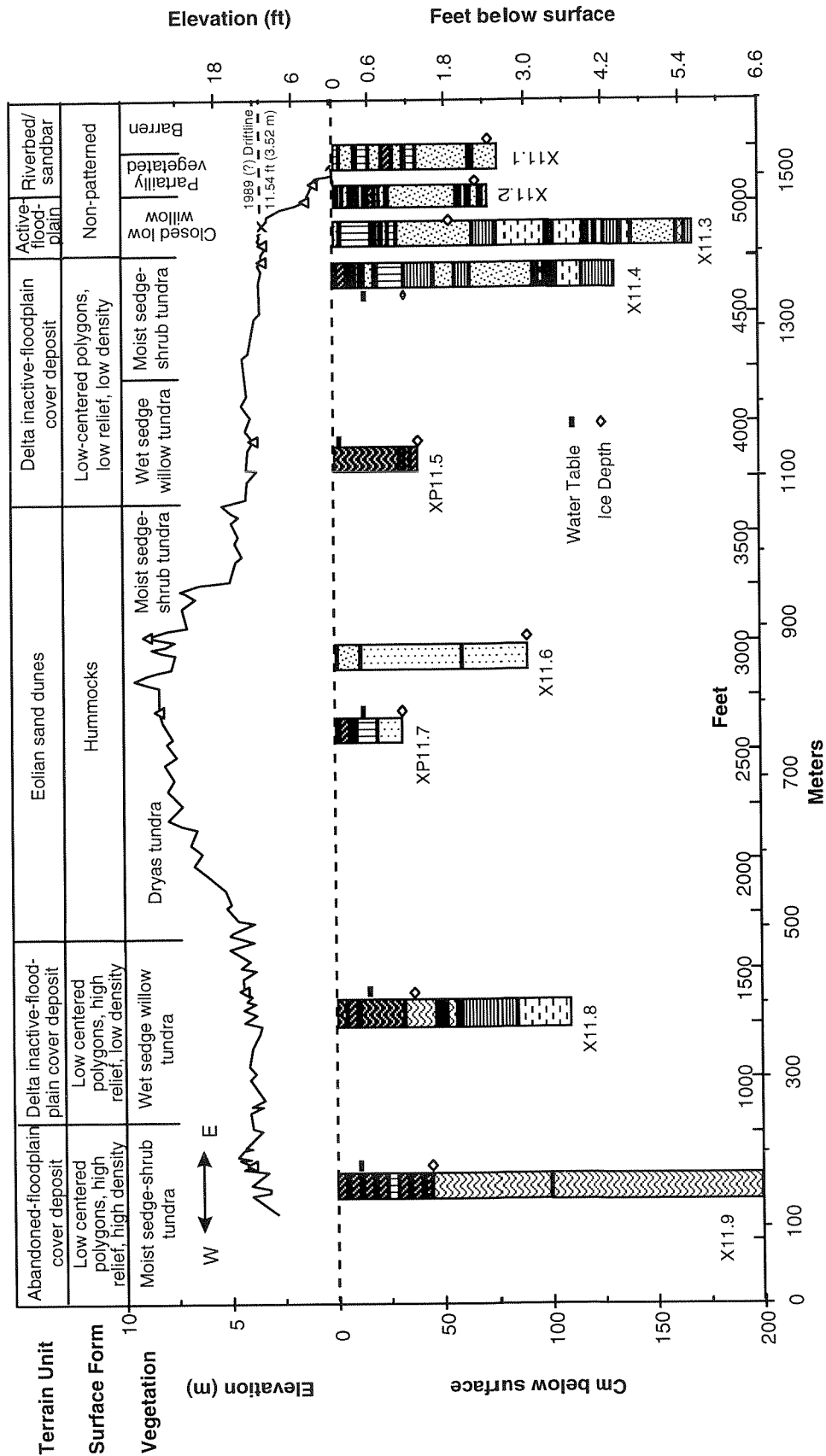


Figure 10-4. Soil stratigraphy along a terrain sequence (Cross Section N7.46) near Nanuk Lake, Colville River Delta, 1995.

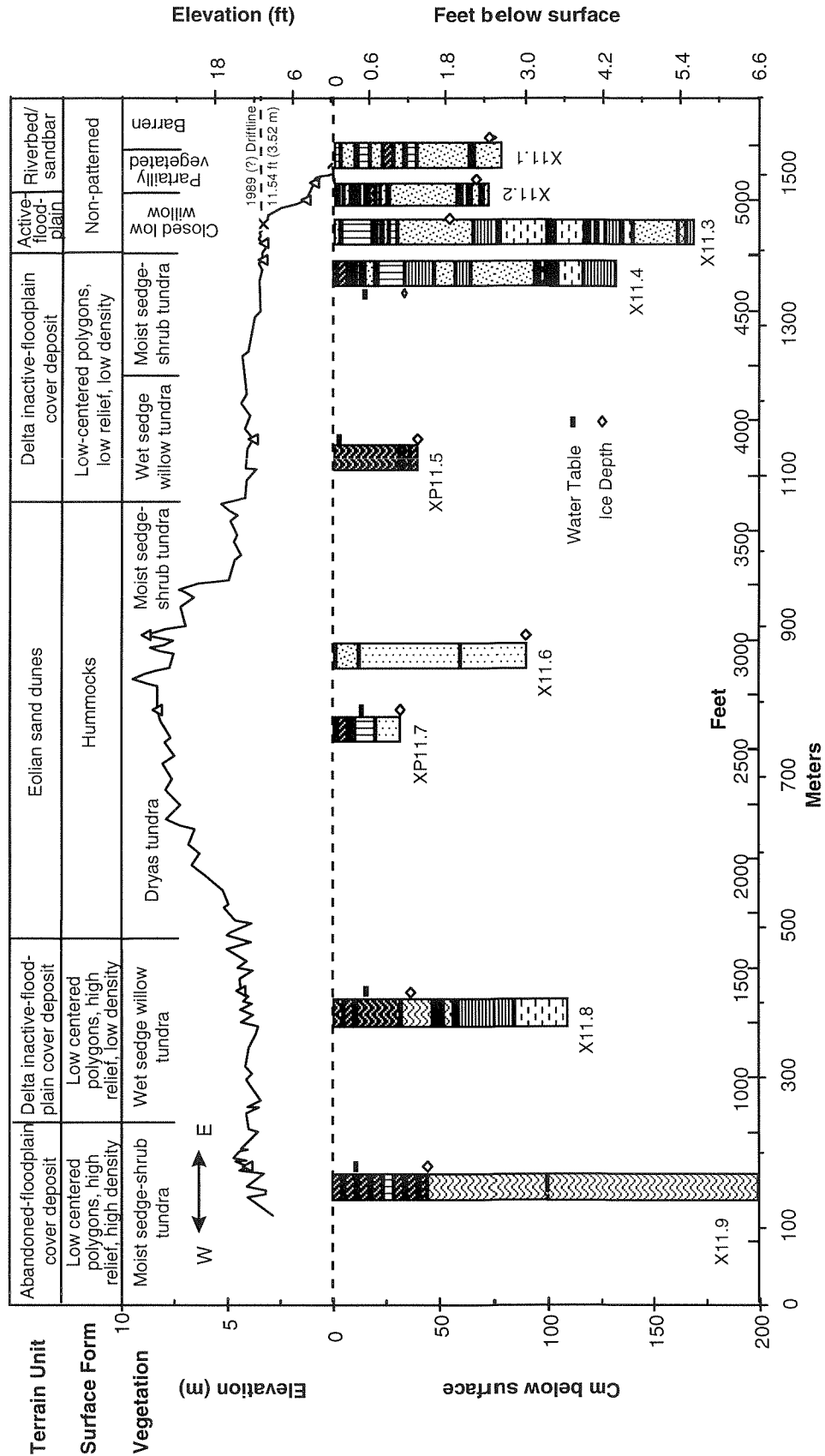


Figure 10-5. Soil stratigraphy along a terrain sequence (Cross Section S9.80) along Sakoonang Channel, Colville River Delta, 1995.

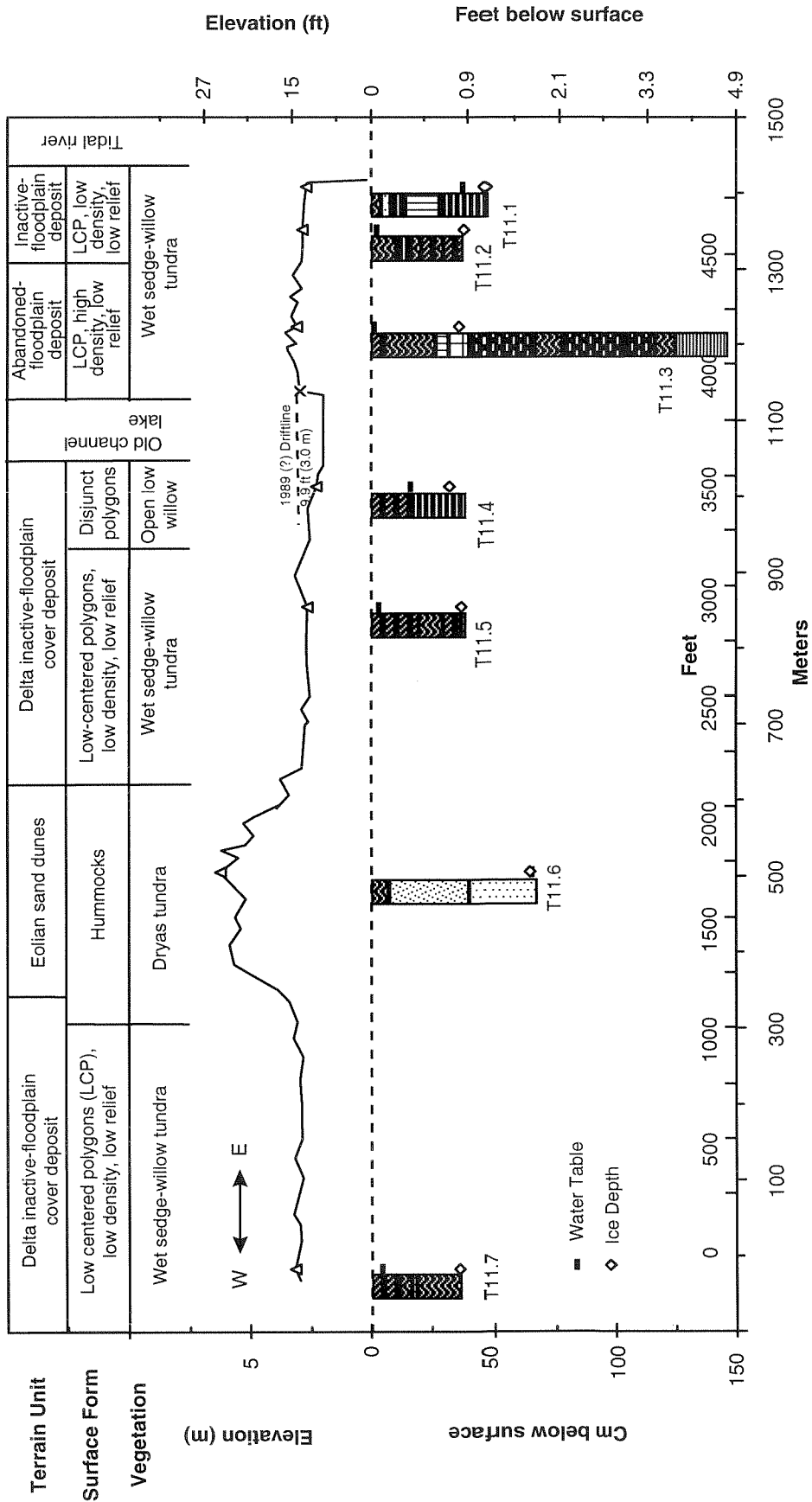


Figure 10-6. Soil stratigraphy along a terrain sequence near Nanuk Lake (Transect 11), Colville River Delta, 1995.

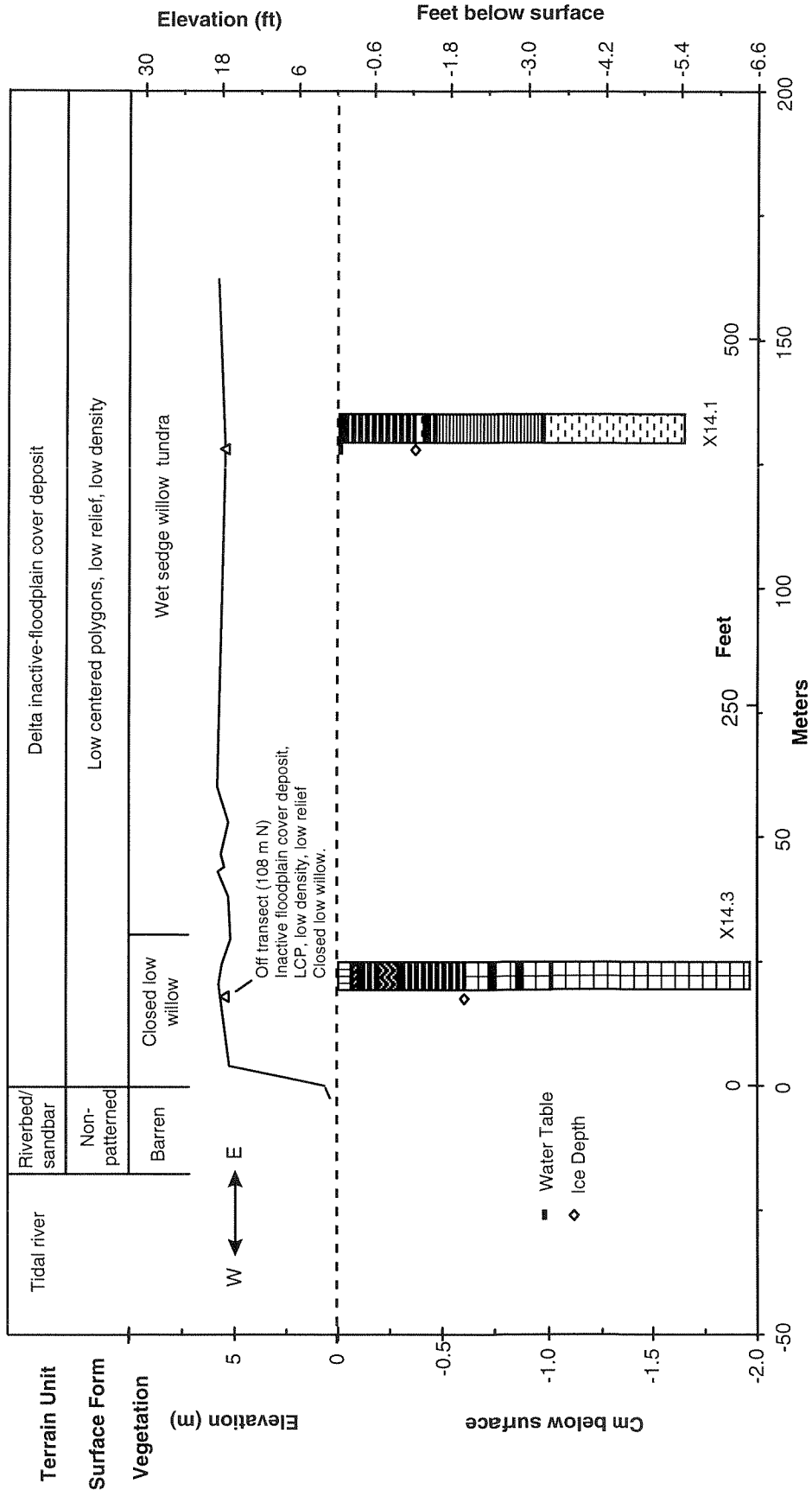


Figure 10-7. Soil stratigraphy along a terrain sequence along the East Channel (Cross-Section E20.56), Colville River Delta, 1995.

lake that is eroding into the ice-rich sediments (Figure 10–5). Transect 12, located across the Nechelik Channel from Cross Section N7.46, does not include the riverbed/sandbar and active-floodplain cover deposits but does include good examples of inactive-floodplain cover and abandoned-floodplain cover deposits (Figure 10–6). Finally, the western bank of Cross Section E20.56 (14) is included because it represents inactive-floodplain cover deposits near one of the proposed pipeline crossings. Borehole log associated with these profiles are proved in Appendix H.

Sediment Characteristics

There were substantial differences in particle-size distributions among the various terrain units (Figure 10–8). The mean percentage of sand in active-layer samples showed consistent decreases from delta riverbed/sandbar (64.4%) to active-floodplain cover (50.4%) to inactive-floodplain cover (35.0%) deposits. In contrast, the percentage of sand increased slightly from inactive-floodplain to abandoned-floodplain (44.0%) cover deposits. The mean percentage of clay more than doubled from riverbed/sandbar (7.4%) to inactive-floodplain cover (18.1%) deposits. Samples obtained with the SIPRE corer showed similar trends (Figure 10–8). Particle-size distribution was analyzed separately for the two sets of samples, however, because particle size was one of the characteristics used to define terrain units.

Changes in particle-size distribution reflect differences in flood frequency, duration, and magnitude and in eolian input among terrain units. The high percentage of sand and low percentage of clay in delta riverbed samples is typical of high-frequency, moderate-energy, depositional environments. In contrast, the higher percentage of clay in inactive-floodplain cover deposits indicates a low-velocity depositional environment.

The increase in the percentage of sand from inactive-floodplain to abandoned-floodplain cover deposits probably was due to eolian input, because sand grains tended to be evenly distributed through the organic matrix, as opposed to occurring in distinct thin layers of silt, as would be seen in fluvial deposition. In addition, the greater age of the abandoned-floodplain cover deposits allowed greater accumulation of eolian material (even

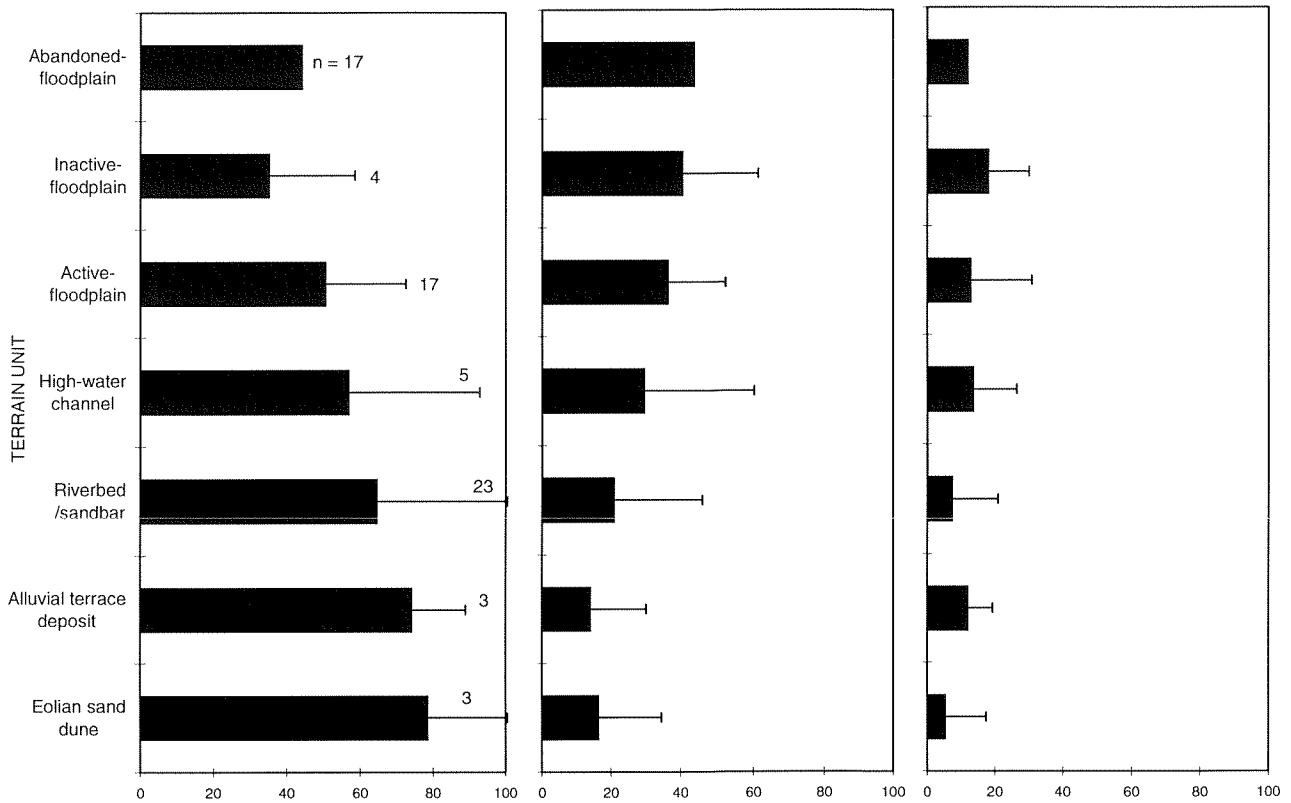
though the rate of eolian deposition may be similar between inactive and abandoned deposits). Although only one sample was analyzed because most soils were highly organic, visual observations also indicated a higher percentage of sand grains in older abandoned-floodplain cover deposits.

Throughout the delta, we observed a mineral horizon near the surface of most inactive-floodplain cover deposits that we attributed to the large flood of 1989. The thickness of the fine deposits (silty sand to organic with some silt) varied from 0.13 ft on inactive-floodplain cover deposits at Cross Section 27.09 (6) at the head of the delta, to 0.06 ft at Cross Section E20.56 across from Putu Channel and Cross Section N7.46 near Nanuk Lake, and 0.03 ft at Cross Section S9.80 near the middle Sakoonang Channel and Transect 1 near the lower Tamayayak Channel. This thin surface layer, which was found both in 1992 and 1996, consistently occurred below the highest driftlines, indicating a close correspondence between the two indicators of flooding.

Both this flood-caused deposition and driftwood also was observed on abandoned-floodplain cover deposits at Cross Sections N7.46 and E20.56 and Transect 10, but was missing at others (Cross Section S9.80 and Transects 1, 11, and 13). This inconsistent occurrence of fluvial sediment and driftwood on the abandoned-floodplain cover deposits at Cross Section N7.46 and Transect 10, but not on similar deposits across the Nechelik Channel (Transect 11), probably resulted from the unusual flooding conditions associated with Nanuk Lake. Nanuk Lake was breached near an outside bend of the Nechelik Channel, and the floodwater entering this lake probably backs up in this area.

Salinity, as measured by electrical conductivity (EC) of soil samples obtained from the active layer in 1992, consistently decreased from riverbed/sandbar deposits (6571 $\mu\text{S}/\text{cm}$) to active-floodplain (2683 $\mu\text{S}/\text{cm}$) and inactive-floodplain (741 $\mu\text{S}/\text{cm}$) cover deposits, but was similar between inactive- and abandoned-floodplain (750 $\mu\text{S}/\text{cm}$) deposits (Figure 10–9). These high values were attributed to the location of their sampling, which was near the coast and resulted in higher-salinity samples being collected in 1992. In 1995, measurements from soil water obtained from SIPRE core samples also revealed decreasing EC values from riverbed

PARTICLE SIZE ANALYSIS FROM ACTIVE-LAYER SAMPLES IN 1992



PARTICLE SIZE ANALYSIS FROM SIPRE CORES IN 1995

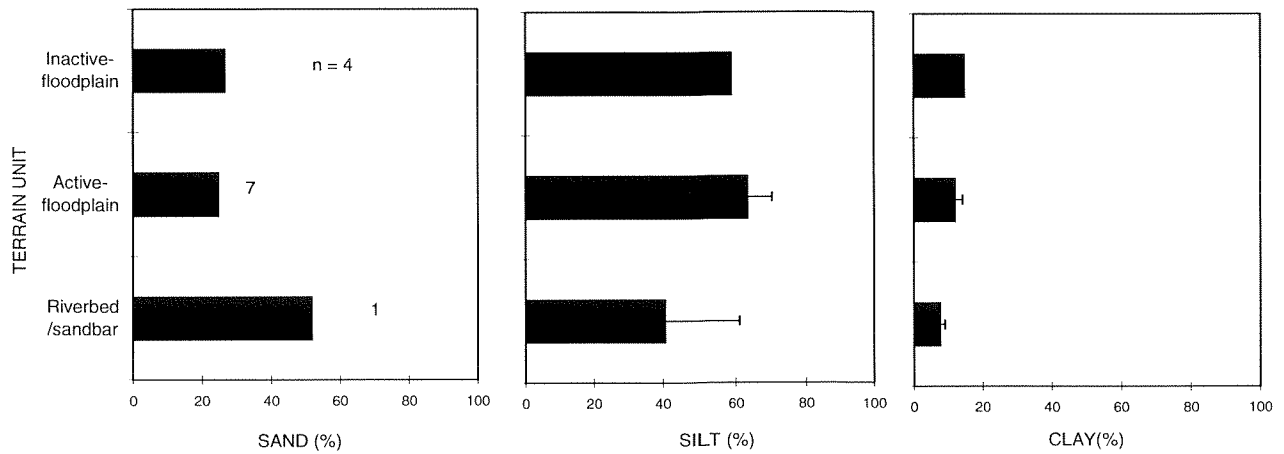


Figure 10–8. Mean (\pm SD) percentages of sand, silt, and clay of soils associated with various terrain units on the Colville River Delta. Samples in 1992 were obtained from the active layer, whereas, samples in 1995 were taken from frozen subsurface layers with a SIPRE corer.

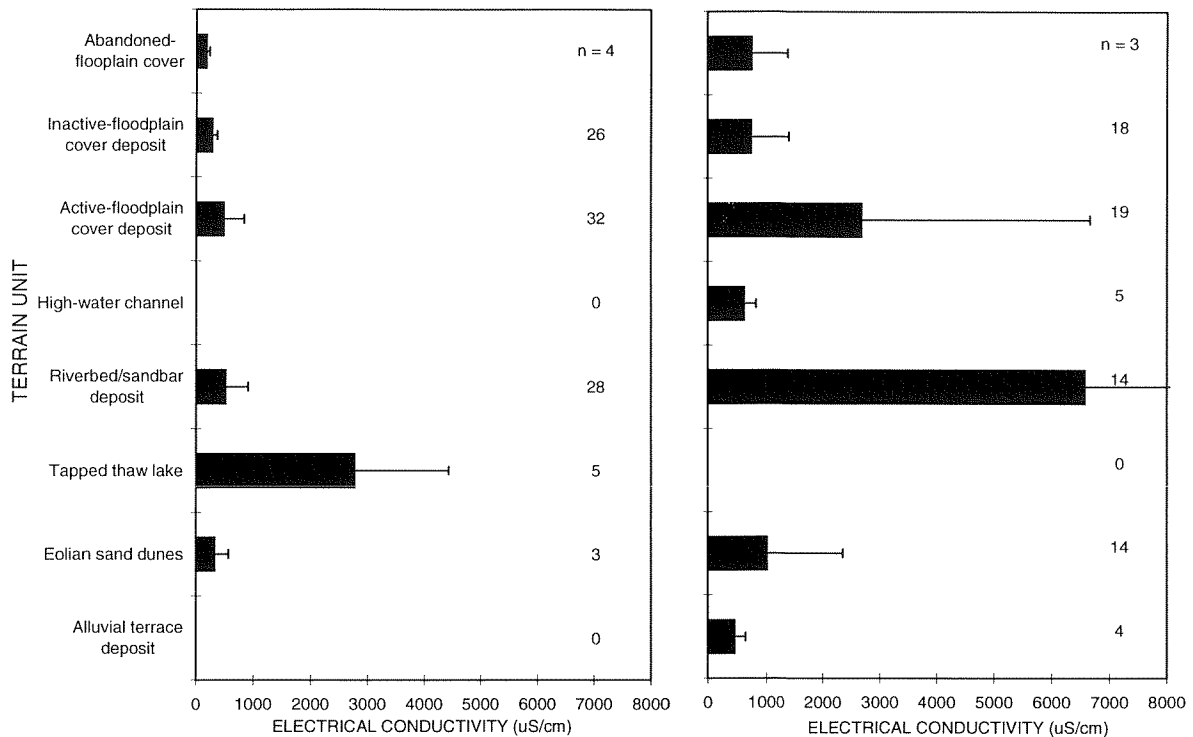


Figure 10-9. Mean (\pm SD) salinity (electrical conductivity) values for soils associated with various terrain units on the Colville River Delta. In 1992, samples were obtained from the active layer, whereas, in 1995 samples were taken from frozen subsurface layers with a SIPRE corer.

deposits (518 μ S/cm) to abandoned-floodplain deposits (286 μ S/cm). In addition, EC values were much higher in delta thaw basin deposits (2774 μ S/cm) than in other deposits.

Accumulation of Organic Matter

Large differences in the mean thickness of the top organic horizon, indicating how much organic material has accumulated since the last significant fluvial deposition, were found in deltaic deposits (Figure 10-10). *In-situ* accumulations of organic material (not including thin layers of drifted peat) were absent on riverbed/sandbar deposits (mean = 0 ft) and nearly absent on active-floodplain cover deposits (0.01 ft). In contrast, mean thicknesses of organic accumulation since the last major depositional event were intermediate for inactive-floodplain cover deposits (0.25 ft) and highest for abandoned-floodplain cover deposits (0.59 ft).

The mean cumulative thickness of organic horizons (organic or organic with trace silt) in the top 1 ft, a long-term indicator of how frequent fluvial deposition has been, also showed large difference among riverbed/sandbar (0 ft), active-floodplain cover (0.01 ft), inactive-floodplain cover (0.64 ft), and abandoned-floodplain cover (0.84 ft) deposits (Figure 10-10). The inactive-floodplain cover deposits generally were characterized by numerous interbedded organic and mineral layers near the surface, but most of this material still was organic in origin. In contrast, most abandoned-floodplain cover deposits were entirely organic or had minor amounts of sand of eolian origin.

Ice Structures and Volumes

Soil borehole descriptions along the terrain sequences from riverbed/sandbar deposits to abandoned-floodplain cover deposits revealed consistent differences among terrain units in structure and ice volumes (Figures 10-3). Seven

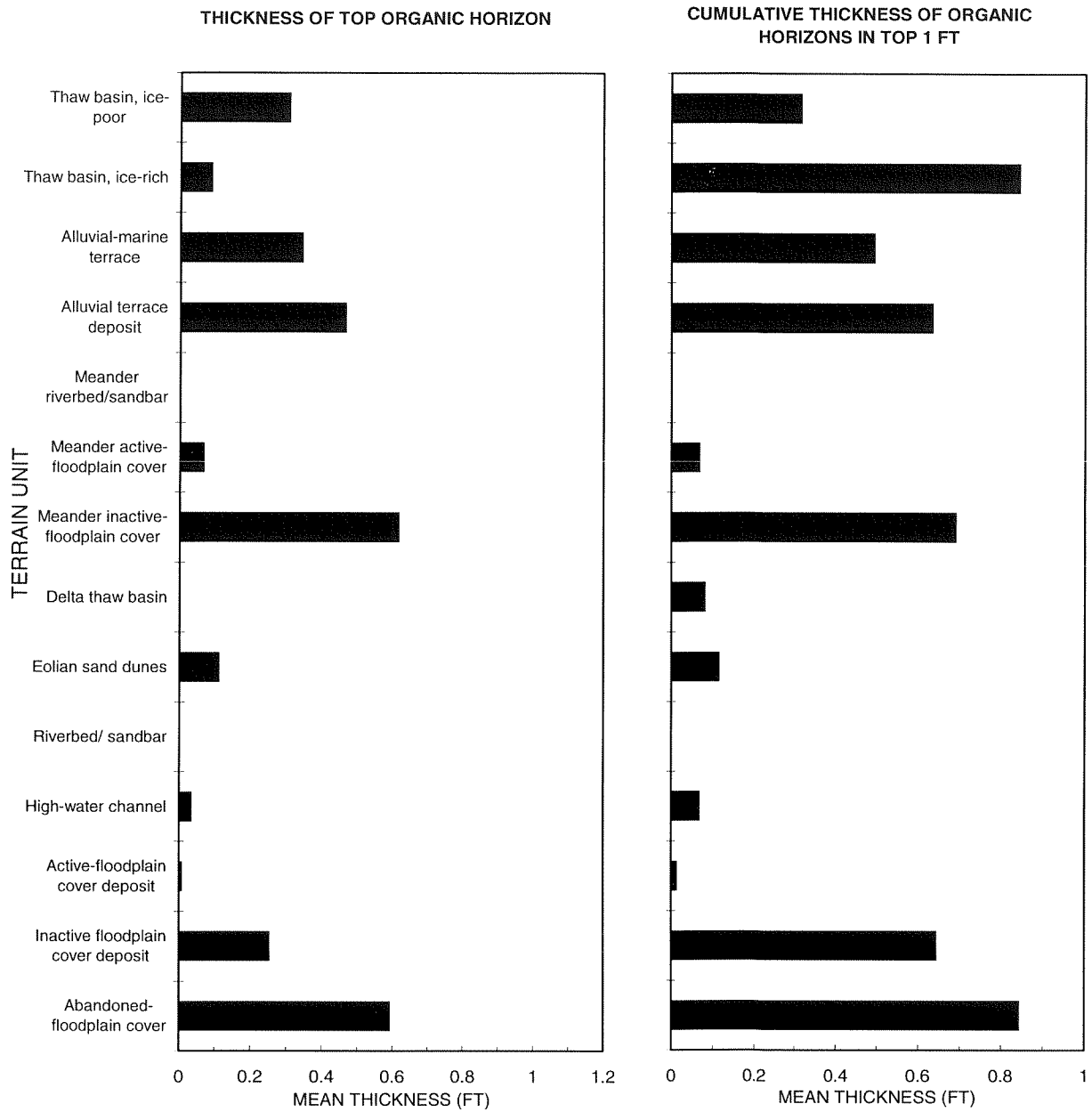


Figure 10–10. Mean (\pm SD) thickness of the top layer of organic matter (left) and cumulative thickness of organic layers in top 1 ft (right) for soils associated with various terrain units on the Colville River Delta, 1995.

types of cryostructures were observed in sediments: structureless, lenticular, layered horizontal beds, layered ice wedges, regular reticulate (ataxitic), suspended, and sheet ice (Figure 10–11). A comparison of profiles indicates that the distribution of cryostructure types was related both horizontally and vertically to the distribution of terrain units.

Riverbed/sandbar deposits (bottom sections of X12.1, X12.2, X12.5, and X11.3) typically did not have visible ice (i.e., were structureless) or occasionally had very thin or low percentages of visible lenticular ice. When riverbed/sandbar deposits were at the surface, ice wedges were absent.

Active-floodplain cover deposits (X12.2 and X11.2) generally had 2–3 ft of ice-rich sediments with mostly lenticular cryostructures, although thin layers of layered ice occasionally were present. Cracks were evident at the surface, indicating the initial development of ice wedges but polygonal rims were not evident.

Inactive-floodplain cover deposits (X12.5, X12.10, X12.11, X11.4, X11.8, X14.1, X14.3, T11.2, and Y3) generally had 2–10 ft of ice-rich sediment (25–50% ice) and sediment poor ice (50–75% ice). The interbedded mineral and organic layers typical of inactive-floodplain cover deposits generally were contained within the active layer but sometimes extended into the permafrost. In the underlying fine-grained sediments that originally accumulated when the deposits received active deposition of sediments, layered, reticulate, and suspended structures were as common or more common than were lenticular structures. At four sites (bottom sections of X12.10, X14.3, T11.2, and Y3), we observed sheet ice, a term we used to describe a type of ice of unknown origin (Jorgenson and Shur 1995). These massive sheets of clear ice with trace amounts of suspended particles were 1–2 ft thick, although the true extent of this type of cryostructure was not determined because it occasionally extended beyond the depth of our coring. Polygonal rims indicating ice-wedges were common, although they were low in density.

Abandoned-floodplain cover deposits (X12.9, T11.3, and X11.9) generally had highly variable subsurface cryostructures. Two sites (X12.9 and X11.9) had ice-rich organic matter with massive layered ice structures, and one of these had several feet of very fine lenticular structures in a sandy

matrix derive of eolian material. At the third site (T11.3), the inactive-floodplain cover deposit below the organic abandoned-floodplain cover deposit generally had sediment-rich ice with suspended structures but also had minor amounts of reticulate and layered structures.

There were substantial differences among terrain units in the ice content of the near-surface frozen soils (Figure 10–12). Mean water contents (% volume) were lowest for riverbed/sandbar deposits (61.1%), intermediate for active-floodplain cover deposits (67.7%), and highest for inactive-floodplain cover deposits (73.4%). Ice contents of ~80% were common in inactive-floodplain cover deposits. We were unable to determine ice volumes for abandoned-floodplain cover deposits because they mostly had organic soils.

Overall, there was little difference in mean ice contents in the top 6–7 ft of soil (64–75%), where both active- and inactive-floodplain cover deposits predominated. Generally, ice contents were slightly lower (49–56%) below that depth, where sandier riverbed sediments predominated. Ice volumes at saturation were assumed to be in the range of 35–40%. Thus, volumes above this amount can be considered excess ice (above what the soil contains at saturation).

Because we purposely avoided ice wedges during our coring, these ice volumes do not include volumes associated with ice wedges. We observed wedge ice as much as 6–10 ft across at the top and extending at least 10 ft below the surface in inactive-floodplain cover deposits along the Nechelik Channel. Although we did not try to measure the volume of ice contributed by ice wedges, it probably is substantial. In the Mackenzie Delta, the total volume of ice composed of ice wedges exceeded 50% of the materials in the upper 3–7 ft of the ground (Pollard and French 1980). Observations in Russian deltas, however, made by one of the authors (Shur) suggests that values of 5–15% for the percent of the total volume contributed by ice wedges is more typical.

Another indicator of very high ice contents in the delta is the abundance and depth of thaw lakes. Most of the abandoned-floodplain cover deposits have been lost to thaw lake processes, so only scattered remnants remain (Figure 10–2). In addition, most thaw lakes in the central delta range

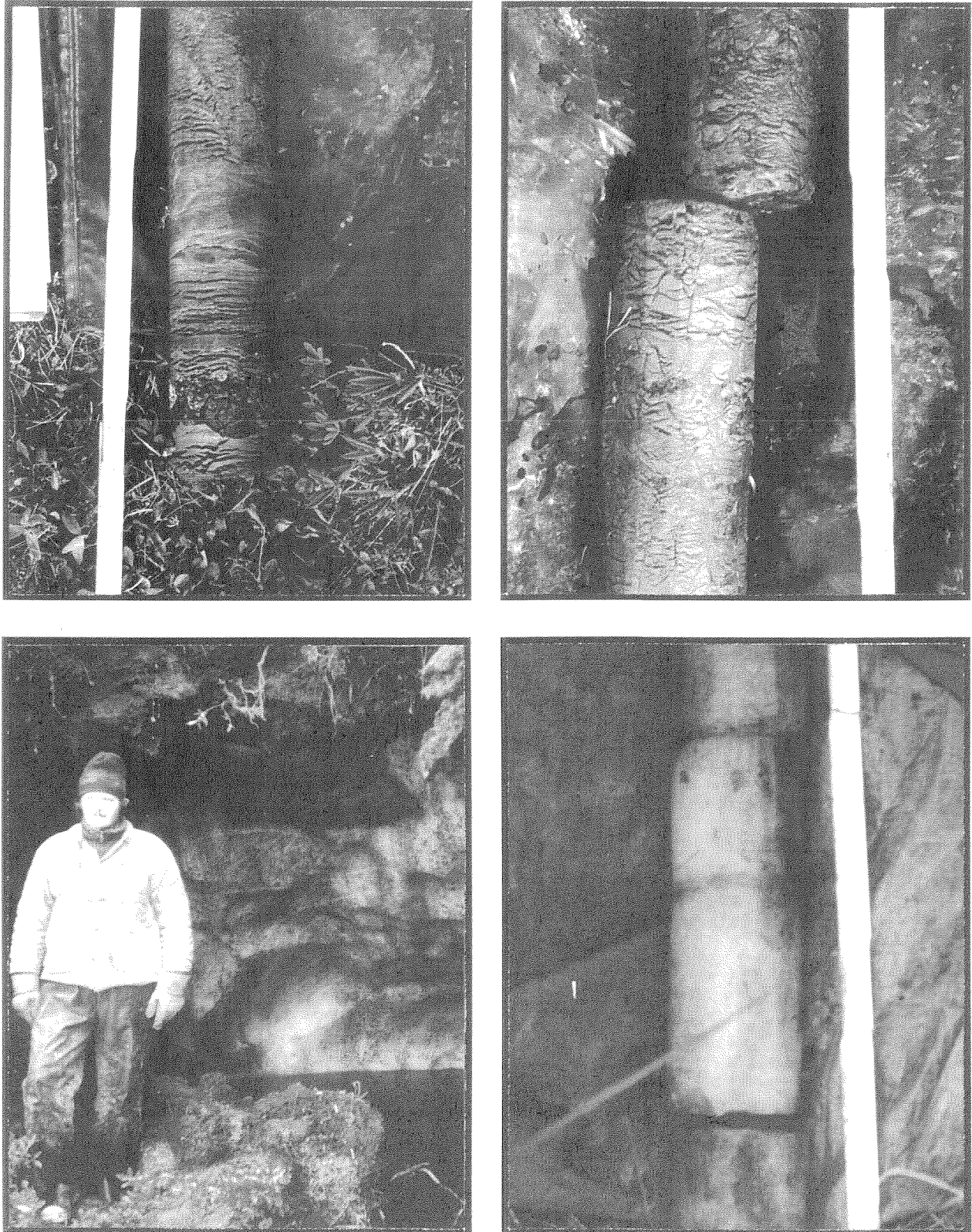


Figure 10–11. Photographs of common ice types: structureless and lenticular ice (upper left), reticulate and suspended ice (upper right), sheet ice (lower right), and wedge ice (lower left) on the Colville River Delta, 1995.

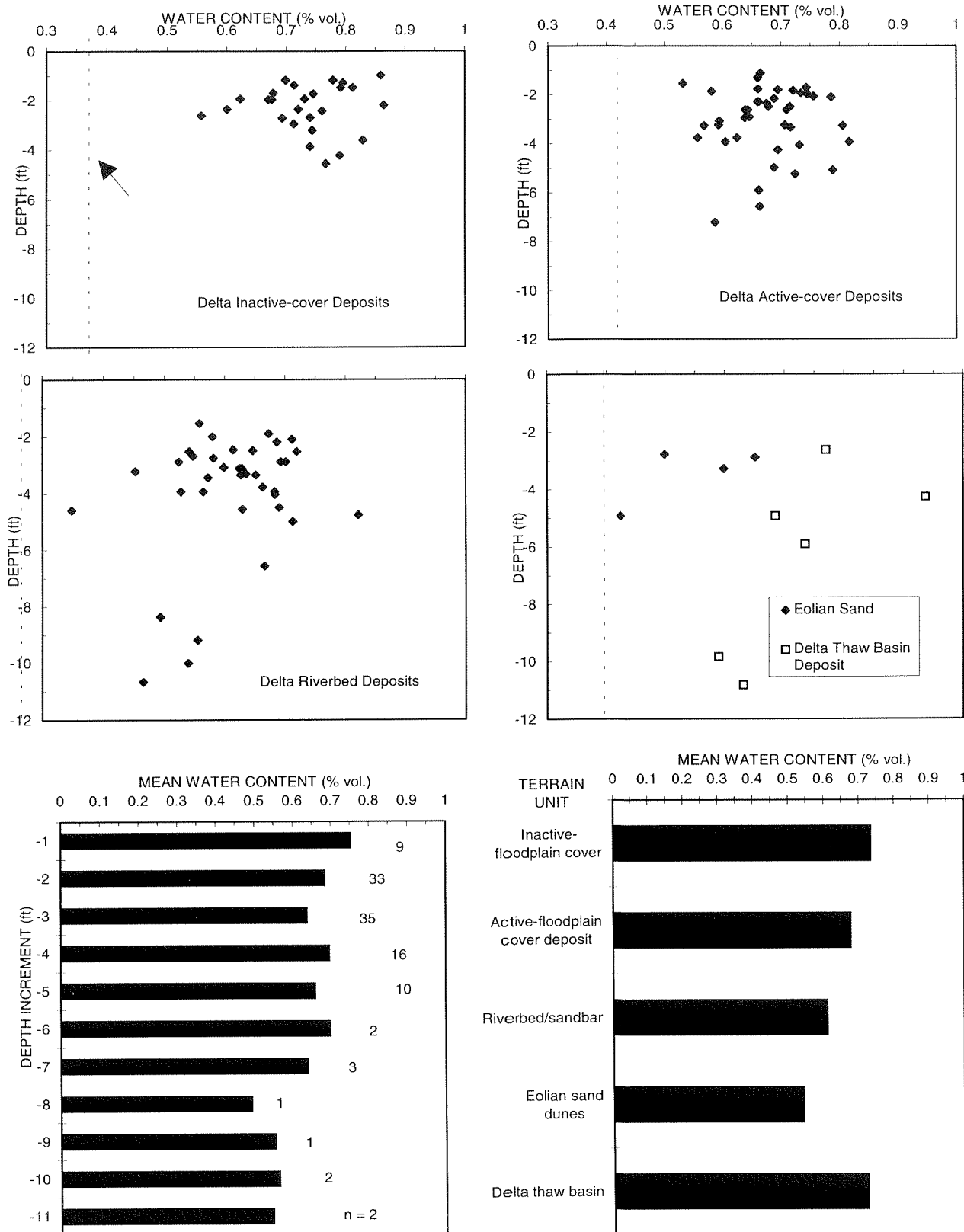


Figure 10-12. Volumetric ice contents near the soil surface grouped by terrain unit (upper four graphs) and summarized by depth (lower left) and terrain unit (lower right) Colville River Delta, 1995.

from 11 to 15 ft deep. Using these water depths for interpreting how much excess ice was present in the deposits before they melted is problematic, however, because the elevations of the adjacent floodplain deposits surrounding the thaw lakes have increased over time, making the lakes deeper.

Overall Accumulation Rates

The rate at which material has accumulated over time within the various terrain units was determined from radiocarbon dating of samples obtained from active-layer samples and SIPRE cores. Large differences in accumulation rates were found among riverbed/sandbar (0.95 ft/100 years), active-floodplain cover (0.33), inactive-floodplain cover (0.24), and abandoned-floodplain cover (0.08) deposits (Figure 10–13).

These rates, however, also include accumulations of sediment, organic material, and ice, so that the actual amount contributed to sedimentation could not be separated. Some generalizations, however, can be made about types of materials. Riverbed/sandbar deposits mostly sediment and had little ice. Active-floodplain cover deposits were mostly sediment and had lesser

mounts of ice. Inactive-floodplain cover deposits were mostly ice with lesser amounts of sediment and organics. Abandoned-floodplain cover deposits mostly were ice and organic material. Another factor that limited the analysis of accumulation rates was the small sample sizes for most terrain units.

GRAVEL RESOURCES

Three moderately deep boreholes were drilled near the proposed drill sites, to determine if there was gravel near the surface that could be used for development. The first borehole, which was in a ice-poor thaw basin deposit in Nanuk Lake, extended to a depth of 13 ft and encountered silty clay loam sediments throughout the profile. The second borehole, which was in a barren riverbed/sandbar deposit in the Nechelik Channel (X12.1), extended to a depth of 15 ft and encountered only interbedded silt and fine sand. The third hole, which was in a barren riverbed/sandbar deposit along the Sakoonang Channel (X11.10), extended to a depth of 15 ft and encountered interbedded silt and fine sand.

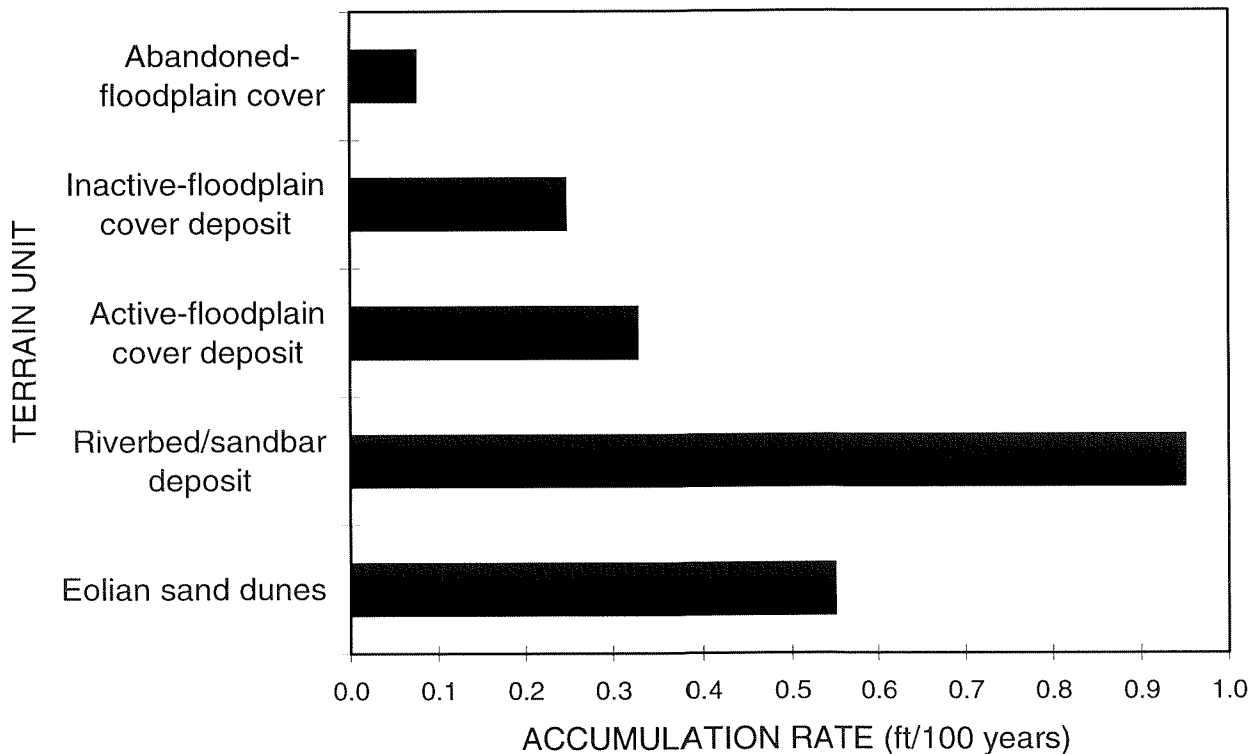


Figure 10–13. Mean (±SD) rates of accumulation of material (sediments, organics, and ice) for various terrain units on the Colville River Delta, 1995.

Data from these boreholes indicate that obtaining gravel from the middle of the delta is impractical. We suspect that there is gravel at greater depths (perhaps 30–50 ft) that was deposited during the late Pleistocene when sea-levels were lower (-66 ft around 10,000 yr ago); however, this gravel would be difficult to extract. Although dredging the Nechelik Channel might be feasible, the depth to gravel there is unknown.

Although obtaining gravel from the middle of the delta does not appear to be feasible, there are other sources of gravel within 8 mi of the proposed drill sites. First, gravel has been dredged from below the Nechelik Channel for use by the village of Nuiqsut (Walker 1994a). Second, riverbed deposits along both the Miluveach and Kachemach Rivers are composed of gravelly sediments. These gravelly deposits are exposed near the surface along most of the Kachemach River and extend to near the mouth of the river. Third, gravel is exposed along the shorelines of several of the large lakes on the eastern margin of the delta floodplain, between the Putu Channel and the Itkillik River. Finally, there probably are gravel deposits beneath the alluvial-marine deposits within the proposed Transportation Corridor, similar to deposits in Kuparuk; however, specific information on depths of these deposits is not available.

CONCEPTUAL MODEL OF FLOODPLAIN EVOLUTION ON THE DELTA

Based on similarities in sediment characteristics, organic matter accumulation, and ice aggradation along the terrain sequences that we examined, some general patterns and processes are evident. These patterns and processes also are similar to those that have been described on Russian floodplains in the Arctic (Shur 1988). In the following discussion, we focus on the general trends that we observed and synthesize these into a conceptual model of floodplain evolution on the delta. This conceptual model is useful for improving our understanding of surficial materials and our ability to use terrain units to predict soil properties across the delta. We then discuss the implications of these patterns and processes for oil development on the delta.

Processes of Accumulation of Delta Deposits

The analysis of the stratigraphy of deltaic deposits revealed that the deposits were formed by four processes: (1) fluvial deposition of mineral material, (2) eolian deposition of mineral material, (3) accumulation of organic material derived from partially decomposed plants, and (4) the accumulation of ice. The relative importance of these processes in the development of delta-floodplain deposits changes during the various phases of floodplain evolution from riverbed/sandbar deposits to abandoned-floodplain deposits (Figure 10–14).

The relative contribution of each process at any phase of evolution depends not only on its own intensity but also on the intensity of the other processes. For example in our field descriptions, we noted considerable amounts of sand in abandoned-floodplain cover deposits and laboratory analyses determined that the percentage of sand, relative to silt and clay, was higher in abandoned-floodplain than in inactive-floodplain cover deposits. Although this difference could be attributed to increased eolian activity, it is more likely due to decreased rates of fluvial deposition and organic matter accumulation, thus making eolian deposition relatively more important. The interplay of the various processes and their resulting patterns are described below.

Permafrost Development and Thaw Stability on Delta Floodplains

Of primary importance to permafrost development on floodplains is the location of the delta in an area where low air and soil temperatures and thin snow cover of high density result in the formation of continuous permafrost and a special type of permafrost formation called syngeneses (Shur 1988). The aggradation of ice during this permafrost formation, and subsequent degradation of the permafrost due to thermal instability, results in a wide range of deposits and surface-forms that are characteristic of arctic deltas.

The formation of syngenetic permafrost in the delta is caused by the addition of new material at the soil surface, a decrease in active-layer thickness, and by the accumulation of ice below the active layer. Over the course of floodplain evolution, new

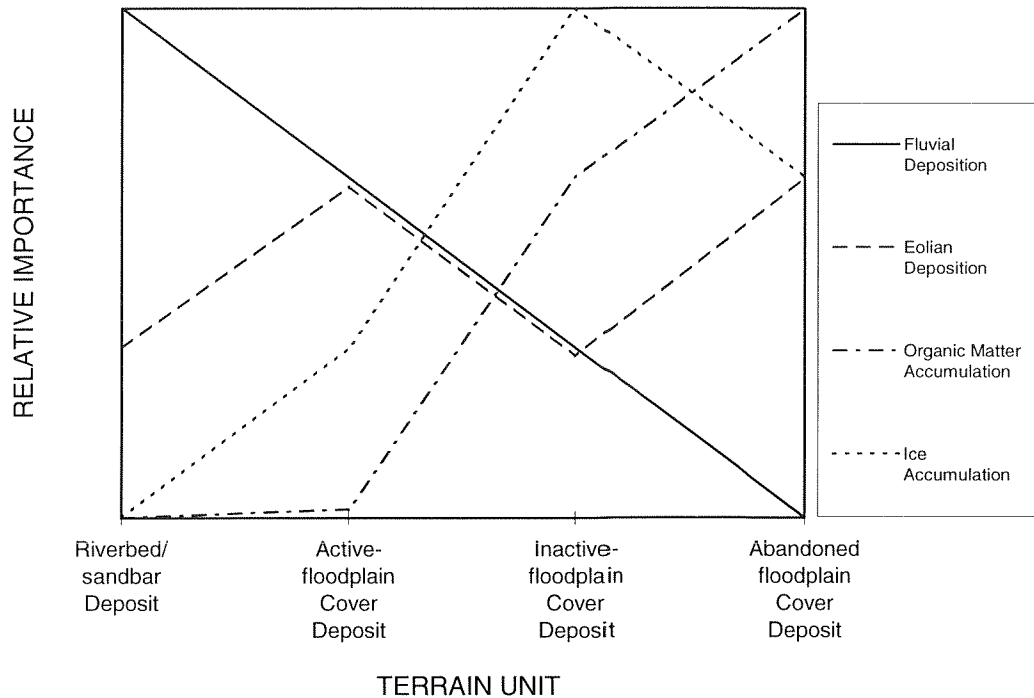


Figure 10-14. Relative importance of the processes of fluvial and eolian deposition, and organic matter and ice accumulation in common floodplain deposits on the Colville River Delta.

material is added to the top of the active layer by deposition of fluvial sediment on the soil surface and accumulation of organic matter. The accumulation of organic material, increased saturation of the active layer, and changes in vegetation structure alter the thermal regime of the soils, causing the thickness of the active layer to decrease. This addition of new material on top and the decrease in active-layer thickness results in new mineral and organic material being incorporated in the top of the permafrost.

At the same time, ice is formed at the bottom of the active layer, because water freezes to the top of the cold permafrost during refreezing of the active layer in the fall. During some summers, not all of the ice produced the previous fall is thawed, and over time, some of this ice accumulates in the underlying sediments. This accumulation of sediments, organic matter, and ice causes the surface to rise over time.

While this is a general description of the process of syngenetic permafrost formation, specific changes in the relative importance of formative processes (fluvial, eolian, organic) associated with the various phases of floodplain

evolution are important to the structure and volume of the ice in the permafrost. Changes in the processes and the resulting patterns of material accumulation during floodplain evolution, as they relate to the most common terrain units, are described below (Figure 10-15). Each of these deposits represent a distinct phase of floodplain evolution.

In delta riverbed/sandbar deposits, frequent (every 1-2 yr) inundation, sedimentation, and scouring prevents the establishment of vegetation, and surface sediments accumulate fairly rapidly (mean of 0.95 ft/100yr). Due to the coarse texture of the soil and lack of vegetative cover, active layer depths are deep (mean of 2.2 ft). Below the active layer, cryogenic structures in the permafrost typically are structureless (massive) and ice contents are low because of the sandy texture of the sediments. Therefore, the rapid rates of deposition move the active layer upward before much ice can be formed at the bottom of the active layer.

Active-floodplain cover deposits are limited to narrow bands along the margins of riverbed deposits. Flooding is still fairly frequent (every 3-4 yr) but the accumulation rate of material (mostly sediment) is substantially lower (0.33 ft/100 yr) than that of

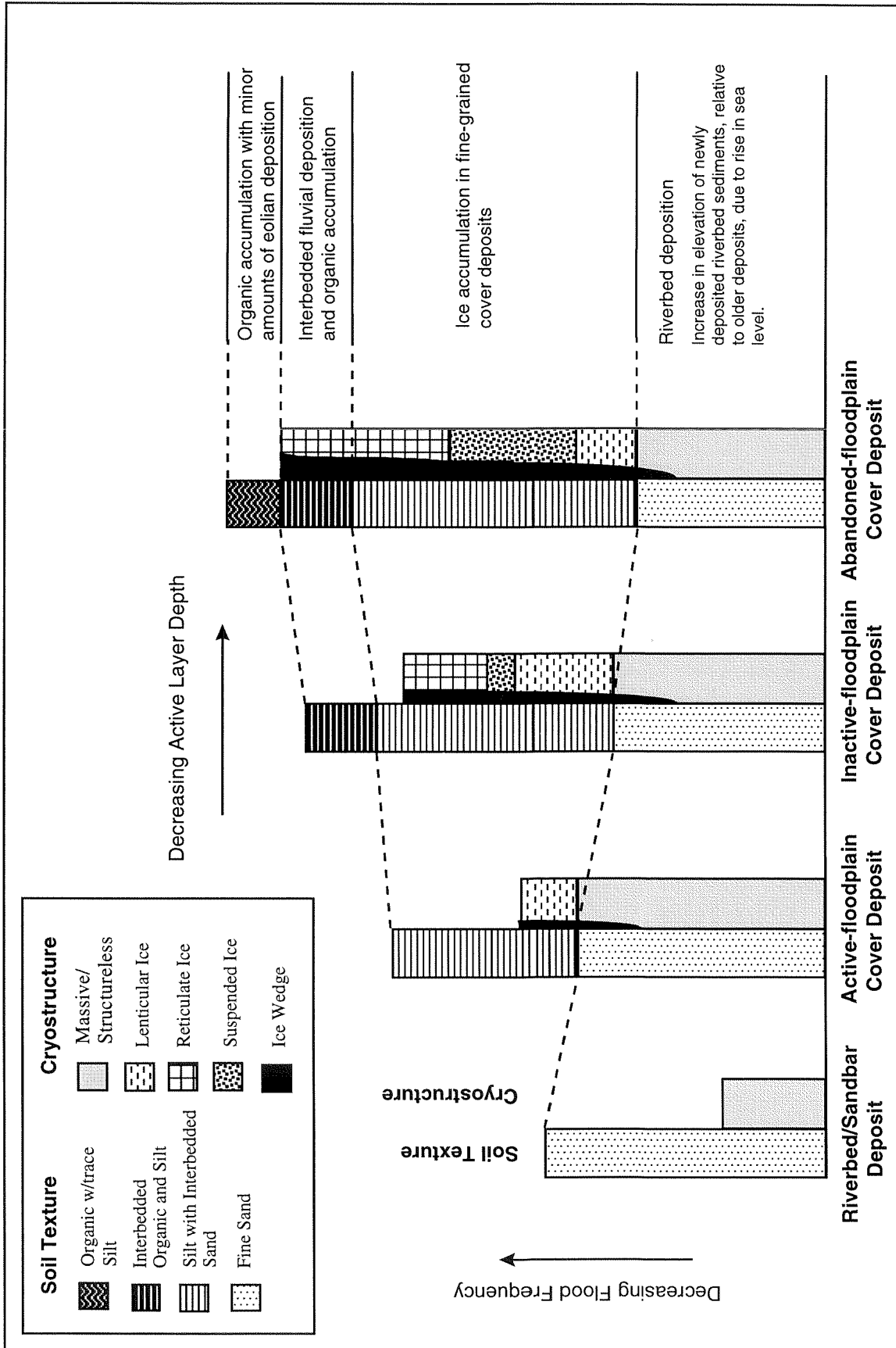


Figure 10-15. A conceptual model of changes in soil texture, active layer thickness, and cryogenic structure during evolution of floodplain deposits on the Colville River Delta.

riverbed deposits (0.95 ft/100 yr). Over time, the added sediment raises the surface, which reduces the frequency of flooding. Both the addition of nutrient-rich sediment from frequent deposition and the well-drained soil conditions favor vigorous growth of shrubs, preventing the development of a moss mat. The mean depth of the active layer is slightly less (1.9 ft) than that of barren riverbed deposits (2.2 ft). Subsurface ice contents remain relatively low, but lenticular structure is more common in the silty active-floodplain cover deposits than in sandy riverbed deposits.

During this active-floodplain phase, approximately 2–4 ft of silty sediment can accumulate on top of the riverbed deposits. It is the accumulation of these fine-grained sediments during this phase that provides the primary material for ice aggradation during the next phase involving inactive-floodplain cover deposits. Eventually, the added sediment and migration of channels reduces the frequency of flooding to a point where peat can start to accumulate. Based on sedimentation rates and the lack of change in these deposits between 1955 and 1992, we estimate that this phase may persist for 100–300 yr.

After these early phases of floodplain evolution, a large transition in permafrost development occurs on inactive-floodplain cover deposits. Flood frequency (every 5–25 yr) and sedimentation rates are substantially lower than those for active-floodplain cover deposits, allowing the build up of organic material and creating the distinctive interbedded structure of silt and peat layers at the surface. The active layer remains saturated throughout the summer, and mean active-layer depths (1.3 ft) decrease substantially in response to changes in vegetation composition and changes in thermal properties of the soil. Both the decrease in the depth of the active layer and the reduced sedimentation occurring during this phase contribute to the accumulation of ice at the top of the permafrost. The accumulation rate of materials (mostly ice, with some organics and sediments) is still substantial (0.24 ft/100 yr), however. The total thickness of the inactive-floodplain cover deposits ranges from 2.5 ft on newly developing deposits to

9 ft on older deposits. This phase may last about 1500 to 2500 yr.

The sediments in the active layer, which were deposited during the previous phase, slowly join the permafrost. The upper layer of permafrost, which forms during this phase from the active layer of the previous phase, is extremely ice-rich and has very distinct cryogenic structures, including reticulate ice (atactic), suspended ice (sediments suspended in ice), and thin lenses of pure ice. The suspended ice and ice lenses may represent periods when the active layer was static (little sediment accumulation or change in active-layer thickness) and ice accumulated at the same place. This combination of distinctive cryogenic structures in the upper horizon of permafrost that is evident in both the Russian and North American Arctic has been termed the "intermediate layer" by Shur (1988). As a result of ice accumulation, the thickness of the intermediate layer can become two or more times greater than the thickness of the active-floodplain cover deposit from which the intermediate layer formed (Shur 1988).

The accumulation of ice in inactive-floodplain cover deposits also includes other types of ice development, such as the formation of ice wedges and sheet ice. The formation of ice-wedges begins near the end of the active-floodplain phase, and they develop into large bodies of massive ice that form a continuous, low-density network of ice wedges in inactive-floodplain cover deposits. The low-centered polygons, which indicate active formation of ice wedges, are typical surface-forms associated with this stage. In addition, massive formations of sheet ice of uncertain genesis occasionally were found near the bottom of inactive-floodplain cover deposits.

Eventually, the inactive-floodplain cover deposits accumulate sufficient ice and organic material, along with minor amounts of fluvial and eolian material, that the surface rarely is flooded. Due to the accumulation of organic material and low thaw depths (average 1.34 ft), the active layer essentially becomes entirely organic and the deposit can be considered an abandoned-floodplain cover deposit. The amount of ice that accumulates as lenses in the frozen peat decreases, and there is a sharp decrease in accumulation rates (0.08 ft/100 yr) of surface materials (mostly organics, ice, and trace amounts of eolian silt and sand). Continued polygonal development (subdivision of large polygons) leads to the formation of high densities of ice-wedge polygons.

Our limited data suggest that this phase occurs 2000–3000 yr after the active-floodplain cover phase.

Finally, so much ice accumulates in the sediments that the deposits become susceptible to thermal degradation and collapse, as indicated by the high areal extent of thaw lakes on inactive-floodplain and abandoned-floodplain cover deposits. Indeed, most of the abandoned-floodplain cover deposits apparently have been lost to melting because most remaining deposits exist as only narrow patches surrounding large thaw lakes in the central delta. Some of these thaw lakes become tapped by river channels and drain. Due to breaching by channels and the lower elevation of the exposed lake bottom, sediment deposition from flood water again becomes frequent.

Complicating this analysis of evolutionary trends are the effects of sea level rise. Sea level has risen from about -13 ft around 5000 yr ago, for an average rise of 0.26 ft/100 yr (Hopkins 1982). Recently, sea level has been rising worldwide at a rate of 0.79 ft/100 yr (Peltier and Tushingham 1989). This increase in sea levels is evident in the soil profiles: the elevations of the surface of newly developing riverbed deposits and of organic horizons in inactive floodplains are considerably higher than the elevations at which these deposits formed in older soil profiles. For example, at Cross Section S9.08, organic material was found at an elevation of 6 ft in an abandoned-floodplain cover deposit, whereas organic material now starts to accumulate only at elevations >11.5 ft.

The rise in sea level probably is increasing the frequency of flooding on the higher floodplain steps, because the rate of sea level rise is faster than the rate of sediment accumulation on inactive-floodplain cover deposits. For example, the current rate of increase in sea levels (0.79 ft/100yr) is similar to the rate of material accumulation for riverbed/sandbar deposits (0.95 ft/100 yr), but is substantially higher than the rates of accumulation for inactive- and abandoned-floodplain cover deposits (0.08–0.24 ft/yr).

Implications for Development

Every surficial deposit within the delta can be considered as a foundation (base) for facilities and transportation systems (roads and pipelines) associated with oil development. Two terrain units, eolian sand and abandoned-floodplain cover deposits, are of particular interest because they occupy the highest elevations in the delta and therefore are least subject to flooding. The eolian sand deposits have the best geotechnical properties, whereas the abandoned-floodplain cover deposits have the most difficult properties to work with.

The eolian sand deposits generally are well drained, have the lowest ice contents in the area, and generally are not subject to flooding. Some ice wedges are expected in sand dunes, but they are much smaller than ice wedges in inactive- or abandoned-floodplain cover deposits. The uneven topography of the dunes appears to be the greatest disadvantage for facility siting. In addition, some dunes are still active, but most, however, have been stabilized by vegetation cover.

The abandoned-floodplain cover deposit is extremely ice rich as a result of well developed segregated ice and wedge ice. The ice-rich intermediate layer, which is located under the active layer, potentially has a thaw settlement of 50% or more, and any increase in the depth of the active layer would initiate the process. Thus, the thermal sensitivity of the active layer must be considered during the design of roads and pads. This thermal sensitivity presents three potential problems, described below.

First, the main principle of design on abandoned-floodplain cover deposits has to be protection of the existing permafrost table; the depth of the active layer under any structures (i.e., gravel fill) should not exceed the depth of the existing one. This protection is already commonly done on the North Slope by placement of foam insulation or sufficient gravel.

Second, when constructing facilities on abandoned-floodplain cover deposits the vegetative cover and organic mat must be protected, because of the occurrence of well-developed ice wedges and the high density of low-centered polygons. The thermal regimes of these features can easily be affected by damage to the vegetation and the surface organic layer that covers and insulates them. When the vegetation or organic soil is disturbed by scraping, or even heavy

dust deposition, it usually leads to complete (or at least deep) thawing of the ice wedges. The process, which may begin in one spot, can propagate to adjacent ice wedges. Prevention of off-road traffic and minimization of on-road traffic during summer, as is common practice, will help avoid this problem.

Third, water potentially may accumulate inside deep ice-wedge polygons as a result of impedance of water flow from surface runoff or impoundment of meltwater from snowdrifts adjacent to roads. The presence of standing water on the surface can alter the thermal regime (Jorgenson 1986), resulting in an increase in the active layer and partial thawing of the ice-rich permafrost over a long period (perhaps 25–100 yr).

The greatest advantage of the area for development is low permafrost temperatures. For the most part, the permafrost is very stable and mitigative measures can be used to minimize the potential problems associated with the high ice contents of inactive- and abandoned-floodplain cover deposits. On balance, we believe the benefits of siting facilities on abandoned-floodplain cover deposits to minimize problems with flood waters outweighs the potential risks of thaw settlement from developing on this ice-rich terrain.

PART 11. LANDSCAPE CHANGE

By Torre Jorgenson and Erik Pullman

BACKGROUND

A substantial amount of information has been collected about rates of geomorphologic change along the Beaufort Sea coast; this information has focused on migration of barrier islands and rates of coastal and riverbank erosion. Knowledge of the rates of erosional and depositional processes is essential for planning locations of oilfield facilities.

Coastal retreat along the Beaufort Sea, some of which is so rapid that it poses a serious hazard to man-made structures, has been summarized by Hopkins and Hartz (1978). Coastal retreat along the mainland coast between Demarcation Point and the Colville River averages 5.3 ft/yr, although storm-driven episodes may cause higher rates of erosion. At Oliktok Point, for example, 36 ft of shoreline was lost within a 2-wk period. Average rates of retreat are highest from Harrison Bay west to Barrow (15.5 ft/yr), primarily because of the fine sediments and ice in the low bluffs along this coastline are easily eroded (Lewellen 1977).

Rates of erosion along riverbanks and lake shorelines within the Colville River Delta also can be rapid, although they often are less dramatic. At two sites along the Nechelik Channel, Walker (1966, 1983) measured erosional rates of just over 3 ft/yr and 6 ft/yr over a 23–30 yr period. However, averaging rates over a long period masks the episodic nature of erosion. Walker and Morgan (1964) observed a maximal erosion of 25–30 ft at a riverbank as a result of a single storm in 1961. They also found that erosion was greater along the eastern banks of the East Channel because southwesterly winds are most common during summer storms. The East Channel is sufficiently wide for sizable waves to develop, so wind-driven erosion has been found to be an important component of the annual amount of erosion.

Although these previous studies provide valuable perspective, they are of insufficient detail for facility siting and engineering design on the delta. Erosional rates, which are affected by characteristics of riverbanks, wave fetch, orientation of the wind and channels, and currents, are site-specific. Thus,

detailed information in potential areas of development is essential to optimal siting and design.

METHODS

To analyze the rates of landscape change within the Alpine Development Area, terrain unit maps were developed using aerial photography from 1955 and 1992. The maps were based on color-infrared photographs (1:18,000 scale) taken in 1992 and black-and-white photographs (1:13,000 scale) taken in 1955. During mapping, terrain units were delineated on acetate overlays of the photography, digitized, and rectified with control points obtained from a SPOT-image base map with a GIS system (AtlasGIS, Strategic Mapping, Santa Clara, CA). Maps from the two years were overlaid and the amount of overlap was analyzed with the GIS. Because of small inaccuracies in registration of maps and generation of thousands of slivers during the overlay process, areas smaller than 1.24 acre (0.5 ha) were deleted from the analysis and map presentation. The various combinations of features created by the overlay were recoded into eight classes that reflected differing erosional and depositional processes. Data obtained from three small areas in the outer part of the delta that were analyzed by Jorgenson et al. (1993) also were included in the analysis.

The accuracy of the GIS method of analyzing landscape change varies with (1) the precision of terrain delineation and (2) the registration accuracy of the 1955 and 1992 digital maps. To assess the accuracy of the analysis, 33 deep, isolated lakes were used to calculate positional accuracy of the 1955 digital map in relation to the SPOT base map. Lake outlines were vectorized from the SPOT 10-m panchromatic raster image and overlain with the 1955 digitized map. Differences in position were measured on 1:32,000-scale print outs with a magnifying reticule to the nearest 0.004 in (0.01 cm). Feature offsets were analyzed for both systematic (east and north) shifts and absolute positional errors. In addition, the accuracy of the mapping approach was compared with measurements of bank erosion made off the photographs at five places each along the banks at Cross Sections 10 and 14. For each year, distances from the banks to topographic features (e.g., ice-wedge polygon intersection) that were easily identifiable on both sets of photographs were

measured and the values were converted to actual distances based on the scale of the photographs.

RESULTS AND DISCUSSION

Overall, the analysis of landscape change in the Alpine Development Area from 1955 to 1992 revealed that 8.2% of the Development Area has been affected by erosion and deposition over the 37-yr period (Figures 11-1 and 11-2a). Most of this change was due to erosion (1.9%) and deposition (4.0%) of sediments within the main channels and adjacent riverbed deposits. A similar percentage of area (2.3%) of higher floodplain steps (i.e., landforms other than riverbed/sandbar, thaw lake, and tidal flat deposits) have been eroded, indicating that they were, for the most part, stable. Results from analyses performed for the other three study areas in 1992 (Jorgenson et al. 1993) found similar rates of change (Figure 11-2a)

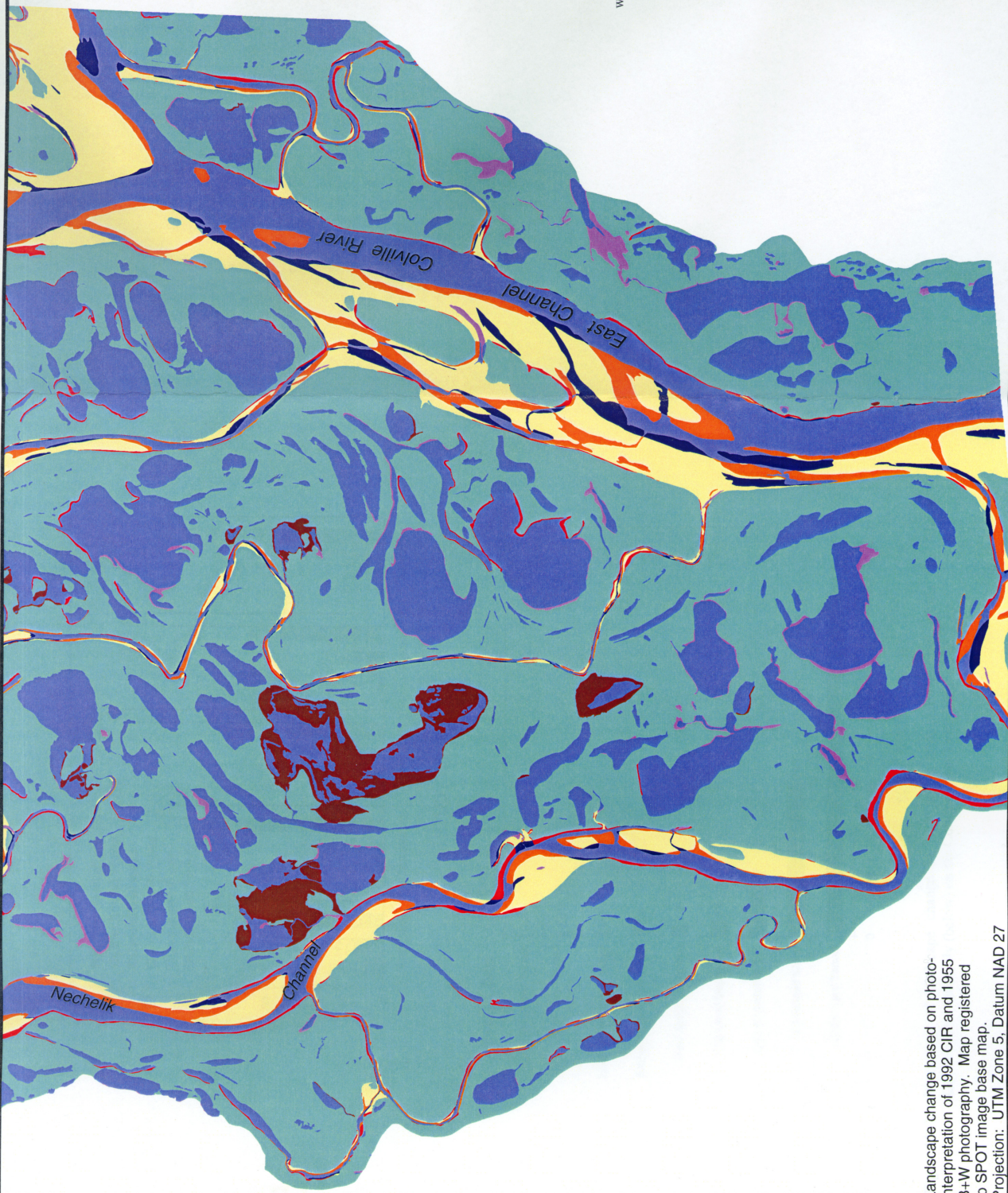
A more detailed evaluation of landscape change for the development area involved an analysis of erosion within differing types of waterbodies (Figure 11-2b). Erosion of higher floodplain sediments by the thermal and mechanical action of thaw lakes was minimal (0.2% of total area) and evident in only a few isolated areas. In contrast, higher floodplain steps that had been eroded by rivers covered 0.7% of the area. Differences in water levels between the two years (Figure 11-1) made it difficult to assess accurately rates of erosion in thaw lakes, but some areas of change that could be directly attributed to changes in water level were identified (0.9% of area)

Change in overall area, however, does not indicate adequately how active geomorphologically some areas are. Consequently, we examined how much change occurred within a particular terrain type. Riverbeds showed the most change: 24.7% of the river surface was replaced with riverbed/sandbar deposits, and 12.4% of the area of riverbed/sandbar deposits was eroded to form new river channels. In addition, the exposure of thaw-basin deposits due to drainage of tapped lakes and deposition of new sediments during flooding reduced coverage of thaw lakes by 8.8% (Figure 11-2b).

The greatest rates of erosion of higher floodplain steps in the development area (landforms other than riverbed) occurred along the cut-banks of the Nechelik and East channels, particularly near the southern end of the Nechelik Channel, where the channel forms sharp bends. In contrast, bank erosion along some straight sections of the East Channel were too small to detect with this approach. Of particular interest is the small amount of erosion along the eastern side of the channel at both Cross Sections 10 and 14. Measurement of erosional rates from the landscape change maps indicates that the mean rates of erosion of these eastern banks at Cross Sections 10 and 14 are 0.5 ± 0.4 ft/yr and 0.8 ± 0.7 ft/yr, respectively. For comparison, measurements taken directly from aerial photographs indicate that mean rates of erosion of the east banks at these locations are 1.2 ± 0.9 ft/yr and 1.1 ± 0.3 ft/yr, respectively.

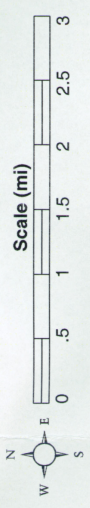
The accuracy of the map-based approach is limited by errors in photointerpretation, boundary delineation, digitizing, and registration. Analysis of positional errors of deep open lakes relative to the SPOT base map gave an average error of 15.7 ± 16.9 ft (4.8 ± 5.4 m), with 90% of tested points having a positional error of <42 ft (12.8 m). Accuracy of the 1992 map was assessed in a similar manner (see Part 12). Another way of assessing accuracy was to compare the GIS and photographic measurements of erosion at Cross Sections 10 and 14 using aerial photographs. On average, measurements of total change after 37 yr made with the GIS method were only slightly less (-16.7 ± 31.1 ft) than the values measured from photos. We estimate that the general accuracy for detecting change in terrain unit boundaries is between 30 and 50 ft (10-15 m). This accuracy is sufficient for siting facilities away from areas prone to erosion.

Although these rates of change are fairly rapid in geologic terms, the data show that, for engineering design, large portions of the development area are sufficiently stable for development. These maps can be used to locate facilities away from locations that are eroding rapidly, thereby providing a sufficient buffer zone so that facilities would not be endangered within hundreds of years.



Terrain Unit Changes 1955-1992

	Area (%)
Eroded Riverbed/Sandbar	1.3
Riverbed/Sandbar Deposition	2.6
Unchanged Riverbed/Sandbar	7.6
Thaw Basin Drainage/Deposition	1.8
Other Eroded Terrain	1.0
Unchanged Terrain	58.8
Lake-level Change	0.9
Unchanged Water	26.1



ARCO Alaska, Inc.	
Colville Geomorphology and Hydrology	
Figure 11-1. Landscape Change Alpine Development Area	
08/15/1996	File:5592CHAN.PRJ

Landscape change based on photo-interpretation of 1992 CIR and 1955 B+W photography. Map registered to SPOT image base map. Projection: UTM Zone 5, Datum NAD 27

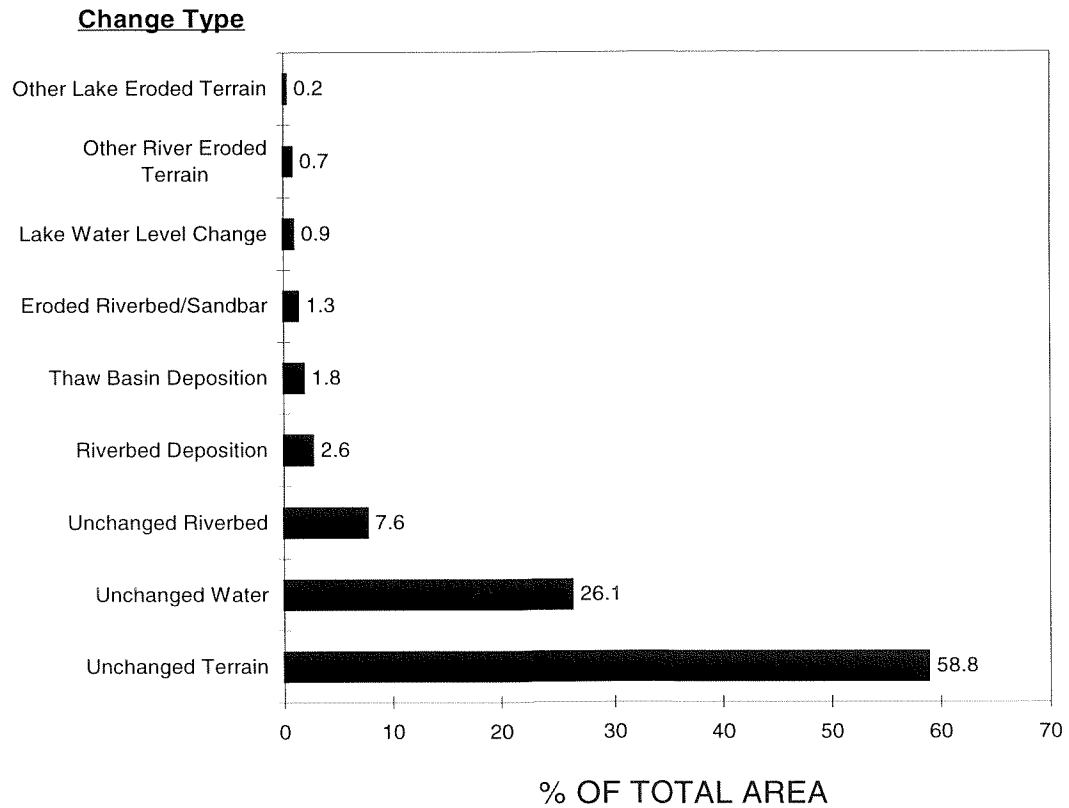
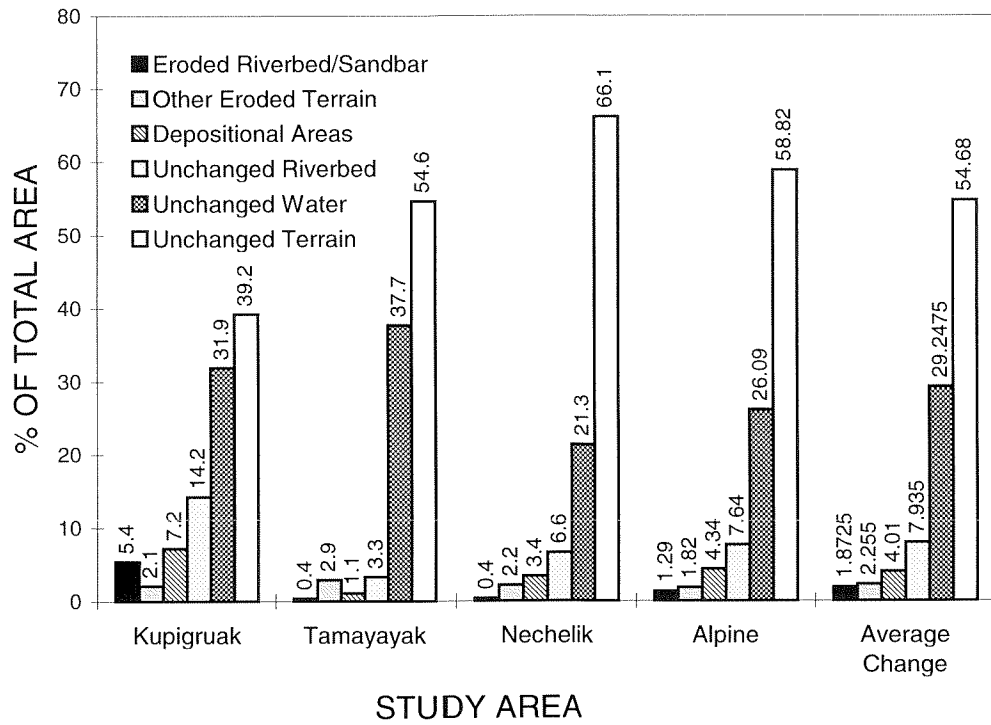


Figure 11–2. Percentage of landscape change in four study areas (above) and within the Alpine Development Area only (below) on the Colville River Delta, 1955–1992.

PART 12. GEODETIC CONTROL NETWORK AND SPOT BASE MAP

By Erik Pullman, Mike Smith, and Torre Jorgenson

BACKGROUND

Creation of a base map of known accuracy is essential to ensure compatibility of mapping data associated with a wide range of environmental and engineering studies being conducted for the proposed Alpine Development. Costs were a concern for developing a map of a remote area with little geodetic control, however. One solution is the use of high-resolution satellite imagery to provide the base for other thematic map efforts. SPOT (Système Probatoire d'Observation de la Terre) satellite imagery (SPOTView, SPOT Image Corporation, Reston, VA) offers both high-resolution (10 m) black-and-white imagery and lower resolution (20 m) color imagery. Recent development of computer processing algorithms allows the fusing of these data types into high-resolution color imagery.

In addition, benchmarks with vertical measurements of high accuracy were needed for the geomorphology and hydrology studies. Differential global positioning system (GPS) technology was used to create a network of high-resolution geodetic control points associated with the hydrologic cross sections. Differential GPS also was used to survey a series of lakes that provided control features to optimize registration of the SPOT images.

METHODS

GEODETIC CONTROL NETWORK

In June 1995, Lounsbury and Associates, Inc., surveyed 14 vertical control points along the Colville River at various cross sections (Figure 12-1). Survey-grade Leica SR299 receivers mounted on tripods were used, and horizontal and vertical controls were tied to the U. S. Coast and Geodetic Survey monument "River." The main control points were referenced to each other with the use of replicate measurement sessions and were adjusted with Leica Ski software (v. 1.09). All supplemental control points were located with Radial Static Survey methods. Standard deviations

of repeated measurements of each benchmark were <0.036 ft. The standard deviation of position fixes also was calculated independently with GPS data logs.

SPOT BASE MAP REGISTRATION AND PRODUCTION

To compensate for the lack of distinct man-made features in the delta available as registration check points, 12 small, deep lakes that could be discerned in the SPOT image were surveyed in the field using a pair of hand-held Magellan Pro Mark X (Magellan Systems Corporation, San Dimas, CA) GPS units (Figure 12-1). Mobile differential GPS techniques were employed, and subsequent post-processing of position data was performed with Magellan software. The stationary base unit was placed on a previously surveyed bench mark referenced to USGS monuments "Fork" and "River." GPS coordinates were converted to a digital vector map of lake outlines and then overlaid with the 10-m SPOT panchromatic image. Lake shorelines were compared between the two maps, and errors in position were averaged and used to calculate the amount of frame shift required for the Colville River Delta and Kuparuk area images. In addition, vector layers of Kuparuk facilities, USGS lakes (1 in = 1-mi scale), and Kuparuk lakes (1 in = 500-ft scale) were used to verify map registration within the Kuparuk image.

Full-scene SPOTView images in both single-band panchromatic (10-m resolution; 0.650- μ m band) and multispectral coverage (20-m resolution; 0.545- μ m, 0.645- μ m, and 0.840- μ m bands) of the delta and Transportation Corridor were used to create the base map. SPOTView scenes were referenced to NAD27 in Universal Transverse Mercator (UTM) Zone 5. Two multispectral scenes taken on 1 July 1990 (429202_9 and 430202_9) and two panchromatic scenes taken 28 August 1992 (429202_8) and 4 July 1995 (433202_9) were combined to produce one integrated scene to cover the entire area. Image processing software (ER Mapper, Earth Resource Mapping, San Diego, CA) was used to mosaic the images from two adjacent flight paths and fuse the panchromatic and multispectral data. Enhancement of visual features was accomplished by sharpening the multispectral

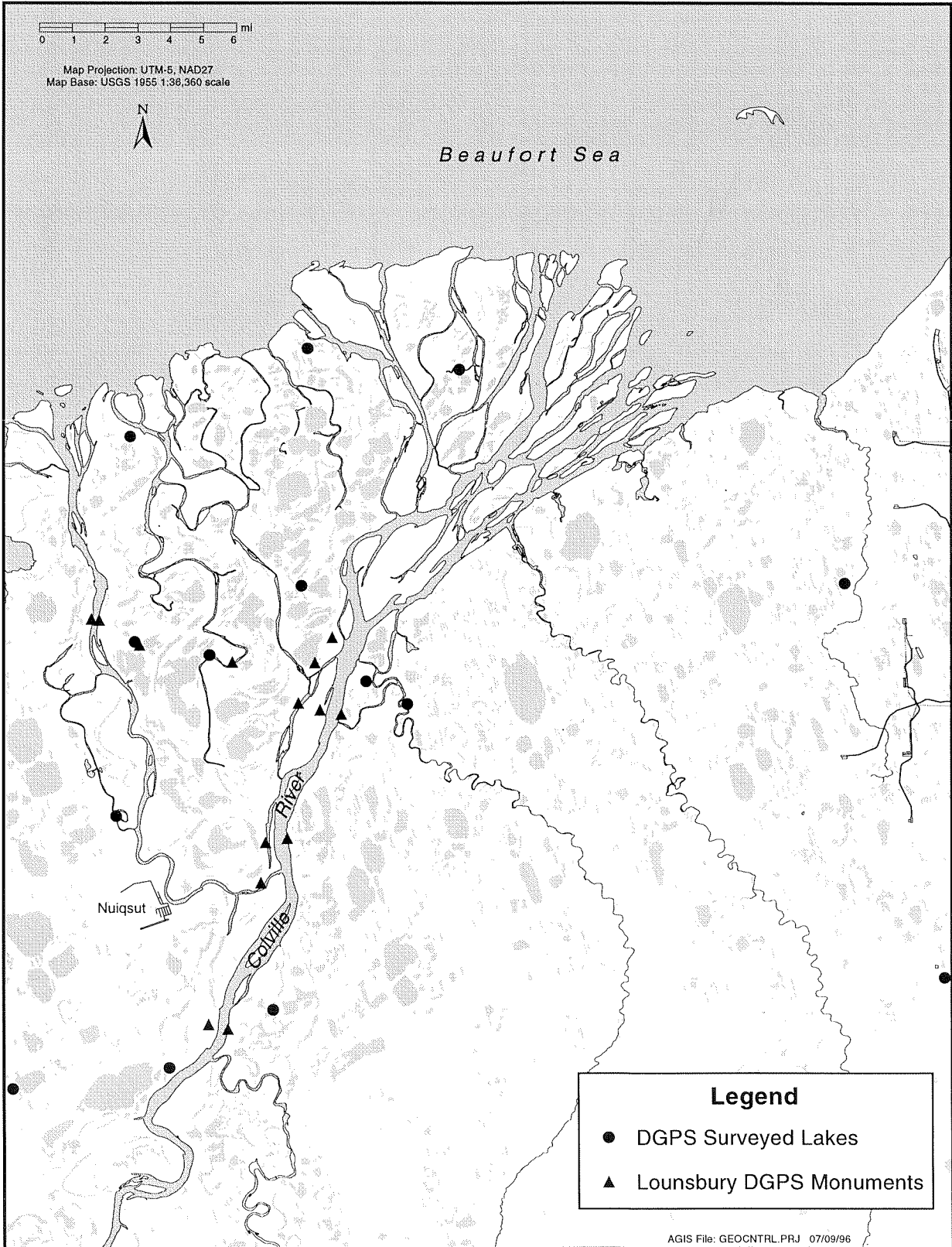


Figure 12-1. Location of new geodetic control monuments and lakes surveyed by differential GPS technology on the Colville River Delta, 1995.

data using the 10-m panchromatic images with a Brovey transformation. The accuracy of image registration was enhanced by comparisons to the network of differential GPS positions and to digital maps (1:6000 scale) supplied by Aeromap. Each SPOT scene then was shifted to optimize agreement with GPS and vector information.

After registration of the SPOT base map, a network of control points for use in digitizing features from aerial photos was created from the 10-m panchromatic SPOT images. The outlines of non-turbid lakes were converted to a separate vector layer with the image processing software. Locations of unique lakeshore features (e.g., inlets, peninsulas) that were visible on both the aerial photo and SPOT image (10–20 per photo) were used as control points.

RESULTS AND DISCUSSION

GEODETIC CONTROL NETWORK

Coordinates for the 14 new monuments are provided for 3 coordinate systems in Table 12–1. Average error for repeated measures of horizontal position was 0.016 ft (0.0049 m) with a range of 0.38 ft (0.01146 m). The vertical error was 0.016 ft (0.005 m) with a range of 0.036 ft (0.011 m).

Most of the monuments were resurveyed in May 1996 by level-loop surveys and some differences between methods are evident. The new elevations obtained in 1996 will be used in future work but earlier work in 1995 was not revised to incorporate the new data.

SPOT BASE MAP

A mosaic of fused SPOT images for the Colville River Delta and the Transportation Corridor are presented in Figures 12–2 and 12–3. The maps have the advantage of the 10-m resolution of the panchromatic images and the color of the 20-m images.

An analysis of the differences between our control features and the final map indicates that the registration is very good in the delta but not as good in the Transportation Corridor (Table 12–2). In the Colville scene, registration was optimized at the Alpine drill site; GPS survey lakes in this area have a nearly perfect alignment with the SPOT image. Within the delta, 90% of positional errors are <32.8 ft (10 m).

Within the Transportation Corridor, 90% of positional errors are <49 ft (15 m). Map control in

Table 12-1. Coordinates of geodetic control points in three coordinate systems for new monuments tied to USGS monument "River", Colville River Delta, 1995.

#ID	Coordinate System									
	Alaska State Plane, NAD 27 (ft)				Alaska State Plane, NAD 83 (m)				UTM Zone 5, NAD 27	
	Northing	Easting	Elevation		Northing	Easting	Elevation		Northing	Easting
1	5968189.37	403584.79	41.99	-	1819030.89	470495.71	12.80	-	583349.62	7803194.00
2	5933373.04	393098.22	48.14	-	1808418.79	467299.77	14.67	-	580680.51	7792440.71
6	5910992.35	383497.64	30.47	29.48	1801597.10	464373.81	9.29	8.99	578097.37	7785484.23
20	5959751.77	407456.80	15.17	14.95	1816459.13	471675.89	4.62	4.55	584657.14	7800683.94
25	5960600.21	404032.71	22.77	23.09	1816717.70	470632.29	6.94	7.04	583602.89	7800890.78
27	5961875.19	400581.58	21.12	20.81	1817106.29	469580.40	6.44	6.34	582532.91	7801226.98
30	5968954.05	390264.05	12.33	12.03	1819263.84	466435.59	3.76	3.67	579286.96	7803227.13
40	5976815.33	369228.71	10.15	9.72	1821659.78	460024.00	3.09	2.96	572765.03	7805303.65
45	5977025.45	368002.65	7.99	-	1821723.79	459650.29	2.43	-	572387.95	7805349.71
60	5940308.97	397713.36	18.86	18.11	1810532.86	468706.37	5.75	5.52	581981.87	7794620.50
65	5939774.99	394161.39	27.92	26.97	1810370.08	467623.76	8.51	8.22	580909.87	7794405.08
101	5972477.65	375505.83	7.49	-	1820337.74	461937.30	2.28	-	574739.57	7804077.36
201	5972105.5	406589.17	28.57	-	1820224.55	471411.39	8.71	-	584206.70	7804431.83
301	5910103.06	386576.74	21.96	-	1801326.06	465312.31	6.69	-	579044.82	7785259.80

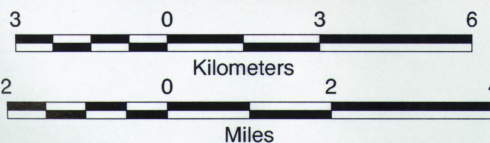
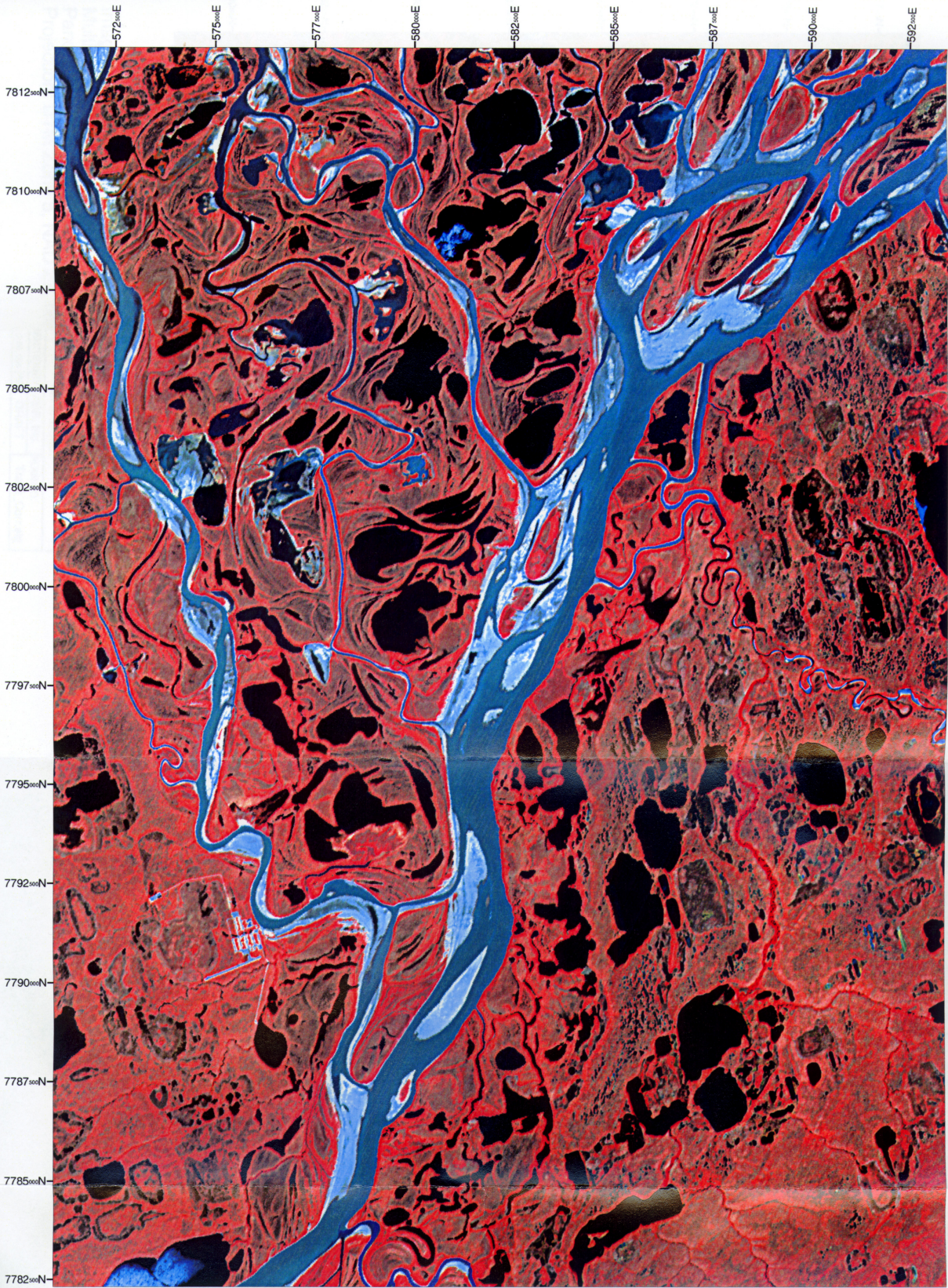
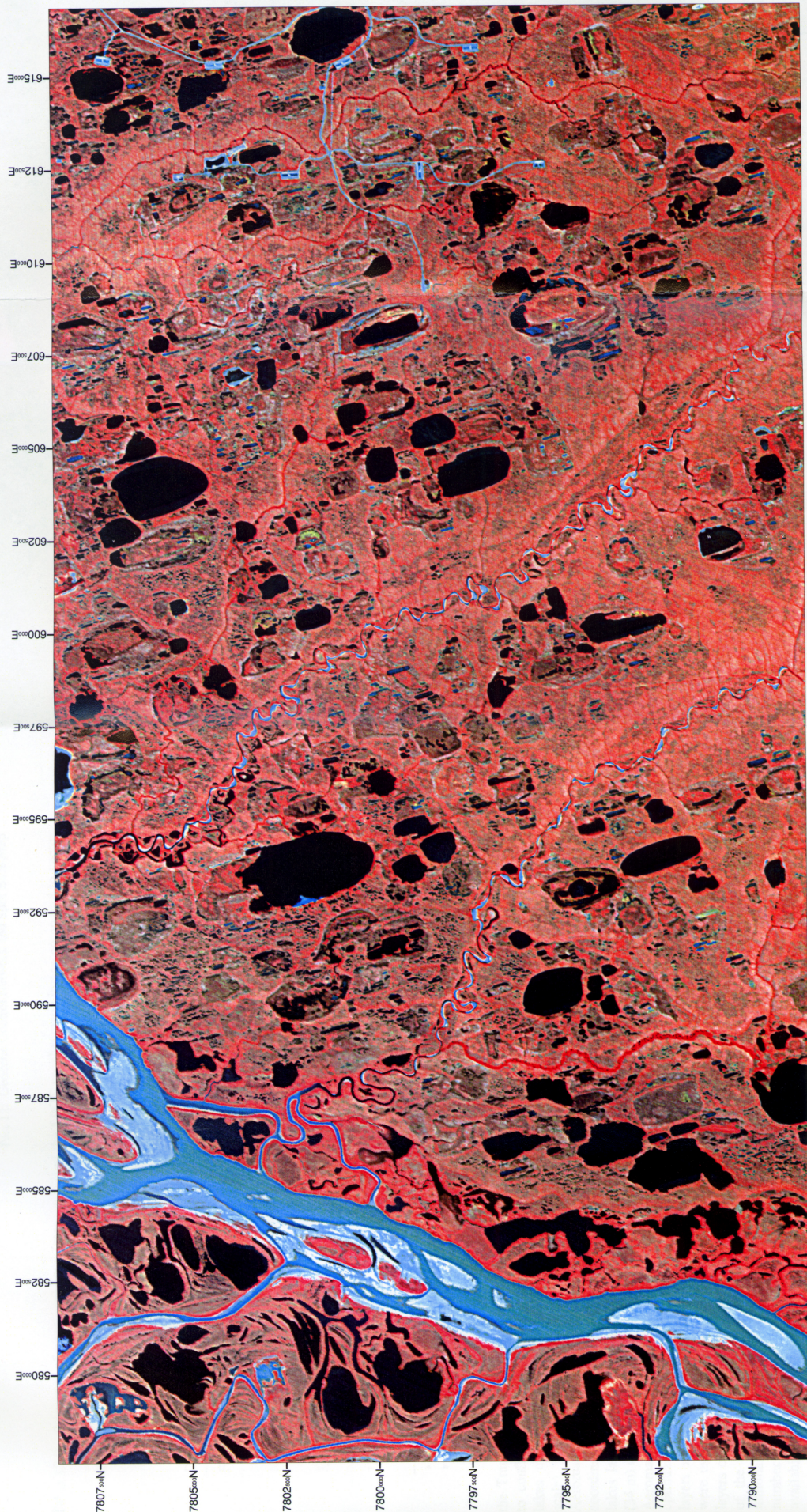


Image produced from mosaiced and fused SPOTView images
 Multispectral: 1 July 1990
 Panchromatic: Kuparuk, 29 August 1992; Colville Delta, 4 July 1995
 Projection: UTM Zone 5, NAD 27, tick marks in meters

ARCO Alaska, Inc.		
Colville Geomorphology and Hydrology Figure 12-2. SPOT image of the Colville River Delta.		
DATE: 03/04/1996	BY: ABR, Inc.	PLAN NO.
SCALE: 1:1,000,000	REF. DRAFT	Colville_Delta.alg



ARCO Alaska, Inc.	
Colville Geomorphology and Hydrology	
Figure 12-3. SPOT image of the proposed Transportation Corridor west of the Colville River Delta.	
DATE: 03/04/1998	BY: ABR, Inc.
SCALE: 1 : 100,000	REF: DRAFT
PLAN NO.	Trans_Corr.alg

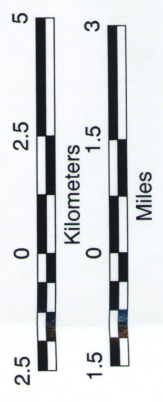


Image produced from mosaiced and fused SPOTView images
 Multispectral: 1 July 1990
 Panchromatic: Kuparuk, 29 August 1992; Colville Delta, 4 July 1995
 Projection: UTM Zone 5, NAD 27, tick marks in meters

Table 12-2. Summary of positional error (mean \pm SE) of the SPOT panchromatic image compared to vector layers from various sources, Colville River Delta, 1995.

Data Layers	Colville Image		Kuparuk Image	
	Average Easting Error (m)	Average Northing Error (m)	Average Easting Error (m)	Average Northing Error (m)
Facilities from Aeromap Map ^a			-0.6 \pm 4.9 ft (-0.2 \pm 1.5 m)	-44.4 \pm 4.4 ft (-13.5 \pm 1.3 m)
Lakes from USGS map ^b	-14 \pm 9.6ft (-4.4 \pm 2.7 m)	-9.58 \pm 8.9 ft- (2.9 \pm 2.9 m)	112 \pm 24.9 ft (34.2 \pm 7.6 m)	93 \pm 41.9 ft (28.4 \pm 12.8 m)
Lakes from Aeromap maps ^a			-10.5 \pm 2.5 ft (-3.2 \pm 0.8 m)	-34.4 \pm 4.4 ft (-10.5 \pm 1.3 m)
Lakes surveyed using GPS	15.9 \pm 6.0 ft (4.85 \pm 1.8 m)	5.5 \pm 4.4 ft (1.6 \pm 1.3 m)	103 \pm 18.1ft (32.4 \pm 5.5m)	69.8 \pm 9.0 ft (21.4 \pm 2.8 m)

^a Aeromap U. S. Inc. 1"=500'-scale maps.

^b Aeromap U. S., Inc. based on USGS 1:63,360 quads.

the Transportation Corridor was more difficult due to conflicting registration between GPS readings, lakes obtained from the USGS maps (1:63,360 scale), and lakes and facilities obtained from Aeromap's digital maps (1:6000 scale). GPS lake coordinates showed good agreement with the USGS lakes layer but were shifted an average of 112 ft (34 m) east and 92 ft (28 m) north in relation to the Aeromap layers. Emphasis was placed on optimizing base map agreement with Aeromap layers of Kuparuk facilities. Survey data for DS-2M were used to verify projection of Aeromap vector layers over the SPOT image. Registration accuracy of the SPOT base map was limited by both the minimal pixel size (10 m) of the imagery and the number of ground-based geodetic control points available for analyzing scene shift.

PART 13. HYDROLOGIC CONSIDERATIONS FOR A PIPELINE CROSSING AT E20.56

by James W. Aldrich

BACKGROUND

This section provides preliminary information about two parameters related to the design of a pipeline crossing in the vicinity of Cross Section E20.56 (Cross Section 14): water-surface elevation and scour depth. Water-surface elevation is used to establish the minimal elevation of an aboveground crossing and to estimate the depth of riverbed scour. Riverbed scour is used to estimate the maximal elevation at which a buried pipeline can be placed and not be uncovered by the river during the design event. It also is used in the design of piers at an aboveground crossing. The estimates provided in this section are intended to be order-of-magnitude estimates that can be used for planning purposes and refined during design.

METHODS

DESIGN FLOOD

The magnitude of the design event at Cross Section E20.56 was estimated based on the flood-frequency relationship developed for the head of the delta (Cross Section E27.09) and the expected split in discharge between the East and Nechelik channels (see Part 1). The expected split in discharge between the two channels was estimated from our observations during the spring of 1995 (62%–38%) and observations made by Arnborg et al. (1966; 80%–20%) in 1962.

The water-surface elevation associated with the design event at Cross Section E20.56 was based on normal depth computations. The channel geometry was developed from an extension of the measured cross section using elevations from USGS topographic maps. Water-surface slope and hydraulic roughness were estimated from measurements made during spring and summer 1995 and were varied with water-surface elevation (see Part 3).

SCOUR DEPTH

The regime depth is the average depth of the river channel when the channel is in regime (dynamic equilibrium). Scour depth is the depth below the water surface to which the bed may move during a large flood. It is estimated by multiplying the regime depth by a constant (i.e., Z-factor) that varies with the severity and erodibility of the bend in the river channel (Blench 1969).

Regime depth estimates were based on Blench's (1969) equations for sand and gravel bed rivers. A range of water-surface elevations, bed material size, and bedload concentrations (also called bedload charge) were considered. The regime depths were estimated for water-surface elevations of 25, 19, 14, and 10 ft. Median bed-material sizes of 0.3 and 5.4 mm were considered at each of the four water-surface elevations. The median bed-material sizes are based on two bed-material samples that were obtained within the deepest part of the channel at E20.56 (see Part 2). Additionally, for each water-surface elevation and bed-material size that was considered, two bedload concentrations were considered. A bedload concentration of 1 ppm was used to represent conditions during clear-water scour. The regime depth estimate associated with this concentration represents the probable upper limit of the regime depth. The second bedload concentration is approximately the lowest concentration estimated with three sediment-transport functions. Bedload concentration for a median bed-material size of 0.3 mm was estimated with the following sediment transport functions: Toffaleti, Laursen (Copeland), and Acker-White (Hydrologic Engineering Center 1992). Bedload concentrations for a median bed-material size of 5.4 mm were estimated with Meyer-Peter-Muller, Yang, and Acker-White sediment transport functions (Hydrologic Engineering Center 1992).

At water-surface elevations of 19, 14, and 10 ft and a median bed-material size of 5.4 mm, only one bedload concentration was used in the analyses. In these situations, the lowest bedload concentration suggested by the sediment transport functions was on the order of 1 ppm.

The regime depth was converted to a total scour depth using a Z-factor. From the criteria in Aldrich and Malcovish (1983), the reach of the river in the vicinity of Cross Section E20.56 is considered

straight. In a straight reach there is a 50% chance that the Z-factor will be less than or equal to 1.1, a 95% chance that the Z-factor will be less than 1.5, and a 99% chance that the Z-factor will be less than 1.7 (Aldrich and Malcovish 1983). For conceptual design purposes with a 200-yr flood, a Z-factor of 1.5 is reasonable.

The total scour depth was converted to a net scour depth by subtracting the thalweg depth from the estimate of total scour depth. Thus, the net scour depth represents the depth from the lowest point in the cross section to the bottom of the portion of the riverbed that may be moved during a large flood.

A second estimate of the net scour depth was based on competent velocity (Neill 1973). This estimate is based on the assumption that scour will proceed until the mean velocity in the cross section is reduced to a value just competent to move the bed material exposed at the scoured depth. The median bed-material size is used as the representative particle for the calculations. For this project, a median bed-material diameter of 0.3 mm was used, and the scour depth was estimated from the average velocity associated with the deepest subsection within Cross Section E20.56. Thus, the deepest subsection was deepened until the velocity was just competent to move a 0.3-mm-diameter particle. The difference between the initial and final depths is the net scour.

The height of dunes that might be present at the time of a large flood was estimated using the method presented by Chang (1988). If dunes are present, the total scour depth is the sum of the general scour depth plus half the height of the dunes.

RESULTS AND DISCUSSION

DESIGN FLOOD

For this assessment, we assumed that the 200-yr flood would be used as the pipeline design flood. Based on the assessment of flood frequency at the head of the delta (Cross Section E27.09), the estimated 200-yr flood is on the order of 1,110,000 cfs. As discussed in Part 1, the distribution of the flow between the East and the Nechelik channels is on the order of 60–80% and 20–40%, respectively. Thus the magnitude of a 200-yr flood in the upper

East Channel may be on the order of 670,000–890,000 cfs.

Based on the normal-depth computations conducted for this analysis, the East Channel is capable of passing a discharge of 525,000–628,000 cfs on the east side of the dunes (located on the west bank), at a water-surface elevation of 25 ft. At or below this elevation, however, it is expected that water will begin to flow west of the dunes. Additionally, water also may begin to flow farther east than the area contained in the cross section used for this analysis. Because a considerable amount of water may flow on the west side of the dunes, we assumed for this task that the water-surface elevation of the 200-yr flood probably will not be greater than 25 ft at E20.56.

SCOUR DEPTH

The various combinations of water-surface elevations, bed-material sizes, and bedload concentrations resulted in estimates of net scour depth ranging from 0 ft to 9 ft (Table 13–1). None of the estimates that involved an estimate of the bedload concentration, based on the hydraulic conditions likely to be present, indicated a net scour. A net riverbed scour was only predicted to occur when it was assumed that the sediment transport rate was 1 ppm, essentially clear water scour conditions. Thus, the actual concentration of bedload likely to be present at the time of the design flood will be critical to estimating the scour depth.

The competent-velocity estimate was calculated at a water-surface elevation of 25 ft and a median bed-material size of 0.3 mm. The result of this computation indicates that the net scour depth is on the order of 5.1 ft.

These scour-depth estimates do not consider the increased depth of bed movement that can occur if dunes are present on the riverbed. Our analyses suggest that if the bed material has a median diameter of 5.4 mm and the water-surface elevation is 25 ft, the likely bedform will be dunes. The height of the dunes will be on the order of 5 ft. If the median diameter of the bed material is smaller than 5.4 mm, the dunes will have a smaller height or may not be present. If the scour-depth estimates are to consider the bedform, one-half of the dune height should be added to the net scour estimate.

Table 13-1. Scour depth estimates based on Blench equations at Cross Section E20.56, Colville River Delta, 1995.

Water-Surface Elevation (ft)	Median Grain Size (mm)	Bedload Concentration (ppm)	Regime Depth (ft)	Thalweg Depth (ft)	Scour Depth ^a (Z = 1.5) (ft)	Net Scour Depth ^b (ft)
25	0.3	1	31.0	37.2	46.5	9.3
25	0.3	300	18.6	37.2	27.9	0.0
25	5.4	1	22.3	37.2	33.5	0.0
25	5.4	20	20.9	37.2	31.4	0.0
19	0.3	1	21.7	31.2	32.6	1.4
19	0.3	100	16.8	31.2	25.2	0.0
19	5.4	1	15.8	31.2	23.7	0.0
14	0.3	1	19.8	26.2	29.7	3.5
14	0.3	100	15.3	26.2	23.0	0.0
14	5.4	1	14.4	26.2	21.6	0.0
10	0.3	1	15.2	22.2	22.8	0.6
10	0.3	40	13.4	22.2	20.1	0.0
10	5.4	1	11.0	22.2	16.5	0.0

^aScour depth is measured from the water surface.

^bNet scour is measured from the thalweg.

Thus, based on the Blench equations and a bedload concentration of 1 ppm, the top of a buried pipeline should be at least 12 ft below the lowest elevation in the bed. Based on the competent-velocity method, the top of a buried pipeline should be at least 8 ft below the lowest elevation in the riverbed. For the purposes of conceptual design, it should be assumed that a buried pipeline will need to be placed at least 10 ft below the lowest elevation in the riverbed at E20.56 to be protected from scour during a 200-yr flood.

To satisfy the above criteria, the top of the pipeline should be no higher than elevation -23 ft (msl). This elevation corresponds to a depth of about 25 ft below the water surface at the time the 25 August 1995 thalweg-profile data were collected

(Figures 2-9 and 2-10). There are several places in the river where the thalweg was this deep or deeper on the day of the thalweg measurements. A few locations had depths in excess of 30 ft, and one location had a depth of nearly 50 ft. However, we believe that the conditions at these locations are more conducive to scour than is the river channel at E20.56. In fact, this crossing location was picked partially because it is located in a particularly straight reach of the channel and has no major tributaries entering the channel at or near this location.

Another check on the reasonableness of assuming that scour or degradation may occur at this crossing is to look at the depth measurements that have been made at E27.09 between 1962 and 1995

(Figure 13-1). These data suggest that the thalweg elevation at this location has changed on the order of 5 ft. However, because this cross section was measured only intermittently (1962, 1977, 1992, 1993, and 1995), the total variation in riverbed elevation experienced during the 33-yr period may be more than 5 ft.

In addition, scour can result from an open-water flood or flow under an ice jam. Only the scour that might occur during an open-water flood has been considered in this analysis. Because the overbank areas are large, scour due to an ice jam may not be more serious than the scour likely to occur during open-water conditions. However, scour at a potential ice jam should be considered prior to detailed design.

ADDITIONAL DATA REQUIREMENTS

As the evaluation, planning, and design of possible oilfield developments on the delta continues, additional information will be required to estimate accurately the magnitude of the design flood and the associated water-surface elevations and scour depths. Ultimately, conditions expected during the design flood will be used to: set elevations and establish the layout of pads and buildings; provide criteria for VSM (vertical-support member) locations and design; set minimal elevations for aboveground pipelines; and set maximal elevations for below-ground river crossings. To provide the information that will be required for final design, the following information should probably be collected.

The largest deficiency in the hydrologic/hydraulic data probably relates to our ability to estimate water-surface elevations during large, infrequent events. This information will be needed for the adequate design of pipelines and facilities. As discussed earlier, large portions of the delta are regularly inundated by spring flooding. To estimate water-surface elevations and velocities that will occur during a large event (e.g., 50-, 100-, or 200-yr floods), it will be necessary to obtain more extensive topographic information than has been collected on the delta to date. It will be necessary to combine this information with estimates of water-surface slope and hydraulic roughness, so that a hydraulic model suitable for estimating water-surface

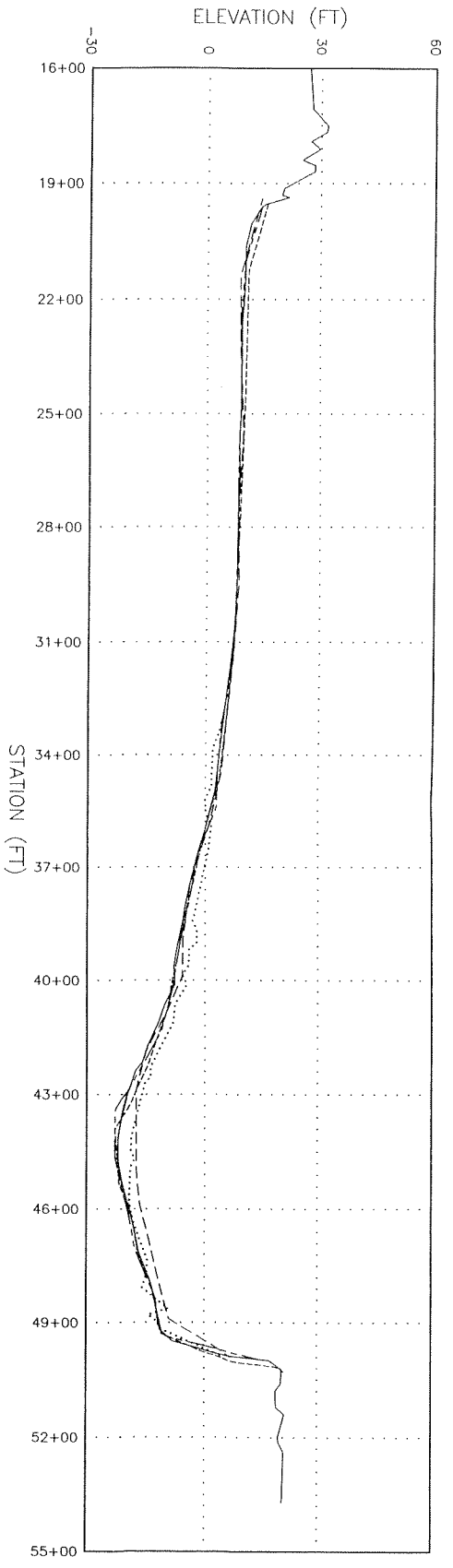
elevations and velocities in the vicinity of proposed pipelines and facilities can be prepared. To increase the accuracy of this model, the collection of water-surface elevation data at selected locations within the delta during the peak of particularly large discharges is desirable. Collection of the necessary data and preparation of this model probably should be the highest priority of any future hydrologic programs.

The estimation of the magnitude of the 1996 spring breakup peak discharge and the relative proportion of flow between the East and the Nechelik channels should also be a high priority for future hydrologic programs. These data are necessary for refining the estimate of the peak discharge at potential development sites. Presently, there are only 6 years of data from which to estimate a flood-frequency relationship for the Colville River at the head of the delta. Every year of data that is added, when so few data exist, has the potential of significantly altering this estimated relationship. This concern is particularly true with regard to the relative proportion of flow between the East and Nechelik channels. To estimate the design discharge at a particular location along these channels, it will be necessary to estimate the design discharge at the head of the delta and the portion of flow likely to pass down each channel. Although this can be estimated with hydraulic models, calibration of the model with one or two events is much more desirable.

Estimating scour depth also will be a significant aspect of the design of a pipeline river crossing. Sediment transport rates are extremely variable from one river to the next and are flow dependent. Measurement of the sediment transport rate during a large flood, such as may occur at breakup, would significantly improve the confidence in scour depth estimates.

Finally, if interest continues in accessing the Alpine Development with barges in the Nechelik Channel, additional bathymetric data should be collected offshore from the mouth of the channel. The collection of additional cross section data along the Nechelik Channel also is desirable.

CROSS SECTION E27.09 (MAIN CHANNEL)
1962 - 1995



KEY

.....	1962
-----	1977
- - - - -	1992
- . - . -	1995

- NOTES:
1. ELEVATIONS ARE BASED ON USCGS MONUMENT "RIVER", ELEVATION= 41.99 FEET.
 2. IN PREVIOUS REPORTS, CROSS SECTION E27.09 HAS BEEN REFERRED TO AS CROSS SECTION 6. DUE TO THE INCREASED NUMBER OF CROSS SECTIONS BEING USED ON THE PROJECT, THE CROSS SECTION DESIGNATION WAS CHANGED SUCH THAT IT IS NOW BASED ON RIVER MILES, MEASURED FROM THE MOUTH.
 3. THE LOCATION OF THE 1962 CROSS SECTION WAS WITHIN SEVERAL FEET OF THE 1992, 1993, AND 1995 CROSS SECTIONS.
 4. THE EXACT LOCATION OF THE 1977 CROSS SECTION IS UNKNOWN. IT IS BELIEVED TO BE WITHIN SEVERAL HUNDRED FEET OF THE 1992, 1993, AND 1995 CROSS SECTIONS.
 5. CROSS SECTION IS LOOKING DOWNSTREAM.

ARCO Alaska, Inc.	
COLVILLE GEOMORPHOLOGY AND HYDROLOGY	
Figure 13-1: Cross Section E27.09	
Date: 13 Feb 1996	File: 2XSEC131.DWG

LITERATURE CITED

- Aldrich, J. W., and C. Malcovish. 1983. A review of scour multiplication factors for gravel-bed rivers. Unpublished report prepared for Alberta Environmental Research Trust, Calgary, AB, Canada, by Hydrocon Engineering Ltd., Calgary, AB, Canada. 33 p.
- Arnborg, L., H. J. Walker, and J. Peippo. 1967. Suspended load in the Colville River, Alaska, 1962. *Geografiska Annaler* 49A: 131-144.
- Arnborg, L., H. J. Walker, and J. Peippo. 1966. Water discharge in the Colville River, 1962. *Geografiska Annaler* 48A: 195-210.
- Blench, T. 1969. Mobile-bed fluviology. University of Alberta Press, Edmonton, AB, Canada. 300 p.
- Black, R. F. 1964. Gubik Formation of Quaternary age in northern Alaska. U. S. Geological Survey, Prof. Pap. 302-C. 91 p.
- Cannon, P. J., and S. E. Rawlinson. 1979. The environmental geology and geomorphology of the barrier island-lagoon system along the Beaufort Sea Coastal Plain from Prudhoe Bay to the Colville River. Pages 209-248 in National Oceanic and Atmospheric Administration, Environmental assessment of the Alaskan Continental Shelf, Annual reports of principal investigators, April 1978 to March 1979. National Oceanic and Atmospheric Administration, v. 10.
- Cannon, P. J., and S. E. Rawlinson. 1981. Environmental geology and geomorphology of the barrier island-lagoon system along the Beaufort Sea Coastal Plain from Prudhoe Bay to the Colville River. Pages 357-444 in National Oceanic and Atmospheric Administration Environmental assessment of the Alaskan Continental Shelf. National Oceanic and Atmospheric Administration, Final Report 34 (1985).
- Cannon, P. J., and T. W. Mortensen. 1982. Flood hazard potential of five selected arctic rivers Arctic Coastal Plain. Report prepared for North Slope Borough Coastal Management Program, Barrow, AK, by Mineral Industries Research Lab, Univ. of Alaska, Fairbanks, 56 p.
- Carter, L. D. 1981. A Pleistocene sand sea on the Alaskan Arctic Coastal Plain. *Science* 211: 381-383.
- Carter, D. L., and J. P. Galloway. 1985. Engineering-geologic maps of northern Alaska, Harrison Bay Quadrangle. U. S. Geological Survey, Open File Rep. 85-256. 47 p.
- Carter, D. L., and J. P. Galloway. 1982. Terraces of the Colville River Delta region, Alaska. Pages 49-52 in W. L. Coonrad, ed., The United States Geological Survey in Alaska: Accomplishments during 1980. U. S. Geological Survey, USGS Circular 884. p.
- Carter, L. D., J. K. Brigham-Grette, and D. M. Hopkins. 1986. Late Cenozoic marine transgressions of the Alaskan Arctic Coastal Plain. Pages 21-26 in J. A. Heginbottom, and J. S. Vincent, eds., Correlation of Quaternary deposits and events around the margin of the Beaufort Sea: Contributions from a joint Canadian-American workshop, April 1984. Geological Survey of Canada, Open File Report 1237.
- Carter, L. D., C. A. Repenning, L. N. Marincovich, J. E. Hazel, D. M. Hopkins, K. McDougall, and C. W. Naeser. 1977. Gubik and pre-Gubik Cenozoic deposits along the Colville River near Ocean Point, North Slope, Alaska. Pages B12-B14 in K. M. Blean, ed., The United States Geological Survey in Alaska: Accomplishments during 1976. U. S. Geological Survey, Circular 751-B.
- Chang, H. H. 1988. Fluvial processes in river engineering. John Wiley & Sons, NY. 432 p.
- Craig, J. D., and G. P. Thrasher. 1982. Environmental geology of Harrison Bay, northern Alaska. U. S. Geological Survey, Open-File Rep. 82-35. 25 p.

- Davidian, J. 1984. Computation of water-surface profiles in open channels. U. S. Geological Survey, Washington, D. C. Techniques of Water Resources Investigations, Book 3, Chapter A15. 48 p.
- Divoky, G. 1983. The pelagic and nearshore birds of the Alaska Beaufort Sea. U. S. Dept. of Comm., Juneau, AK. NOAA-OCEASP Final Rep. 114 p.
- EarthInfo. 1993. USGS Peak Values, 1993 (revised). Boulder, CO. (CD-ROM)
- Foster, D. S. 1988. Quaternary acoustic stratigraphy between the Colville River and Prudhoe Bay, Beaufort Sea Shelf, Alaska. U. S. Geological Survey, Open-File Rep. 88-0276. 108 p.
- Gilliam, J. J., and P. C. Lent. 1982. Caribou/Waterbird impact analysis workshop. Proceedings of the National Petroleum Reserve in Alaska (NPR-A). U. S. Alaska State Office, Bureau of Land Manage., Anchorage, AK. 29 p.
- Helmericks, J. 1996. Personal communications of September 15, 1995 and January 2, 1996. Golden Plover Lodge, Colville River, AK.
- Henderson, F. M. 1966. Open channel flow. Macmillan Publishing, Inc., New York. 521 p.
- Hopkins, D. M. 1982. Aspects of the paleogeography of Beringia during the late Pleistocene. Pages 3–28 in D. M. Hopkins, J. Matthews, C. E. Schweger, and S. B. Yount, eds., *Paleoecology of Beringia*. Academic Press, New York.
- Hopkins, D. M., and R. W. Hartz. 1978. Coastal morphology, coastal erosion, and barrier islands of the Beaufort Sea, Alaska. U. S. Geological Survey, Open-File Rep. 78–1063. 54 p.
- Interagency Advisory Committee on Water Data. 1982. Guidelines for determining flood flow frequency. U. S. Geological Survey, Office of Water Data Coordination, Washington, DC. Bulletin 17B.
- Jones, S. H., and C. B. Fahl. 1994. Magnitude and frequency of floods in Alaska and conterminous basins of Canada. U. S. Geological Survey, Anchorage, AK. Water-Resources Investigations Report 93–4179. 122 p.
- Jorgenson, M. T. 1986. Biophysical factors affecting the geographic variability of soil heat flux. M.S. Thesis, Univ. of Alaska, Fairbanks, AK. 109 p.
- Jorgenson, M. T., J. W. Aldrich, J. G. Kidd, and M. D. Smith. 1993. Geomorphology and hydrology of the Colville River Delta, Alaska, 1992. Unpublished annual report prepared for ARCO Alaska Inc., Anchorage, AK, by Alaska Biological Research, Inc., Fairbanks, AK. 79 p.
- Jorgenson, M. T., J. W. Aldrich, and C. J. Hammond. 1994a. Geomorphology and hydrology of the Colville River Delta, Alaska, 1993. Unpublished annual report prepared for ARCO Alaska Inc., Anchorage, AK, by Alaska Biological Research, Inc., Fairbanks, AK. 36 p.
- Jorgenson, M. T., J. W. Aldrich, and C. J. Hammond. 1994b. Geomorphology and hydrology of the Colville River Delta, Alaska, 1994. Unpublished data report prepared for ARCO Alaska Inc., Anchorage, AK, by Alaska Biological Research, Inc., Fairbanks, AK. 9 p.
- Jorgenson, M. T., R. M. Burgess, E. R. Pullman, A. A. Stickney, M. Raynolds, and A. Zusi-Cobb. 1996. Ecological land survey of the Colville River Delta. Unpublished draft report prepared for ARCO Alaska, Inc., Anchorage, AK, by ABR, Inc., Fairbanks, AK.
- Jorgenson, M. T., and Y. L. Shur. 1995. Sheet ice associated with polygons in the Colville River Delta. Page F244 in Proceedings of 1995 Fall Meeting, American Geophysical Union, Washington, DC. (abstract).
- Katasonov, E. M. 1969. Composition and cryogenic structure of permafrost. Pages 25–36 in Permafrost investigations in the field. National Research Council of Canada, OT. Technical Translation 1358.

- Klute, A., ed. 1986. Methods of soil analysis: Part 1. Physical and mineralogical methods. Amer. Soc. of Agron., Madison, WI. 1188 p.
- Kreig, R. A., and R. D. Reger. 1982. Air-photo analysis and summary of land-form soil properties along the route of the Trans-Alaska pipeline system. Alaska Division of Geological and Geophysical Surveys, Geol. Rep. 66. 149 p.
- Lewellen, R. I. 1977. A study of Beaufort Sea coastal erosion, northern Alaska. Pages 491–527 *in* Environmental Assessment of the Alaskan Continental Shelf, annual reports of principal investigators for the year ending March, 1977. U. S. National Oceanic and Atmospheric Administration, v. 15.
- Moulten, L. J. 1986. Colville River 1985–1986 under-ice temperatures and salinity monitoring. Unpublished progress report No. 1 prepared for ARCO Alaska, Inc., Anchorage, AK, by Entrix.
- Moulten, L. J. 1995. The 1994 Endicott Development Fish Monitoring Program, Volume II: the 1994 Colville River fishery. Unpublished final report prepared for BP Exploration (Alaska) Inc., Anchorage, AK, and North Slope Borough, Barrow, AK, by MJM Research, Bainbridge Island, WA.
- Murton, J. B., and H. M. French. 1994. Cryostructures in permafrost, Tuktoyaktuk coastlands, western arctic Canada. *Can. J. Earth Science* 31: 737–747.
- Naidu, A. S., and T. C. Mowatt. 1975. Depositional environments and sediment characteristics of the Colville and adjacent deltas, northern arctic Alaska. Pages 283–309 *in* M. L. S. Broussard, ed., Delta models for exploration. Houston Geological Society, TX.
- Neill, C. R. 1973. Guide to bridge hydraulics. University of Toronto Press, Toronto, ON, Canada. 191 p.
- NOAA-OCSEAP. 1983. Sale 87. Harrison Bay synthesis. U. S. Dept. Comm., National Oceanic and Atmospheric Administration, Outer Continental Shelf Environmental Assessment Program, Juneau, AK. 81 p.
- Peltier, W. R., and A. M. Tushingham. 1989. Global sea level rise and the greenhouse effect: might they be connected. *Science* 244: 806–810.
- Philainen, J. A., and G. H. Johnston. 1963. Guide to a field description of permafrost. Associate Committee on Soil and Snow Mechanics, National Research Council, OT. Tech. Memo. 79.
- Pollard, W. H., and H. M. French. 1980. A first approximation of the volume of ground ice, Richards Island, Pleistocene Mackenzie Delta, Northwest Territories, Canada. *Can. J. Earth Sciences* 17: 509–516.
- Rawlinson, S. E. 1993. Surficial geology and morphology of the Alaskan Central Arctic Coastal Plain. Alaska Div. Geol. and Geophy. Surv., Fairbanks, AK. Report of Investigations 93-1. 172 p.
- Reed, J. C., and J. E. Sater. 1974. The coast and shelf of the Beaufort Sea. Arctic Institute North America, Washington, D.C. 648 p.
- Reimnitz, E., S. M. Graves, and P. W. Barnes. 1985. Beaufort Sea coastal erosion, shoreline evolution, and sediment flux. U. S. Geological Survey, Open-File Report 85–380. 66 p.
- Reimnitz, E., S. M. Graves, and P. W. Barnes. 1988. Map showing Beaufort Sea coastal erosion, sediment flux, shoreline evolution, and the erosional shelf profile. U. S. Geological Survey, Denver, CO. Misc. Invest. Series Map I-1182-G.
- Rothe, T. C., C. J. Markon, L. L. Hawkins, and P. S. Koehl. 1983. Waterbird populations and habitat analyses of the Colville River delta, Alaska, 1981 summary report. U. S. Fish and Wild. Serv., Anchorage, AK. Special Studies Prog. Rep. 67 p.

- Schell, D., and G. Hall. 1972. Water chemistry and nutrient regeneration process studies. Pages 3–28 *in* P. J. Kinney, and others, eds. Baseline data study of the Alaskan arctic aquatic environment. University of Alaska, Fairbanks, AK. Institute of Marine Science Report R72-3.
- Shur, Y. L. 1988. The upper horizon of permafrost soil. Pages 867–871 *in* K. Senneset, ed., Proceedings of the Fifth Intern. Conf. on Permafrost. Tapir Publishers, Trondheim, Norway.
- Simons, Li & Associates. 1982. Engineering analysis of fluvial systems. Simons, Li, and Associates, Fort Collins, CO.
- Simpson, S. G., J. Barzen, L. Hawkins, and T. Pogson. 1982. Waterbird studies on the Colville River delta, Alaska, 1982 summary report. U. S. Fish and Wild. Serv., Anchorage, AK. Special Studies Prog. Rep.
- Soil Survey Division Staff. 1993. Soil survey manual. U. S. Department of Agriculture, Washington, D.C. Handbook No. 18. 437 p.
- Strahler, A. N. 1952. Dynamic basis of geomorphology. Geological Society of America Bulletin 63:923–938.
- University of Alaska (Fairbanks UAF). 1972. Baseline study of the Alaska arctic aquatic environment. Institute of Marine Science, University of Alaska, Fairbanks, AK. Report R72-3. 275 p.
- U. S. Army Corps of Engineers. 1992. Hydrologic design package for flood control channels (SAM Ver. 3.04). Unpublished draft computer program manual. U. S. Army Corps of Engineers, Waterways Experiment Station, Vicksburg, MS.
- U. S. Geological Survey. 1978. Water resources data for Alaska, water year 1977. Water Resources Division, Anchorage, AK.
- U. S. Geological Survey. 1980. Water resources data for Alaska, water year 1979. Water Resources Division, Anchorage, AK.
- U. S. Geological Survey. 1981. Water resources data for Alaska, water year 1980. Water Resources Division, Anchorage, AK.
- U. S. Geological Survey. 1982. Water resources data for Alaska, water year 1981. Water Resources Division, Anchorage, AK.
- U. S. Geological Survey. 1994. Water resources data for Alaska, water year 1993. Water Resources Division, Anchorage, AK. 373 p.
- U. S. Geological Survey. 1995. Water resources data for Alaska, water year 1994. Water Resources Division. Anchorage, AK. 289 p.
- Walker, D. A., K. R. Everett, P. J. Webber, and J. Brown. 1980. Geobotanical atlas of the Prudhoe Bay region, Alaska. U. S. Army Corps of Engineers, Cold Regions Research and Engineering Lab., Hanover, NH. Lab. Rep. 80-14. 69 p.
- Walker, H. J. 1966. Permafrost and ice-wedge effect on riverbank erosion. Pages 164–171 *in* International Conference on Permafrost, 1963, Proceedings. National Academy of Sciences, National Research Council Publication 1287, Washington, D.C.
- Walker, H. J. 1973a. Salinity changes in the Colville River Delta, Alaska, during breakup. Pages 514–527 *in* Proceedings of the Snow and Ice in Hydrology Conference. Banff, AB, Canada.
- Walker, H. J. 1973b. Morphology of the North Slope. Pages 49–92 *in* Proceedings of the 25th Anniversary Celebration of the Naval Arctic Research Laboratory. Arctic Institute of North America, Arlington, VA. Technical Paper No. 25.
- Walker, H. J. 1974. The Colville River and the Beaufort Sea: Some interactions. Pages 513–540 *in* J. C. Reed, and J. E. Sater, eds., The coast and shelf of the Beaufort Sea. Arctic Institute of North America, Washington, DC.

- Walker, H. J. 1976. Depositional environments in the Colville River Delta. Pages C1–C22 *in*, T. P. Moller, ed., Recent and ancient sedimentary environments in Alaska. Alaska Geological Society, Anchorage.
- Walker, H. J. 1978. Lake tapping in the Colville River Delta. Pages 233–238 *in* Proceedings of the Third International Conference on Permafrost, Edmonton, AB. National Research Council of Canada, OT, Canada.
- Walker, H. J. 1983a. Colville River Delta, Alaska, guidebook to permafrost and related features. Alaska Division of Geological and Geophysical Surveys, Fairbanks, AK. Guidebook 2 for Fourth International Conference on Permafrost. 34 p.
- Walker, H. J. 1983b. The Colville River Delta. Section G: The delta's distributaries. Unpublished report prepared for North Slope Borough, Barrow, AK. 41 p.
- Walker, H. J. 1994a. Environmental impact of river dredging in arctic Alaska (1981-89). *Arctic* 47: 176–183.
- Walker, H. J. 1994b. Nechelik Channel investigations—1994. Unpublished report prepared for North Slope Borough, Barrow, AK, by Louisiana State University, Baton Rouge, LA.
- Walker, H. J., and L. Arnborg. 1966. Permafrost and ice-wedge effect on riverbank erosion. Pages 164–171 *in* Proceedings, Permafrost International Conference, 1963, Lafayette, IN. National Academy of Sciences, Washington, DC, National Research Council Publication 1287.
- Walker, H. J., and Y. Matsukara. 1979. Barchans and barchan-like dunes as developed in two contrasting areas with restricted source regions. Pages 43–46 *in* Annual Report. Institute of Geoscience, Tsukuba, Japan.
- Walker, H. J., and J. M. McCloy. 1969. Morphologic changes in two arctic deltas. Arctic Institute of North America, Arlington, VA. Research Paper No. 49. 91 p.
- Walker, H. J., and H. M. Morgan. 1964. Unusual weather and river bank erosion in the delta of the Colville River, Alaska. *Arctic* 17: 41–47.
- Williams, J. R., L. D. Carter, and W. Yeend. 1978. Coastal Plain deposits of NPR-A. Pages B20–B22 *in* The United States Geological Survey in Alaska: Accomplishments during 1977. U. S. Geological Survey, Circular 772-B.